



HELMHOLTZ
CENTRE FOR
ENVIRONMENTAL
RESEARCH – UFZ

PhD Dissertation 09/2011

Evaluation of groundwater recharge in Najd aquifers using hydraulics, hydrochemical and isotope evidences

Khalid Salim Ahmed Al-Mashaikhi

ISSN 1860-0387

EVALUATION OF GROUNDWATER RECHARGE IN NAJD AQUIFERS
USING HYDRAULICS, HYDROCHEMICAL AND ISOTOPE
EVIDENCES

For the obtainment of the academic degree doctor rerum naturalium
(Dr. rer. nat.)

Submitted to the Council of the Faculty of Chemistry and Geosciences
of the Friedrich-Schiller-Universität Jena

by

Khalid Salim Ahmed Al-Mashaikhi,

Born on: 01/01/1967, in Sultanate of Oman

ABSTRACT

This study presents a multi-indicator approach about the Najd region in south-west Oman; a significant area for groundwater resources and a future of agricultural development. The Najd area mainly consists of marine limestone of Tertiary age and hydrogeologically classified to four aquifers A to D following the order from groundlevel, downwards. Aquifer A is located in the Rus formation, the upper deposits, whereas the aquifers from B to D are restricted with the Umm Er Radhuma formation (UER).

On the north side of the recharge area at the Jabal chain, only aquifer D exists, whereas the other aquifers are dry due to geological structural influences. This dominance leads us to believe that aquifer D is the main aquifer in Najd. This aquifer has the potential to collect recharge from the Jabal chain and the nearby north side. This occurs particularly during cyclone events and in monsoon season. The aquifer conducts the water through faults and fissures to upper aquifers further north.

Results were detected from monitoring the level of water in boreholes during flood period occurrences. It is evident that these observations support the idea that cyclone events are a significant source of recharge to Najd groundwater. Thus, the estimated time for recharge to reach the groundwater was calculated between a range from 7 days to 6 months depending on the cyclone intensity and longevity, the aquifer characteristics and distances between the recharge occurrence locations and the monitored boreholes. In comparison to water levels are declining in central Najd in all aquifers A to D on the range between 0.12m to 2.05m annually. However, the highest decreases are found at Helat Ar Rakah in aquifer C, with a depressive affect extending more than 30 km.

In general, groundwater mineralization in all aquifers increases in a northeastward direction. With exception of the Jabal chain, Najd groundwater does not meet with the Omani standard for human drinking water. However, the majority of groundwater in all aquifers is classified as suitable for agricultural purposes, ie. Irrigation, according to SAR and EC concentrations, follow the order of $D > C > A > B$.

The stable water isotopes reveal that ^2H and ^{18}O are depleted in all aquifers within the flow direction. They reflect the isotopic composition of cyclone events as well as in fossil groundwater. However, enrichment in ^2H and ^{18}O is found in or at least close to the Jabal chain and two other locations further north: at Thumrait (MOD-15) and at the Poultry Farm (332/014) at Hanfeet. This enrichment indicates recent groundwater along the recharge direction as one of the findings in this study. Tritium was detected in the Jabal chain, at Shsir in aquifer A and in DEP-9 in aquifer B reflecting sub-modern groundwater recharge. These arguments conclude that groundwater hydrochemistry and water stable isotopes are mainly controlled by geological structures and that aquifer properties contain a certain quality and quantity of recharge. As a result, heterogeneity of aquifers was observed.

^{14}C data and model age calculations show that the groundwater age in Najd aquifers varies between modern and up to 22,000 years. However, majority of groundwater belongs to the Holocene period (<10,000 yr). With exception of the Jabal chain several boreholes from different aquifers were indicated as modern or containing a young groundwater age, such as Helat Ar Rakah, Shsir, the South of Qitbit and east Al Mazyunah. The data analyses of ^{14}C , $^{13}\text{C}_{\text{DIC}}$ and ^{18}O confirm three sources of the origin of groundwater: monsoon, recent and paleo-cyclones.

The noble gases temperature (NGT) reveals paleo-climate conditions, keeping in mind the recharge to groundwater in the past, which occurred under colder climate conditions compared with recent times. Additionally, the groundwater temperature increases towards the northeast which supports the hypothesis of humid or colder climates near the Jabal in the past than further north in the interiors of Najd. The Ne/He and $^3\text{He}/^4\text{He}$ data presents an atmospheric helium source in aquifers A, B and D as an evidence of recent recharge, however, radiogenic helium in aquifer C points to a paleo-recharge.

Zur Untersuchung der bedeutenden Grundwasserressource in der Wüstenregion Najd, einem landwirtschaftlichen Entwicklungsgebiet im Südwesten des Omans, wird ein Multi-Indikator-Ansatz verwendet. Das Najd-Grundwasserreservoir besteht aus vier Aquiferen (A-D) tertiären Alters. Aquifer A ist in der oberen Rus-Formation ausgebildet, die Aquifere B bis D gehören der Umm Er Radhuma-Formation (UER) an. Auf der Nordseite der Jabal-Kette, dem Neubildungsgebiet, ist nur Aquifer D flächig ausgebildet, während die anderen Aquifere strukturell geologisch begründet trocken fallen. Daher ist Aquifer D quasi Hauptaquifer für die gesamte Najd-Region und ist geeignet, die Grundwasserneubildung der Jabal-Kette und des angrenzenden Nordteils weitestgehend aufzunehmen. Monsun und Zyklon-Niederschläge sind dominierende Quellen für die Neubildung. Das Grundwasser aus Aquifer D erreicht über Störungen und Spaltensysteme die oberen Aquifere im nördlichen Najd-Gebiet.

Ergebnisse des Wasserstandsmonitorings in Bohrungen während Flutperioden werden diskutiert und geschlussfolgert, dass Niederschläge aus Zykloneignissen eine entscheidende Quelle der Grundwasserneubildung in der Najd-Region sind. Aus den Messungen konnte eine Fließzeit zwischen Niederschlag und Grundwassereintritt im Intervall von 7 Tagen bis zu 6 Monaten ermittelt werden. Die Fließzeiten hängen dabei von der Niederschlagsintensität und -länge, der Aquifermatrix und der Entfernung zwischen Niederschlags- und Messlokation ab. Der Vergleich der Wasserstände zeigt, dass in allen Aquiferen eine jährliche Absenkung zwischen 0,12m und 2,05m zu verzeichnen ist. Die höchste Grundwasserdepression wurde in Helat Ar Rakah im Aquifer C mit einem 30km Depressionstrichter beobachtet.

Die Mineralisation des Grundwassers nimmt generell in nordöstliche Richtung zu. Mit Ausnahme von Vorkommen im Jabal-Gebiet eignet sich das Grundwasser der Najd-Region gemäß den omanischen Wasserstandards nicht vorrangig als Trinkwasser. Allerdings ist der Großteil des Grundwassers den SAR- und Leitfähigkeitswerten nach für landwirtschaftliche Zwecke, beispielsweise Bewässerung, als geeignet klassifiziert worden. Die Wasserqualität nimmt in der Folge der Aquifere von D über C und A nach B ab.

Die stabilen Wasserisotope weisen aus, dass das Grundwasser in allen Aquiferen entlang der Fließrichtung in ^2H und ^{18}O abgereichert ist. Sie widerspiegeln die Isotopensignatur rezenter Zykloneignisse als auch die fossiler Wasser. Nur im Einflussbereich der Jabal-Kette und an zwei Entnahmehäusern weiter nördlich (Thumrait, MOD-15, und Geflügelfarm Hanfeet, 332/014) werden an ^2H und ^{18}O angereicherte Grundwässer gefunden. Diese Anreicherung deutet auf einen Einfluss rezenter Grundwassers entlang der Fließrichtung, wie er erstmalig in dieser Studie nachgewiesen wurde. Tritium als Indikator sub-moderner Grundwasserneubildung wurde in der Jabal-Region, in Shisr und in DEP-9 (Aquifer B) nachgewiesen. Aus den hydraulischen, hydrochemischen und isotopischen Ergebnissen lässt sich schlussfolgern, dass die Hydrochemie und die Isotopie des Grundwassers vorwiegend durch geologische Strukturen (Bruchstörung, Karst) und Eigenschaften der Aquifermatrix (Speicherkapazität, Durchlässigkeiten), die eine starke Heterogenität der Aquifere zur Folge haben, kontrolliert werden.

^{14}C -Analysen und Berechnungen von Modelaltern weisen auf Grundwasseralter zwischen modern und 22.000 Jahren. Vorwiegend im Holozän (<10.000 Jahre) wurde die Mehrheit des Grundwassers gebildet. Außer in der Jabal-Region wurden nördlich davon in einigen Brunnen in unterschiedlichen Aquiferen junge Grundwasseralter bestimmt: Helat Ar Rakah, Shisr, südlich Qitbit und östlich Al-Mazyunah. Die Isotopendaten von ^{14}C , $^{13}\text{C}_{\text{DIC}}$ und $^{18}\text{O}_{\text{H}_2\text{O}}$ bestätigen drei Quellen der Wasserherkunft: Monsun, rezente und Paläo-Zyklonsysteme,

Edekgastemperaturen (NGT) ermöglichen Aussagen zu Paläoklimaeinflüssen während der Grundwasserneubildung im Vergleich zu rezenter Neubildung. Im Najd-Gebiet nehmen die Grundwasserbildungstemperaturen nach Nordost zu. Dies weist auf humidere Bedingungen nahe der Jabal-Kette in der Vergangenheit hin im Vergleich zum Inneren des Najd. Rezenter Recharge in A, B und D und fossiler Recharge im C-Aquifer lässt sich aus atmosphärischen bzw. radiogenen He-Anteilen der Ne/He- und $^3\text{He}/^4\text{He}$ -Verhältnisse ableiten.

تركز هذه الدراسة على طرق ومؤشرات التغذية الجوفية بمنطقة النجد الواقعة في جنوب سلطنة عمان والتي تعد أحد أهم مصادر المياه الجوفية ومستقبل التنمية الزراعية هناك. وتتشكل منطقة النجد بصورة أساسية من رواسب الحجر الجيري ذات الأصل البحري التابعة للعصر الجيولوجي الثلاثي والتي تضم مجموعة من التكاوين الجيولوجية مثل الدمام، الرس و أم الرضوم التابعة لمجموعة حضرموت. ومن الناحية الهيدروجيولوجية تقسم الطبقات الحاملة للمياه بمنطقة النجد إلى أربع خزانات جوفية تصنف من الأعلى إلى أسفل (أ، ب، ج، د)، حيث ينحصر الخزان الأول (أ) في تكوين الرس وما يعلوه بينما تتواجد الخزانات الثلاثة (ب، ج، د) في طبقة أم الرضومة.

ويعتبر الخزان الجوفي (د) هو الخزان الرئيس من ناحية انتشاره حيث يتواجد على عموم منطقة النجد، وكذلك كونه ينفرد بتواجده على السطح الشمالي لسلسلة جبال ظفار ويستقطب كميات من مياه الأمطار والسيول التي تسقط على السطح الشمالي لسلسلة جبال ظفار ومن ثم تأخذ طريقها عبر الفوالق والكسور من الخزان (د) إلى الخزانات الجوفية التي تعلوه (ج - أ). وتعد الأمطار الإعصارية هي المصدر الأول للتغذية الجوفية في منطقة النجد بينما تأتي الأمطار الموسمية المعروفة محليا بالخريف في المصدر الثاني. وقد استنبطت هذه المعلومات من مقارنة بيانات الفيضانات مع التأثيرات الايجابية لمناسيب المياه في العديد من آبار مراقبة مناسيب المياه الجوفية من مختلف الخزانات، وبناءً على ذلك تم حساب اقصر فترة لوحظت لارتفاع مناسيب المياه الجوفية مقارنة بفترة حدوث الفيضان. تم رصد فترات زمنية تراوحت ما بين 7 أيام بالقرب من السلسلة الجبلية في الخزان (أ) إلى حوالي ستة أشهر في الخزان (ج). بصفة عامة فإن مناسيب المياه بمنطقة النجد تتناقص سنويا في جميع الخزانات بمعدل يتراوح ما بين 0,12 متر في الخزان الجوفي (أ) إلى 2,05 متر في الخزان (ج). وتعتبر منطقة هيلة الراكه هي أكثر المناطق تأثرا بانخفاض مناسيب المياه حيث تعدى هبوط مناسيب المياه 39 متر في نهاية 2009م.

وتشكل جودة المياه إحدى التحديات الأبرز حيث بينت الدراسة أن جودة المياه الجوفية تتناقص في جميع الخزانات بمنطقة النجد باتجاه الجريان من الجنوب والجنوب الغربي إلى الشمال والشمال الشرقي، وباستثناء المنطقة الجبلية والتي تتأثر بالأمطار الموسمية فإن المياه بمنطقة النجد لا تتطابق مع المواصفات العمانية لمياه الشرب للاستخدام الأدمي، بينما صنفنا معظمها ضمن نطاق المياه الصالحة للزراعة بناءً على تراكيز معدل امتصاص الصوديوم (SAR) والموصلية الكهربائية (EC)، وعليه فقد صنفنا هذه الخزانات من حيث جودتها للري كالتالي: $d < c < a < b$.

كما تشير بيانات النظائر المشعة مثل 2H ، ^{18}O والتي تستخدم للاستدلال على حداثة المياه الجوفية عندما تكون غنية، إلى أنها تستنفذ باتجاه جريان المياه الجوفية باتجاه الشمال بينما تكون غنية في سلسلة جبال ظفار والمناطق المجاورة. كما تم الاستدلال بواسطة النظائر الأثقل على وجود خط تغذية جوفية في الخزان (د) يمتد من منطقة الجبل في الجنوب مرورا بثمريت (MOD-15) ومزرعة الصفا بشرق حنفيت (332/014) باتجاه وادي بن خوطار، إضافة إلى ما سبق تشير نتائج تحاليل 3H إلى وجود مسار آخر في الخزان الجوفي (أ) يمر عبر وادي غدون إلى منطقة شصر، بينما لوحظ وجود مؤشر تغذية في الجهة الغربية عبر وادي عديم مرورا بققع (DEP-9) وباتجاه الجريان.

ويتضح من الدراسة أن عمر المياه بمنطقة النجد يقدر ما بين مياه حديثة إلى قديمة يصل عمرها إلى 22 ألف سنة (BP) وباستثناء منطقة الجبل يعود أصلها إلى فترة الهالوسين ($<10000yr$). كما تشير البيانات المستوحاة من نتائج ^{18}O ، ^{14}C في هذه الدراسة إلى وجود ثلاثة مصادر لأصل المياه الجوفية وهي: موسمية، وإعصارية (قديمة وحديثة). أما درجات حرارة المياه حين دخولها للخزان في الأزمنة الماضية والتي تم قياسها باستخدام الغازات الخاملة (NGT) قد بينت أن درجة حرارة المياه تزداد من أسفل إلى أعلى أي من الخزان الجوفي (د - أ) وأن الظروف المناخية التي تمت بها التغذية في السابق كانت أكثر برودة إذا ما قورنت بالظروف الحالية، وحسب بيانات ($^3He/^4He$ ، Ne/He) يتضح أن التغذية في الخزان (ج) أكثر قداما (paleo-recharge) من بقية الخزانات الأخرى.

ACKNOWLEDGMENTS

I would like to express my sincere gratitude to all the people who contributed to this work. Particularly to:

His Excellency Abdullah Salim Al Ruwas, minister of Regional Municipality and Water Resources and his undersecretary Eng. Ali Mohammed Al Abri for financial support and encouragement.

Prof. Dr. Sabine Attinger and Prof. Dr. Georg Büchel (Jena University) for the worthy discussions and supervision.

Dr. Gerhard Strauch (UFZ, Leipzig), for his valuable comments and excellent dealing.

The staff of the UFZ-Departments; Isotope Hydrology and Hydrogeology, and to Dr. Andreas Musolff for his help with software analyses.

The staff of DG of Water Resources Assessment, Department of Water Resources in Dhofar, Laboratory of Water Quality, Manpower Center, PDO, Salalah Airport, GIS, DG of Environment and Climate Affairs in Dhofar and DG of Water in Dhofar.

My colleagues Eng. Hamad Al-Hatimi, Dr. Abdulaziz Al-Mushaikhi, Eng. Salim Alesh, Ghassan Al-Tamimi, Abdullah Bawain, Mansoor Amer Jeed and Ahmed Al Mawali for their support during samples collection.

My special thanks go to my family for their patience and understanding over my years of study.

LIST OF FIGURES	Page
ABSTRACT	i
ZUSAMMENFASSUNG	ii
خلاصة	iii
ACKNOWLEDGMENTS	iv
LIST OF FIGURES	viii
LIST OF TABLES	iv
ABBREVIATIONS	x
1. CHAPTER: INTRODUCTION	1
1.1. Motivation	1
1.2. The Goal of the Study and Hypotheses	4
2. CHAPTER: STUDY AREA	6
2.1. Topography	6
2.2. Demography	7
2.3. Maps System and Data Source	7
2.4. Hydrology	7
2.4.1. Climate of Dhofar Governorate	7
2.4.2. Climate data source	8
2.4.3. Temperature	9
2.4.4. Evaporation and relative humidity	9
2.4.5. Rainfall	9
2.5. Surface Water	11
2.5.1. Wadi flow	11
2.6. Geological Structure and Units Classifications	13
2.6.1. Geological structure	14
2.6.2. Geological units classifications	16
2.6.3. Recent alluvium	17
2.6.4. Fars Group	17
2.6.5. Hadhramaut Group	18
2.6.5.1. <i>The Dammam Formation</i>	19
2.6.5.2. <i>The Rus Formation</i>	21
2.6.5.3. <i>The Umm er Radhuma Formation</i>	21
2.6.6. Shammar Shale	24
2.7. Conclusion	24
3. CHAPTER: AQUIFER PROPERTIES AND DEVELOPMENT OF GROUNDWATER LEVELS	25
3.1. Description of Hydrogeological Units	25
3.2. Aquifers Characteristics	26
3.2.1. Aquifer A	27
3.2.2. Aquifer B	29
3.2.3. Aquifer C	31
3.2.4. Aquifer D	33
3.3. Groundwater Movement	34
3.4. Indications for Trends of Water Level	37
3.4.1. Aquifer A	38
3.4.2. Aquifer B	40
3.4.3. Aquifer C	41
3.4.4. Aquifer D	44
3.5. Recharge Processes	46
3.5.1. Evidence of recharge associated with cyclone events	46
3.6. Conclusion	54

4. CHAPTER:	
GROUNDWATER ASSESSMENT AND MECHANISMS OF RECHARGE WITHIN THE AQUIFERS	55
4.1. Sampling and Analytical Methods.....	55
4.2. Data Choices.....	60
4.3. Correlation Matrix and Factor Analysis.....	63
4.4. Evaluation of the Groundwater Hydrochemistry.....	67
4.4.1. Characterisation of water types.....	67
4.4.2. Hydrochemical signature.....	71
4.4.3. Trace Elements.....	76
4.4.4. Saturation Index (SI)	78
4.4.5. Lithology of aquifer matrixes.....	81
4.5. Environmental Isotopes in Groundwater of the Najd Aquifers.....	87
4.5.1. Stable isotopes of water and tritium.....	87
4.5.2. Sulphate and oxygen isotopes of sulphate	93
4.6. Multiple Influences on Groundwater Recharge Processes.....	102
4.6.1. Groundwater flow dynamic in the upper aquifer A.....	102
4.6.2. Faults influences in the groundwater flow and behavior.....	103
4.6.3. Hydrochemistry and isotopes evidences.....	104
4.6.4. Recharge direction	111
4.7. Water Quality.....	112
4.7.1. Potable water.....	113
4.7.1.1. Fluoride source and distribution	114
4.7.1.2. Nitrate	119
4.7.1.3. Total Hardness	119
4.7.2. Irrigation water for agriculture purposes.....	120
4.7.2.1. Salinity	120
4.7.2.2. Cl/Br ratio	122
4.7.2.3. Sodium Adsorption Ratio (SAR)	123
4.8. Conclusion.....	126
5. CHAPTER:	
EVALUATION OF GROUNDWATER AGE IN ALL AQUIFERS WITH REGARDS TO PALEO-ENVIRONMENTAL DEVELOPMENT	128
5.1. Dating of Groundwater Using ¹⁴ C.....	128
5.1.1. Radiocarbon in groundwater and the problems of age dating	128
5.1.2. ¹⁴ C in groundwater of the Najd region – data and corrections.....	130
5.1.3. Interpretation of ¹⁴ C data in relation to the carbon sources and the water origin	136
5.1.4. Comparison of ¹⁴ C data with data from other sources	142
5.2. Estimation of Paleo-Recharge Temperatures by Noble Gas Thermometry	143
5.2.1. Noble gases importance and types of applications	143
5.2.2. Noble gases interpretations and evidence of recharge	145
5.3. Conclusion.....	149
6. CHAPTER: NAJD GROUNDWATER SITUATION AND FUTURE MANAGAMENT	150
7. REFERENCES	156
8. ANNEX	163

1.1 Location of the Study Area in Dhofar with the proposed agriculture sites (<i>bold black</i>)	5
2.1 Total rainfalls in Thumrait and Qeroon Hiritti stations for the period (1977 – 2009).....	10
2.2 Comparison between different wadis flow in each year	12
2.3 Total monthly cumulative flows from four wadi Gauges (1985-2008)	13
2.4 Distribution of faults in the Study Area	16
2.5 Simplified geological map of the Study Area and cross sections locations	18
2.6 Isopleths for the base of the upper UER in Najd area	23
3.1 Schematic South-North (A-A) and West-East (B-B) hydro-geological cross sections along the Study Area (see Figure 2.5, directions)	29
3.2 Groundwater flow direction (arrows) in aquifer C	35
3.3 Groundwater flow direction (arrows) in aquifer	36
3.4 Variation in water level for aquifer A and B up to 2009	39
3.5 Water level variations in Helat Ar Rakah (aquifer A) for the period (1991-2008).....	40
3.6 Water level variations in Hanfeet (aquifer B) for the period (1992-2009).....	41
3.7 Variation in water level for aquifer C up to 2009	42
3.8 Water level variations in Helat Ar Rakah (JICA-6) and Hanfeet (001/016) in aquifer C for the period (1990-2009)	43
3.9 Variation in water level for aquifer D up to 2009	45
3.10 Water levels variations in Hanfeet (aquifer D) for the period (1992-2009) ..	46
3.11 Locations of wadi gauges, boreholes responding with flood events and wadi flow direction (dark arrows)	48
3.12 Comparison between borehole Mathira1 water level and Wadi Ghadun flood event	49
3.13 Comparison between borehole KHT-A water level and Wadi Thahboon flood events	50
3.14 Monitoring well (001/007) in Shsir with some respond related to flood events	51
3.15 Comparison between boreholes RBK-C and Ribkut1 water level and Wadi Thahboon flood events	53
4.1 Sampling locations from all aquifers	60
4.2 Overall dominant major ions in Najd groundwater	69
4.3 Dominant major ions in different Najd aquifers	69
4.4 Piper diagram from all groundwater samples of Najd area including four developed hydrochemical facies	70
4.5 Comparison between major ions in Najd aquifers	71
4.6 Total dissolved solids (TDS) versus Na/Na+Cl	72
4.7 Total dissolved solids (TDS) versus Mg/Mg+Ca.....	72
4.8 Total dissolved solids (TDS) versus Ca/Ca+SO ₄ ratio	73
4.9 Total dissolved solids (TDS) versus Cl/sum anions ratio	74
4.10 SO ₄ versus HCO ₃ /sum anions ratio compared with rainfall and sea water ...	74
4.11 Earth's alkaline-alkaline ratio relative to the salt forming (Cl/SO ₄ ratio in the Najd aquifers	75
4.12 Fe versus As for different aquifers of Najd	77
4.13 Fe versus B for aquifers A to D	77
4.14 As versus Cu for all aquifers	78

LIST OF FIGURES	Page
4.15 Saturation index in different aquifers versus Total dissolved solids (TDS) ...	79
4.16 Aquifer matrix compositions in different aquifers	83
4.17 Sulphur in aquifer matrix and sulphate in groundwater in different aquifers ...	85
4.18 Calcium and magnesium in aquifer matrix of Najd aquifers based on X-RF analyses	86
4.19 Comparison of trace element in the matrix of different aquifers	87
4.20 $\delta^2\text{H}$ - $\delta^{18}\text{O}$ diagram of groundwater, spring water, and precipitation from the Dhofar region and the different Najd aquifers (Najd Groundwater Line [NGL]: black line bold); further: Northern Oman Meteoric Water Line (NOMWL: dotted), Southern Meteoric Water Line (SOMWL: dashed-dotted), Global Meteoric Water Line (GMWL) are depicted for reference	89
4.21 Relation of S and O isotopes in groundwater sulphate from the different aquifers.....	96
4.22 $\delta^{34}\text{S}_{\text{sulphate}}$ vs $\delta^{13}\text{C}_{\text{DIC}}$ in groundwater of Najd aquifers	98
4.23 $\delta^{34}\text{S}_{\text{sulphate}}$ vs sulphate concentration in groundwater from all aquifers	98
4.24 Distribution of $\delta^{34}\text{S}_{\text{sulphate}}$ in groundwater of aquifer C and D	102
4.25 Profiles constructed in different aquifers based on the consistent relationship between hydrochemistry and isotope data, for an example from each aquifer (see Figure 4.26)	106
4.26 (a-p) Characteristic profiles reporting the hydrochemical and isotope development of the groundwater in aquifers A to D. The profiles follow the main directions of the groundwater flow: in aquifer A (a, b = A) and aquifer B (c, d = B) south to north, in aquifer C (e, h = C1, C2)	109
4.27 $\delta^2\text{H}$ distribution in aquifer D and direction of the recharge in dot line shows decrease of monsoon influence along the flow line; high depletion of ^2H could also point to strong pumping activities because of fossils water with depleted ^2H ...	111
4.28 Cl (mg.L^{-1}) distribution in aquifer D and proposed recharge direction in dot line	112
4.29 Sr versus F in aquifer A	116
4.30 Distribution of fluoride in aquifers C and D	117
4.31 Total dissolved solids (TDS) versus Fluorite (SI).....	118
4.32 Electrical conductivity ($\mu\text{S.cm}^{-1}$) distributions in aquifers A, C and D	121
4.33 Cl versus Br compared with sea water	123
4.34 Sodium Adsorption Ratio (SAR) from the different aquifers	126
5.1 Groundwater age in different aquifers	136
5.2 Groundwater age in years BP from all aquifers using Mod-1 with ^{13}C (AMS)..	138
5.3 Groundwater age versus ^{14}C concentration.....	139
5.4 Comparisons between ^{13}C and ^{14}C showing three types of influences, (^{14}C values were plot in DIC and AMS for each aquifer).....	140
5.5 ^{18}O of water versus ^{14}C classified the source of groundwater in Najd to three groups, (^{14}C values were plot in DIC and AMS for each aquifer)	141
5.6 ^{18}O versus $^{13}\text{C}_{\text{DIC}}$ for different aquifers in Najd, reflecting soil organic matter and mixing processes	141
5.7 Ne/He versus $^3\text{He}/^4\text{He}$ ratio in aquifers A to D as evidently for influence of different inputs: atmospheric and radiogenic.....	145
5.8 NGT versus ^4He in aquifers A to D	146
5.9 Groundwater age in comparison with NGT for different aquifers	147
5.10 Groundwater age versus NGT in different aquifers	148

2.1 Meteorological data collected from Thumrait station during the period from 1986 to 2009	11
2.2 Summary of the hydrogeological units in the Study Area (after GRC, 2008)..	20
3.1 A summary of hydraulic characteristics from the Najd aquifers (saturation zone) (modeled after GRC, 2008)	31
3.2 Estimated recharge periods to reach aquifers based on water level and flood events.....	48
4.1 Results of the hydrochemical analyses of groundwater and precipitation in the Najd region	61
4.2 Correlation coefficient matrix water parameters for all Najd aquifers	64
4.3 Principle component varimax rotated factor analysis for Najd water parameters (n=79)	66
4.4: Range of total dissolved solid (TDS) concentrations in each aquifer	68
4.5: Average of major ions concentration and their percentage in each aquifer ...	68
4.6 Saturation index (SI) of the groundwater	80
4.7 (a-b) Lithological results for 9 boreholes in Najd analyzed by using XRF ...	82
4.8 Elements obtained from borehole WWD-25 by using (XRF) analysis.....	84
4.9 Minimum and maximum concentration of isotopes in each aquifer	88
4.10 Results of isotope analyses of water, sulphate, DIC and tritium from water, in addition to ^{13}C of lithology	92
4.11 Enrichment factor for sulphate reduction (ϵ) along selected directions	99
4.12 The FAO standards for the safe upper limits of total salts in water for stock in arid countries	120
5.1. ^{14}C data and age calculations by different models	132
5.2. Comparison between NGT, helium isotopes and groundwater age	146

ANNEX

A-1 Results of chemical data and precipitation collected in 2008 and 2009 (mg.L^{-1}).....	163
A-2 Results of chemical analyses and precipitation collected in 2008 and 2009 (meq.L^{-1})	167
A-3 Stable isotopes and tritium for groundwater and precipitation analyses collected during 2008 and 2009	171
A-4 Results of trace elements and precipitation collected in 2008	174
A-5 Results of noble gases collected in 2009	176

ABBREVIATIONS

CCEWR	Council for Conservation of Environment and Water Resources
DG	Directorate General
FAO	Food and Agriculture Organisation of the United Nations
GIS	Geographical Information System
GRC	Geo-Resources Consultants
GTZ	Deutsche Gesellschaft für Technische Zusammenarbeit
IAEA	International Atomic Energy Agency
IPCC	Intergovernmental Panel on Climate Change
JICA	Japanese International Corporation Agency
MAF	Ministry of Agriculture and Fisheries
MEW	Ministry of Electricity and Water
MMI	Mott MacDonald International
MMP	Mott MacDonald and Partners
MOC	Ministry of Communications
MOD	Ministry of Defence
MPM	Ministry of Petroleum and Minerals
MRMWR	Ministry of Regional Municipalities and Water Resources
MWR	Ministry of Water Resources
NWI	National Well Inventory
PAWR	Public Authority for Water Resources
PDO	Petroleum Development Oman
UFZ	Helmholtz Centre for Environmental Research
WBCSD	World business council for sustainable development
BP	before present
CDT	Cañon Diablo Troilite standard
DIC	Dissolved Inorganic Carbon
DOC	Dissolved Organic Carbon
GMWL	Global Meteoric Water Line
GPS	Global Positioning System
ID	Identity
ITCZ	Intertropical Convergence Zone
ka	kilo annum (thousand year)
L.UER	Lower Umm Er Radhuma
m.agl	meter above ground level
m.amp	metres above measuring point
m.amsl	metres above mean seal level
m.bgl	metres below ground level
m.bmp	metres below measuring point
mm	mili metres
Mm ³	million cubic meters
NGL	Najd Groundwater Line
NGT	Noble Gases Temperature
NOMWL	Northern Oman Meteoric Water Line
pmC	percentage of modern carbon (¹⁴ C)
S.A.S	Study Area south (boundary)
SOMWL	South Oman Meteoric Water Line
SWL	standing water level
TDS	Total Dissolved Solids
U.UER	Upper Umm Er Radhuma
UTM	Universal Trans Mercator
VPDB	Vienna Pee Dee Belemnite
VSMOW	Vienna Standard Mean Ocean Water
WGS	World Geographic Spheroid
WL	Water level

INTRODUCTION

The Study Area is located in the Dhofar Governorate in southern Oman. The region is called Najd and covers an area of about 88,000 km². The borders of the Study Area are regulated by the international border with the Kingdom of Saudi Arabia from the north, the Republic of Yemen from the west, the Al Wusta area (middle of Oman) from the east and the Dhofar Mountain (Jabal) Chain from the south (Figure 1.1).

The Najd region is an essential groundwater reservoir for Oman. This is my motivation to contribute, through my study, a better understanding of the groundwater development and to determine the sustainability of this resource. The integration of groundwater hydrochemistry, environmental isotopes and noble gases analyses were used to evaluate water quality, water age and paleo-climate conditions finally to assess the recharge processes and mechanisms of Najd aquifers A to D.

1.1 Motivation

Water plays a pivotal role for sustainable development and reduction of poverty globally. The competition for water demands has increased over the last two decades; a decrease in both water shortages and water quality have seriously affected the developments sectors such as economics, politics and ecosystem integrity (UN, 2010). On 'World Day of Water' held on the 22nd of March 2010 the United Nations announced that 1 billion people in the world have a scarcity of drinking water and that 2.4 billion are lacking clean water. In addition, two thirds of the world populations are likely to live in a country with moderate or severe water shortages by the year 2025. Nevertheless, domestic use does not exceed 10% of the total consumption, with the remaining 90% being divided between agriculture at 70% and industry at 20% (WBCSD, 2005).

Asia, Central and South America and the Middle East are the most affected regions by aridity. Particularly, the Middle East and in North Africa the water resources are anticipated to decline in the next century due to a decrease of rainfall in the range between 10-25%, and increases of evaporation between 5-20%, which is being associated with a surge in the demand of water consumption (IPCC, 2008).

Typically, countries restricted with arid zones depend on groundwater for more than 60% of their daily consumption due to the limitation or absence of other sources such as rivers or springs. It can occasionally occur that good quantities of water are found in arid zones as mixed or fossil water. However, due to water quality decline the groundwater is not potable and is usually only used for agriculture purposes. Therefore, this issue requires intensive study about the source of the water itself, in order to establish sustainable management. Due to the demand of water, analysis is essential in several fields; in all quantities, qualities, origin and recharge of groundwater.

Semi-arid zones are covered around many places worldwide, including Middle East and the North of Africa (UN, 2010). The hydrogeological conditions, however, are often different in contrast with the Najd Study Area in Oman, except for the Arabian Peninsula. Here, the Tertiary formation of the Umm Er Radhuma (UER) is distributed in all of the Gulf States. This formation is one of the most important aquifer structures in the Arabian Peninsula. The focus of the research should evidentially be on groundwater and its availability to the UER and connected aquifer units. With the investigation of the Najd aquifers we have the chance to compare the results of the UER in other parts of the Arabian Peninsula. This comparison will generally emphasise the aquifer condition, the mechanism of recharge and water quality.

According to the investigations conducted by Sharaf (2001) for hydrogeological and hydrochemical aspects of groundwater in UER in the Arabian Peninsula, it was concluded that the UER is a semi-confined to confined aquifer system. Furthermore, recharge was limited and appears at the outcrops on the west part of Saudi Arabia. The study also concludes that groundwater mineralization increases with a flow direction from west to east. These results represent an overview about groundwater in the UER and take into account the UER formation as one aquifer system. The comparison with Najd is not detailed, since it is categorized by three aquifers. However, similarities were observed between aquifer properties, (PAWR, 1986) recharge occurrence and mineralization increase with the flow direction in UER aquifers in both countries (GRC, 2008).

The Study Area is classified as one of the most arid zones in the world due to high temperatures, evaporation and low rainfall (Roppin, 1986). The recharge to Najd groundwater has been discussed in previous studies, for example Clark (1997) who concluded that it originated in the paleo-climate and is unrelated to modern precipitation in the recharge area; this is based on evidence of environmental isotopes collected from aquifer C in the artesian zone. However, the groundwater in Najd has also been recharged recently by monsoon and cyclonic events (Macumber et al., 1995). The cyclone events' influence was observed in groundwater level responding to several boreholes from different aquifers. In 2008 GRC mentioned aquifers A and B started dewatering in the Hanfeet area (80 km north of the recharge area of the Jabal chain) from beneath aquifers C and D. This evidence supports the idea that aquifer D dominates the recharge in/or close to the Jabal chain in the south, where other aquifers A to C were dry.

The recharge mechanisms in the Najd aquifers are controlled by several parameters including the amount and intensity of rainfall, soil density, faults, fractures, fissures, distance from the recharge area, weather conditions and the aquifers properties. However, it is cyclone events that seem to be the main cause of recharge in the Study Area, with limited monsoon contributions expected in the Jabal chain.

Several hydrogeological studies have been conducted in Najd since the 1970s by Authorities of Oman. Most of them were restricted by a limited area due to the shortage and distribution of boreholes or because of a focus predominantly on aquifer C; subsequently they do not involve aquifer categories in detail. Recent studies attempt to describe the general hydrochemical parameters.

With the exception of the Jabal chain groundwater in Najd, it does not fit with the potable water standard; however it is significant for agriculture purposes. This essential region is one of the vital groundwater reservoirs that need a sustainable water management in Oman.

Due to limited knowledge in the previous investigations - especially in the recharge processes to the aquifer system – the idea of this multi-methodical study was developed. With the water situation in semi-arid and arid zones, I believe that a comprehensive study of groundwater in all Najd aquifers is necessary to answer such

questions; when, where and how the groundwater had originated and which recharge processes occurred. Due to complicated recharge processes a reasonable quantification is required far more than simple, basic knowledge. The approach is derived from the multi-methodical approach of hydraulic, hydrochemical and isotope analyses and is a part of this study goal.

1.2 The Goal of the Study and Hypotheses

The goal of this study is to evaluate the groundwater quality rather than volume in Najd aquifers A to D. Furthermore, the recharge process is to assess in all aquifers, a meteorological, hydrochemical and isotopes data analyses. This study aims to contribute to further investigations and applications as well as management strategy recommendations. Moreover, it will improve the understanding about groundwater development in arid zones and may help authorities when they plan for a future of sustainable groundwater management.

This guides me to three hypotheses as follow:

☒ Groundwater recharge is usually related to flood events reflecting development of the groundwater levels

This can be achieved by analyzing static water levels in aquifers A to D, and to create piezometric water levels to determine the groundwater flow direction. At the same time, we can compare the responding boreholes with flood events and how they fit with the subsurface flow.

☒ The groundwater quality is controlled by active recharge, aquifer matrix, dissolution processes, geological structure and the aquifer characteristics

This hypothesis focuses on several comparisons between aquifers using hydrochemical data such as major ions which is in order to categorize the water type in each aquifer, and to understand what the relationship is between aquifers. The hydrochemical data is compared with stable isotopes among contour maps and profiles in order to assess probability of recharge mechanisms and direction.

☒ The groundwater age and recharge processes over the Najd is the result of changing climate conditions during a period of more than 20 thousands years

This hypothesis mainly emphasises the groundwater age by using radiocarbon methods and comparing the data with the geological structure and the paleo-climatical conditions. This is obtained from noble gases analysis which was introduced in the Najd area for the first time. This data can provide evidence of the recharge occurrence and climatic conditions in the past as a result of groundwater age and noble gas temperature (NGT) in all aquifers.

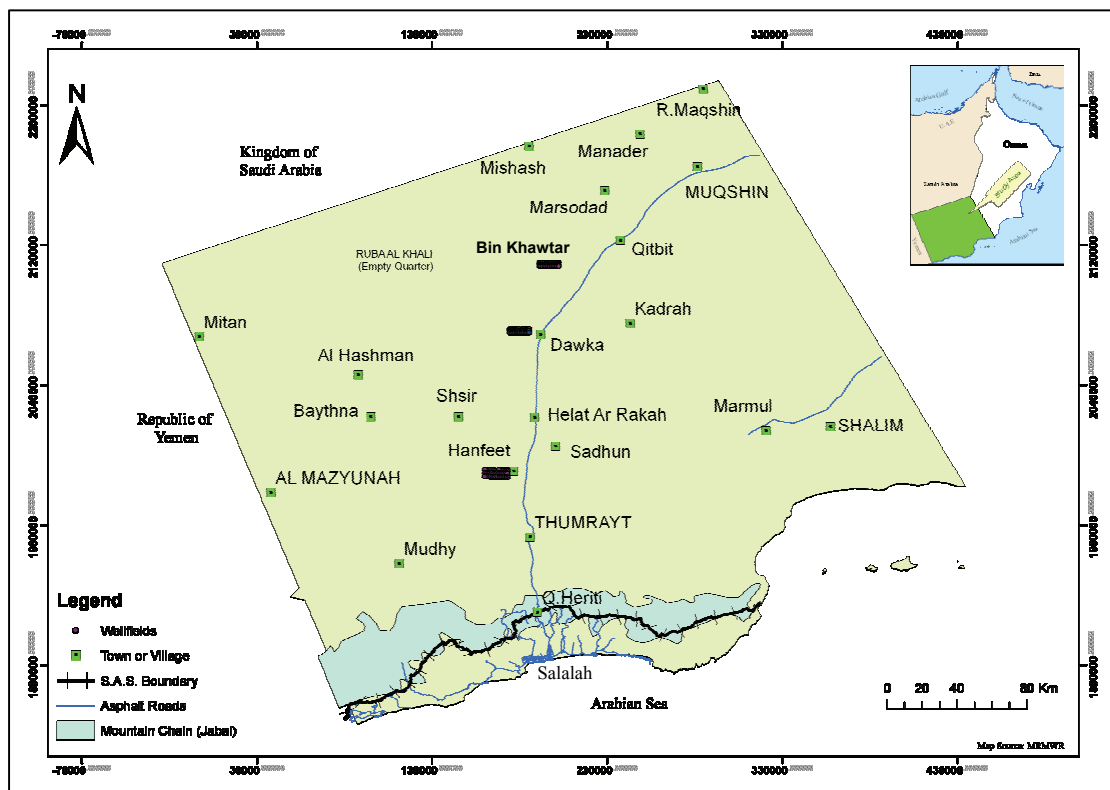


Figure 1.1 Location of the Study Area in Dhofar with the proposed agriculture sites (bold black)

STUDY AREA

This chapter aims to specifically describe the Study Area and its topography, demography, hydrology and geological properties. It emphasizes climate conditions such as temperature, evaporation, humidity and rainfall. In addition, it discusses geological structures and presents some new faults added for the first time on the geological map. At the same time this chapter discusses the historical geology of Najd and different classifications of the existing geological groups and formations including new maps especially for the Umm Er Radhuma formation (UER).

The Study Area is located in Dhofar Governorate in the south of Oman, in the region of Najd and covers an area of about 88,000 km². The borders of the Study Area are established by the international border of the Kingdom of Saudi Arabia from the north, the Republic of Yemen from the west, the Al Wusta area (middle of Oman) from the east and the crest of the Jabal chain in the south which separates the Najd from the coast of the Arabian Sea -30 km off shore- (Figure 1.1). It consists of a flat area penetrated by major wadis (valleys), small hills and sand dunes on the north edge of the Ruba Al Khali desert (translate as *Empty Quartre desert*). Vegetation is sparse and mainly consists of desert shrubs. More substantial vegetation can be found in the vicinity adjacent to the Jabal chain in south.

2.1 Topography

Land surface profiles show the general level of the land to descend from approximately 1000 m.a.s.l on the crest of the Jabal chain to a mainly flat land surface with an elevation of less than 94 m.a.s.l. There are general slopes towards the north-east ranging between 0.0024 m.m⁻¹ at DWS-15 and 0.00032 m.m⁻¹ at WWD-37 with an overall general slope of 0.002 m m⁻¹. The Najd desert consists of a stony plain and alluvial deposits are concentrated within the main wadi channels and sand dunes. The sand dunes occupy a north portion along international border of Saudi Arabia. Several wadis emerge from the Jabal chain and through the centre of the Study Area, eventually disappearing down the sand dunes. These wadis follow the general direction of the topography and represent old drainage patterns. The largest wadis

between the Jabal and central Najd are Aydim, Gharah, Ghadun in the west merging in wadi Milhait; and Ribkut, Thahboon and Andhur, and in the east merging in wadi Qitbit. Furthermore, wadis are compiled together either from the west or east of the Study Area and in wadi Maqshan within the sand dune portion.

2.2 Demography

The Najd area contains four cities: Thumrait, Mazyunah, Shalim and Maqshan and several villages scattered along the area. The total population is around 20953, and is distributed as follows: Thumrait (9590), Mazyunah (5670), Shalim (5123), Maqshan (570) based on the Ministry of National Economy census of 2003. However, more than two thirds of them are concentrated in Thumrait and Al Mazyunah. The main income for the population is agriculture, livestock cultivation and government employment.

2.3 Maps System and Data Source

Data is plotted using UTM WGS84 system coordinates which are provided by the Ministry of Regional Municipality and Water Resources (MRMEWR). The data covers an area extending two UTM zones, UTM 39 and 40. Spatial representation of this data was possible by converting all sites located within UTM 39 to equivalent locations in UTM 40. This was achieved using the Arc GIS Projection Utility. Several various ArcView compatible shape files (.shp) were made available from the MRMEWR which related to international boundaries, roads, wadi orientation and geological maps. These were used for enhancing base-map presentation. In view of the large amount of spatial data that it has been necessary to collect, automatic contour plotting of data using SURFER software was used.

2.4 Hydrology

2.4.1 Climate of Dhofar Governorate

The Study Area, located in arid to semi-arid zones are classified as one of the most arid zones in the world due to high temperatures and evaporation as well as low rainfall (Roppin, 1986). Worldwide Asia, Central and South America and Middle East

are the most influenced by aridity (IPCC, 2008). The Najd area is affected by the movement of the inter-tropical convergence zone (MMI, 1991). This phenomenon varies with the seasons and occurs in the combination of southern and northern winds. Additionally, the air temperature and topography play a role in the phenomenon between land and sea. The climate in the south of Oman which includes the Najd area is defined to three seasons by Pedgley, (1970) and Schemenaver (1989) (MMI, 1991). This classification done based on wind fields characteristic as following:

- The period from July to September is associated with the west monsoon and brings warm, moist air to the southeastern coastline, which is locally called 'Khareef'. This phenomenon is restricted to the south border of the Study Area and mainly on the opposite side. The monsoon generated in the Arabian Sea and Indian Ocean move towards the south mountain with warmer air and blanket clouds. During this monsoon, rainfall occurs in low intensity and long duration.
- The inter-tropical convergence zone moves southwards and the northeast trade wind replace the southwest monsoon due to decreasing temperatures and which usually occurs between November and January.
- The south-western winds become predominant during February to June and October in a northeast direction. The difference in temperatures between the land and the sea helps in the generation of this wind. By the end of June the south western winds become a Monsoon and are generated in the Khareef at the Mountains front.

2.4.2 Climate data source

Meteorological data from the Thumrait weather station which belongs to the Ministry of Transport and Communication is located at 80 km north of the Salalah Airport. It was chosen as a reference for this study because of the availability of an intensive database regarding historical weather patterns including air temperatures, rainfall, relative humidity, and evaporation (Table 2.1). The station has a period record exceeding 23 years. Despite the use of this station, being the most relevant to the Najd climate, temperatures are higher in the sand dunes of Ruba Al Khali, (200 km north of Thumrait), particularly in summer.

The nearest station which can be taken into account is Qeroon Hiritti located 50's km away to the south edge of the Study Area on the Jabal chain. This station is affected by the monsoon rainfall and will be used for references of the recharge contribution from the Jabal.

2.4.3 Temperature

Based on Koeppen (1923) PAWR (1986), it was stated that monthly minimum and maximum temperatures range between 27.4 °C and 45.4 °C. Data obtained from Thumrait Station from the period between 1986 and 2009, show averages of extremely low to extremely high temperatures to be between 6.2 °C to 44.7 °C, with a mean of 26.3 °C. The highest temperatures occur in the period from May to July, and the lowest between the periods from December to February annually.

2.4.4 Evaporation and relative humidity

In this hot, arid, semi-dry region, evaporation has an average of 161.44 mm. yr⁻¹ (13.5 mm.month⁻¹). Annually maximum average evaporation occurs in the period between April to June and the minimum average recorded in the period from December to February. Simultaneously, minimum and maximum averages of evaporation are 3.2 mm.month⁻¹ and 28.3 mm.month⁻¹ respectively. The average relative humidity ranges between 3.7% and 97.3%, with an annual mean of 46.6%. The months of March, April, May and October have the lowest mean of humidity with the highest mean occurring in July and August annually.

2.4.5 Rainfall

Rainfall is irregular in Najd and is affected by cyclone events. The previous studies mentioned the annual average rainfall to be in the range 30mm to 40mm. However, the data obtained from Thumrait Station for a period of 29 years (1980 -2009) gives an average of 30 mm.yr⁻¹. The records for maximum total rainfall are in 1983, 1989, 1992 and 2007 are 144.6mm, 227mm, 131.5mm and 76mm respectively. At the same

time the station did not receive any rainfall during the years 1984, 1999, 2000, 2001 and 2006 (Figure 2.1).

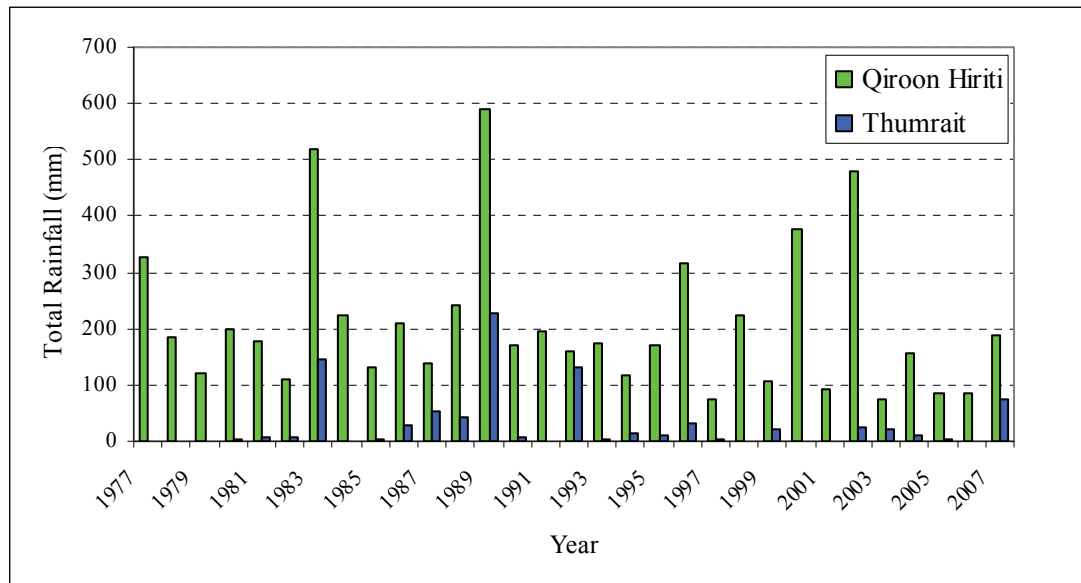


Figure 2.1 Total rainfalls in Thumrait and Qeroon Hiritti stations for the period (1977 – 2009)

The highest rain was recorded in March, June and May; and the lowest in February, April and January. The difference in the annual rainfall between the previous studies and more recent ones may be related to the length of the record. Due to the fluctuation of rainfall and in order to find reasonable average value the record should not be less than 25 years. The nearest meteorological station is Qeroon Hiritti Station, which located 50 km south of Thumrait on the edge of the Study Area. This station is affected by the monsoon rainfall, which is locally called (Khareef) and generated annually in the Arabian Sea during the period between June and September. The annual average rainfall for this station is 197mm from 1977 to 2007. Most of the monsoon rainfall falls in the opposite direction to the Jabal chain towards the Arabian Sea and may not give a significant rain contribution to the Najd area except within the Jabal chain. This is because the rainfalls as a light shower or drizzle and not commonly associated with runoff. Moreover aquifer D starts from the Jabal in the south where monsoon rainfall occurs and collects an amount of water from the Khareef season. As a result, the Khareef contributes to Najd annually, however this amount is difficult to detect through water level monitoring wells at the north side.

CHAPTER 2

Studies indicate that rainfall is too small or the infiltration period is longer due to the rainfall intensity, in comparison with flood events.

Table 2.1 The meteorological data collected from Thumrait station during the period from 1986 to 2009

Year	Air temperature °C					Relative humidity %					Evaporation mm.month ⁻¹			Rainfall mm.yr ⁻¹	
	Mean	Mean	Mean	Extreme	Extreme	Mean	Mean	Mean	Extreme	Extreme	Mean	Extreme	Extreme	Total	Max
	Mean	Max	Min	Max	Min	Mean	Max	Min	Max	Min	Mean	Max	Min		24h
1986	25.7	33.4	19.1	43.9	4.4	47.8	70.7	25.0	98.0	2.0	15.5	21.7	10.1	30	18
1987	26.2	34.1	19.3	44.6	7.0	47.5	70.4	24.3	98.0	1.0	16.1	37.0	3.3	53	34
1988	26.3	34.3	19.1	44.4	4.0	46.7	70.0	23.4	100.0	3.0	15.1	29.6	2.0	43	43
1989	25.5	33.4	18.1	43.3	1.6	50.0	73.0	26.0	100.0	5.0	13.6	28.7	2.7	227	107
1990	26.6	34.5	19.6	46.0	6.8	51.0	75.0	26.0	100.0	4.0	13.2	33.5	1.4	6	2
1991	26.3	34.2	18.8	44.5	7.0	48.0	72.0	25.0	96.0	2.0	13.5	26.2	5.3	0	0
1992	26.0	33.6	18.7	44.3	3.6	48.0	72.0	24.0	99.0	4.0	14.2	28.5	1.1	132	101
1993	26.1	33.8	19.4	44.2	4.4	48.0	71.0	24.0	98.0	3.0	13.3	27.5	1.2	2	1
1994	26.7	34.5	19.8	44.8	7.0	44.0	68.0	21.0	95.0	2.0	13.8	28.0	5.0	14	1
1995	26.3	34.0	19.7	44.4	8.6	45.0	69.0	23.0	99.0	4.0	13.7	35.0	0.8	9	5
1996	25.3	32.8	19.5	42.4	7.1	50.0	72.0	28.0	99.0	4.0	12.7	25.8	0.3	33	12
1997	26.3	34.4	20.0	44.6	8.2	49.0	72.0	24.0	98.0	4.0	13.4	27.6	1.0	3	2
1998	26.5	34.2	20.6	45.5	5.4	49.0	71.0	27.0	99.0	5.0	12.9	26.4	3.5	0	0
1999	26.4	34.4	19.9	45.5	8.6	46.0	69.0	24.0	95.0	2.0	11.0	36.0	3.0	20	11
2000	26.1	34.4	19.6	45.1	8.6	46.7	68.1	24.5	98.0	4.0	11.5	34.0	4.1	0	0
2001	26.3	34.3	19.2	45.3	6.1	45.6	69.6	22.9	99.0	4.0	13.8	27.0	4.9	0	0
2002	26.0	33.9	19.8	43.5	6.8	49.1	71.4	26.5	99.0	5.0	13.6	27.4	3.8	24	23
2003	26.7	34.8	20.0	46.1	7.9	49.2	72.5	25.4	97.0	5.0	13.5	24.6	3.8	21	13
2004	26.6	34.0	20.1	45.3	6.0	43.3	66.0	21.5	97.0	4.0	13.5	28.3	3.2	10	6
2005	26.5	34.0	20.2	44.5	7.6	45.6	67.9	22.3	94.0	3.0	14.8	25.4	3.2	4	2
2006	26.5	34.1	20.3	45.1	7.0	45.7	69.1	21.9	95.0	5.0	11.5	22.0	4.7	0	0
2007	26.9	34.1	20.7	44.6	4.5	42.4	64.7	21.5	96.0	5.0	11.9	21.8	3.0	76	20
2008	25.7	33.3	19.2	45.8	3.8	40.0	61.0	20.0	93.0	4.0				7	3
2009	26.9	34.5	20.3	45.9	5.6	42.0	65.0	19.0	93.0	4.0				5	3
MIN	25.3	32.8	18.1	42.4	1.6	40.0	61.0	19.0	93.0	1.0	11.0	21.7	0.3	0	0
MAX	26.9	34.8	20.7	46.1	8.6	51.0	75.0	28.0	100.0	5.0	16.1	37.0	10.1	227	107
AVER	26.3	34.0	19.6	44.7	6.2	46.6	69.6	23.8	97.3	3.7	13.5	28.3	3.2	30	17
STDEV	0.4	0.5	0.6	0.9	1.9	2.8	3.1	2.2	2.2	1.2	1.3	4.4	2.1	52	29

Data Source Salalah Airport (Station Elev = 466.9 m.a.s.l)

2.5 Surface Water

2.5.1 Wadi flow

The Najd area is penetrated by several wadis running from south or southwest to north and northeast directions. From the dozens of wadis, only four of them are monitored

by the Ministry of Regional Municipalities and Water Resources (MRMWR) staff in Salalah since 1985. The wadis are in the following order from the west to the east: Gharah, Ghadun, Thahboon and Andhur (see chapter3, Figure 3.11). The total amount of water passing through these four wadis is 233.75 Mm³ with a general annual average of 10.2 Mm³ for the period from 1985 to 2008. The highest amount of water is recorded in the wadi Thahboon (115 Mm³) and the lowest in wadi Gharah (21.19 Mm³). This indicates that the amount of water from floods seems to be more in the east (Thahboon and Andhur) of Najd than in the west (Gharah and Ghadun). The highest amount of water was recorded in the year 2007 at the eastern wadis and at the same time the cyclone year could be detected as well from Figure 2.2.

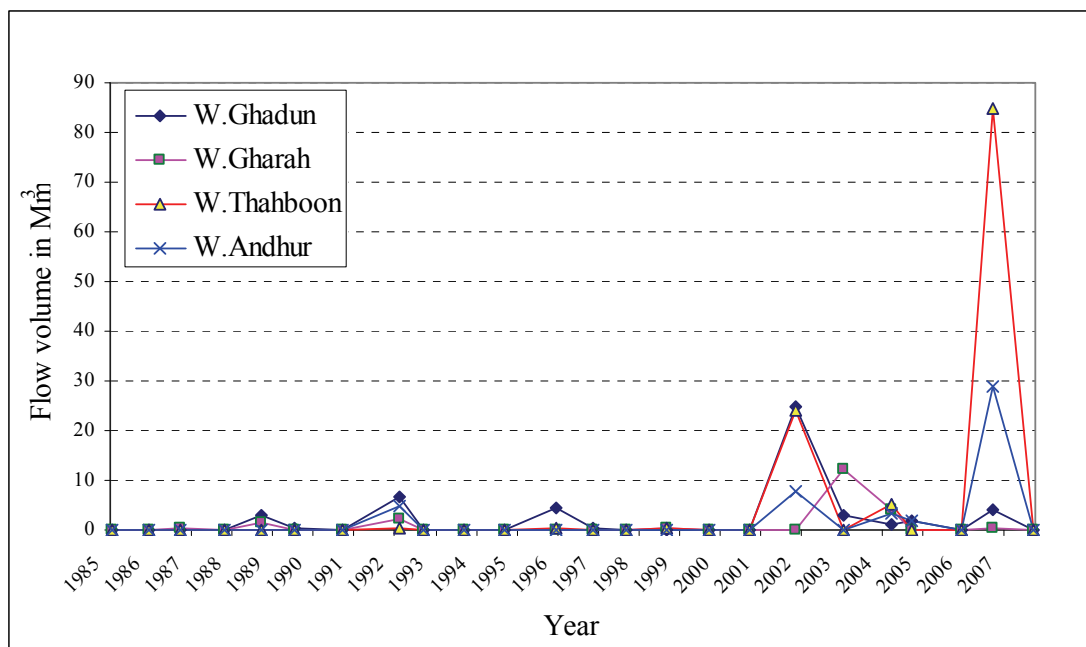


Figure 2.2 Comparison between different wadis flow in each year

The majority of cyclones occur in the months of May and June. These two months captured 73% of the total water flow amount of Najd since 1985; however the months of December and January were the lowest affected annually (Figure 2.3).

These wadis are affected by huge runoff's caused by cyclone events rather than monsoon rainfall. A Wadis flood can sometimes take several days of travel and pass more than 200 km before disappearing behind the sand dunes in the north; this depends on the amount and intensity of the rainfall on the recharge area (Jabal). A particular event occurred in 2004 when a tropical storm started on the 30th September

and continued to October 1, 2004. The tropical storm started in the south (Jabal chain), even though no rain appeared in the whole Najd. The flood reached the village of Qitbit on Sunday morning at 6 am, 3rd of October 2004, and continued to flow toward the sand dunes in the north until the next day. This flood created a lagoon more than 1 km wide near Kadhrat Qitbit, 55 km south of the Qitbit village. The two stations of Thahboon and Andhur which are located in this direction, together recorded a total volume 11.4 Mm³ of water, and 96% of this flood amount was generated on the first day.

In general most cyclones result in large runoffs reaching the sand dunes because the wadis are connected together about 100 km and compile into one predominant wadi. Consequently, these large floods can reach the edge of the Rub Al Khali sand dunes. Moreover, there are a lot of wadis such as Aydim affected by cyclone events and flooded to Najd, which are unfortunately not covered by monitoring gauges. The actual amount of runoff to Najd still remains uncertain.

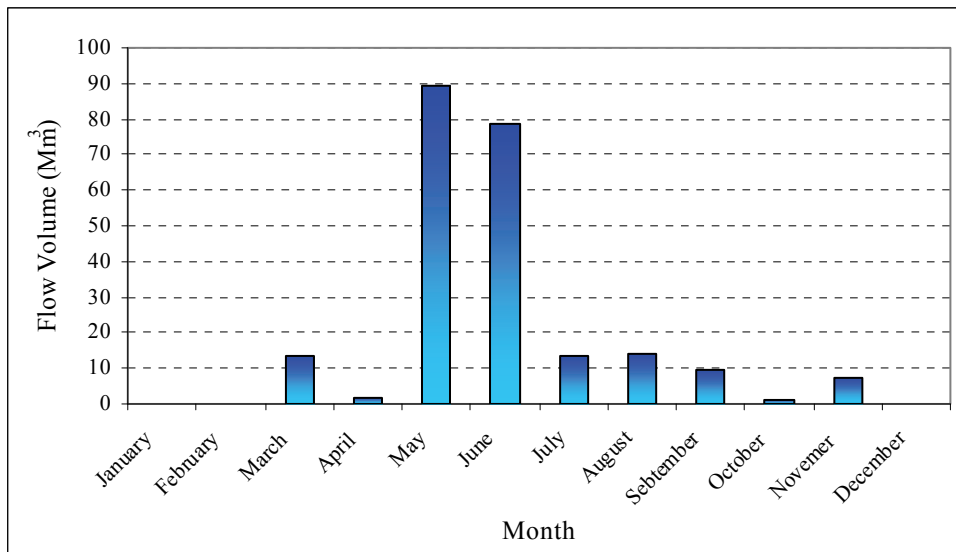


Figure 2.3 Total monthly cumulative flows from four wadi Gauges (1985-2008)

2.6 Geological Structure and Units Classifications

The Study Area is affected by several faults varying in length and generally laying in a south to northeastly direction. Additional faults observed from seismic surveys and conducted in the Study Area in 2009 by a number of oil companies (Figure 2.4). This

survey gives the picture of the geological structure in Najd, in particular, around Helat Ar Rakah and Hanfeet. At the same time, data collected from more than 120 boreholes were used for formation thickness calculations and to create contour maps for the base of upper UER (Figure 2.5).

2.6.1 Geological structure

In general, there are layers which dip from south to north in the east part, and from southwest to northeast in the west of the Study Area near Yemen's international border. The average hydraulic gradient is assumed by PAWR (1986) to be 0.002 and following the flow direction south to north or south to northeast. Furthermore, the hydraulic gradient calculated by GRC (2005a) for the base of the Rus and the U.UER was found to be 0.00198 m m^{-1} and 0.00269 m m^{-1} respectively.

The interpretation of the structure of the Najd area is complicated due to a large surface area which has not been properly covered by research and additionally, due to the distance between existing boreholes. Sharing data with oil companies working in Najd is further complicated due to the countries restriction rules. According to previous information, different studies have been conducted by several ministries. The latest project in Hanfeet and the north side of the Jabal exploration wells, lead us to assume that the Najd area is affected by two major faults. The actual direction of these faults is not clear, however, the first one passes through the middle of the Hanfeet well field between boreholes HAD-33, HAD-34, HAD-43 and HAD-44 (GRC, 2005a). This fault has contributed to different water level heads between the east and west part of the well field. It strikes clearly from south to north or south to northeast. The other significant fault is assumed to start from the Jabal foot (north side) at about 30 km east of Thumrait from south to north or to north east, and extends to wadis Qitbit. These two major faults form a Graben structure between them, and lift up at both sides (thrust faults).

Recently, two oil companies conducted seismic surveys by running several profiles. The first survey started between Thumrait and Shsir and followed south to northeast from Thumrait-Al Mazyunah to north east of Helat Ar Rakah at UTM Easting coordinate 210000 with a total length about 50-60 km. These profiles recorded data

below a depth of 260 m in the L.UER formation to Cretaceous formations. Several faults have been detected yet they are scattered, and do not form as big a fault as expected. In general, most of these faults are parallel and have the direction of south to north or northeast. The Hanfeet well field is affected by two of them: one crossing the well field, and the second hitting south of the well field.

The second survey is located on the east side and starts near Thahboon village at about 10 km north of DEP-5. The survey runs for about 60 km to the east and 90 km to the north. One major fault and several smaller to medium sized faults have been detected in this survey. The fault crosses three wadis and runs towards the northeast direction for about 60 km. However, the other faults (5) have various lengths ranging between 3 and 15 km in different directions.

From these seismic surveys, previous thoughts about two major faults may be not justified because the survey does not show any major fault on the western side between the Hanfeet well field and Helat Ar Rakah. More than 16 faults exist, with an approximate direction from south to north, however no major fault appeared. On the east side, one major fault is known, but its direction is southwest to northeast. This fault which was detected by an oil company in 2009 near Thahboon (north DEP-5) supports the previous idea about the eastern major fault. In addition, the general trends of faults or lineaments in the Najd take a direction of west to east or southwest to northeast. The faults' lengths are usually less than 40 km and are expected to extend for more than 100 km (NWAA, 2000a).

The lineament (surface features), mentioned by WAA (2005b), in Wadi Qitbit and its extension to the village of Qitbit to the north, lies under the Rub Al Khali sand dunes. GRC (2008) assumed an extension up to the WWD-34 location. At this time the key concern was to find a connection between the Jabal chain in the south and the confined layers southwest of Qitbit at WWD-24, which has better water quality than other locations. Compiling both hypotheses of fault structures and the occurrence of a lineament in the Najd area (Figure 2.4), it seems possible to have a connection from the recharge area near the borehole Lop Fr (103/372) through Thumrait (MOD-15), east of Hanfeet (332/014) and to northeast towards the area southwest of Qitbit (WWD-24).

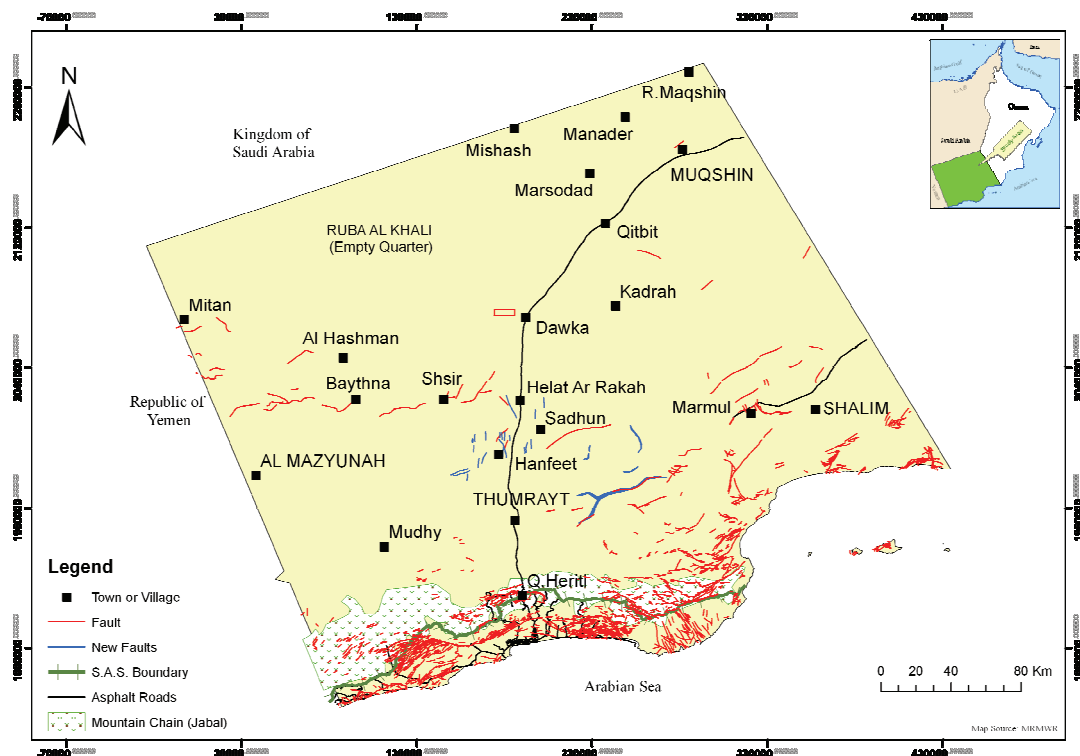


Figure 2.4 Distribution of faults in the Study Area

The wells most recently drilled were parallel to the border of the Republic of Yemen - in Tosnat and south and north of Al Mazyunah – and show that the base of the Rus formation is found at a depth of 60m in the south, and at 81m in the north sector at roughly 12 km behind the main road to Mitan. This is in spite of the Damman outcrops which exist in the north. The data reveals that the depth of the UER is very thin and tends to dip north or northeast after Al Mazyunah (GRC, 2005a). Two hydrogeological cross sections have been conducted in the Study Area in directions S-N (A-A) and W-E (B-B) as they printed on Figure 2.5; refer to chapter 3 for further details (see Figure 3.1).

2.6.2 Geological unit's classifications

The Study Area consists of recent Alluvium and two geological units called the Fars Group and the Hadhramaut Group (MMI, 1991; Roger et al, 1992), as they are shown on the geological map of Dhofar Governorate (Figure 2.5). These two groups of tertiary age formed the geology of Najd; however the Hadhramaut Group distribution

dominates. Each Group Formation and hydrogeological characteristics are summarised in Table 2.2.

2.6.3 Recent alluvium

Alluvium thickness is in the range of zero to 4 m over the Study Area. These materials, which belong to the Quaternary age, are composed of Aeolian sand and often, boulders. The Alluvium deposits may be found more in the wadi channels with a thickness of 15-30 m. Consequently, alluvium deposits are not considered as an aquifer in Najd.

2.6.4 Fars Group

The Fars group of Tertiary age (Oligocene to Miocene) outcrops began in the central and north of the Study Area. The thickness increases towards the north and reaches its' pinnacle near the international border of Saudi Arabia. This variable thickness ranges from several meters in central and northeast Najd near borehole WWD-36 (5m) to 78m North al Hashman at borehole WWD-12. Recently (GRC 2005a) and the Ministry of Petroleum and Minerals (MPM) classified four members in the Fars Group in the Najd: Marsawdad, Shsir, Montasar and Dawkah (Table 2.2), as the following description:

- Marsawdad Formation: This sequence comprises of inter-bedded reddish to yellowish siltstone and grey silty limestone.
- Shsir Formation: This sequence comprises of reddish conglomerates, siltstones and limestone.
- Montasar Formation: This sequence comprises of grey to white micritic limestone, and in places brecciated limestone.
- Dawkah Formation: This sequence comprises of brecciated lacrustine limestone.

2.6.5 Hadhramaut Group

The Hadhramaut Group of the Tertiary age is found over large areas over the south and east of the Arabian Peninsula. The formations which make up this group were first described in Saudi Arabia by Powers et al. (1966). It was Roger et al. (1992) which described the Hadhramaut Group in the geological study of the Dhofar Region, including the Najd area. All the group formations in the Study Area form the target area for groundwater. These formations are in order from top to bottom, as following (Table2.2):

- Dammam: Middle Eocene to, possibly, Lower Eocene.
- Rus: Lower Eocene.
- Umm Er Radhuma (UER): Lower Eocene to Palaeocene.

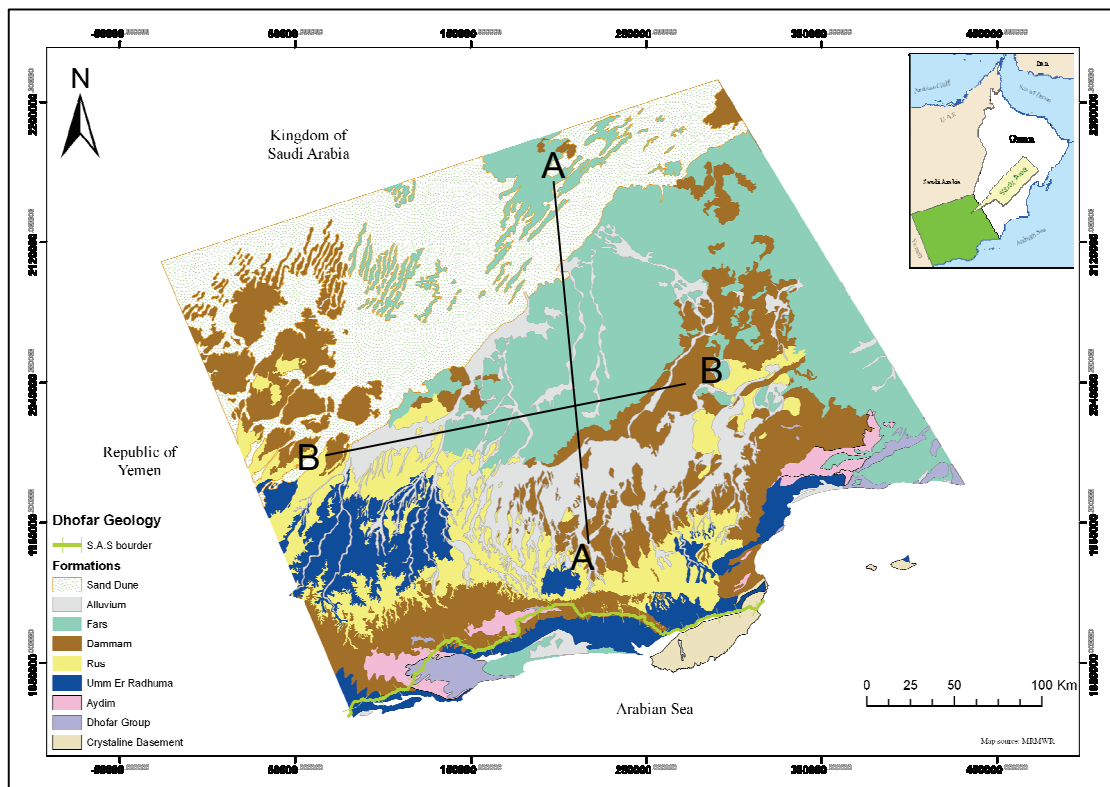


Figure 2.5 Simplified geological map of the Study Area and cross sections locations

The depth of the formations have been discussed in studies done by the Council for the Conservation of Environment and Water Resources (PAWR, 1986), Geo-Resources Consultancy (GRC, 2005a, stated thicknesses of Dammam (10-100m), Rus

(30-254m), UER (U.UER 50–300m, and L.UER; 250-300m). However, often these results are restricted to specific portions of Najd because of such drilling projects carried out at particular sites.

Therefore, this study attempts to compile old data records with recent ones in order to ascertain a reasonable thickness of these formations. As result of data collected from more than 120 boreholes (except 11 boreholes from L.UER) distributed in Najd, a more differentiated estimation can be given with an average data of 22m, 113m, 100m and 291m for Dammam, Rus, U.UER and L.UER respectively (Table 2.2). Also, minimum and maximum amounts range between 4-51m, 9-229m, 27-260m and 199-349m respectively. Many boreholes drilled to L.UER, however, only had a small number of crossed the base to Shammar Shale. Only 11 boreholes were involved in this data collection for L.UER.

2.6.5.1 The Dammam Formation

The Dammam formation (in the Middle Eocene) underlies the Fars Group. The formation was characterized for the first time near the city of Dammam in Saudi Arabia. The formation thins out or discontinues in the south and west of the Study Area because of erosion processes; the formation becomes exposed on the surface. However, the formation sediments increase when it is overlaid by other deposits such as the Fars Group. The Dammam sediments were recorded in many boreholes, but unfortunately many of them are not specified with the exact thickness, otherwise they only account for it with the Fars Group, due to uncertainty and mixing. It is only 123 boreholes that were accounted for in order to calculate the thickness of the Dammam sediments. The thickness of these sediments ranges between 4m at DEP-14 and 51m in borehole WWD-26 near Qitbit with an average of 22m. The formation becomes thicker in the area between WWD-26, WWD-25 and WWD-32, and narrow in the west of the Study Area.

The formation compressed with thin, massive bedded nodular limestone with marl and yellow to orange shale with marl and limestone (Table 2.2). Fossils like *Nummulites beaumonti* were recorded at boreholes WWD-12, WWD-22, WWD-29 and WWD-31. This fossil, in addition to the lithological description such as blue-

grey, brown shales, yellow earthy marls and impure limestone (e.g. WWD-29) are used to differentiate the Dammam from its adjacent formations.

The Dammam Formation is divided into three members: Uyun, Qara and Andhur (Roger et al., 1992). The lithologic characteristics of these members are as follows:

Uyun Member. This comprises of a thin-bedded, nodular, grey to pink bioclastic limestone with large molluscs

Qara Member. This comprises of a massive-bedded, nodular, white bioclastic limestone with large molluscs.

Andhur Member. This comprises of yellowish shale with of white to yellowish bioclastic limestone, green marl with oyster at the base.

Table 2.2 Summary of the hydrogeological units in the Study Area (after GRC, 2008)

Age	Group	Formation	Aquifer	Thickness range, Average (m): [n=data]	Lithological description		
unconformity							
Cenozoic	Tertiary	Oligocene to Miocene	Fars	Marcawdad	A	Interbedded reddish to yellowish siltstone and grey silty limestone	
				Shir		Reddish conglomerates, siltstones and limestone.	
				Montasar		Grey to white micritic limestone, and places of brecciated limestone.	
				Dawqah		Brecciated and lacustrine limestone.	
	~Pre-Neogene Unconformity~						
		Eocene	Hadhramaut	Dammam	4 - 51 22 123	Massive and thin bedded nodular limestone with marl, yellow to orange shale with marl and limestone.	
				Rus	9 - 229 113 143	Breccia, chalky dolomite, marl and laminated gypsum.	
				Upper UER	B	27 - 260 100 120	Grey to brown dolomitic limestone, very weak white and brown biomicrite and blue-grey shale. Brown granulated and fossiliferous limestone at base.
		Paleocene		Lower UER	C&D	199 - 349 291 11	Moderately weak olive, sparry limestone interbedded with brown fossiliferous limestone.
				Shammur Shale		?	Grey brown, dark grey limestone and blue shale. Green mudstone interbeds.
unconformity							
Mesozoic							

2.6.5.2 The Rus Formation

The Rus Formation (Lower Eocene) underlies the Dammam where it exists in the Study Area. Its thickness varies between 9m at borehole DEP-10 near the southwest of the Study Area and 229 m in borehole WWD-7 in Ramlat Mitan near the Saudi Arabia's border, at an average of 113m. The Rus outcrops are visible near the main road of Salalah-Thumrait between Hareet, near the Jabal and Thumrait City. The formation consists lithologically of a white, creamy-brown limestone. Yellow-brown marl limestone inter-bedded with gypsiferous units and classified to two members as it stands below (MMI, 1991):

Upper member (Gahit). This comprises of white, cream to brown or spotted limestone with some yellow fragmented limestone and yellowish brown marl.

Lower member (Aybut). The lithology of the lower part of the Rus is similar to the upper member but contains massive crystalline gypsum and occasionally thin beds of dolomite and chalk. Cavities are common in this subdivision of the Rus.

The Upper and Lower members characteristic of the Rus formation seem to be similar in the Study Area. This is because of the weak light coloured dolomitic limestone, inter-bedded with grey marl and gypsum (e.g. WWD-22, WWD-6, WWD-8) (GRC. 2005a).

Even though fossils are acknowledged in previous studies, during most recent projects, it is claimed that fossils have never been in this formation. From the formation we can be recognize its typical lithology and the appearance of upper UER containing an index fossil. The formation is of vital importance for industrial use because it provides a good amount of gypsum. At the Rawya village which is located 18 km south of Thumrait, a gypsum mine produces raw material from the Rus hills from several years ago, and still running up to date.

2.6.5.3 The Umm Er Radhuma Formation (UER)

The Umm Er Radhuma Formation (UER) (Lower Eocene to Palaeocene) of the Tertiary age exists along the whole Study Area. It contains abundant marine fossils of

Lower Eocene to Palaeocene age, and is broken down into either two (upper and lower UER) or three (upper, middle and lower UER) units. Previous thoughts about the formation thickness are between 450 m to 600 m, which decreases northward to become less than 100 m near the border of Saudi Arabia (PAWR 1986). However, Sharaf (2001) mentioned the thickness of UER in the east of Saudi Arabia being 243m. By referring to recent data obtained from MRMWR projects after 2003, the thickness of UER varies from 226 m to 609m with an average of 390m. Furthermore, the formation thickness was recorded at 380 m in the northeast corner of the Study Area at WWD-37, in Ramlat Maqshan. In the south east of Najd, about 40 km east of Thumrait and north of the main road to Marmul, it's thickness about 348 m at DEP-3.

The UER formation is mainly classified in two parts, the Upper and the Lower, and sometimes also divided in three parts (Upper, Middle and Lower) based on the formation age (Powers et al. 1966, D. Parker 1985). During several drilling projects conducted in Najd by PAWR and MRMWR, the UER was classified to upper and lower parts based on an index of microfossils and lithology. However, these tools are unsuccessful in identifying the difference between M.UER and L.UER. Consequently, this type of microfossil could be the best for identification of upper and lower UER in comparison with other tools.

The lithology and foraminifera of the Upper- and Lower-UER formations in the Najd are characterised as follows:

Upper UER Formation (U.UER): Based on the data collected from 120 boreholes, results show the thickness of U.UER is in the range between 27m at DEP-8 to 260m at borehole DEP-3 and the average is 100m. Typically, the top of the U.UER is placed into contact between the weak, light coloured dolomitic limestone above and the generally stronger grey to brown dolomitic limestone below (GRC, 2005a). The U.UER formation is detected by the first occurrence of the foraminifera *Sakesari cotteri* and *Nummulities deserti* appearing at the top of this formation. Further down, the sequence consists of dolomitic limestones, brown biomicrite, brown micritic limestone and finally a bluish grey shale and marl. Below the shales and marl, near the base of U.UER, brown, crystalline, granular and highly fossiliferous dolomite limestones usually occur.

The U.UER dips towards the north and northeast (Figure 2.6). Data obtained from 67 boreholes located between the top of the Jabal in south and the rest of Najd area show dipping in the base of U.UER from around 540 m above sea level to -300 m below sea level near the border of Saudi Arabia which follows the flow direction.

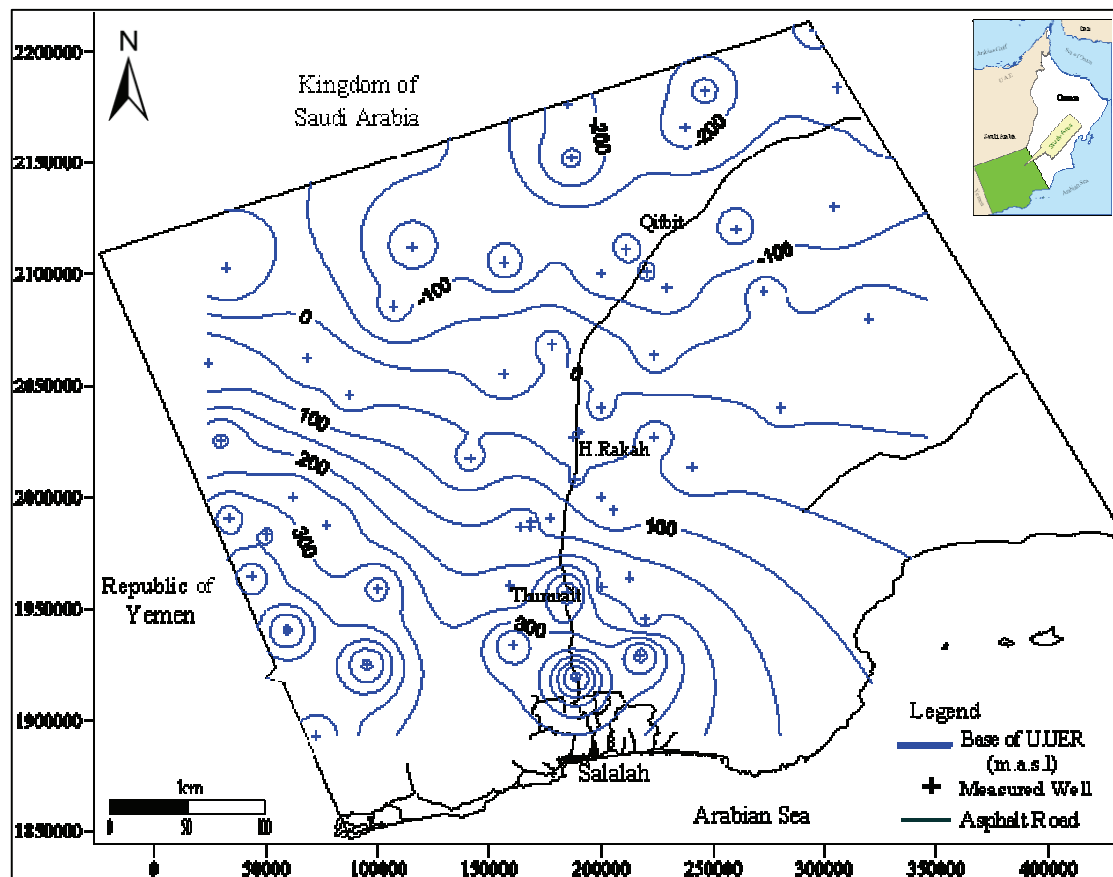


Figure 2.6 Isopleths for the base of the upper UER in Najd area

Lower UER Formation (L.UER): The thickness of this part ranges from about 199m at borehole AFAR-1 (BE428528AA) to 349m at WWD-14 near Saudi Arabia border with an average of 291m. The top of this formation can be detected by the first appearance of Palaeocene index microfossils. These fossils such as *Sakesaria dukhani* and *Dictyokathina simplex* are available in almost all boreholes of the Study Area and are easily identified. The other microfossils: *Kathina major* and *Lockhartia diversa* were recorded in boreholes that negate this formation. In addition, the lithology of the top of the L.UER was fairly distinct from the U.UER in western Najd particularly around WWD-6, WWD-8 and WWD-11. It is characterised by a moderately weak

olive limestone interbedded with faint brown fossiliferous limestones. Further down at L.UER the sequences of grey micritic limestone, thin sequences of shales, and dark grey and black moderately strong crystalline dolomite are common. This lithologic description of the L.UER is recognisably similar to that given by MMI (1991) for southern Oman. In central and eastern Najd lithological is distinguished between U.UER and L.UER is not yet available. Thus, the index fossils are the best parameter for this determination. L.UER sediments were compressed with weak brown fossiliferous limestones occurring across the contact with the boreholes WWD-22, WWD-25, WWD-32.

2.6.6 Shammar Shale

Shammar Shale underlies the UER formation and is described as a part of the Cretaceous formation (MMI, 1991). The Ministry of Water Resources (MWR) in 1993 declared that this was the age of Shammar Shale to the Cretaceous. Shammar Shale is comprised of black shale and greyish brown dark grey limestone, with green mudstone inter-beds. Several boreholes penetrate the Lower UER to the Shammar Shale. The maximum thickness of this layer is 12m at WWD-37. The lithology of these boreholes consists of a massive sequence of dark grey and black shales interbedded with dark grey and light brown L.UER limestones. GRC (2005a) proposed this description which suggests a match with the Shammar Shale age mentioned in 1991 by MMI. The Shammar Shale is described as bedrock in relation to the main aquifers, and functions as an impermeable layer in Najd.

2.7 Conclusion

Overall, the Najd area is affected by faults with lengths less than 60 km, and probably stills more which are not yet determined. The graben at the Hanfeet area does not exist. Based on, the recent siesmic survey having been done by oil companies a couple of years ago and represented in this chapter. However the area is influenced by several faults, which take the general direction southwest to northeast. The layers thicknesses are increased to north or northeast direction. However, these layers are thinning to the west of the Study Area near the border of the Republic of Yemen, and increase towards north and northeast.

AQUIFER PROPERTIES AND DEVELOPMENT OF GROUNDWATER LEVELS

This chapter discusses the aquifer systems in the Study Area which appear to be controlled by geological structures. The structures have a high altitude, and the aquifers characteristics development is mainly represented by aquifer D as the dominant aquifer in the Jabal chain and the nearby north side. However, the other aquifers such as A to C were often dry in that area. Therefore the recharge processes may occur among aquifer D then passes to the above aquifers C to A. The majority of the recharge to the Najd aquifers is related to cyclone events; even contribution from monsoons can be expected. Two simplified hydrogeological cross sections have been constructed along the Study Area from south to north and west to east directions. Water level data was used to represent the abstraction effect and to create contour maps for determining the groundwater flow direction. In addition, the floods were compared with a few monitoring wells from different aquifers; consequently groundwater recharge and traveling time was calculated between the occurrence date and borehole response.

3.1 Description of Hydrogeological Units

The alluvial deposit in the Study Area is very thin and is usually 0-4 m except in some main wadi deposits. These deposits are always dry and are not accounted for as an aquifer. Therefore it can be ignored for the purposes of groundwater exploration.

Two main groups located in the Study Area are the Fars Group and the Hadhramaut Group. The Fars sediments are found in central, north and northeast of the Study Area through the Dawkah and Shsir formations. The sequence thicknesses vary from 10 m in the central Najd at the MRMWR branch in borehole 103/395 (H.R.C) to 78 m in WWD-12 in the north. Nevertheless several experimental drillings conducted in the area did not detect water in the sediments. Consequently, the Fars Group is not a significant unit for water resources in the Najd area. It appears to be significant on the opposite side of the Study Area towards the Arabian Sea.

The Hadhramaut Group carbonates are distributed in the Najd area with a maximum depth of about 890 m. It dips gently to the north-east direction of the Study Area. The Hadhramaut Group sediments consist of sequences including three formations starting with the Dammam at the top and ending with Umm Er Radhuma (UER) above the Shammar Shale. The base of UER can be detected by the presence of Shammar Shale, posing as an aquiclude between the Tertiary and underlying Cretaceous units (MWR, 2000a). The formations of Dammam, Rus and UER are distributed in all of Najd, however the Dammam is a significant factor for groundwater in the Jabal chain, at the south edge of the Study Area. The most extensive aquifers occur within the Rus and UER formations.

3.2 Aquifers Characteristics

The Study Area consists of four layers which are identified as aquifers after (Hydrotechnica, 1985) from the top (A) to the bottom (D) (see chapter 2, Table 2.2) as follows:

- Aquifer A located in the Dammam and Rus formations is unconfined to semi-confined.
- Aquifer B is a confined aquifer located in the U.UER.
- Aquifer C is a confined aquifer located in the upper part of the L.UER .
- Aquifer D is a confined aquifer located in the lower part of the L.UER.

These aquifers appear through a series of fractures and fissures rather than karst, excepting aquifer C which is found with karst (GRC, 2008). However, they separate each other by thin layers of shale, with a thickness often less than 3m. In 2008 GRC measured the porosity in these formations by using specific yield to be (0.7% to 5.9%). These values compare with estimates of 0.5% by JICA (1989) around Helat Ar Rakah and values between 0.4 to 10% estimated by MWR (1993) in other parts of the Najd.

To illustrate the aquifer sequence, two hydrogeological cross sections have been created in the Study Area directing from south to north (A-A), and west to east (B-B) (Figure 3.1). These cross sections extend through a distance of more than 230 km and pass among small deposits of the Alluvium and Fars Group which are too small to be represented. As a result of the deposits such as Alluvium and the Fars Group, they could appear on the geological map, however at times are not detected from cross sections.

The cross section A-A is constructed from boreholes located in aquifer C and D. This line shows the dipping of all layers northward and the appearance of the Fars Group north of borehole W.Bharna1 (001/280). The piezometric surface of the water level could be detected above the ground level surface (artesian) and between boreholes W.Bharna1 and Bin Kh (BF080077AA). The expected faults are highlighted in the cross section, especially between DEP-5 and DEP-3, and between Bin Kh and WWD-25.

The second cross section (B-B) is conducted through the middle of Najd using boreholes located in aquifers B, C and D. It starts from the west near the border of the Republic of Yemen to borehole Ranada1 in the northeast of Marmul. It includes borehole WSW-3 at Marmul Rahab Farm located 50 km south of the line (B-B). It was drilled to the end of L.UER and passes to the Shammar Shale (below the base of LUER).

The cross section shows that the U.UER and Rus formations are very thin in the west and increase towards the east, particularly after Shsir area (Ubar Fm). However, the thickness of L.UER decreases towards the east.

3.2.1 Aquifer A

Aquifer A is occupied in the Dammam and Rus formations and from additional sediments above. The lithological composition of interbedded thin layers of chalk and marl beds are in addition to the relative thickness reducing the aquifer's potential. In Najd this aquifer is found nearly within Rus formation with high discharge of more than Dammam, despite them being accounted for as one aquifer. Aquifer A has been

suggested unconfined to semi-confined and the water that exists in the upper zone of the Rus where gypsum horizons are present (PAWR, 1986).

The aquifer is restricted in the Rus formation, and if it exists has a general EC between $909 \mu\text{S.cm}^{-1}$ (SHTH spring) in the recharge area and $9880 \mu\text{S.cm}^{-1}$ in the north east of the Study Area at WWD-30. With an exception in the north east corner with $15000 \mu\text{S.cm}^{-1}$ recorded during the borehole WWD-36 drilling.

Aquifer A is significant between Shsir, Hanfeet and Helat Ar Rakah (MWR, 1995a). Moreover, data obtained from MWR drilling reports in the period from 1992 to 1995, north of the above mentioned locations, highlight aquifer A in Wadi Bin Khawtar as a significant aquifer at BG117784AA [KhT-A] in surrounding area. Further drilling was carried out by MRMWR in 2004 and also confirms the importance of aquifer A at WWD-24 and the surrounding area. In this specific area, the aquifer has the potential to produce a good amount of water of good quality. The maximum yield was recorded at 48 L.sec^{-1} and the minimum at 14.7 L.sec^{-1} . The quality of water was found in the range of $1603 \mu\text{S.cm}^{-1}$ to $2060 \mu\text{S.cm}^{-1}$ in EC, and 1.23 mg.L^{-1} , 1.7 mg.L^{-1} in fluoride concentrations.

These wells may have the best water quality in aquifer A, compared to the whole of the Najd. Consequently, aquifer A has the potential to yield considerable amounts of water to the Wadi Bin Khawtar area. The absence of gypsiferous layers in this area could be the main reason for the waters good quality (GRC, 2005a). The summary of hydraulic characteristics from the Najd aquifers (saturation zone) can be detected from Table 3.1. It becomes more active, when overflowing artesian conditions are evident. Therefore data interpretation should take into account the possible influence of artesian wells in the case of them not being properly cased or cemented. This evidence draws the attention of expected accelerating seepage to aquifer A from beneath the artesian aquifer. Therefore, the presence of shallow groundwater at a depth of less than 10m in the north portion of the artesian zone from WWD-45 to WWD-36 of the Study Area is probably due to the seepage from beneath the aquifers' acting as Sabkha system. The water quality in that portion is common with high mineralization, ranging from $10000 \mu\text{S.cm}^{-1}$ to $15000 \mu\text{S.cm}^{-1}$ and increasing from west to east ward.

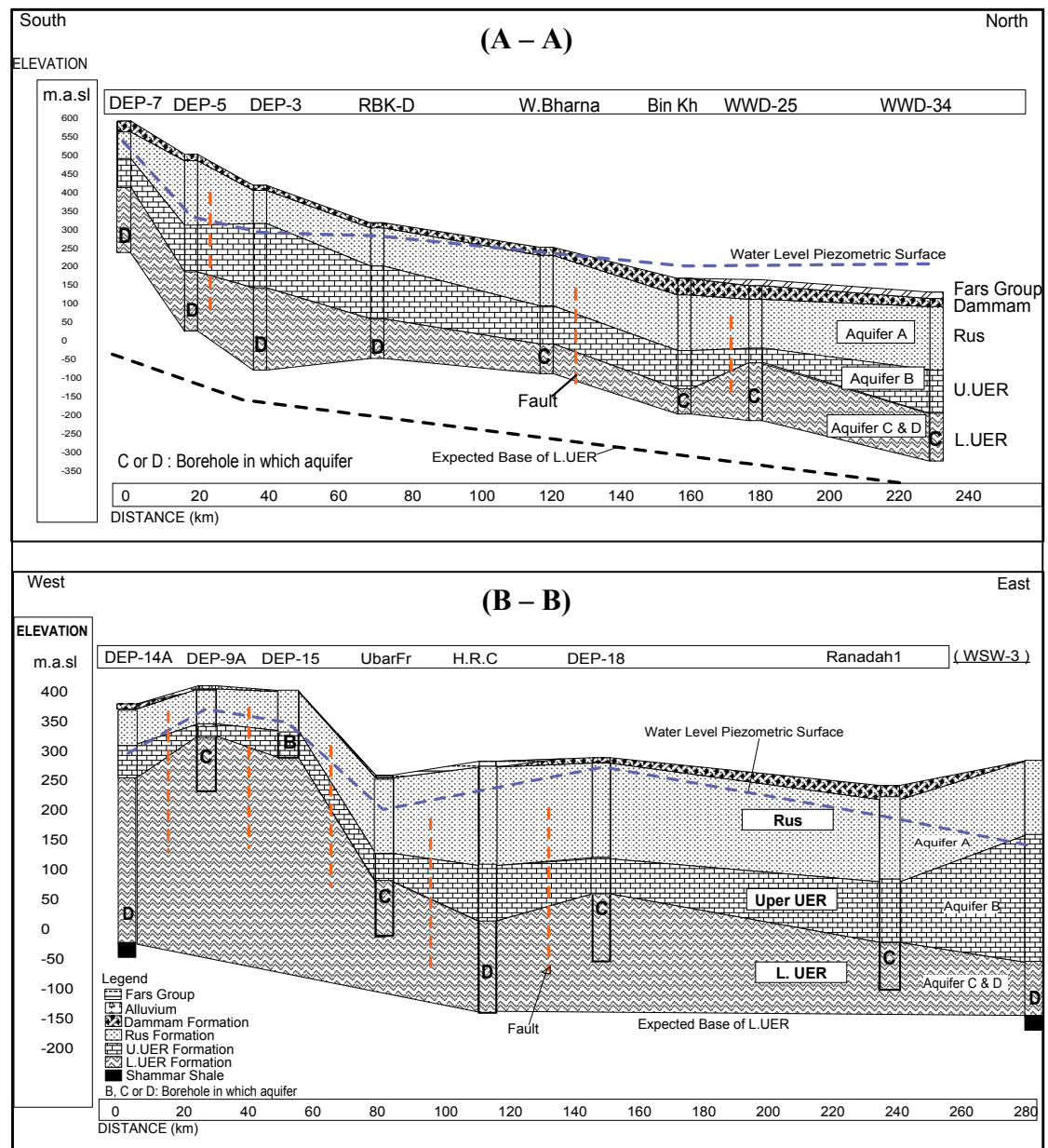


Figure 3.1 Schematic South-North (A-A) and West-East (B-B) hydro-geological cross sections along the Study Area (see Figure 2.5, directions)

3.2.2 Aquifer B

Aquifer B is located at the upper part of UER (U.UER). It is confined (CCEWR, 1986b) and extends in the west and central Najd. Several previous studies conducted in Najd such as MMI (1991, 1994) and MWR (2000a) suggest that aquifer B is

significant in all of Najd. This was based on the historic scattered drilling information by MWR in the period from 1992 to 1995. 17 monitoring wells were drilled down to aquifer B in central and east Najd. These boreholes yield a range between zero to 48 l sec⁻¹, and among 13 of them with <5 L.sec⁻¹. The remaining 4 boreholes have a good yield, but bad quality with higher mineralisation associated with EC of 5000 µS.cm⁻¹.

On the other hand, more than 15 boreholes drilled in aquifer B in the south and east of the Study Area, by different authorities since 1970s or 1980s, although most of them seem to be incorrectly ordered to aquifer B. They were drilled by private companies or Petroleum Development Oman (PDO) for water supplies, road constructions and oil exploration purposes and not supervised by water resources authorities sector at that time.

After 2003 the MRMWR conducted several projects in central and west Najd, covering most of the Study Area except the south east portion. Data revealed that the saturation zone of aquifer B was between 1m to 43m and averaged 15m (Table 3.1). It's dipping was similar with the groundwater flow direction from north and northeast and usually had one water strike.

The yield recorded during drilling among the v-notch ranged from zero to 140 L.sec⁻¹. Boreholes located east of Mazyunah (DEP-9, DEP-15) have the highest yield, however the yield decreases in either a north or east direction with a yield of <3 L.sec⁻¹ in the sand dune portion, and <5 L.sec⁻¹ east of Helat Ar Rakah, respectively. Aquifer B can be detected at or above UTM WGS84 with nothing (1978362 N) around the borehole DEP-17, south of this coordinate (<5 km) where it may be possible to hit. The aquifer pressure increases with the groundwater flow direction. As a result the artesian condition seems to develop due to layers dipping. Consequently, an overflow exists at WWD-19, WWD-5 and WWD-13 located in Shsir, north Mitan and Al Hashman, respectively. The other aquifer characteristics are summarised in Table 3.1.

This aquifer is significant in the east of Al Mazyunah and around Shsir, but is of minor significance in the area between West Hanfeet and Helat Ar Rakah; and the sand dunes portion.

Table 3.1: A summary of hydraulic characteristics from the Najd aquifers (saturation zone) (modeled after GRC, 2008)

Aquifer		Thickness (m)	discharge (L.s ⁻¹)	T (m ² .d ⁻¹)	Storage- coefficient	Formation
A	<i>Count</i>	45	40	485	3.2 x 10⁻⁶	Above UER (Rus & Dammam...act)
	Min	1	0.75			
	Max	112	201			
	Mean	32	24			
B	<i>Count</i>	38	33	680	1 x 10⁻⁶	Upper UER
	Min	1	0.2			
	Max	43	140			
	Mean	15	16.6			
C	<i>Count</i>	89	89	556	1.5 x 10⁻⁴	Upper of L.UER (or Middle)
	Min	1	0.6			
	Max	69	138			
	Mean	28	48			
D	<i>Count</i>	13	20	13	-	Lower of L.UER
	Min	133	2			
	Max	351	43			
	Mean	79	18			

3.2.3 Aquifer C

Aquifer C is found in the upper part of the lower or middle UER formation and extends to cover almost all of the Najd area. This aquifer is confined (CCEWR, 1986b) and partially artesian. The artesian pressure zone increases towards the north and north east generally within the groundwater flow direction. Two or three water strikes are expected when drilling into this aquifer. This water strike can be found at few meters (7-8m) from the upper of L.UER in the west of Najd, and can reach a maximum depth of 70m in east of Najd near Qitbit (MWR, 2000a).

Although it was historically thought that aquifer C covered all the Najd area, but recent projects do not support this idea. Several boreholes (DEP-10, DEP-6, LobFr (103/372), DEP-5 and DEP-7) were drilled in parallel at the south side of the Study

Area and did not detect aquifer C, except seepage in DEP-7 ($<1 \text{ L}\cdot\text{sec}^{-1}$). Thus, aquifer C can be expected to be more north than initially assumed. It is located north of the UTM WGS84 (1959600 N) and covers the entire Najd area. Further south the aquifer is dry along the parallel portion with the Jabal chain except the southeast edge which is still unknown (GRC, 2008). The aquifer dips with the groundwater flow direction. Therefore, the top of aquifer C is reached when drilling is required to a depth of 100 m in the west near DEP-14A, to 237m in Hanfeet well field near HAD-49, and 393m in the north portion at WWD-12.

The aquifer thickness mentioned in this text refers to the saturated zone which is detected with water and when there is no more increase in discharge or change in EC. In aquifer C this zone ranges between 1 m to 69 m with an average of 28m. The maximum yield recorded in aquifer C through the drilling of 88 boreholes was $138 \text{ L}\cdot\text{sec}^{-1}$ in northeast of the Study Area at borehole WWD-32, however the minimum was $5.5 \text{ L}\cdot\text{sec}^{-1}$ recorded in borehole DEP-12 with a general mean of $48 \text{ L}\cdot\text{sec}^{-1}$. These two boreholes WWD-32 are located in the northeast of Study Area and DEP-12 is restricted to the border of Yemen at 15 km north of Mazyunah. The groundwater flow direction in aquifer C is similar to aquifer B southwest to northeast direction. The transmissivity of aquifer C was obtained from previous studies to be in the range $166\text{-}380 \text{ m}^2\cdot\text{day}^{-1}$ (MWR, 1994d, 1995a) in Helat Ar Rakah. However, the average transmissivity for aquifer C is $556\text{m}^2\cdot\text{day}^{-1}$ based on the recent data and storage coefficient of 1.5×10^{-4} (Table 3.1).

The cross section A-A (Figure 3.1) show that the piezometric surface water level starts as an artesian north of Dawkah and before borehole Bin Kh (BF080077AA). This is due to the pressure zone which increases from the south to the north/northeast, generally along the direction of the water flow. The pressure in this zone has been decreasing gradually during last two decays and tends to move north or north eastwards. For instance, borehole W.Baharna (001/280) is located 15 km northeast of MRMWR branch in Helat Ar Rakah the water level dropped from $-3.6(\text{m}\cdot\text{a}\cdot\text{g}\cdot\text{l})$ in July1993 to $2.49(\text{m}\cdot\text{b}\cdot\text{g}\cdot\text{l})$ in June1996. Moreover several artesian boreholes were flowing previously in the area near Shsir and Dawkah; however they have completely stopped or have only seepage only at the moment. Pressure decrease in these

boreholes is mainly related to three reasons (i) dipping of the layers with the flow direction, (ii) layers permeability which makes such aquifers confined and (iii) the huge column of water existing in the aquifer. Therefore, the abstraction of this aquifer should be taken into account which will reduce the pressure and decrease the artesian system. In addition the discharge tends to be more in the artesian zone and increases with the groundwater movement towards the north.

3.2.4 Aquifer D

Aquifer D is located below aquifer C and is occupied by the lowest part of L.UER. It is confined and is usually encountered 50 to 100 metres below Aquifer C, which extends to the base of the L.UER. Data collected from 21 boreholes penetrate to L.L.UER, however less than half of them only reach or nearly reach the Shammar Shale. Aquifer D thickness (saturated zone) ranges from 35m to 133m, with an average of 79m. The thickness was recorded at HAD-49 at the Hanfeet wellfield and the lowest was at the borehole DEP-3 in wadi Thahboon. In addition the aquifer thickness at the northeast corner (WWD-37) was found to be 61m.

Aquifer D is distributed in all Najd and is usually associated with more than one water strike. The aquifer becomes artesian in the north and northeast of the Study Area, increasing with the groundwater flow direction. The v-notch yield during drilling in this aquifer is various between 2 L.s⁻¹ to 43 L.s⁻¹ with an average of 18 L.s⁻¹ (Table 3.1). The boreholes drilled until the base of the L.UER (Shammar Shale) or those close to the end of L.UER. Often they have a relatively high yield more than others, which does not reach or pass the L.UER. This was observed at boreholes DEP-6 (10 L.s⁻¹) and WWD-6 (43 L.s⁻¹) which have a yield greater than 10 L.s⁻¹. This was related to the opportunity to find more water strikes while continuing drilling to the base of L.UER. The first transmissivity calculation for aquifer D was done by GRC in 2005a using 13 boreholes pumping test data and which eventually found 26 m².d⁻¹. The absences of observation boreholes in this aquifer make other calculations such as storage coefficient difficult to measure.

Comparing all aquifers, the D aquifer is the only widely distributed one, as it starts on the northern side of the Jabal chain and covers the entire region. It is also suggested that this portion of the formation possesses the highest saturated thickness, but lower transmissivity than aquifer A, B, or C. The D aquifer also produces at a lower discharge rate than aquifer C (MWR, 2000a). This aquifer seems to be wider in the Study Area because it covers all Najd. It is assumed to be responsible for conducting groundwater from the recharge area at Jabal chain and the nearby northside to Najd aquifers C to A. This thought was developed and based on the recent drilling data in the northside of the Jabal chain and isotopes results signatures such as ^2H and ^{18}O (discussion in chapter 4).

3.3 Groundwater Movement

The groundwater flow direction is from southwest to northeast and south to north. It starts from the Jabal chain and is divided near borehole QISB in the south running north to the Ruba Al Khali sand dunes. The gradient elevation is the strongest component controlling this flow. Piezometric contour maps constructed reveal that for aquifer C and D are the dominant aquifers in Najd. Boreholes previously used for water level variation surface mapping were also used. As a result, groundwater flow direction can be detected from the maps which supports the previous directions in aquifer C and D (Figure 3.2 and 3.3).

In fact all aquifers from A to D are restricted by a part of the Study Area, except aquifer D. This aquifer is unique and is located in direct contact with the recharge area in the south. Further north other aquifers A, B and C are presented in different places; however aquifer C is wider spread and more essential than A and B. Nevertheless the thought that each aquifer is different and connected to the Jabal may not be supported anymore. Due to latest drilling investigations carried out by MRMWR after 2004 results, it is suggested that aquifer D is distributed over all the Najd area. Moreover the groundwater piezometric surface in this aquifer varies from 544 m above sea level at DEP-7 to less than 50.5 (m.a.s.l) at WWD-37 (Figure 3.3).

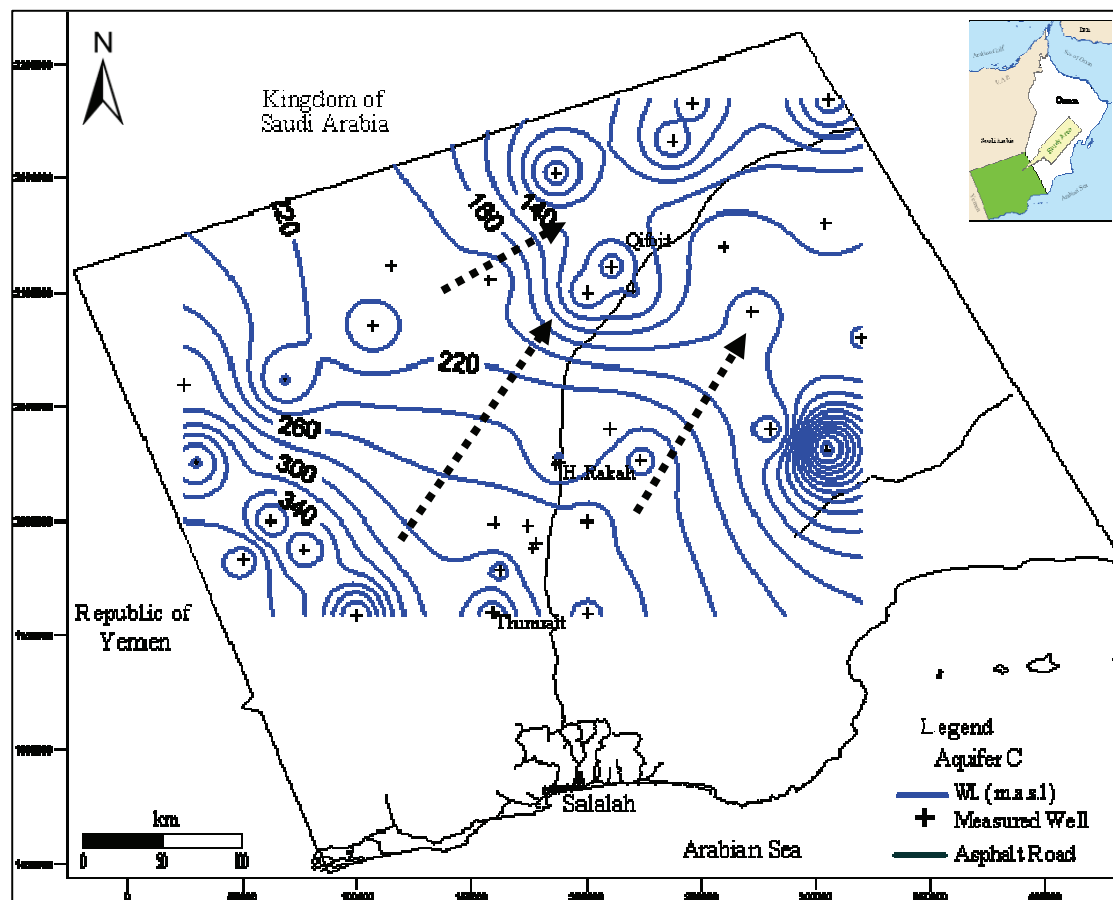


Figure 3.2 Groundwater flow direction (arrows) in aquifer C

From the above evidence the groundwater movement mechanism seems to be the following process: Aquifer D captures groundwater from the recharge source area (Jabal) then it move with the flow direction. The elevation, water pressure, faults and fractures are conducted the groundwater from aquifer D to aquifer C. The majority of dewatering could be occurred after 40 km from the surface watershed north of borehole QISB for aquifer C and after 60 km for aquifers A to B in the north towards Hanfeet. The other directions in the east or west vary depending on the appearance of the aquifers. Additional processes such as natural or non-natural leakage occurs later on and should not be ignored.

The natural leakage between aquifers A to D is expected through faults, fractures and future processes developed in the groundwater system. However the processes of this leakage are from aquifer D to above aquifers and not in the reverse order, with an exception of the shallow layers (accounted with aquifer A) in Jabal chain, such as

borehole Mathira1 and the spring SHTH. The natural leakage exists due to artesian boreholes located in semi to artesian zones with poor design or cementing. Data obtained from boreholes located east of Al Mazyunah at about 50 km from the Jabal towards the north; show no leakage between aquifer's B and C (DEP-16A & DEP-16) or C and D (DEP-14 & DEP-14A). Pump tests conducted in these two locations did not find any leakage between aquifers as shows the following: the static water levels in DEP-16 and DEP-16A before the start of the pumping test were 31.83 m.bmp and 61.49 m.bmp, respectively. At this location the hydraulic head in Aquifer C (DEP-16) was 29.66 m above Aquifer B (DEP-16A) and no groundwater drawdown was recorded in DEP-16A during the constant pumping test.

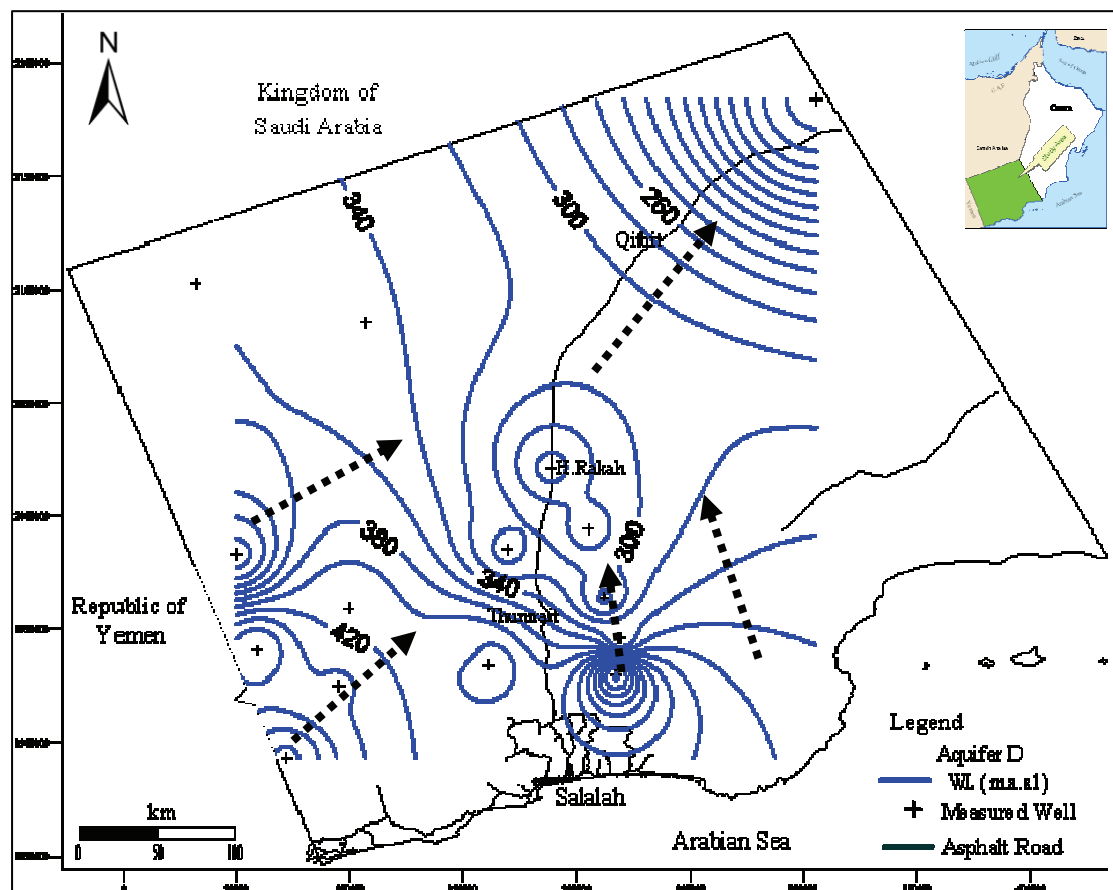


Figure 3.3 Groundwater flow direction (arrows) in aquifer D

On other hand, the static water level in DEP-14 before the start of the pumping test was at 69.08 m.bmp. The static water level in DEP-14A was 68.36 mbmp. At this location the hydraulic head in Aquifer D (DEP-14A) was 0.72 m above Aquifer C

(DEP-14) and no groundwater drawdown was recorded in DEP-14A during the constant test DEP-14. The leakage between aquifer C and B was not detected at DEP-9 and DEP-9A located 50 km east of Al Mazyunah. Consequently the leakage between aquifer C and B or D was not observed. In addition, pumping test analyses in previous studies mentioned a delay yield in several boreholes in aquifer B, C, and D at Hanfeet wellfield, Tosnat and DEP-16 (GRC, 2008).

In fact leakage between aquifers exists in the area close to the Jabal chain and in most of the Study Area due to two reasons. Firstly, (i) The appearance of aquifer D only one in the contact with recharge area; and secondly, (ii) the continuous gentle drawdown in borehole 001/018 located at Hanfeet area in aquifer B as well as with borehole BE094486AA (RBK-D) located in aquifer D without any pumping affect in the surrounding area before 2000 from the same aquifers (see section 3.4).

The groundwater movement follows the direction southwest to northeast and south to north. The process is started with capturing water from or nearby the recharge area by aquifer D only then at further north aquifer D feeds the other aquifers. This idea is supported by absent or weak evidence of other aquifers A to C in contact with the recharge area. The biggest difference in piezometric elevation in aquifer D in addition with faults, fractures is controlling these processes. Leakage between aquifers is not observed in the west of Najd, close to Al Mazyunah at boreholes DEP-9, DEP-14 and DEP-16. However this phenomenon seems to occur in central Najd around Hanfeet and Helat Ar Rakah. This evidence came from monitoring borehole records in aquifer B (001/018) and D (RBK-D), in addition with a delayed yield mentioned by GRC, 2008 at Hanfeet wellfield.

3.4 Indications for Trends of Water Level

Despite many boreholes being distributed in the Study Area, the study is concentrated only on those with a known design, even though they are limited in number. The source of data for water level and wadi flow, which are involved in this study was MRMWR data base either in Salalah or Muscat. Unfortunately, the water level routine monitoring was stopped during the period from 2006 to 2009 in the Najd area due to technical problems. Therefore, missing data of that period is observed in the

hydrographs. Boreholes included in this study sampling campaign had an opportunity for measurement in that period.

The groundwater level is affected by two components: abstraction of agricultural purposes and a few artesian boreholes which still flow on the ground for longer than 30 years. The abstraction was concentrated in the area and forms the triangle (Helat Ar Rakah, Shsir and Hanfeet) with approximate dimensions of 50x50x40 km. This area controls approximately 85% of the total water consumption in Najd. Therefore the majority in decline of water level is observed in these areas and the circle of decline radius increases specifically around Helat Ar Rakah. The circle radius is not less than 60 km, based on the latest water level data which expands annually. On the other hand, some boreholes were drilled before in 1950 and 1980 and left open until now. These boreholes drilled by different agencies, such as oil companies for supporting oil exploration purposes in the artesian zone, which were not cased or cemented properly afterwards. In this case the boreholes continuous overflow or leakage to other aquifers. As a result, these boreholes participated and accelerated groundwater level decline in the long term, particularly when they penetrated to artesian layers.

3.4.1 Aquifer A

This aquifer is significant in Helat Ar Rakah, Hanfeet, Shsir; and Bin Khawtar southwest of Qitbit. The development in these areas started at the beginning of the 1990s with small farms using diesel generator power. Many people established their farms after constructing hand dug wells in aquifer A. Later, around the middle of the 1990s and beginning of 2000 most of the small farmers ignored the fact due to the high cost of the power. In 2004, the government connected electricity between Helat Ar Rakah, Hanfeet and Shsir, which encouraged the old farmers and others to rehabilitate their farms and to dig new boreholes mostly in aquifer A.

There are very few monitoring wells in aquifer A because almost all of them are privatised and are used for daily pumping or constructed recently and not have a long record. Moreover the limitation and scattered state of monitoring wells in this huge

area can not strongly describe the water level trends indeed. Therefore 15 wells used to produce a recent water level deficit map for aquifer A. Data involved in this map were collected from 10 wells with record pre 1994 to January 2010, however the other 5 wells were involved in monitoring network since 2004 only and have records up to end of 2009 (Figure 3.4).

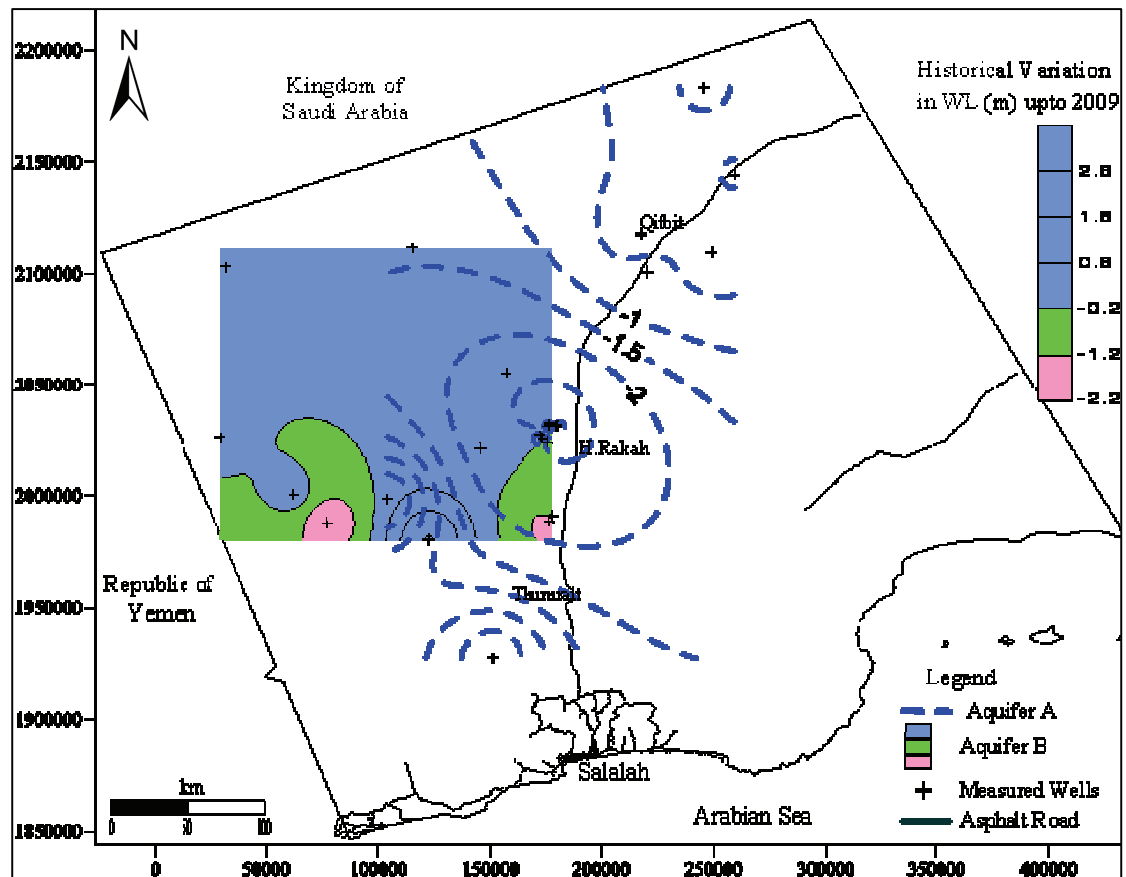


Figure 3.4 Variation in water level for aquifer A and B up to 2009

On the other hand, two selected wells with a historical record of water level were used as representatives for this aquifer. These wells are HRB-19 (210/902) and HRB-21 (210/850) located in Helat Ar Rakah have a very intensive consumption. The monitoring data shows steep decreases from 1991 to 1994 followed by recovery in 1995 and reflected the direct response to agriculture activities. This recovery became close to the initial level in 1997. The water level remained stabilised afterwards until 2005, then decreased again. These declines exceed the highest drawdown found since 1991. Also, both wells were recorded with a maximum deficit between October 1991 and January 2010 of -3.0 m and -6.27m respectively (Figure 3.5).

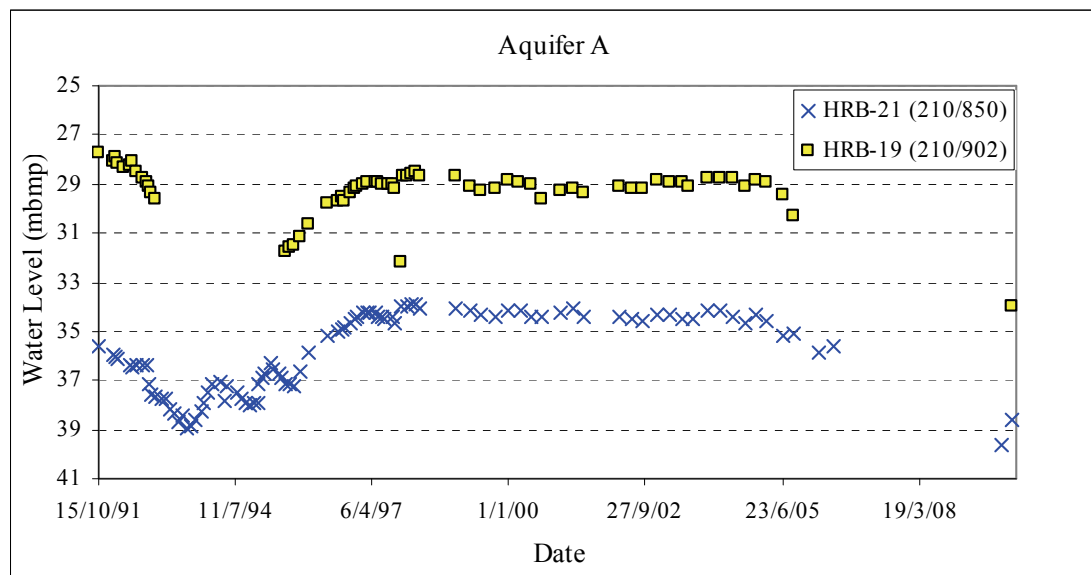


Figure 3.5 Water level variations in Helat Ar Rakah (aquifer A) for the period (1991-2009)

3.4.2 Aquifer B

This aquifer is concentrated in west and central Najd. Many boreholes penetrated aquifer B; however few of them can be used in order to evaluate difference or piezometric of water levels. This is because many of those boreholes are not completed in the specific layer. As a result, 12 boreholes were selected to represent the water level deficit in aquifer B (Figure 3.4). The borehole ZV182823BA (001/018) was chosen as an example because it had the longest monitoring record and maximum drawdown in aquifer B. The borehole started gently decreasing since October 1992 up February 2010 with a deficit in water levels of -2.23 m (Figure 3.6). The deficit not too much in comparison with the monitoring record period; however in areas like Hanfeet it does not have any activities and using aquifer B seems to be considerable. This decline could be reflected as the abstraction influence in Hanfeet from aquifer C which was recorded as a steep drawdown from 1995 to 1996 with more than 29m. Another source of the effect could be the abstraction at Helat Ar Rakah which is located 30 km northward. It appears that either this or that aquifer B seems to be responding with the aquifer C drawdown. Therefore this relationship is

probably assessed as a leakage which is based more on bad borehole construction than design problems because it was a well known construction.

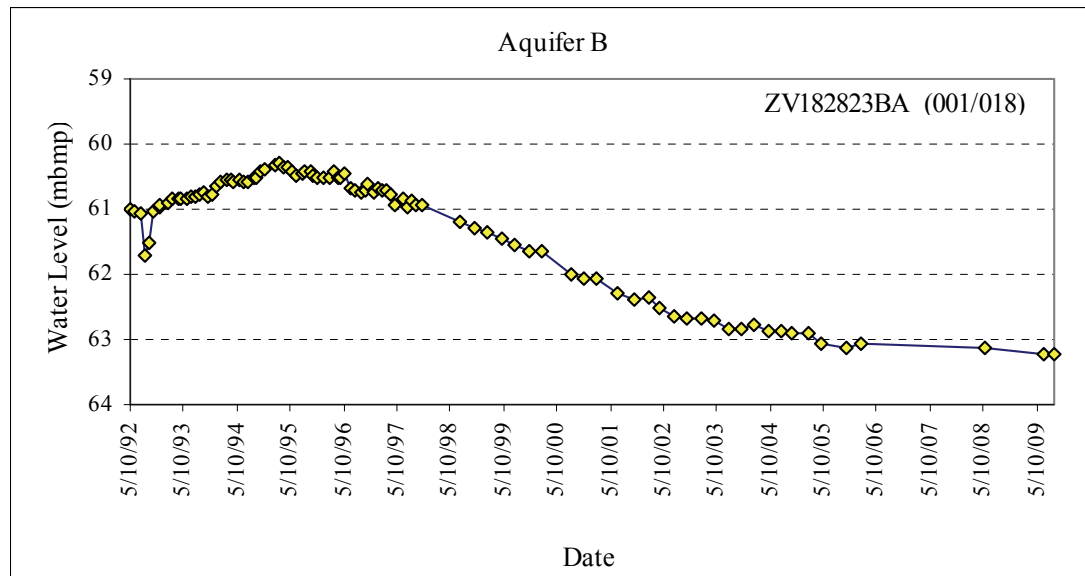


Figure 3.6 Water level variations in Hanfeet (aquifer B) for the period (1992-2009)

3.4.3 Aquifer C

The most intensive abstraction is concentrated in aquifer C. This withdrawal is represented by the concentration of all Grasses farms on C aquifer as a main source of water supply. JICA in 1988, 1989 concluded that water levels in central Najd (Hanfeet and Helat Ar Rakah) declined in the range of 0.15 to 0.3m.yr⁻¹. Unlimited use of water over the last three centuries resulted with a drop of groundwater level for more than 30 m in Helat Ar Rakah and Hanfeet, based on the latest measurement in February 2010. The greatest decline occurred in the period from 1994 to 1997 with 40-50%. Even though, the water level still decreases annually in this aquifer. For more contrast, the data collected from 44 monitoring wells were used to plot a historical deficit contour map for the full record up to end of 2009. The map shows the highest depletion concentrated around Helat Ar Rakah which extends for more than 30 km, specially south and southwest directions (Figure 3.7).

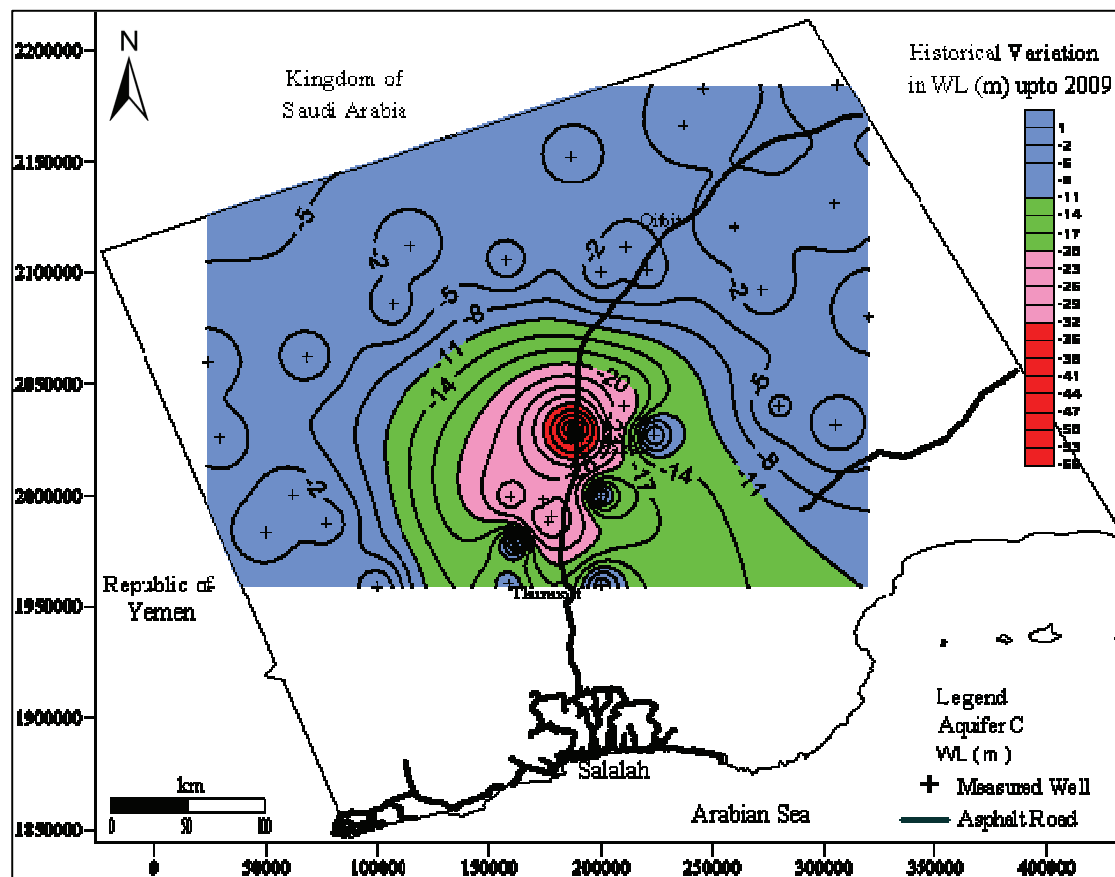


Figure 3.7 Variation in water level for aquifer C up to 2009

In addition two monitored boreholes were selected to represent the historical trend of the water level in high depleted areas. The boreholes are AF825206AA (JICA-6) from Helat Ar Rakah and ZV193045AA (001/016) from Hanfeet (Figure 3.8). In general, both boreholes hydrographs were reflected as having a steady state condition in the water level before 1994, then steeply dropping until 1997. After that there was a gentle decline until 2006, which was observed in Helat Ar Rakah; however borehole 001/016 recovered for about 10m then continued to decrease as well as JICA-6. After 2006 to February 2010 JICA-6 water levels dropped more than 13m, however 001/016 is also decreasing at a low rate (3.2m).

The steep drop in the water level after 2006 which followed a stabilised period in Helat Ar Rakah (JICA-6) is related to the presence of additional production boreholes established by the Royal Court at Zinat Al Sahara Farm. On the other hand, borehole 00/016 at Hanfeet (30 km south Helat Ar Rakah) is located near Grasses farm which had abstracted a huge amount of water before 1998. The Farm was discontinued by

the end of 1997. As a result, the borehole was recovered but could not reach the initial water level, and continued gently declining due to the high abstraction in Helat Ar Rakah.

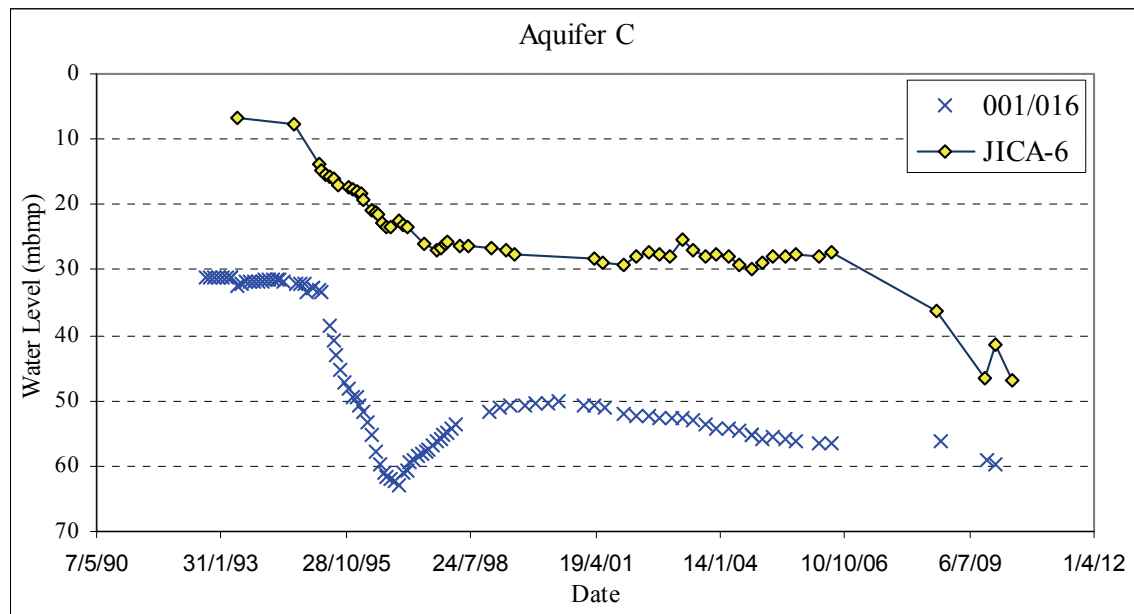


Figure 3.8 Water level variations in Helat Ar Rakah (JICA-6) and Hanfeet (001/016) in aquifer C for the period (1990-2009)

Data analysis for boreholes JICA-6 (=17yr) in Helat Ar Rakah and 001/016 (=18yr) in Hanfeet show that water levels are declining at the rate of 2.05 and 1.59 m.yr⁻¹ respectively. However if the period was reduced to the last 13 or 14 years when both boreholes become more stabilised, the annual decline rate will be 1.20m in JICA-6 and 0.74m in 001/016. Further affects were recorded 35 km east of MRMWR (Helat Ar Rakah camp) in the new borehole DEP-18 which was drilled in 2008 were recorded with drops in water levels of 1.67m after one year. Moreover, boreholes such as JICA-3 are located close to the well field of Zinat Al Sahara Farm and have more drawdown; however that was under because of pumping (dynamic water level).

In addition, the water level was measured twice in the monitoring wells close to Zinat Al Sahra farm in Helat Ar Rakah before the wellfield stopped and before starting the next day. The first measurement started on 6/6/2010 at (14:00) followed by the next measurement on 7/6/2010 (7:00 AM) after 16 hours shutdown and before the pumps

were switched on. As a result, the borehole water level was found at JICA-1 (61.35m), JICA-3 (60.77m), JICA-5 (57.65m) and JICA-6 (47.22m). The recovery after 16 hours was 57.65m, 56.5m, 53.69m and 46.86m. The result was that the maximum recovery recorded was 3.27m, 4.27m, 3.96m and 0.36m respectively, despite the first three boreholes being located within the well field.

3.4.4 Aquifer D

In general this aquifer is distributed all over the Study Area. Limited numbers of borehole are completed in aquifer D; even though several penetrations to the lower UER pass aquifer C and reach D aquifer. However, those boreholes were not completed in aquifer D and were isolated from other aquifers. Therefore they were excluded from water level applications. Data collected from 16 boreholes are used in this study for water level assessment. Almost of them drilled between 2004 and 2008 have the series WWD, DEP and DWS. Data gathered from both new and old boreholes were used to establish water level variations of the surface contour map for aquifer D. Water level records involved in this calculation consist of the initial reading compared with 2009 (Figure 3.9). The map shows two depressions around boreholes DEP-5 and RBK-D (BE094486AA) with maximum declining of -22.67 m (=2yr) and -8.9m (=21yr). In fact, the high drawdown DEP-5 is related to new borehole constructions nearby with a distance of less than 100 m. The last reading was taken during the pumping influence of the other borehole; therefore the reading may reflect the dynamic water level rather than the static. At the sametime the borehole was probably influenced by the major fault which was detected less than 10 km northward. However the other borehole RBK-D reflects the aquifer's actual circumstances in that area due to its long record.

The overall water level in aquifer D is affected as well as with other aquifers in Najd. The historical record detected from borehole BE094486AA (RBK-D) located east of Hanfeet shows a gentle declining since 1992 up to January 2010 (Figure 3.10). Despite the abstraction in the surrounding areas, from before 2000 it was not from aquifer D; however it was from boreholes completed into aquifer C. In 2000 a new poultry farm was constructed 10 km south of the borehole RBK-D and drilled 4

boreholes in aquifer D, but the graph does not show any response for period after 2000 rather than normal decline. The water level record for RBK-D shows annual decline in aquifer D at the rate of 0.42m. On other hand, continuous drawdown in this area reflects regional affect of all aquifers by each other. Therefore the visible source of this declining seems to be high abstraction at Helat Ar Rakah, even though it is 30 km far away with the flow direction.

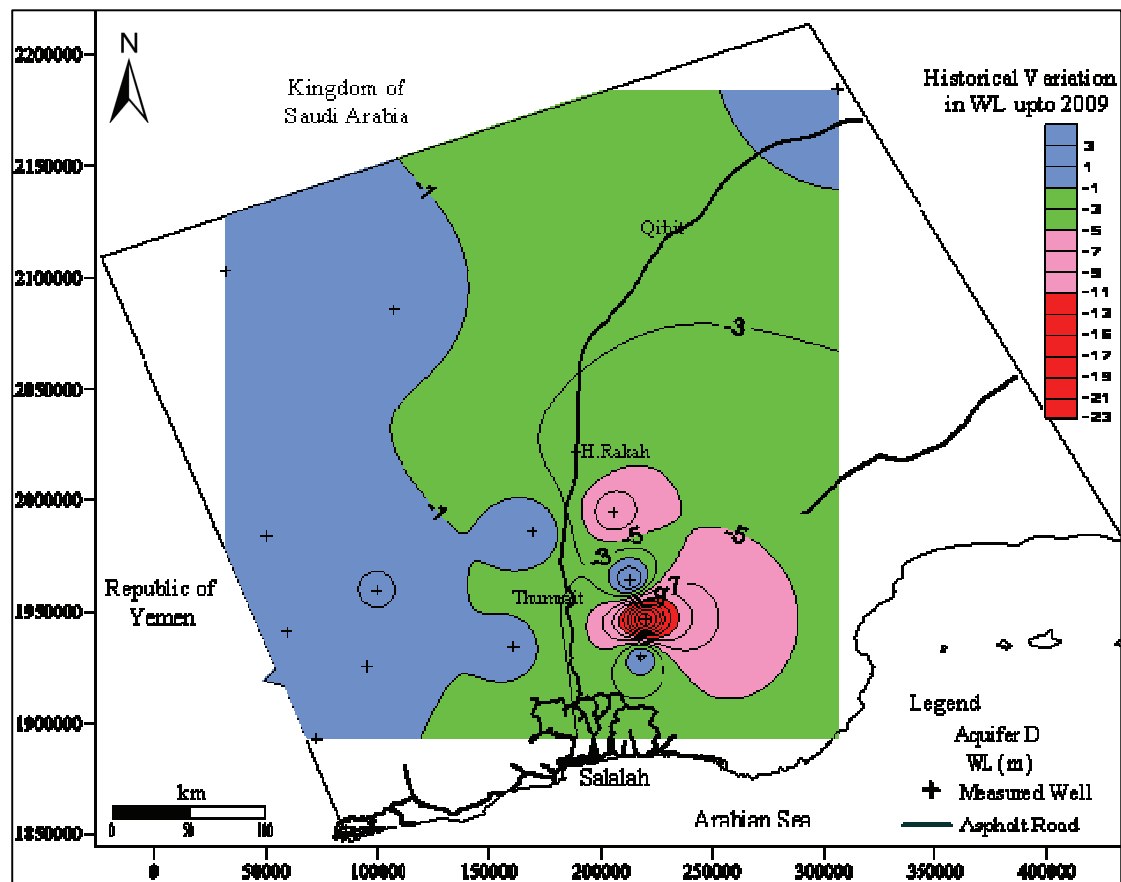


Figure 3.9 Variation in water level for aquifer D up to 2009

Generally water level is declining in aquifers A to D. This decline is concentrated more in aquifer C than A, B or D. The groundwater in Najd seems to be in a steady state condition pre 1994; followed by intensive abstraction caused by drawdown varying from one aquifer to another. The maximum drawdown recorded in February 2010 was; 6.27m, 2.23m, 34.79m and 8.9m in aquifers A to D respectively. Boreholes from aquifer C and D with drawdown values of more than the previous such as JICA-5 and DEP-5 may have a dynamic water level rather than a static. They

were therefore avoided. During the last period all aquifers failed to recover from the deficit to reach its initial water level.

On the other hand, water levels in aquifers B and D are still decreasing even though they are not being used intensively. As a result, these aquifers are feeding each other through some faults or fractures depending on the pressure and the permeability existing between them. The aquifers from A to D decline at a rate of 0.33m, 0.12m, 2.05m and 0.42m annually.

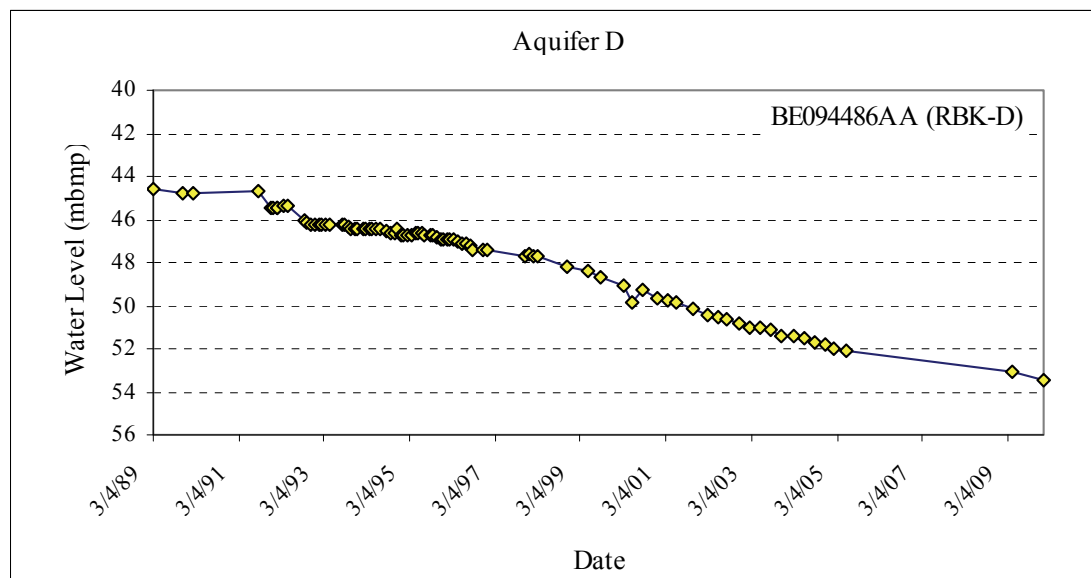


Figure 3.10 Water levels variations in Hanfeet (aquifer D) for the period (1992-2009)

3.5 Recharge Processes

More than one parameter contributes to groundwater recharge in the Study Area. The flood events, faults, fissures, fractures and aquifer characteristics share the responsibility of the recharge which varies between aquifers and the directional flow. The efficiency of each of these parameters affects groundwater hydrochemistry and isotopes behaviour. Therefore, the following explanations will emphasize some of these parameters' influences and the evidence observed as a result.

3.5.1 Evidence of recharge associated with cyclone events

The monitoring network reveals boreholes from different aquifers rising in water level after flood events (Figure 3.11) which is explained as recharge to groundwater. Therefore several water levels of boreholes as well as wadi flood events were

analyzed and compared with each other. At least one borehole was determined in each aquifer from A to C (Table 3.2). However aquifer D was excluded from this list due to (i) most boreholes being completed in this aquifer drilled after 2004, and have short record periods (ii) the majority of boreholes which existed before were used for a water supply and the limited wells that were monitored did not show any response with flood events.

The different boreholes from aquifers A to C were used to estimate the travel time from the flood occurrence until water level rises were observed. Nevertheless, the selected boreholes were reflected responding to water level rise more than once; however it is not easy to access the date of recharge reaching the borehole. This is because the boreholes are monitored manually and the routine visit is not frequent; approximately 3 months, especially in central Najd. Despite some shorter periods having been detected from these boreholes, these periods were compared with flood events duration, borehole water level before and after the flood occur.

In aquifer A two boreholes were selected; Mathira1 (YV826752AA) located close to the recharge area upstream of wadi Ghadun Station. The other borehole is KHT-A (BG117784AA) is located north of Najd about 250 km northward from the Jabal chain downstream of the Wadi Thahboon Station. These boreholes have records from 1988 until May 2009 and January 2010 respectively. Data analyses of these boreholes show corresponding floods occurred several times during their monitoring period. However it is strongly expressed and appears faster in borehole Mathira1 (YV826752AA) (Figure 3.12) than borehole KHT-A (Figure 3.13). The borehole Mathira1 in aquifer A is located close to the Jabal chain which is an unusual existence due to the dominance of aquifer D. However, springs restricted to the top layers of the Jabal such as SHTH and NKR or seepage were accounted for in aquifer A. Therefore, the existence of Mathira1 in aquifer A in the area close to the Jabal chain seems to be related to feeding from surface pool called Uyun which is located upstream from the borehole. Another further 10 km's north of Mathira1, the flow direction is caused by more than one borehole drilling, however aquifer A is not detected.

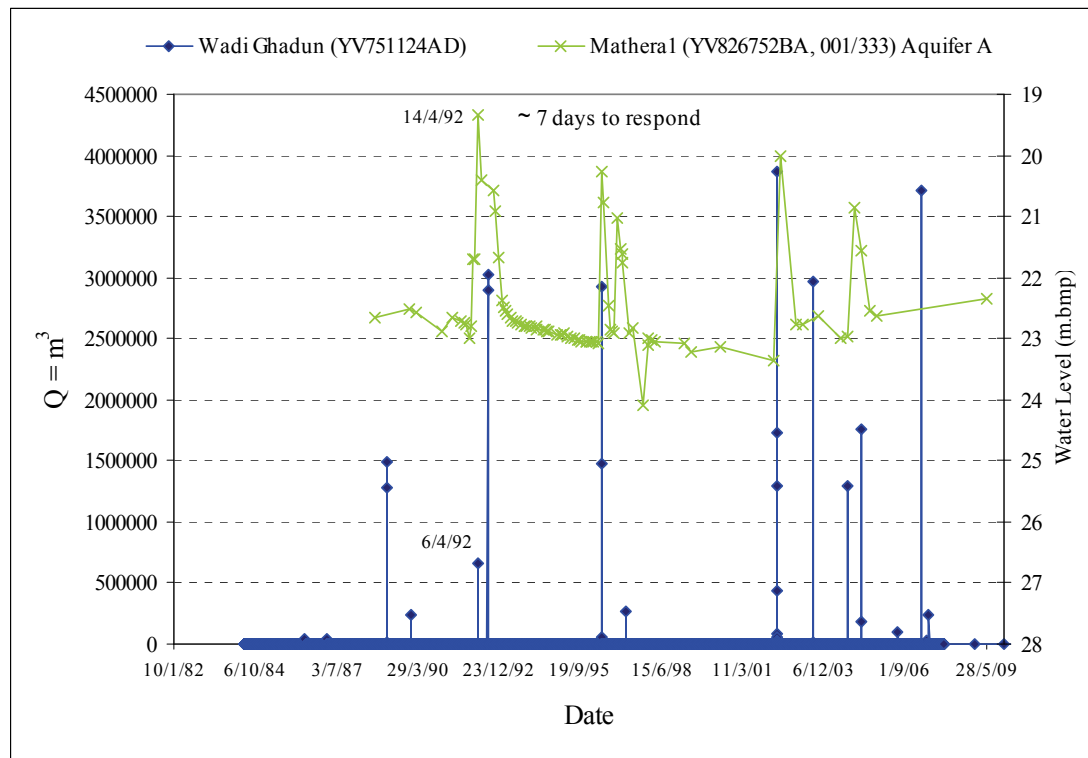


Figure 3.12 Comparison between borehole Mathira1 water level and Wadi Ghadun flood event

At borehole BG117784AA the response to floods seems to be less. The comparison between both records; borehole water level and Wadi Thahboon Station are slightly affected (Figure 3.13). However the reflection of this response takes a longer time due to the distance from the recharge source. The time seems to range between 5 and 6 months. This period is calculated based on the flood which occurred on September 30th, 2004, (Table 3.2). Moreover several floods were recorded among the Wadi Thahboon Station since 1988 to 2007, passing further north of Qitbit, east of this borehole and continuing to the sand dunes. However before 2006 not one of these floods gave a direct response to the borehole water levels. The flood in 2007 was given recovery from the last reading in September 2005 and the recent measurement in October 2008 of 0.41 m in the borehole. Overall, these results are a guide to the thought that the direct infiltration to aquifer A in this area is avoidable, which means a regional recharge could occur.

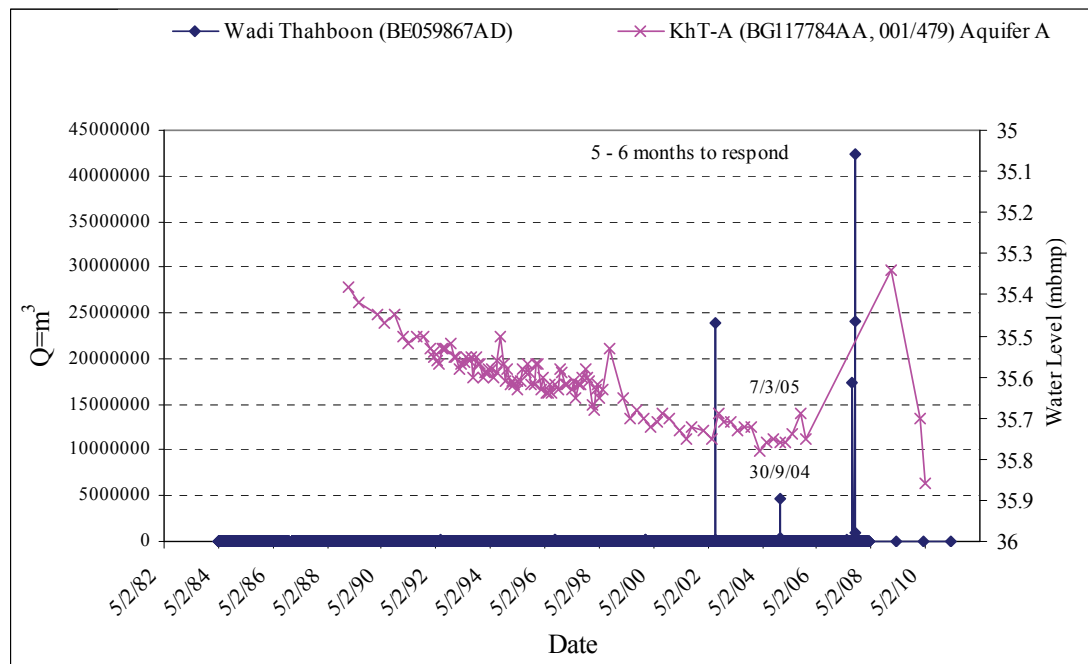


Figure 3.13 Comparison between borehole KhT-A water level and Wadi Thahboon flood events

The relationship between water level response and cyclone events in aquifer B is difficult to detect in many places due to a shortage in number of boreholes prior to 2004. These new boreholes' historical records are too short in comparison with cyclone events which are irregular and occur roughly once every ten years. Therefore only three boreholes have long records, but two of them are located in the Hanfeet area and do not show any response with flood events. The other borehole YA715978BA (001/007) which is located downstream of Wadi Ghadun in the Shsir area will be used for the comparison of aquifer B. In addition, the missing data is due to the disconnecting of the monitoring programme in the Najd from 2006 until end of 2009.

The borehole was monitored since 1986 until February 2010, with exclusive years being 2007 and 2008. The graph shows the general decreases in water levels. Even though, several rises in water level were observed in the borehole responding with periods following flood events. The 2007 flood seems to be the effective one, despite the borehole not being measured since 2006, until February 2010. However, the borehole recorded an excess recovery of 8.31 m above the last measurement in June

2006 (Figure 3.14). Therefore the recharge effect needs 3 to 4 months to pass more than 120 km before it gives a contribution to the groundwater at the Shsir area. This analysis is based on the comparison of measurements dated on the September 30th 2004 flood event and the borehole (001/007) water level associated with that flood (Table 3.2). For instance, the flood was recorded in the period from May 10 to 23, 2002, and 85% of it was given within the first two days. The borehole measured in September 7th had little response; however the first increases in water levels was seen in December 17 with an excess recovery of 1.04 m. Also the borehole water level was recorded to be continuously rising up to March 15, 2003, with extra 0.52m.

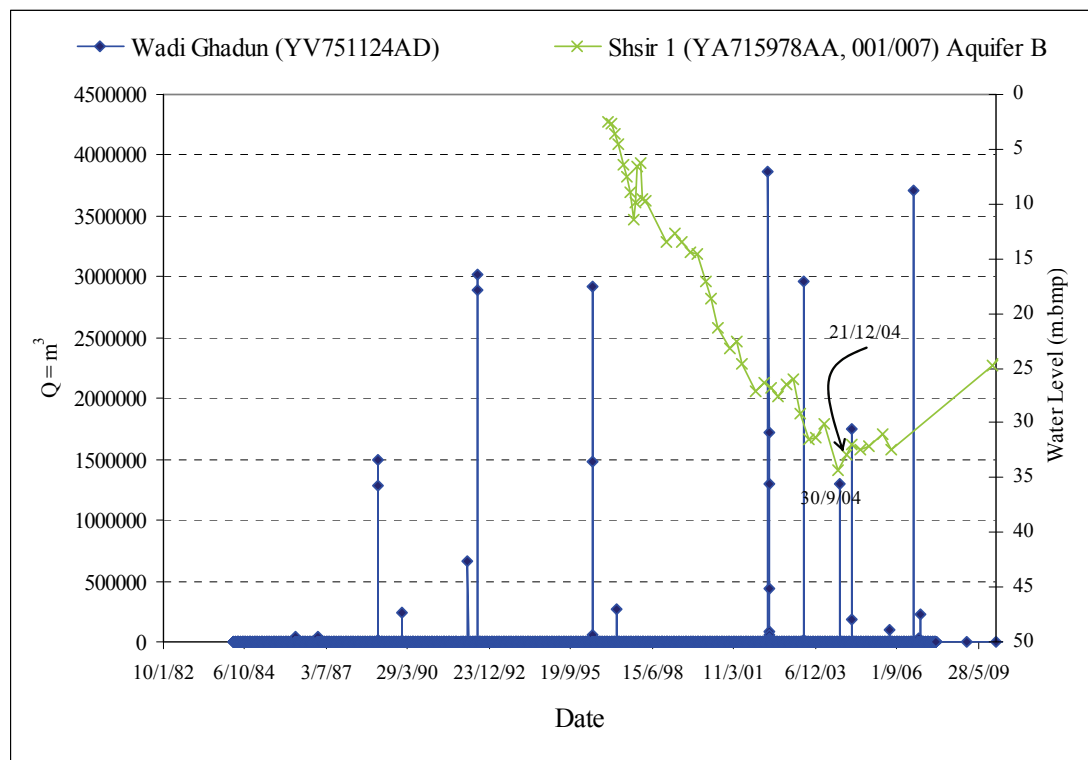


Figure 3.14 Monitoring well (001/007) in Shsir with some response related to flood events

The groundwater monitoring network of the MRMWR in the Study Area recorded the rise in water level associated with the cyclone events which was counted as a recharge to aquifer C. Therefore two boreholes BE050838AA (RBK-C) and BF000000AA (001/283) were selected for recharge comparison. RBK-C is located in wadi Ribkut on the west side of the wadi Thahboon station and 001/283 is located downstream of

the wadi Thahboon. Both boreholes are about 50 km to 100 km from the recharge area and have been monitored since 1996 and 1993 respectively. The borehole records are compared with the flood station of wadi Thahboon because it is the closest (Figure 3.15).

The borehole RBK-C was affected by several floods especially those of 2002 and 2007. The period from the flood event and the borehole response can not be calculated accurately because of the data absent at the borehole, and the expansion of monitoring frequencies. Borehole monitoring data in comparison with the flood event which occurred in the period May 10-12, 2002, shows the first water level responding on June 18, 2002, of 0.85 m. The water level in the borehole continued to rise up to the next measurement which indicated an uncompleted influence of recharge. Respectively, the period assumed for the recharge influence to reach this borehole was about 28 days.

The borehole BF000000AA (001/283) responds to flood events particularly in 2002 and 2007. Based on monitoring data the first measurement on June 23, 2002, after the flood occurred (10-12 May 2002) the water level was raised 3.16 m. Due to the shortage of readings for the duration between flood events, the first measurement after the flood was taken on June 23, 2002. Therefore this reading was suggested to be a period for borehole responding with recharge, which calculated a maximum of 1.5 a month.

In aquifer D the comparison between flood events and the responding of boreholes close to the recharge area was not available. This is because the limited existing boreholes were previously pumping wells used continuously for water supply and was excluded from the monitoring routine. On other hand, recent boreholes were drilled after 2004, with short records not exceeding 3 years. Further northward the numbers of wells are very limited and scattered with limited records, except BRK-D. The borehole RBK-D is located in east Hanfeet at about 10 km north borehole 332/014 has a long record (Figure 3.10) but it does not show any response with flood events. However, it may affected by the discharge in the area or pressure drop due to the feeding in of other aquifers and do not show any response of recharge.

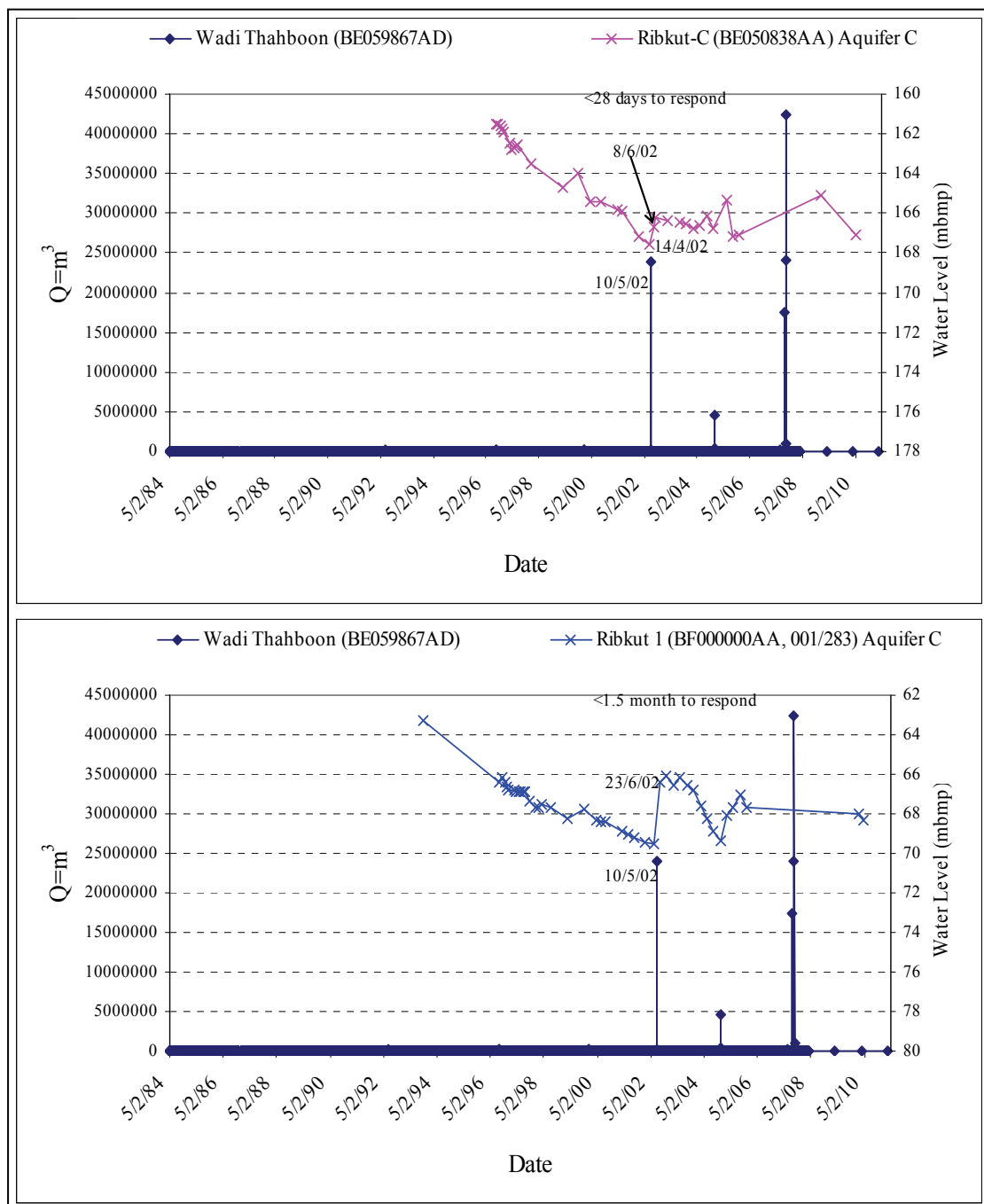


Figure 3.15 Comparison between boreholes RBK-C and Ribkut1 water level and Wadi Thahboon flood events

More than one borehole reflected rise in water levels due to flood events. These boreholes are from different aquifers and they are in varied distances from 50 to 250 km. The time recorded for recharge to reach the boreholes was varied between 8 days in borehole Mathira1 (YV826752AA) near the Jabal and 5-6 months at KhT-A (BG117784AA) in aquifer A west of Qitbit as well in borehole YA715978BA located

in aquifer B in Shsir. Additionally, the influence of recharge was observed after 28 days in RBK-C (BE050838AA) east of Thumrait, and 1.5 months at BF000000AA (00/283) in aquifer C northeast of borehole 332/014. The response of boreholes does not mean the recharge has already reached its location, however it indicates the pressure generated in the aquifers was due to additional water, even from far away.

Furthermore, the period needed for the recharge to reach the borehole in different aquifers depends on the gaps between the water level's reading date and the flood events which occur, and then seeing how to match them. These trails sometimes have successes when that gap is minimized; otherwise it seems to be difficult. Sometimes the data analysis of the flood and the nearby borehole shows a possibility of determining the time needed for the recharge to reach the aquifer. However these periods are not absolute because they depend on several factors like rainfall intensity, flood volume, distance, aquifer matrix and monitoring systems.

3.6 Conclusion

Based on the knowledge gathered from water levels on contour maps, groundwater in all aquifers generally flows south and southwest towards north and northeast. The monitored data reveals that water levels are declining in all aquifers; however aquifer C is more affected. The abstraction in Helat Ar Rakah which was concentrated in aquifer C, was sworn a declining influence for more than 30 km. The natural and non-natural leakages between aquifers exist due to faults, fissures, fractures or old boreholes with a destroyed casing. As a result, together with extensive abstraction, piezometric levels decreases annually, moving towards the north.

The period from 1985 to 2008 when cyclone events occurred in 2002 and 2007 were found with the highest positive influence at groundwater level. This is detected from water level hydrographs in several wells from different aquifers which respond with flood events and considered recharge occurrences in some parts of Najd. At the same time, most of the flow is likely to be generated among wadi Thahboon and Ghadun.

It is evident that the cyclone events are the dominant source of recharge to Najd aquifers despite a small contribution from monsoon in the Jabal chain, which can be expected. The recharge will be discussed later in Ch. 4 and Ch. 5, with a focus on hydrochemistry, stable isotopes, radioactive (^{14}C) and noble gases evidence.

GROUNDWATER ASSESSMENT AND MECHANISMS OF RECHARGE WITHIN THE AQUIFERS

This chapter concentrates on the analysis and discussion of the results of comprehensive data collected from the Study Area during the period from 2008 to 2009, and includes: covered groundwater hydrochemistry, environmental isotopes, noble gases, lithology, soil carbon dioxide and precipitation. For better understanding of the quality of the data and the reliability relationship between elements check, correlation matrix and factor analysis were applied to the hydrochemical results. The groundwater hydrochemistry data was used to evaluate characteristics of water types in all aquifers and to distinguish homogenous directions in parallel with environmental isotopes in the Study Area. In this chapter several conceptual models were performed to present the recharge processes and suggested direction. In addition, water quality was assessed with recommended uses included.

4.1. Sampling and Analytical Methods

The sampling locations were selected with the intention of characterizing the groundwater chemistry in the majority of Najd formations, as to gain a representative overview of chemical and isotopic dynamics in this groundwater system (Figure 4.1).

Special concentration during sampling was given to wells that were built by the MRMWR because they were reliable and designed according to modern day standards. In addition to the MRMWR wells, five thrust-design wells and three springs were included in the sampling regime. The sampling campaign was conducted during 2008 and 2009, as well as for several samples in 2010. Samples were collected from sites covering A to D aquifers (N=80), including three springs, and one monsoon rainfall event from June to August 2008.

Two methods of sampling were used for hydrochemical and isotope analytics: (i) 30 groundwater samples out of the 80 total were collected by bailer, and (ii) the remaining samples (N=50) were extracted from the aquifer by direct pumping or collection of spring discharge.

The rainfall sample was collected by a precipitation sampler during the monsoon season of June to August, 2008. Hydrological parameters such as electrical conductivity (EC), pH, temperature, Eh, alkalinity were performed on-site during the sampling. Samples collected for hydrochemical analyses for major ions (N=80) and trace elements (N=69) were filtered prior to collection in the HDPE and glass bottles, labeled, and stored at 4° C until analytical procedures were performed. Major ions and trace elements analyses were conducted at the MRMWR laboratory in Muscat and all isotope analyses were performed at Isotope Laboratory of the UFZ-Department Isotope Hydrology in Halle/Saale, Germany.

The campaigns consisted of sample collection for chemical, stable isotopes, radioactive isotopes and noble gas analyses. However, trace elements, radioactive isotopes and noble gases were performed in each one.

The stable isotopes of water, deuterium (^2H), oxygen (^{18}O), the sulphate isotopes ^{34}S , ^{18}O , and ^{13}C of dissolved inorganic carbon (DIC) were conducted for every site that was sampled (N=80). Samples for radioactive isotopes and other chemical analyses were distributed as follow: ^{14}C (N=39), Tritium (^3H) (N=39), $^{13}\text{C}_{\text{lithology(carb)}}$ (N=9) and $^{13}\text{C}_{\text{soil/gas}}$ (N=4).

The ^2H , ^{18}O and ^3H samples were collected directly from the source with no additions or filtering prior to testing in 30ml and 1000 ml HDPE bottles, respectively.

The isotope ratios for $^2\text{H}/\text{H}$ and $^{18}\text{O}/^{16}\text{O}$ were measured using the equilibration technique (Gehre *et al.*, 2003) coupled to a isotope ratio mass spectrometer (IRMS) XL-plus (ThermoElectron) with an accuracy of 1‰ for $\delta^2\text{H}$ and 0.1‰ for $\delta^{18}\text{O}$. Standard δ -notation is used for reporting, so that:

$$\delta = [(R_{\text{sample}}/R_{\text{standard}}) - 1] 1000 \quad (\text{‰}) \quad (\text{eq. 1})$$

with R equal to changes in heavy and light isotopes compared to the Vienna Standard Mean Ocean Water (V-SMOW) for both $\delta^{18}\text{O}$ and $\delta^2\text{H}$.

The ^3H analyses were performed by Liquid Scintillation Counter (LSC) with a detection limit of 0.2 TU (tritium unit).

The groundwater for ^{14}C analysis was collected by two different methods; precipitation (N=10) for conservative β -counting method and for Acceleration Mass

Spectrometry (AMS) (N=28) analysis. The precipitation method was carried out in the field using the Clark (1997) procedure. In this method two components were added, first $(\text{Ba}(\text{OH})_2 \cdot 8\text{H}_2\text{O})$ in order to raise the pH then followed by $(\text{BaCl}_2 \cdot 2\text{H}_2\text{O})$ into a container of a 60 L capacity. The amount of the components required adding and the volume of distilled water for each sample was determined based on SO_4^{2-} and HCO_3^- concentrations. After 24 hours the final residual precipitation was collected in 1000 ml HDPEs bottles.

The AMS samples were collected from boreholes directly in 1000 ml HDPE bottles after adding 2-3ml of HgCl_2 solution (30g/100ml). They were measured for $\delta^{13}\text{C}$ in (‰) and for ^{14}C in pmC (%) for ^{14}C as defined by Stuiver and Polach (1977). The analysis has been done in the Mannheim laboratory for both ^{13}C and ^{14}C having a STD comprised for error counting with a detection limit between 0.08 to 0.23‰. The ^{14}C was measured by Accelerator Mass Spectrometer (AMS) at the CEZ Archäometrie GmbH in Mannheim with accuracy about 0.3 pmC.

In total, 27 samples were collected for noble gases analysis and distributed as follows: 5, 6, 7 and 8 in aquifers from A to D respectively. The collection method according to Kipfer (1991), Hahm and Kim (2001) and Hahm et al. (2004) had taken place after the pumping of 3 times the borehole water volume. All samples were collected during the pump running to achieve representative groundwater samples, and also to maintain the pressure inside copper tubes for noble gases around 4 Bar. The samples were filled in special copper tubes at the field, and then well packed in selected wooden and aluminium boxes. The noble gases and AMS samples were then sent to the Isotope Laboratory of the Institute for Environmental Physics, University of Heidelberg, Germany.

Noble gases were measured by using Mass Spectrometer (MS 5400) in Heidelberg with the reproducibility: He : 0:2%, Ne : 0:3%, Ar : 0:3%, Kr : 0:7%, Xe : 1:2%.

The measurement details of ^{14}C using the AMS method and the preparation for estimation of noble gases will be discussed in a Diploma thesis by Christian Herb (2011) at the Heidelberg University.

Five sites consisting of 9 boreholes in Najd aquifers A (WWD-20 & WWD-24), B (WWD-13), C (WWD-25, WWD-12 & WWD-36) and D (WWD-14, WWD-37 & DEP-6) were selected for lithological analyses. The lithological samples were collected by picking up about 50g from each metre of the saturation zone. Consequently the samples will be compiled and mixed together before delivery to the UFZ laboratory in Germany for analysis. The test method used was X-ray fluorescence analysis (XRF), and covered the following elements and oxides: Na₂O, MgO, Al₂O₃, SiO₂, P₂O₃, S, K₂O, CaO, TiO₂, V, Cr, Mn, Fe₂O₃ and Sr.

The same samples were used to measure $\delta^{13}\text{C}_{\text{Carb}}$ from the aquifer matrix. This process was carried out by grinding a small amount of each sample, sieving with 100 micro screens. About 20 g of the sample was prepared from the same method and used for ^{13}C which will later explain and measure $^{13}\text{C}_{\text{Carb}}$ concentration.

The dissolved components as sulphate and DIC were collected in 1000 ml bottles with the addition of barium chloride (BaCl₂.2H₂O), sodium hydroxide (NaOH) and zinc acetate Zn(OOCCH₃)₂.2H₂O at the field in order to precipitate sulphate and DIC as insoluble barium salts and to prevent any microbiological reaction (Zn). After only one day, the precipitation at the bottom of the bottle with about 100 ml to 120ml was transferred in a small bottle and sent for analyses.

^{13}C , $^{34}\text{S}_{\text{Sulphate}}$ and $^{18}\text{O}_{\text{Sulphate}}$ analysis started with samples preparation by decanting the sample under nitrogen gas (N₂) and then flowing into the vacuum filtration and sucking it off, then washing the precipitation neutral with distilled water (pH=7). The reason for N₂ gas flow during samples filtration processes is to avoid any adsorption of air CO₂ on the alkaline sample precipitation. Hereafter, the precipitation heats to about 70 °C for drying. The dry precipitation is scraped off the filter and divided into two parts, one for $^{13}\text{C}_{\text{carbonate}}$ and the other for $^{34}\text{S}/^{18}\text{O}_{\text{Sulphate}}$ as following:

- **Preparation of carbonate precipitation for measuring of ^{13}C :**

In this step amount, 1-2 mg of a carbonate-sample put in a bottle with membrane a cap under nitrogen gas flows until the bottle has filled completely with the sample and nitrogen gas. The second step was to inject of 1-2 drops of concentrated H₃PO₄ to

remove CO₂ before the samples are connected via the autosamples to the mass spectrometer, for carbon analysis.

- **Preparation of Sulphate for measuring of ³⁴S_{Sulphate} and ¹⁸O_{Sulphate}:**

The sample was separated into two parts and each put in crucibles. HCl was added to both precipitations to remove carbonate. After that there was a heating of 600 °C then a scraping of the precipitation from the crucibles and putting in to a mortar and homogenizer. Finally weighing the precipitation in the crucibles for ³⁴S_{Sulphate} and ¹⁸O_{Sulphate} perform the measurements.

Eventually, ³⁴S and ¹⁸O were analysed by using “delta S” and delta plus XL with pyrolysis TC/EA with an accuracy of 0.8‰ for δ³⁴S and 1.0‰ for δ¹⁸O. The ¹³C (DIC) analyses are measured by IRMS “delta S” with an accuracy of 0.1‰.

The ¹³C_{Soil} was collected from 4 locations using the methods of Doerr and Mueanich (1980). The sampling technique was performed by dipping 30 cm stainless steel tube (1 cm diameter) into the soil. The steel tube was connected to a plastic bottle through a flexible tube. The bottle contained a solution consisting of (BaCl₂ + NaOH) and was conducted with a pump. The task of the pump was for sucking CO₂ from the soil through the alkaline solution. The pumping device is DIGIFLAM 3000 OFD, an infrared device used for gas measurements of air, CO₂ and CH₄. The BaCl₂ solution reacts with CO₂ and produces precipitation consisting of BaCO₃ which is prepared in the laboratory by the conventional technique used for ¹³C.

Major ion determination was conducted by Ion Chromatography (IC) at a detection limit of 1 mg.L⁻¹ for every ion except fluoride limit of (0.1 mg.L⁻¹).

For trace metals the emission spectrometry with a technique of inductively coupled plasma (ICP-OES) was used. The measuring accuracy are at 0.04 mg.L⁻¹ for Al, Ni Pb and 0.008 mg.L⁻¹ for Cd, Fe, Cu, Co, Cr, Mn, Mo, V and Zn.

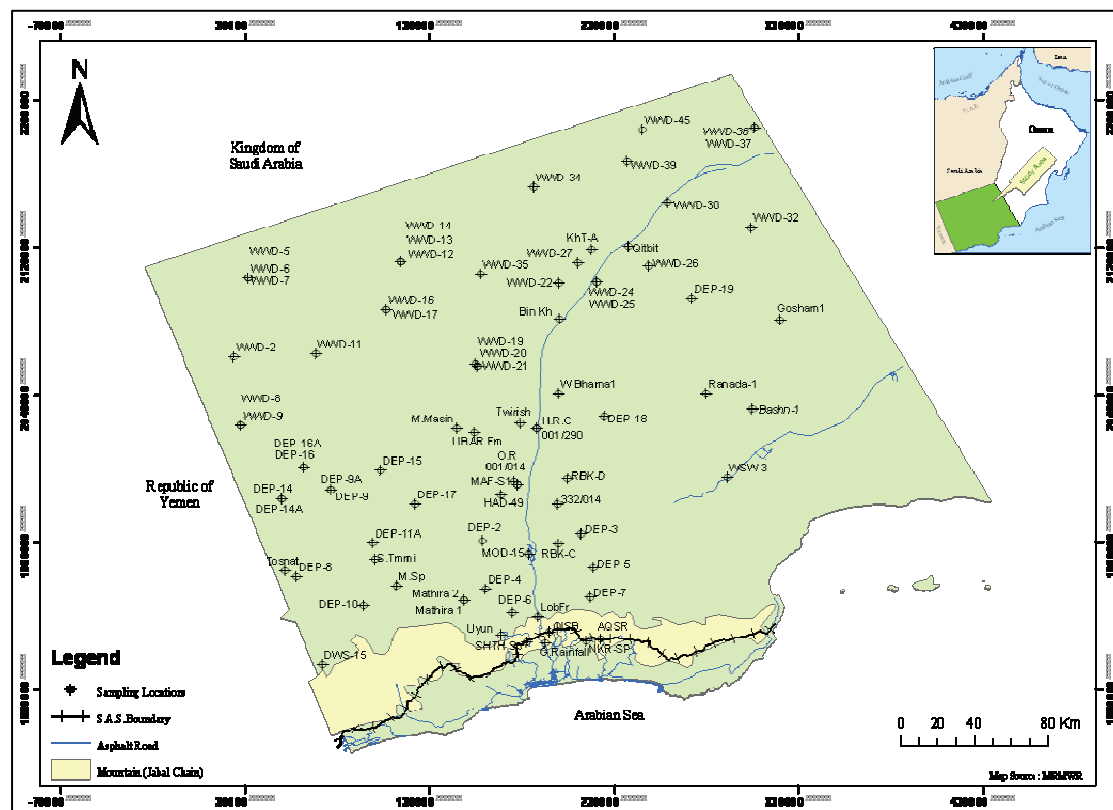


Figure 4.1 Sampling locations from all aquifers

4.2 Data Choices

During the period between 2008 and 2009, three campaigns of sampling were carried out. The data results were compiled together in (Annex: A-1 to A-5) for chemical, isotopes, trace elements and noble gases analyses. They were then selected to complete the record per well or spring if there is more than one record. Despite most samples having been selected from 2009, priority was given for completed analysis records regardless the year. The purpose of this procedure was to form one final table for each of the following type of analyses: hydrochemistry (Table 4.1) and isotopes (Table 4.10) to be used for different correlation plots and diagrams, and for the discussion of the data. Other types of data such as ^{14}C , noble gases, $^{13}\text{C}_{\text{lithology}}$, $^{13}\text{C}_{\text{Soil}}$, aquifer matrix composition and tracer metals which have an unique reading were used as is. Reliability of the data was taken to account after comparing records with each other and historical data of the boreholes if they exist.

CHAPTER 4

Table 4.1 Results of the hydrochemical analyses of groundwater and precipitation in the Najd region

Local Name	Site ID	Aquifer	Sample Date	Temp °C	pH	EC $\mu\text{S cm}^{-1}$	Ca ²⁺ meq.L ⁻¹	Mg ²⁺ meq.L ⁻¹	Na ⁺ meq.L ⁻¹	K ⁺ meq.L ⁻¹	Si ²⁺ meq.L ⁻¹	HCO ₃ ⁻ meq.L ⁻¹	Cl ⁻ meq.L ⁻¹	SO ₄ ²⁻ meq.L ⁻¹	NO ₃ ⁻ meq.L ⁻¹	F ⁻ meq.L ⁻¹	Br ⁻ meq.L ⁻¹	Si mg.L ⁻¹	SiO ₂ mg.L ⁻¹	SAR	TDS mg.L ⁻¹	T.Hardness mg.L ⁻¹
KhT-A	BG117784AA	A	3/5/09	31.3	8.4	2095	6.4	2.6	12.1	0.4	0.1	0.4	17.1	3.6	0.0	0.1	0.0	0.6	1.2	5.7	1252	452
M.Masin	YA729072AA	A	20/4/09	32.6	7.2	2460	10.8	6.8	10.5	0.1	0.2	2.9	14.9	10.8	0.3	0.1	0.0	13.9	29.2	3.5	1739	886
Mathira 1	YV826752BA	A	26/5/09	32.8	8.0	1449	1.6	2.8	8.0	0.2	0.2	0.9	9.1	3.5	0.0	0.2	0.0	0.3	0.7	5.3	785	224
NKR-SP	BE105632AC	A	24/5/08	26.4	7.2	1275	6.3	2.0	3.7	0.3	0.0	4.8	6.2	1.2	1.3	0.0	0.0	8.2	17.1	1.8	771	417
O.R	ZV191273AA	A	5/4/09	32.8	7.4	2864	10.1	5.9	14.1	0.2	0.1	2.3	17.1	10.9	0.5	0.1	0.0	12.0	25.2	5.0	1870	806
SHTH Sp	AE803515AC	A	24/5/08	26.0	8.1	909	4.7	1.6	3.5	0.0	0.0	3.8	4.7	1.0	0.3	0.0	0.0	11.5	24.1	1.9	580	321
TWIRISH	AF123492AA	A	5/4/09	33.2	7.1	2590	12.5	6.6	11.0	0.1	0.2	2.9	14.5	15.3	0.4	0.2	0.0	15.2	31.9	3.6	1988	960
WWD-20	YA859494BA	A	6/5/09	30.1	8.1	5400	21.7	14.2	23.4	1.2	0.2	0.1	22.8	41.8	0.0	0.5	0.0	9.7	20.4	5.5	4088	1809
WWD-24	BG200046CA	A	3/5/09	29.0	8.8	1537	2.2	2.7	9.1	0.3	0.1	0.6	9.7	4.7	0.0	0.1	0.0	0.4	1.0	5.8	885	247
WWD-26	BG409917AA	A	3/5/09	33.7	8.6	2902	13.5	5.8	11.6	0.3	0.2	0.5	15.6	17.8	0.0	0.2	0.0	0.5	1.0	3.7	2049	970
WWD-30	BG549421AA	A	3/5/09	32.9	8.6	9880	31.3	16.5	59.7	1.2	0.3	0.6	70.1	45.3	0.0	0.2	0.0	0.7	1.5	12.2	6932	2400
WWD-45	BG485361BA	A	21/4/09	32.3	8.2	2982	14.4	7.2	16.2	0.4	0.2	0.5	16.7	24.2	0.0	0.2	0.0	0.5	1.1	4.9	2537	1088
DEP-15	YV399518AA	B	21/5/08	32.3	7.9	981	3.2	3.0	4.6	0.2	0.1	1.7	5.0	3.9	0.0	0.1	0.0	2.2	4.7	2.6	638	317
DEP-16A	XV997655BA	B	12/4/09	29.9	11.1	2126	8.4	0.5	10.9	1.4	0.4	-2.2	10.7	8.0	0.0	0.1	0.0	2.3	4.7	5.2	1339	446
DEP-17	YV578833AA	B	11/4/09	35.9	7.5	1467	5.4	5.1	7.0	0.1	0.4	3.7	8.3	4.6	0.0	0.1	0.0	18.6	39.2	3.1	1008	525
DEP-9	YV182483AA	B	12/4/09	32.1	8.9	904	0.9	2.5	5.3	0.1	0.1	0.7	5.8	1.7	0.0	0.1	0.0	0.2	0.4	4.0	506	172
MAF-SI(001/015)	ZV193035AA	B	18/11/09	35.0	7.0	2420	8.8	8.5	9.0	0.5	0.0	0.0	11.5	10.8	0.0	0.0	0.0	0.7	1.5	1.7	3306	2136
WWD-13	YB406953BA	B	31/3/09	33.2	9.2	3840	26.6	15.9	7.8	1.1	0.3	0.1	5.7	44.1	0.0	0.2	0.1	0.7	5.8	3.1	3962	2182
WWD-17	YA389228BA	B	31/3/09	31.6	8.6	4170	26.9	16.4	14.5	1.3	0.3	0.1	6.8	53.2	0.0	0.3	0.2	2.8	21.6	1.0	3031	2017
WWD-19	YA859494AA	B	6/5/09	31.5	8.5	3990	23.5	16.5	4.6	0.8	0.2	1.0	4.9	41.3	0.0	0.3	0.0	10.3	0.7	1.7	3314	2126
WWD-5	XA694716BA	B	13/4/08	31.5	9.8	3057	26.5	15.7	8.0	0.8	0.4	0.2	6.7	44.2	0.0	0.2	0.0	0.4	0.7	1.7	3314	2126
WWD-9	XA612881BA	B	4/5/08	31.7	8.8	2067	2.9	7.9	17.3	0.5	0.2	0.6	14.1	6.0	0.0	0.1	0.0	0.8	1.6	7.4	1386	545
001/014	ZV193035BA	C	28/4/08	36.2	7.6	2132	5.4	7.3	10.9	0.7	1.3	1.9	13.8	6.5	0.0	0.3	0.0	10.9	23.0	4.3	1368	640
001/290	AF829201AA	C	6/4/09	35.5	7.4	1795	5.9	6.4	8.3	0.3	0.5	2.3	11.4	7.1	0.0	0.3	0.0	9.6	20.3	3.3	1238	620
Bashn-1	CF035107AA	C	5/5/09	32.4	9.3	1691	3.9	2.8	10.5	0.4	0.2	0.5	10.5	6.7	0.0	0.1	0.0	0.1	0.2	5.7	1084	337
Bin Kh	BF080077AA	C	3/5/09	34.1	7.9	1717	4.1	5.8	6.1	0.4	0.1	2.2	7.4	7.7	0.0	0.3	0.0	9.5	19.9	2.7	1045	503
DEP-14	XV876910AA	C	4/5/08	32.3	9.0	1071	1.6	3.6	6.5	0.3	0.0	1.0	5.8	3.8	0.0	0.1	0.0	0.6	1.4	4.0	661	266
DEP-16	XV997655AA	C	12/4/09	29.0	8.5	1372	1.9	6.8	5.2	0.1	0.6	1.8	5.9	6.1	0.0	0.2	0.1	1.4	2.9	2.5	824	443
DEP-18	BF223760AA	C	2/5/09	32.0	8.6	1349	1.7	2.9	6.7	0.7	0.2	1.2	6.1	5.3	0.0	0.2	0.0	1.3	2.7	4.4	764	233
DEP-19	BF792149AA	C	3/5/09	32.5	9.0	2575	2.5	3.6	17.4	0.7	0.4	0.6	17.8	5.5	0.0	0.3	0.0	0.3	0.5	9.9	1440	308
DEP-2	YV955966AA	C	8/4/09	31.1	8.6	2229	3.4	7.7	13.5	0.3	0.5	0.9	19.3	5.2	0.0	0.3	0.0	2.9	6.0	5.7	1573	562
DEP-9A	YV182483BA	C	12/4/09	32.9	8.5	1329	2.7	7.7	6.0	0.1	0.6	1.4	6.5	7.7	0.0	0.3	0.0	0.6	1.2	2.7	954	521
Goshami	CF179989AA	C	5/5/09	32.6	8.5	3441	4.0	8.1	22.1	0.6	0.2	1.3	23.0	11.3	0.0	0.2	0.0	0.4	0.8	9.8	1211	614
M.Sp	YV439388AC	C	6/5/08	29.8	7.9	1859	6.3	3.9	10.7	0.3	0.1	2.8	10.7	5.5	0.2	0.1	0.0	10.1	21.3	4.7	2203	515
Qitbit	BG317999AA	C	3/5/09	37.8	7.7	2962	7.4	10.5	13.1	0.8	0.5	1.8	13.9	16.1	0.0	0.3	0.0	10.3	21.6	4.3	1961	904
Ranada-1	BF840101AA	C	5/5/09	31.8	8.8	1088	1.4	2.1	6.6	0.3	0.3	0.8	7.1	2.7	0.0	0.3	0.0	0.3	0.7	4.9	626	179
RBK-C	BE050838AA	C	18/8/09	32.6	9.3	1879	1.8	2.3	14.0	0.4	0.2	0.4	15.2	1.3	0.0	0.2	0.0	0.0	0.1	9.7	1018	209
S.TMMI	YV347775AA	C	11/4/09	33.0	7.4	1814	6.6	6.1	8.8	0.0	0.4	3.7	10.0	6.5	0.0	0.2	0.0	10.7	22.4	3.5	1216	639
UbarFm	YA819821AA	C	29/4/08	36.3	7.4	1332	2.7	3.9	5.9	0.3	0.7	2.6	5.6	4.6	0.0	0.3	0.0	9.8	20.5	3.3	782	331
W.Bhaml	BF040020AA	C	2/5/09	31.5	8.9	1576	2.1	5.1	9.7	0.4	0.4	0.7	12.1	4.0	0.0	0.3	0.0	0.3	0.7	5.1	992	366

CHAPTER 4

Table 4.1 Continued

Local Name	Site ID	Aquifer	Sample Date	Temp °C	pH	EC $\mu\text{S cm}^{-1}$	Ca ²⁺ meq.L ⁻¹	Mg ²⁺ meq.L ⁻¹	Na ⁺ meq.L ⁻¹	K ⁺ meq.L ⁻¹	SP ²⁺ meq.L ⁻¹	HCO ₃ ⁻ meq.L ⁻¹	Cl ⁻ meq.L ⁻¹	SO ₄ ²⁻ meq.L ⁻¹	NO ₃ ⁻ meq.L ⁻¹	F ⁻ meq.L ⁻¹	Br ⁻ meq.L ⁻¹	Si mg.L ⁻¹	SiO ₂ mg.L ⁻¹	SAR	TDS mg.L ⁻¹	T. Hardness mg.L ⁻¹
WWD-11	YA051882AA	C	13/4/08	36.7	8.1	1733	6.8	9.5	6.6	0.5	0.6	3.2	6.1	12.2	0.0	0.3	0.1	11.7	24.7	2.3	1354	823
WWD-12	YB406944AA	C	31/3/09	37.4	8.0	2277	9.9	11.1	6.7	0.6	0.4	1.2	7.4	20.4	0.0	0.3	0.0	12.0	25.2	2.1	1824	1054
WWD-16	YA389227AA	C	31/3/09	38.6	7.6	2163	11.6	11.7	6.9	0.6	0.5	2.2	6.7	21.8	0.0	0.3	0.1	14.2	29.9	2.0	1949	1170
WWD-2	XA557476BA	C	13/4/08	36.6	8.3	1564	5.2	3.9	6.0	0.2	0.6	3.6	4.9	7.6	0.0	0.2	0.0	12.1	25.4	2.8	984	460
WWD-21	YA858545AA	C	6/5/09	36.5	8.0	1585	4.6	6.8	5.5	0.4	0.6	2.8	7.2	9.4	0.0	0.3	0.0	11.8	24.8	2.3	1145	575
WWD-22	BG200046AA	C	17/4/08	36.6	7.8	2050	8.6	9.4	7.9	0.8	0.6	1.8	7.8	12.8	0.0	0.3	0.1	10.1	21.2	2.6	1476	908
WWD-25	BG00002AA	C	16/4/08	37.6	7.8	1875	7.3	8.8	7.5	0.7	0.5	2.0	7.1	11.3	0.0	0.3	0.0	8.9	18.6	2.6	1339	809
WWD-27	BG110099AA	C	3/5/09	38.3	7.5	2159	5.3	8.0	6.7	0.6	0.5	1.9	7.4	11.0	0.0	0.4	0.0	10.5	22.0	2.6	1265	669
WWD-32	CG034063BA	C	5/5/09	31.4	9.0	5100	6.3	8.4	34.1	0.9	0.4	0.3	43.4	8.8	0.0	0.3	0.0	0.3	0.6	12.5	3048	743
WWD-34	AG856280BA	C	17/4/08	35.3	8.3	2855	13.8	12.7	14.9	1.1	0.5	1.4	14.3	22.4	0.2	0.3	0.1	11.6	24.3	4.1	2495	1331
WWD-35	YB809472AA	C	17/4/08	38.5	8.0	2169	11.4	10.7	6.8	1.0	0.5	1.7	6.0	15.5	0.1	0.3	0.0	12.2	25.7	2.1	1605	1111
WWD-36	CG085491AA	C	5/5/09	35.0	8.2	8460	9.0	14.0	63.8	1.4	0.6	2.0	72.1	18.5	0.0	0.4	0.0	10.7	22.5	18.7	5411	1163
WWD-39	BG367633AA	C	21/4/09	36.6	8.0	4150	10.2	11.4	25.8	1.0	0.5	1.8	28.6	21.8	0.0	0.4	0.2	11.7	24.6	7.8	3128	1088
WWD-7	XA694716DA	C	1/4/09	30.7	8.5	1742	6.1	10.4	6.9	0.4	0.5	0.8	7.6	13.9	0.0	0.3	0.0	5.5	11.5	2.4	1415	830
WWD-8	XA612881AA	C	4/5/08	32.4	9.2	2049	4.7	1.6	17.9	1.6	0.3	0.2	14.5	6.6	0.0	0.1	0.0	0.3	0.6	10.0	1431	317
332/014	AE989051AA	D	28/4/08	38.6	7.5	1885	4.8	5.7	9.9	1.1	1.3	1.7	11.7	5.0	0.0	0.3	0.0	14.3	25.4	4.3	1182	528
AQSR	BE202783AA	D	10/5/08	30.8	7.3	2522	11.9	10.8	16.9	0.3	0.5	5.2	15.8	6.7	0.2	0.1	0.0	9.2	19.4	5.0	1848	1143
DEP-10	YV32265AA	D	13/5/08	33.8	7.3	1515	4.8	4.9	6.6	0.2	0.3	3.6	6.8	6.7	0.0	0.2	0.0	10.6	22.2	3.0	1017	491
DEP-11A	YV356616BA	D	11/4/09	31.1	9.2	1395	1.3	5.0	8.8	1.7	0.2	1.0	6.8	6.8	0.0	0.3	0.0	0.4	0.9	4.9	981	314
DEP-14A	XV876910BA	D	12/4/09	31.7	8.8	1540	1.7	6.7	8.9	0.4	0.3	1.3	7.1	8.2	0.0	0.2	0.0	0.5	1.1	4.3	1048	429
DEP-3	BE162450AA	D	25/5/09	32.6	8.8	1299	0.9	2.5	9.8	0.4	0.1	0.8	10.4	0.4	0.0	0.4	0.0	0.3	0.5	7.4	739	173
DEP-4	YV937394AA	D	26/5/09	32.2	11.7	5610	22.1	0.4	13.5	0.6	0.3	-19.3	15.0	2.1	0.0	0.0	0.0	2.4	5.0	4.0	1999	1125
DEP-5	BE149620AA	D	25/5/09	30.8	9.0	1320	0.7	2.3	7.9	0.6	0.1	0.7	7.4	1.6	0.0	0.3	0.0	0.3	0.7	6.4	642	152
DEP-6	YV123115AA	D	28/4/08	32.7	7.2	2101	5.9	5.2	11.7	0.3	0.7	3.2	13.5	5.0	0.0	0.2	0.0	10.2	21.4	4.9	1308	560
DEP-7	BE127955AA	D	25/5/09	28.0	9.0	2273	5.5	5.9	11.7	0.2	0.5	3.8	15.0	5.4	0.0	0.3	0.0	9.1	19.2	4.9	1388	574
DEP-8	XV935678AA	D	13/5/08	32.3	8.8	1042	2.0	3.5	5.9	0.2	0.2	0.6	5.7	4.2	0.0	0.2	0.0	0.3	0.6	3.5	655	280
DWS-15	YU181909AA	D	24/4/08	31.2	7.2	1098	5.3	3.7	3.6	0.1	0.1	3.1	3.0	5.6	0.1	0.1	0.0	8.7	18.3	1.7	736	452
H.R.C(103/395)	AF828170BA	D	6/4/09	33.0	9.5	1243	0.9	1.9	9.8	0.5	0.1	0.3	7.9	4.4	0.0	0.3	0.0	0.3	0.7	8.2	819	143
HAD-49	ZV084571AA	D	6/4/09	30.5	9.0	878	0.6	1.8	5.5	0.5	0.1	0.9	5.2	1.7	0.0	0.4	0.0	0.3	0.6	5.0	500	123
LobFr	AE818982AA	D	3/6/09	31.6	7.5	1807	6.0	4.7	7.1	0.1	0.1	4.0	10.2	3.0	0.3	0.1	0.0	6.8	14.4	3.0	1009	540
Mathira 2	YV826752AA	D	26/5/09	33.0	8.1	1541	4.2	5.3	6.2	0.1	0.2	3.5	7.4	4.5	0.0	0.3	0.0	13.2	27.8	2.8	920	480
MOD-15	AE853383AA	D	15/3/10	35.2	7.7	3070	9.7	10.8	9.0	0.1	0.0	0.0	16.4	5.0	0.2	0.2	0.0	8.6	18.2	2.4	1996	1028
QISB	AE915009AA	D	2/6/09	30.0	7.4	1140	4.0	2.2	4.3	0.1	0.0	5.0	3.7	2.5	0.2	0.1	0.0	0.4	0.8	10.8	838	123
RBK-D	BE094486AA	D	2/5/09	32.5	9.0	1567	0.8	1.7	12.0	0.5	0.1	1.1	11.9	0.6	0.0	0.3	0.0	0.4	0.8	3.0	1009	540
TOSNAT	XV849043AA	D	14/5/08	33.6	7.5	1480	4.7	5.4	5.0	0.4	0.4	3.8	5.2	8.1	0.0	0.2	0.0	8.4	17.6	2.2	1002	510
WSW-3	BE991437AA	D	5/5/09	35.0	7.5	1287	3.4	2.7	5.6	0.1	0.2	3.7	5.0	3.4	0.1	0.1	0.0	9.0	19.0	3.2	718	306
WWD-14	YB406954CA	D	31/3/09	39.5	7.5	3101	7.8	7.7	21.6	0.6	0.7	2.3	22.4	13.4	0.0	0.4	0.2	14.3	30.1	7.8	2326	777
WWD-37	CG085490BA	D	21/4/08	32.0	8.8	14910	16.1	21.0	156.2	1.9	1.3	0.4	167.0	11.1	0.0	0.8	0.4	0.5	1.1	36.1	10747	1871
WWD-6	XA694716CA	D	1/4/09	34.0	7.9	1837	7.0	9.1	8.0	0.2	0.7	3.5	8.5	10.6	0.0	0.3	0.0	9.8	20.7	2.8	1391	816
Geogib Rainfall	AE902477AF	Rainfall	Jul-Aug2008			229	0.0	0.1	0.0	0.1	0.0	1.8	0.6	0.2	0.0	0.0	0.0	0.4	0.9	0.0	91.05	3

Data reliability checking

Based on the chemical compositions (Table 4.1), ion charge balance between cations and anions were tested for data reliability using the equation:

$$\text{Data Reliability} = (\text{sum cations} - \text{sum anions}) / (\text{sum cations} + \text{sum anions}) \times 100.$$

With the exception of the rainfall sample, all samples (n=79) involved in the former calculation were found within an acceptable ratio which should be less than 10% (Datta and Subramanian 1997; Singh and Hasnain 1998; Bahar and Reza 2010), except five of them. These five samples were collected from (DEP-4, AQSR, MOD-15) from aquifer D and (WWD-9) in aquifer B and WWD-35 in aquifer C. However, four of them were represented with values ranging between 12% and 18%, and the fifth one was at 36%. These different percentages may relate to some missing data of bicarbonate or one of the following: sampling performance collection due to using bailer when boreholes were not pumping or analytical mistakes.

4.3 Correlation Matrix and Factor Analysis

For a better understanding of the relationship between different elements in each aquifer, the final list of chemical and tracer metals elements were compared with each other by using Factor Analysis Varimax (optimization) Extraction method equal to that of principle component analysis. The correlation coefficient is used to establish the relation between two variables. This type of statistic can predict the matching of one element with others. The measurements were conducted by using PHREEQC Aquachem package program (Parkhurst, 1995) for each aquifer separately. The correlation matrices results are significant to 1% and included EC, TDS and major ions (Table 4.2).

Additional statistic methods between variables were applied in order to determine the variables pattern origin and distribution. These classifications were conducted based on several variables including pH, Ca, Mg, Na, K, Sr, SiO₂, HCO₃, Cl, SO₄, F and Br. The factor analysis with varimax rotation (optimization) extraction method (principle component analysis) was performed using SPSS software to extract factors. As a result, four factors were extracted to present the contribution of chemical composition to groundwater in aquifer A and C. However two and three were

extracted at aquifer B and D. These factors were represented by accumulative variance (%) of about 94.09%, 87.04%, 83.13% and 83.43% of total samples in aquifers from A to D (Table 4.3).

The factor analysis reveals that the first two strongest relationships between TDS and the other elements occur with Ca, Na in aquifer A; SO₄, Ca in aquifer B and Na, Cl in both aquifers C and D. However this relation seems to be stronger in aquifer C and D. Major ions among themselves were found with strong correlations. In addition, the strongest relationship between ions was observed in Na-Cl in aquifers A, C and D; whereas between Ca-SO₄ in aquifer B. However aquifer D occupied the highest correlation percentage.

Table 4.2 Correlation coefficient matrix water parameters for all Najd aquifers

Aquifer A (n=12)	EC	pH	Ca ²⁺	Mg ²⁺	Na ⁺	K ⁺	Sr ²⁺	Cl ⁻	SO ₄ ⁻²	HCO ₃ ⁻	NO ₃ ⁻	F ⁻	Br ⁻	TDS
EC	1	0.30	0.95	0.94	0.98	0.86	0.69	0.97	0.91	-0.43	-0.39	0.59	-0.42	0.99
pH		1.00	0.17	0.16	0.37	0.42	0.13	0.34	0.27	-0.74	-0.31	0.20	-0.09	0.28
Ca ²⁺			1.00	0.96	0.89	0.82	0.69	0.87	0.95	-0.34	-0.42	0.63	-0.61	0.97
Mg ²⁺				1.00	0.87	0.86	0.76	0.83	0.98	-0.43	-0.52	0.78	0.01	0.96
Na ⁺					1.00	0.82	0.66	0.99	0.84	-0.44	-0.47	0.49	-0.27	0.97
K ⁺						1.00	0.53	0.77	0.88	-0.55	0.89	0.78	-0.22	0.87
Sr ²⁺							1.00	0.63	0.75	-0.57	-0.54	0.70	0.58	0.71
Cl ⁻								1.00	0.79	-0.39	-0.44	0.40	-0.01	0.95
SO ₄ ⁻²									1.00	-0.52	-0.54	0.81	-0.50	0.94
HCO ₃ ⁻										1.00	0.76	-0.62	0.18	-0.43
NO ₃ ⁻											1.00	-0.57	-1.00	-0.46
F ⁻												1.00	-0.45	0.63
Br ⁻													1.00	-0.48
TDS														1
Aquifer B (n=10)	EC	pH	Ca ²⁺	Mg ²⁺	Na ⁺	K ⁺	Sr ²⁺	Cl ⁻	SO ₄ ⁻²	HCO ₃ ⁻	NO ₃ ⁻	F ⁻	Br ⁻	TDS
EC	1	0.17	0.93	0.91	0.23	0.74	0.50	-0.20	0.93	-0.31	0.00	0.93	0.91	0.96
pH		1.00	0.24	-0.04	0.21	0.66	0.42	0.04	0.20	-0.92	0.00	0.00	-0.56	0.17
Ca ²⁺			1.00	0.91	0.03	0.69	0.53	-0.43	0.99	-0.26	0.00	0.87	0.90	0.98
Mg ²⁺				1.00	0.11	0.44	0.34	-0.32	0.93	-0.02	0.00	0.92	0.91	0.94
Na ⁺					1.00	0.39	0.28	0.73	0.09	-0.35	0.00	0.15	0.72	0.22
K ⁺						1.00	0.58	0.00	0.66	-0.80	0.00	0.57	0.50	0.70
Sr ²⁺							1.00	0.24	0.44	-0.22	0.00	0.33	0.38	0.52
Cl ⁻								1.00	-0.44	-0.23	0.00	-0.31	-0.33	-0.27
SO ₄ ⁻²									1.00	-0.24	0.00	0.92	0.96	0.99
HCO ₃ ⁻										1.00	0.00	-0.16	0.31	-0.28
NO ₃ ⁻											1.00	0.00	0.00	0.00
F ⁻												1.00	1.00	0.92
Br ⁻													1.00	0.96
TDS														1

Table 4.2 Continued

Aquifer C (n=33)	EC	pH	Ca ²⁺	Mg ²⁺	Na ⁺	K ⁺	Sr ²⁺	Cl ⁻	SO ₄ ⁻²	HCO ₃ ⁻	NO ₃ ⁻	F ⁻	Br ⁻	TDS
EC	1	-0.01	0.42	0.56	0.96	0.62	0.13	0.96	0.48	-0.08	-0.10	0.39	0.57	0.97
pH		1.00	-0.47	-0.45	0.17	0.08	-0.44	0.15	-0.38	-0.77	0.17	-0.42	-0.16	-0.08
Ca ²⁺			1.00	0.80	0.23	0.52	0.21	0.21	0.90	0.27	-0.50	0.38	0.19	0.58
Mg ²⁺				1.00	0.36	0.37	0.37	0.37	0.89	0.19	-0.58	0.63	0.23	0.69
Na ⁺					1.00	0.60	0.05	0.99	0.29	-0.19	0.66	0.24	0.58	0.91
K ⁺						1.00	0.07	0.54	0.52	-0.30	-0.64	0.18	0.34	0.66
Sr ²⁺							1.00	0.09	0.18	0.29	-0.78	0.52	0.12	0.16
Cl ⁻								1.00	0.26	-0.19	0.73	0.30	0.47	0.90
SO ₄ ⁻²									1.00	0.16	-0.40	0.48	0.32	0.64
HCO ₃ ⁻										1.00	0.59	0.14	0.48	-0.04
NO ₃ ⁻											1.00	-0.49	1.00	-0.10
F ⁻												1.00	0.23	0.44
Br ⁻													1	0.5
TDS														1
Aquifer D (n=24)	EC	pH	Ca ²⁺	Mg ²⁺	Na ⁺	K ⁺	Sr ²⁺	Cl ⁻	SO ₄ ⁻²	HCO ₃ ⁻	NO ₃ ⁻	F ⁻	Br ⁻	TDS
EC	1	0.23	0.70	0.76	0.96	0.63	0.63	0.96	0.39	-0.30	0.42	0.64	0.95	0.98
pH		1.00	0.23	-0.26	0.11	0.32	-0.20	0.10	-0.31	-0.83	-0.32	0.10	-0.27	0.09
Ca ²⁺			1.00	0.47	0.48	0.20	0.47	0.50	0.30	-0.58	0.43	0.04	0.94	0.59
Mg ²⁺				1.00	0.79	0.45	0.74	0.80	0.70	0.24	0.27	0.61	0.90	0.84
Na ⁺					1.00	0.68	0.62	1.00	0.42	-0.08	0.33	0.77	0.94	0.99
K ⁺						1.00	0.52	0.66	0.31	-0.22	0.00	0.66	0.64	0.65
Sr ²⁺							1.00	0.63	0.59	0.04	0.03	0.54	0.92	0.67
Cl ⁻								1.00	0.41	-0.08	0.48	0.76	0.94	0.99
SO ₄ ⁻²									1.00	0.23	-0.20	0.41	0.60	0.48
HCO ₃ ⁻										1.00	0.53	0.10	-0.20	-0.12
NO ₃ ⁻											1.00	-0.52	0.00	0.36
F ⁻												1.00	0.94	0.72
Br ⁻													1.00	0.96
TDS														1.00

The presence of major cations (Na, Ca, Mg) and Cl with high positive values indicates the salt water signature (Bahar and Reza, 2010). Overall the factors shows a presence of Ca, Mg, Na, K, SO₄ and Cl may relate to marine deposits such as gypsum and evaporites which may increase due to lithological dissolution. Whereas Sr and F are positive correlations in aquifers from B to D and this could be related to dissolution of carbonates such as aragonite and ion exchange. In addition, the positive correlation of SiO₂ and HCO₃ in all aquifers indicates dissolution of carbonate minerals or sulphate reduction of organic matters in the case of bicarbonate which is possible (Bahar and Reza, 2010). The Br samples involved in these calculations were 3, 4, 12 and 7 in aquifers from A to D. Therefore, Br positive correlation in A, B and D is not significant, however Br presence indicates influence by marine environmental condition and evaporites dissolutions.

The positive correlation between NO₃ and K (+0.89) in aquifer A are probably due to the fertilizers influences. The strongest relation in aquifer A rather than others exists in Shsir, Hanfeet and Helat Ar Rakah. The depth of the water strike in these areas varies between 20m to 30m. Therefore, fertilizers may reach the aquifer either through direct infiltration in the case of shallow aquifers or among the well head, which is often not protected in the private wells.

Table 4.3 Principle component varimax rotated factor analysis for Najd water parameters (n=79)

Parameter	Aquifer A				Aquifer B		
	Factor 1	Factor 2	Factor 3	Factor 4	Factor 3	Factor 2	Factor 3
pH	0.27	0.84	0.28	-0.22	0.20	0.82	0.27
Ca	0.89	0.32	-0.07	0.13	0.87	0.31	-0.25
Mg	0.83	0.52	-0.07	0.17	0.88	0.33	-0.12
Na	0.96	0.15	-0.18	-0.06	0.16	0.33	0.91
K	0.71	0.56	-0.26	-0.23	0.86	0.46	-0.05
Sr	0.57	0.37	-0.38	0.52	0.74	-0.11	0.18
SiO ₂	-0.13	0.20	0.88	0.28	0.08	-0.95	-0.02
HCO ₃	-0.24	-0.29	0.89	-0.05	-0.57	-0.75	-0.01
Cl	0.97	0.05	-0.14	-0.05	-0.30	-0.04	0.91
SO ₄	0.78	0.53	-0.20	0.14	0.89	0.36	-0.22
F	0.33	0.87	-0.32	0.17	0.94	-0.26	-0.03
Br	-0.02	-0.10	0.21	0.93	0.67	0.50	0.08
Variance	58.98	15.31	11.02	8.78	53.96	20.87	12.21
Cumulative % of variance for each aquifer	94.09				87.04		
Parameter	Aquifer C				Aquifer D		
	Factor 1	Factor 2	Factor 3	Factor 4	Factor 1	Factor 2	
pH	0.12	0.03	0.12	0.85	0.05	0.93	
Ca	0.95	0.14	0.11	-0.03	0.88	-0.37	
Mg	0.79	0.25	0.43	0.01	0.96	-0.06	
Na	0.19	0.93	0.11	0.12	0.90	0.33	
K	0.60	0.58	-0.09	0.25	0.57	0.61	
Sr	0.14	0.01	0.90	0.02	0.92	-0.08	
SiO ₂	0.65	-0.22	0.32	-0.60	0.15	-0.87	
HCO ₃	0.15	-0.39	0.35	-0.67	-0.05	-0.90	
Cl	0.14	0.94	0.18	0.09	0.90	0.31	
SO ₄	0.91	0.23	0.20	0.07	0.72	-0.31	
F	0.25	0.34	0.76	-0.12	0.73	0.52	
Br	0.43	0.00	0.43	0.44	0.91	0.28	
Variance	41.30	21.92	10.08	9.83	55.38	28.04	
Cumulative % of variance for each aquifer	83.13				83.43		

4.4 Evaluation of the Groundwater Hydrochemistry

4.4.1 Characterisation of water types

The geological structures, aridity and aquifers' characteristics together with water residence time control groundwater behavior and quality in Najd area (PAWR, 1986). Hence, aquifers (A, B & C) displays were restricted with the specific places of the Study Area, whereas aquifer D was distributed in whole Najd and acted as the dominant one. The evidence may suggest the influence of tectonic movements had affected the upper aquifers A to C more than with D. As a result, groundwater conduct from deeper (aquifer D) to higher aquifers probably occurs due to these fissures.

Groundwater chemistry varies among the different aquifers, notwithstanding that three of them are located within the same formation (UER). Due to the geological characteristics of this formation, it was difficult to determine a simple linear vector for groundwater-flow direction. However, in general, water in the western part of Najd is less mineralized than water from the eastern part of this region. Mineralization increases as one move toward the north/northeast in the direction of groundwater flow.

The total dissolved solid (TDS) of the 79 samples range between 500 to 10,747mg.L⁻¹ with general average of 1,682mg.L⁻¹. The lowest and highest TDS values were recorded in aquifer D at HAD-49 with 500mg.L⁻¹ and WWD-37 with 10,747mg.L⁻¹ respectively (Table 4.4). On average, the concentrations of dissolved ions reach about 2,123 mg.L⁻¹ in aquifer A and 2,055 mg.L⁻¹ in aquifer B, and are less concentrated with around 1,537 and 1,519 mg.L⁻¹ in the aquifers C and D.

The pH values range between 7.0 and 11.7, however the highest value was recorded at DEP-4 in aquifer D and the lowest was found at borehole MAF-S1(001/015) in aquifer B. The relationship between the electric conductivity ($\mu\text{S.cm}^{-1}$) and the total dissolved solids (mg.L⁻¹) was determined to be linear, which is generally known to be true (TDS = 0.725 EC [Hölting, 1992]), with the equation TDS = 0.71 EC - 57.38 ($R^2 = 0.95$) describes the relationship between these two parameters.

Table 4.4: Range of total dissolved solid (TDS) concentrations in each aquifer

Aquifer	TDS	TDS	EC	pH	Total samples
	Range [mg.L ⁻¹]	Average [mg.L ⁻¹]	Average [μ S.cm ⁻¹]	Range	
A	580 - 6932	2123	3029	7.1 - 8.8	12
B	506 - 3962	2055	2502	7.0 - 11.1	10
C	626 - 5411	1537	2277	7.4 - 9.3	33
D	500 - 10747	1519	2394	7.2 - 11.7	24

A mean distribution of the predominant ions of the groundwater from the different Najd aquifers shows in Table 4.5. For purposes of water type calculation, ions with total percentages less than 4 % were ignored, which was agreed with the same result obtained from Aquachem program calculation.

Table 4.5: Average of major ions concentration and their percentage in each aquifer

Average concentration of major ions [meq.L ⁻¹]											
Aquifer	Ca ²⁺	Na ⁺	Mg ²⁺	K ⁺	Si ²⁺	HCO ₃ ⁻	Cl ⁻	SO ₄ ²⁻	NO ₃ ⁻	F ⁻	Count
A	11.29	15.24	6.24	0.39	0.16	1.69	18.22	15.02	0.23	0.16	12
B	13.33	8.91	9.20	0.68	0.24	0.58	7.95	21.78	0.00	0.16	10
C	5.65	12.31	7.12	0.57	0.46	1.67	13.43	9.93	0.02	0.26	33
D	5.50	15.07	5.62	0.46	0.35	1.43	16.21	5.25	0.04	0.25	24
Abundance of major ions [meq%] and water types											
Aquifer	Ca ²⁺	Na ⁺	Mg ²⁺	K ⁺	Si ²⁺	HCO ₃ ⁻	Cl ⁻	SO ₄ ²⁻	NO ₃ ⁻	F ⁻	Water Type
A	16.4	22.2	9.1	0.6	0.2	2.5	26.5	21.9	0.3	0.2	Na-Ca-Cl-SO ₄
B	21.2	14.2	14.6	1.1	0.4	0.9	12.6	34.7	0.0	0.3	Ca-Mg-Na-SO ₄ -Cl
C	11.0	23.9	13.9	1.1	0.9	3.2	26.1	19.3	0.0	0.5	Na-Mg-Cl-SO ₄
D	11.0	30.0	11.2	0.9	0.7	2.8	32.3	10.5	0.1	0.5	Na-Ca-Mg-Cl-SO ₄
Average	14.9	22.6	12.2	0.9	0.5	2.4	24.4	21.6	0.1	0.4	

In general, representative dominant ions in the Najd aquifers all together follow the pattern of Cl⁻ (24.4%) > Na⁺ (22.6%) > SO₄²⁻ (21.6%) > Ca²⁺ (14.9%) > Mg²⁺ (12.2%) (Figure 4.2). These ions are forming 95.7% of the major ions, whereas the remaining 4.3% consists of subdominant ions. However these percentages were expected to be different in the comparison between individual aquifers (Figure 4.3).

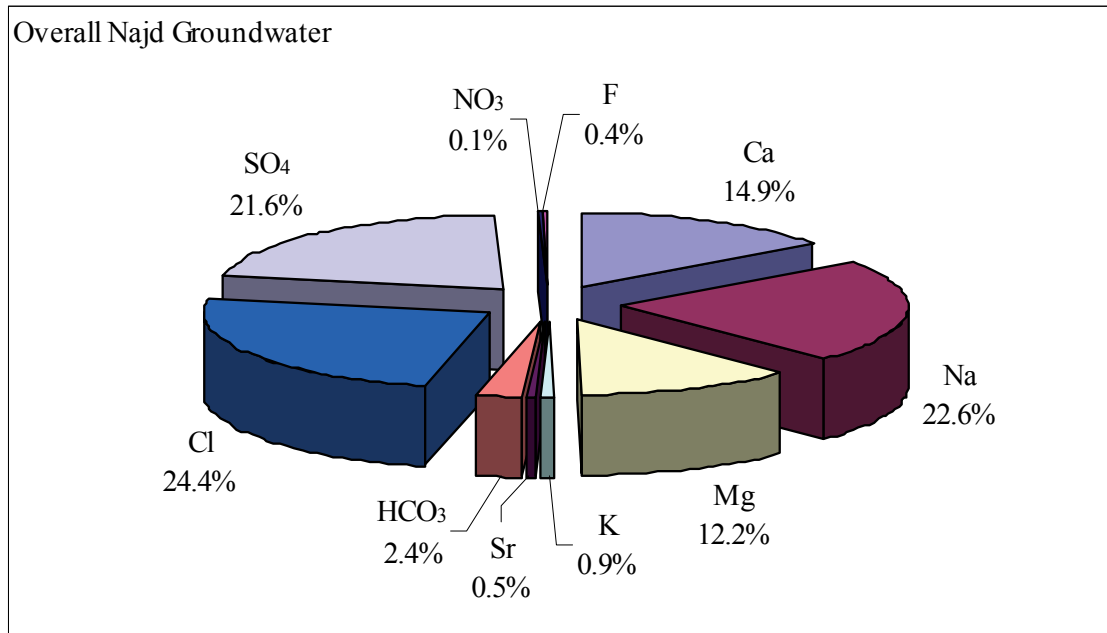


Figure 4.2 Overall dominant major ions in Najd groundwater

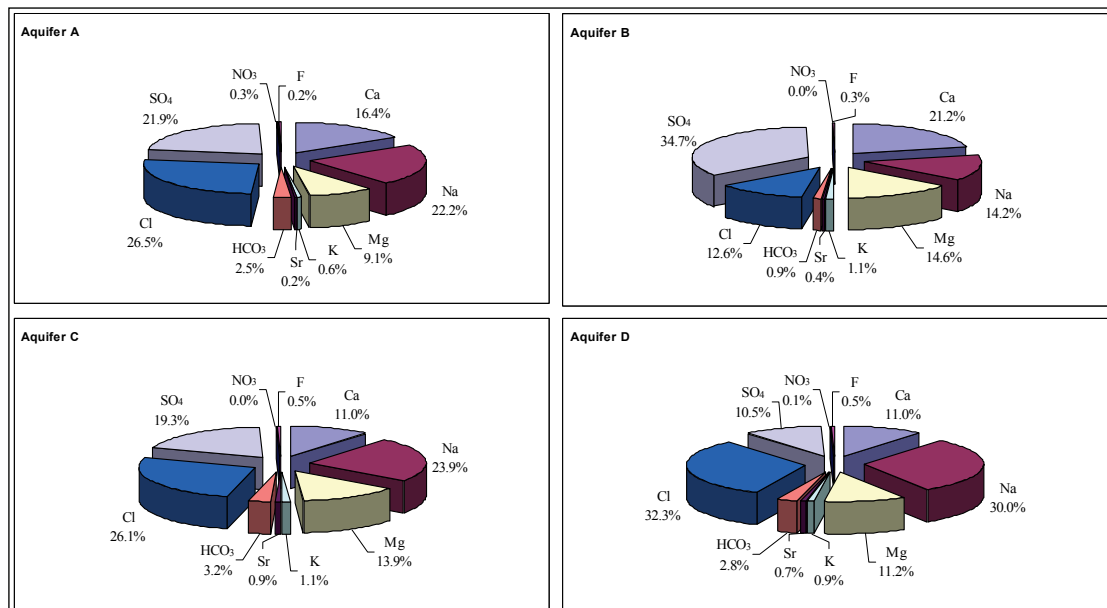


Figure 4.3 Dominant major ions in different Najd aquifers

The piper plot (Figure 4.4) provided above, shows the relationship of the major ions and reiterates that the majority of the groundwater chemistry consists of Na⁺, Ca²⁺, Mg²⁺, Cl⁻ and SO₄²⁻. Consequently, the water types of the Najd groundwater are characterized as earth alkaline-alkaline sulphate types occurring in the aquifers A and B. In the aquifer C and D, an alkaline-earth alkaline sulphate-chloride type is dominant with increasing chloride content in aquifer D.

Relative ion concentrations reached more than 70% for sulphate, chloride and sodium, and were between 20% and 60% for calcium and magnesium. Chloride, sodium and sulphate and calcium were the most abundant ions in the aquifers A and B, sodium and chloride were dominant in the deeper C and D aquifers. The presence of magnesium depends on the dissolution of dolomite-limestone or ion exchange calcite or aragonite (see below: Saturation index), and bicarbonate was the most abundant in the spring waters of aquifer A, near the recharge area in the Jabal.

By dividing the trilinear piper diagram into four (1,2,3,4) hydrochemical facies based on 50% of each direction, the water types determination could be detected (Bahar and Reza, 2010). Therefore the diagram distinguishes types of groundwater as the following: (1) Ca-Mg-HCO₃, (2) Na-K-HCO₃, (3) Na-K-Cl-SO₄ and (4) Ca-Mg-Cl-SO₄. Based on these classifications, data from all aquifers matched with types (3) and (4) which consist of Na-K-Cl-SO₄ and Ca-Mg-Cl-SO₄. The diagram also reveals mixing in groundwater between all aquifers, in which distinguishing them is difficult.

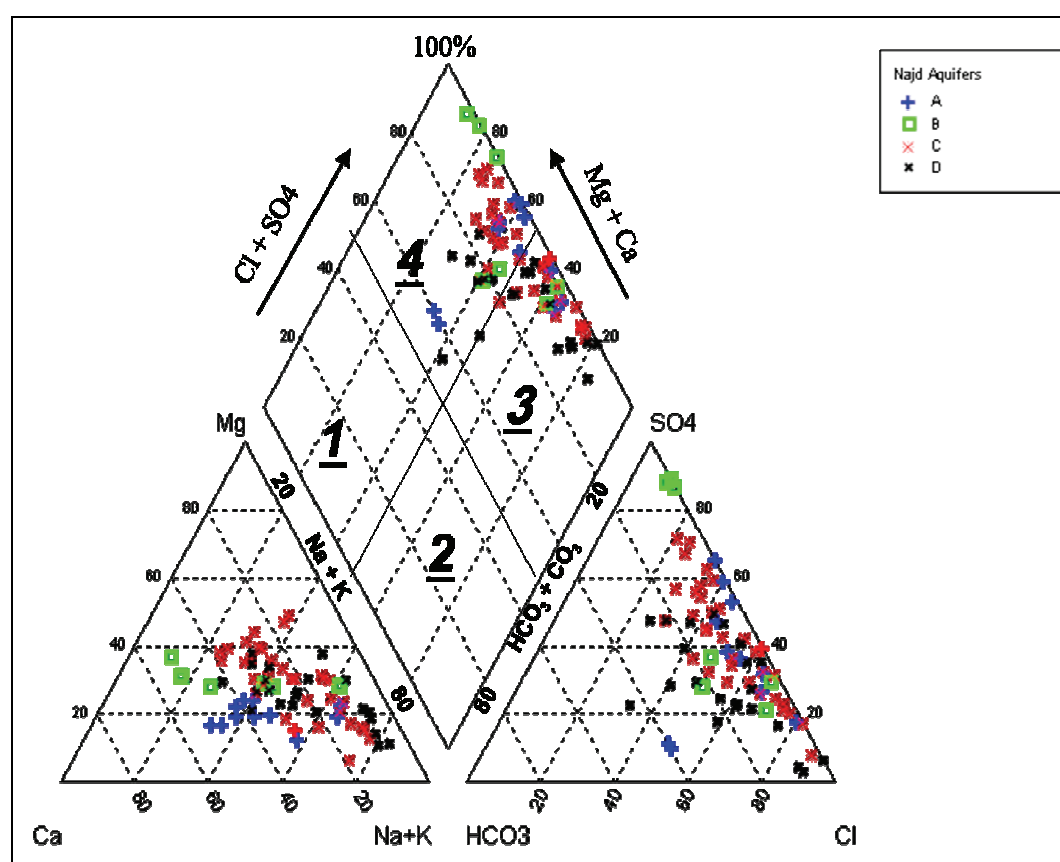


Figure 4.4 Piper diagram from all groundwater samples of Najd area including four developed hydrochemical facies

4.4.2 Hydrochemical signature

The ion percentages (Table 4.5) of dominant elements in each aquifer show clear distinguished patterns between calcium-sulphate characters in aquifer B and sodium-chloride characters in all other aquifers. These variables also highlight a general trend, where sulphate levels are highest at shallow depths (aquifer A & B) and sodium and chloride concentrations decrease from aquifer A to B, then increase with the increasing distance downward from the surface (deeper aquifers C-D). Magnesium concentration value is 9.1% in aquifer A and decreases with the depth from aquifer B (14.6%) to D (11.2%). High levels of sulphate detected percentages that were observed in aquifer B. Bicarbonate was present in the formations in relatively constant percentages and was recorded the lowest value of 0.9% in the B aquifer and the highest of 3.2% in aquifer D. In general, calcium, magnesium and sulphate follow similar trends which show the increase from aquifer A to reach the peak in aquifer B then decreasing from B to D. The reverse trends relationship is observed with sodium and chloride (Figure 4.5).

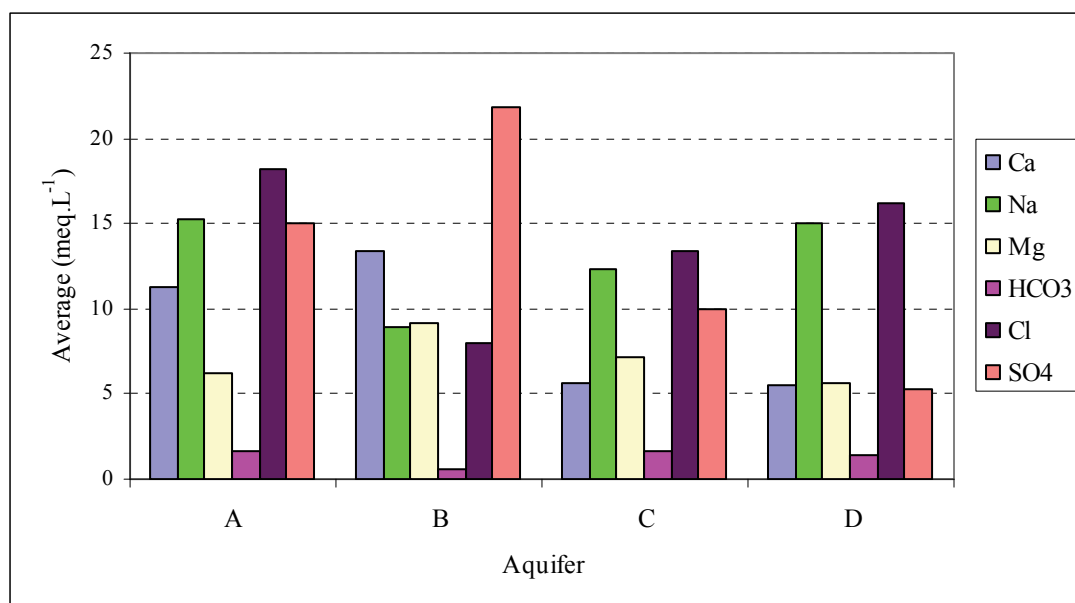


Figure 4.5 Comparison between major ions in Najd aquifers

The hydrochemistry plot (Figure 4.6) shows a mixing between aquifers, as it was explained by the relationship between mineralization and $\text{Na}/\text{Na}+\text{Cl}$. By referring to the figures, the values of $\text{Na}/\text{Na}+\text{Cl}$ they were generally within the range 0.4 to 0.55. Respectively, the data indicates sodium source which may result from one or both processes such as ion exchange and dissolution of aquifer matrix.

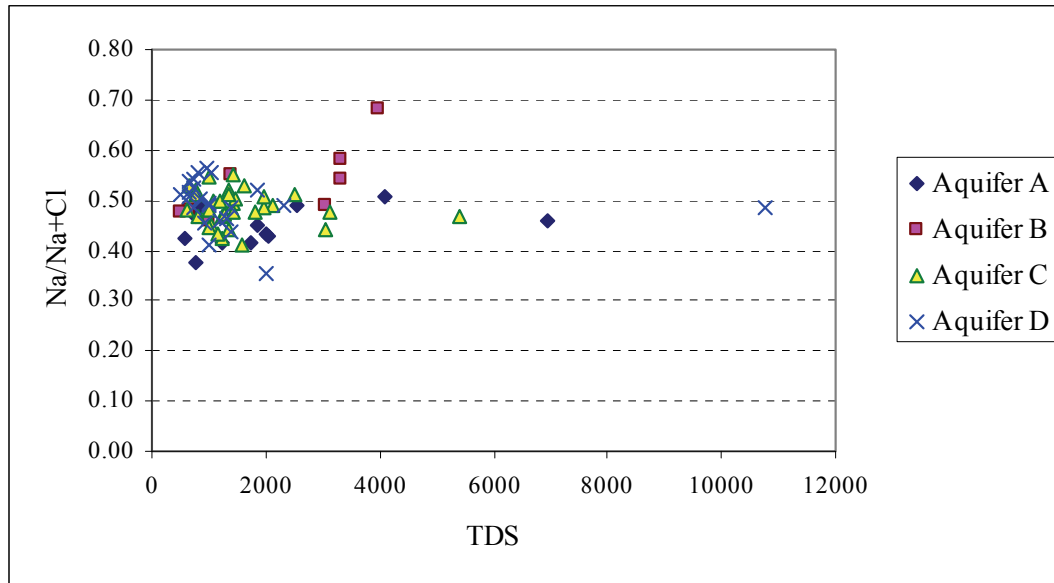


Figure 4.6 Total dissolved solids (TDS) versus Na/Na+Cl

The figure 4.7 shows an excess of calcium above magnesium in aquifer A which decreases the Mg/Mg+Ca ratio below 0.5. The similarity was observed in some boreholes located in aquifer B, C and D, however the majority of groundwater in these aquifers were indicated as having an excess of Mg over Ca. These different ratios were reflected with limestone-dolomite weathering in aquifer A and in some parts of the other aquifers (ratio <0.5). Another possibility is dolomite dissolution or calcite precipitation in aquifers C and D. By referring to saturation index calculation (SI) dolomite and calcite were over-saturated, therefore the chance of precipitation of either dolomite or calcite was probably expected rather than dissolution.

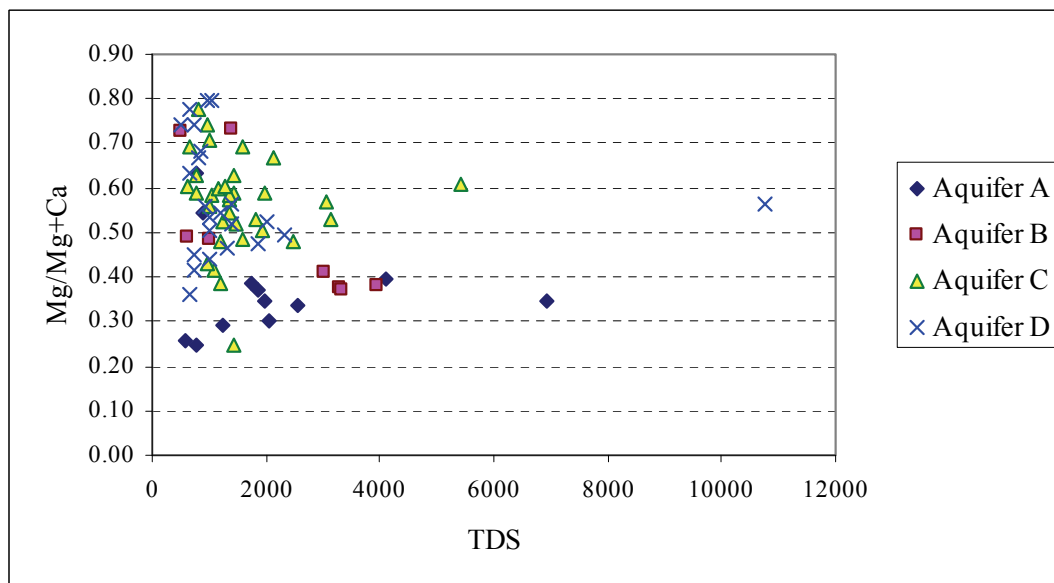


Figure 4.7 Total dissolved solids (TDS) versus Mg/Mg+Ca

The scattered plot (Figure 4.8) reflects an excess of sulphate over calcium (ratio <0.5) for the majority of the groundwater from aquifers A to D with the exception of minor wells from aquifer D and springs in aquifer A. The data shows groundwater mixing between all aquifers. The sulphate contribution may relate to dissolution of some gypsum layers in aquifer A and B. However, in aquifers C and D the minor gypsum layers in addition with sulphate reduction of inorganic matters as well as ion exchange between Ca and other elements played the role in this excess.

Moreover the data suggested calcium removal from groundwater as an ion exchange and calcite precipitation. In addition gypsum dissolution was assumed a part of aquifer A and D (ratio >0.5) which also agreed with SI result for gypsum and anhydrite.

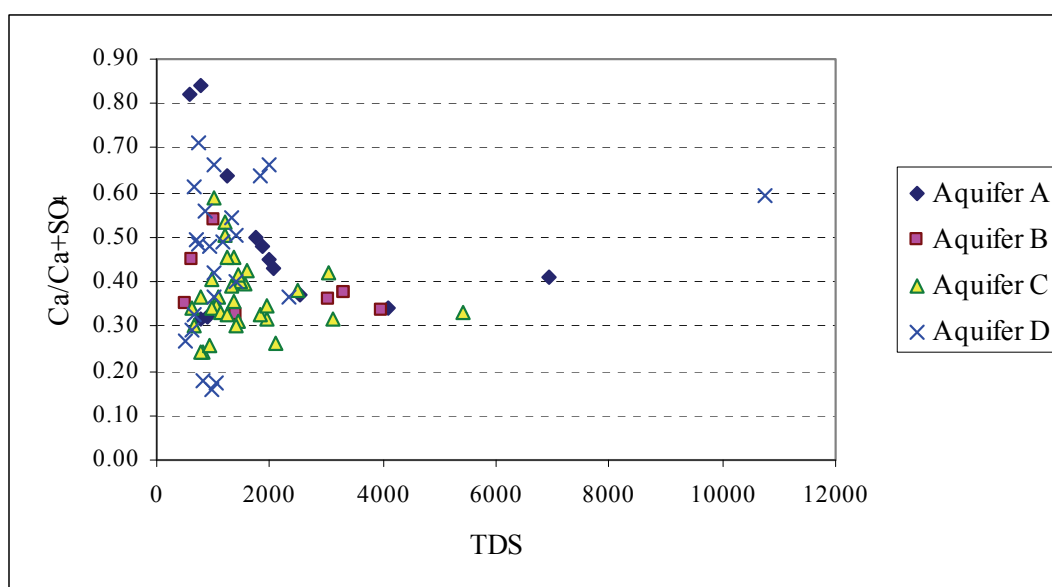


Figure 4.8 Total dissolved solids (TDS) versus $\text{Ca}/\text{Ca}+\text{SO}_4$ ratio

The linear plot (Figure 4.9) of TDS versus $\text{Cl}/\text{sum anion}$ (meq.L^{-1}) shows general mixing between aquifers. The anions become enrich (<0.3) in or near the recharge area at boreholes such as QISB, Tosnat and DWS-15 in aquifer D, and too by moving northward in the northwest of the Study Area around boreholes WWD-5, WWD-13 and WWD-17 in aquifer B; and in WWD-12 and WWD-16 in aquifer C. However the $\text{Cl}/\text{sum anion}$ ratio (>0.5) indicates enrichment of chloride over the sum anions. The ratio (>0.5) occurs in central Najd and increases northeastward. The differences between west and east of the Najd are probably due to mineralization increases with the flow direction or/and exist of brine and evaporites water.

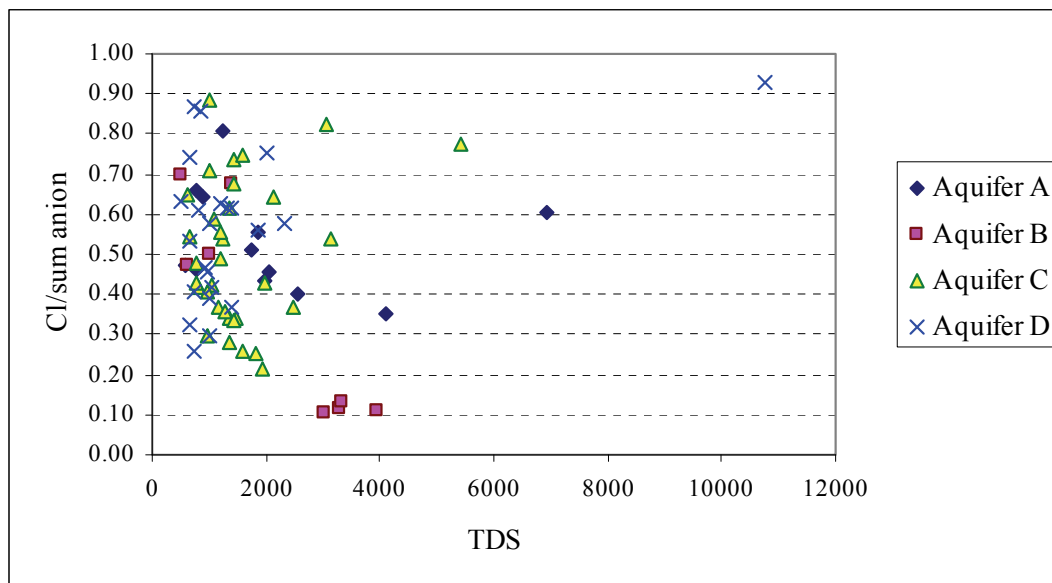


Figure 4.9 Total dissolved solids (TDS) versus Cl/sum anions ratio

In the X-Y plot (Figure 4.10) for SO_4 versus $\text{HCO}_3/\text{sum anions}$ Gogib rainfall and sea water samples were included. The plot shows a decreasing in $\text{HCO}_3/\text{sum anions}$ ratio from the recharge area towards the north. At the same time aquifer D and two springs in the Jabal chain were recorded with the highest ratio which indicates enrichment in bicarbonate. The excess of sulphate was observed to increase from deeper to shallow aquifers D to A. The sulphate concentration tends to increase in the direction of sea water especially in aquifers A and B and remarkably in C as well as with the flow direction. This may make sense in the relation of these waters sources. However the evidence is probably related to brine water sources.

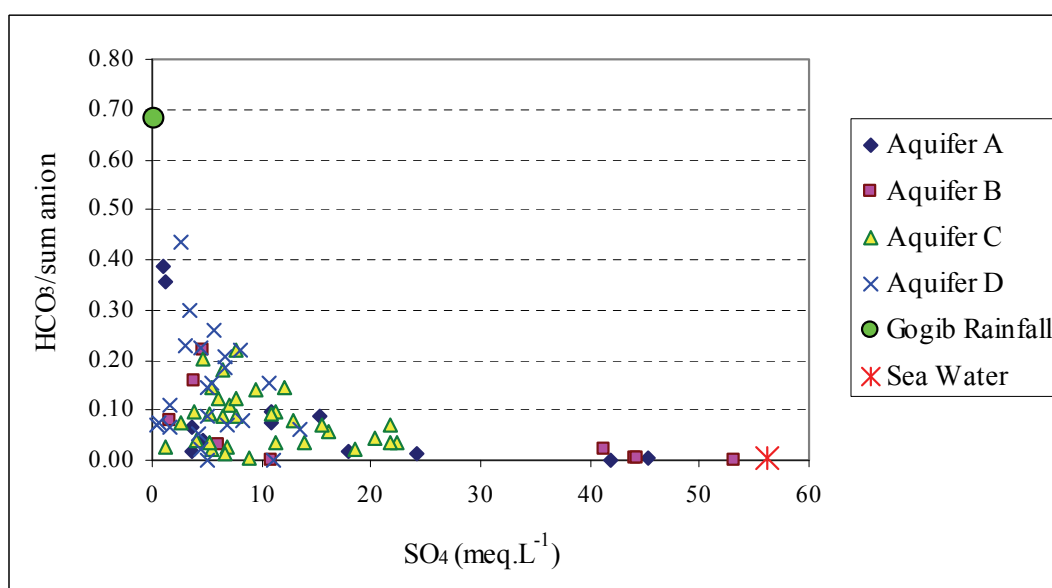


Figure 4.10 SO_4 versus $\text{HCO}_3/\text{sum anions}$ ratio compared with rainfall and sea water

A clustering of the hydrochemical signature was detected in the aquifers C and D, but also in B. This process seems to shift the water type in aquifer D to a sodium chloride dominated system in northern part of aquifer D. This obvious mixing and/or separation behavior is clearly expressed in the log-plot of major ion ratios (Figure 4.11). For example, the log-plot of ionic ratios of $(Ca^{2+} + Mg^{2+})/(Na^{+} + K^{+})$ versus (Cl^{-} / SO_4^{-2}) shows an increasing dominance of chloride and sodium along the C and D aquifer flow.

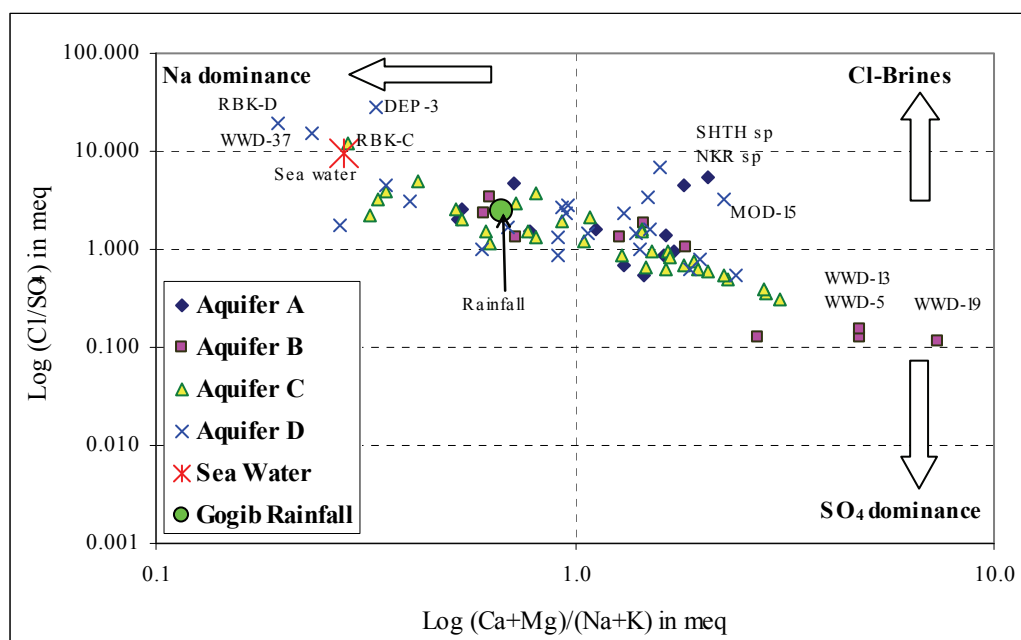


Figure 4.11 Earth's alkaline-alkaline ratio relative to the salt forming (Cl^{-} / SO_4^{-2}) ratio in the Najd aquifers

On account of the presence of gypsum in the formation matrices and the dissolution of gypsum common in the upper UER, sulphate-dominant groundwater reduces consequently the ionic ratio (Cl^{-}/SO_4^{-2}) in aquifer B. The increase of groundwater salinity and dominance of chloride and sodium as observed at well WWD-37 in the northeast of the Study Area tends to support the observation of gypsum dissolution in the different parts of the UER matrix.

4.4.3 Trace Elements

In total 69 samples were collected in the Study Area for trace elements analysis (Annex A-4). These analyses covered Fe, Pb, As, B, Mn, Cu, Ni, Cr, Zn, Al, Cd and Co from all aquifers. The correlation coefficient conducted by Aquachem Package for all the data together except Fe shows a very weak relationship between the elements. The maximum positive relation obtained was 0.3%. In order to evaluate these elements distribution several plots have been created. The elements appear to be controlled by redox conditions in the aquifers (Kebede, et al, 2010). In addition, the absences of pesticide and sewage contamination in most of the Najd area probably explain the low relationship between elements. In spite of this, four elements were used as examples to explain some of these relationships, as we may associate with oxidation processes and form this metal. At the same time it has the possibility to form sulphides and to present an element in sulphide. The element could be adsorbed on hydrous iron or the releases of the elements on the other hand. This occurs when iron is associated with elements become more active. Also involved is biochemical processes such as dimethyl arsenic and methyl arsenic acids (Hem, 1989). This is part of pesticides and is therefore present in groundwater close to the agriculture area. It indicated contamination of agricultural drainage or waste disposal water. The element is undesirable in water supply and classified as toxic for humans with a value greater than 0.01mg.L^{-1} . As nominated in several studies as harmful and can cause problems like skin cancer and bladder-based diseases. Based on this information, As is considered to be the priority substance for removing out of the drinking water (GTZ & DCo, 2009).

X-Y plots of Fe versus As (Figure 4.12) show mixing between all aquifers groundwater, even though some boreholes were recorded with a regular excess of Fe. However, there is no diagnostic trend for these elements. These often occurred in the oxides form and their low concentration may relate to the reactions with aquifers matrixes.

All boreholes were recorded with values of As within the permissible limit. Boreholes with relatively high level such Ubar Fm may relate to influence of fertilizer reaction with aquifer matrixes.

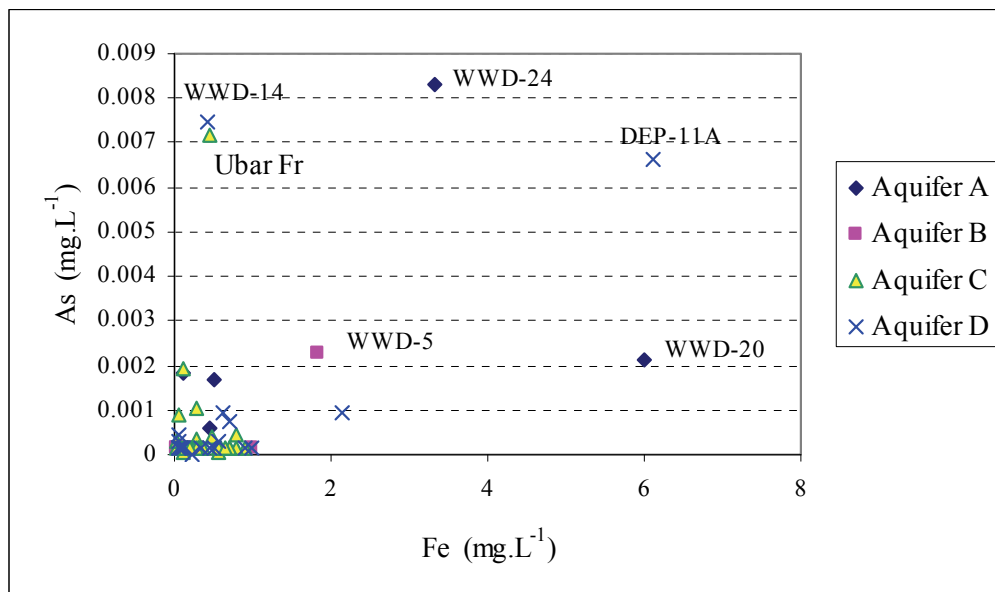


Figure 4.12 Fe versus As for different aquifers of Najd

Boron is important for plant growth yet concentrations greater than 1 mg.L⁻¹ of Boron can become harmful to many plants. Boron occurs in groundwater naturally, however detergents and waste water are the main sources for Boron concentration build up. Boron is found in many hydroxide such as B(OH)₄⁻ and some times replaced by F⁻. The maximum permissible limit for human drinking water is 0.5mg.L⁻¹ (Hem, 1989). Boreholes (Figure 4.13) with high concentration such as WWD-20 (Aquifer A) and WWD-17 (Aquifer B) are associated with sulphate concentrations exceeding 2000 mg.L⁻¹ which may due to some reduction.

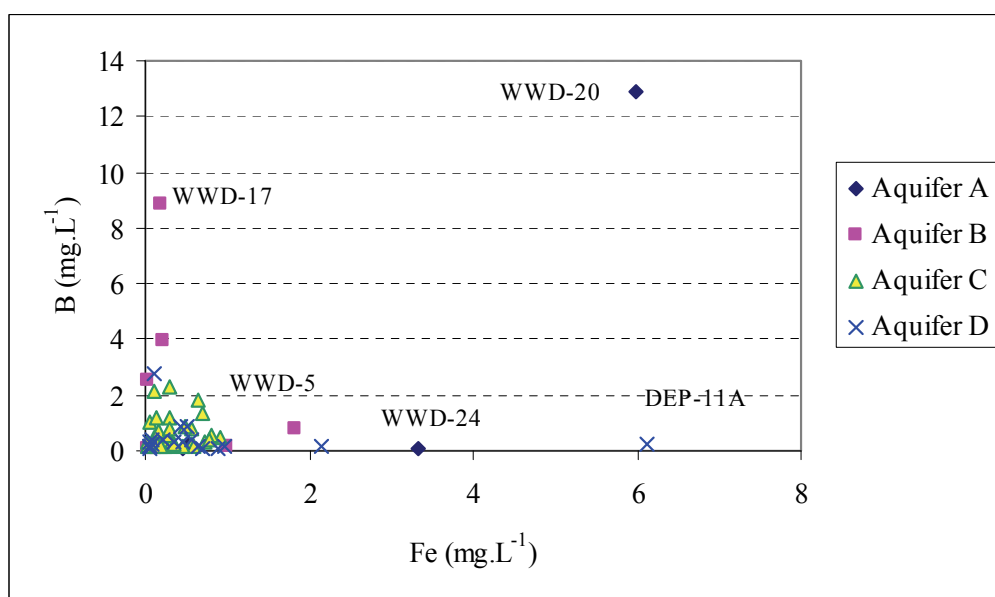


Figure 4.13 Fe versus B for aquifers A to D

The linear plot of As versus Cu (Figure 4.14) shows general excess of Cu concentration over As. The Cu element has the capability to form $\text{Cu}(\text{OH})_4^-$ and CuCO_3 which may cause low solubility. Therefore Cu concentration increases, and at the same time As decreases, which could be related to adsorption of As on iron oxides or manganese oxides (Hem, 1989). Both element concentrations are fitting with human drinking water ($\text{As} < 0.01 \text{ mg.L}^{-1}$, $\text{Cu} < 2 \text{ mg.L}^{-1}$). However, the slight rise of these elements' concentrations at borehole Ubar Fm is probably due to influence of fertilizer reaction with aquifer matrixes.

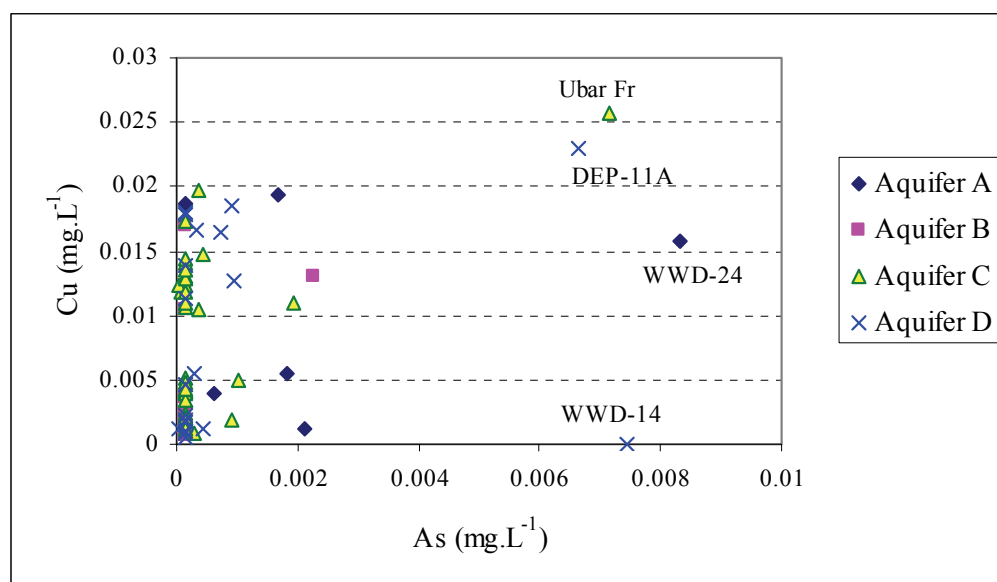


Figure 4.14 As versus Cu for all aquifers

4.4.4 Saturation Index (SI)

The limestone dominance in the aquifer matrix of the aquifers B to D influences the groundwater quality due to mineral dissolution and precipitation. The calculation of the saturation index helps us to understand the basic processes within the aquifers. Values of the saturation index are less than zero indicated under saturation; zero indicates saturation, and values greater than zero point to saturated ratios with regard to typical salt compounds (Table 4.6). Using the PHREEQC program package (Parkhurst, 1995) SI values were calculated for all water samples. When the

correlation of TDS (mg.L^{-1}) is plotted against $\text{SI} = \log(\text{IAP}/K_s)$ for calcite, dolomite, gypsum and halite, the outcome reveals that calcite and dolomite are generally oversaturated within the aquifer complex (Figure 4.15). However, groundwater and spring water are under-saturated with respect to evaporated minerals such as gypsum and halite. These waters also tend to precipitate carbonate minerals such as dolomite, calcite, and aragonite. This observation is indicative of non-significant dissolutions of calcite, and indicates that a Ca^{2+} addition would increase the calcite precipitation in this formation.

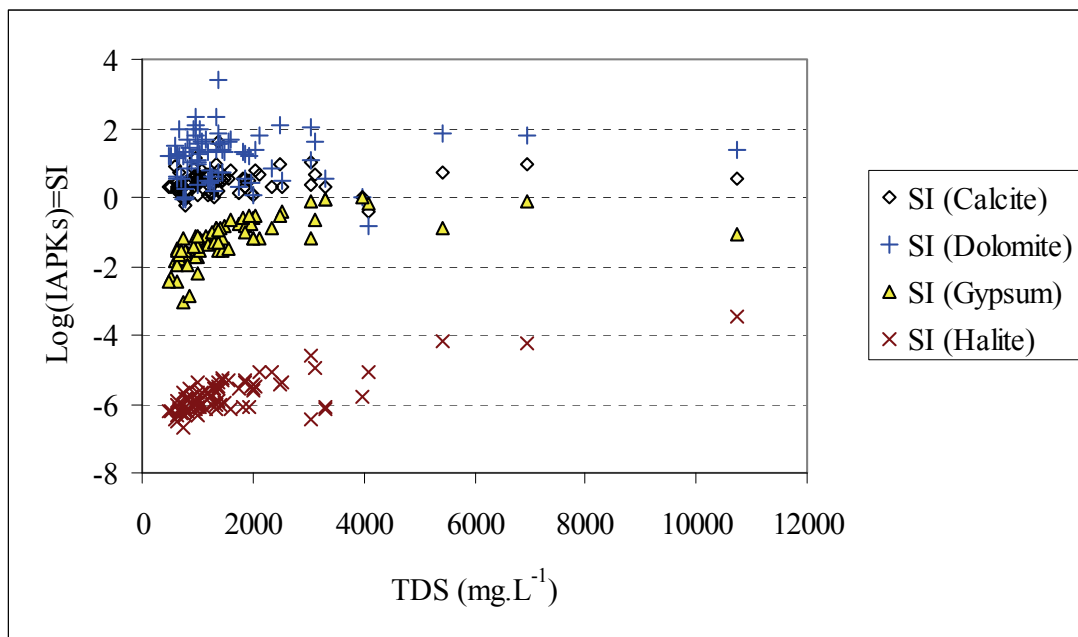


Figure 4.15 Saturation index in different aquifers versus Total dissolved solids (TDS)

Table 4.6 Saturation index (SI) of the groundwater

Local Name	Site ID	Aquifer	Calcite	Dolomite	Gypsum	Halite	Fluorite	Anhydrite	Aragonite
KhT-A	BG117784AA	A	0.3	0.5	-1.3	-5.4	-0.6	-1.5	0.2
M.Masin	YA729072AA	A	0.1	0.3	-0.8	-5.6	-0.2	-1.0	0.0
Mathira 1	YV826752BA	A	-0.3	-0.1	-1.8	-5.9	-0.4	-2.0	-0.4
NKR-SP	BE105632AC	A	0.2	0.0	-1.8	-6.3	-1.3	-2.0	0.0
O.R	ZV191273AA	A	0.3	0.5	-0.8	-5.4	-0.4	-1.0	0.1
SHTH Sp	AE803515AC	A	0.9	1.5	-1.9	-6.5	-1.4	-2.1	0.8
TWIRISH	AF123492AA	A	0.1	0.0	-0.6	-5.6	0.0	-0.8	-0.1
WWD-20	YA859494BA	A	-0.4	-0.9	-0.2	-5.1	1.0	-0.4	-0.6
WWD-24	BG200046CA	A	0.4	1.0	-1.6	-5.8	-0.9	-1.8	0.3
WWD-26	BG409917AA	A	0.8	1.4	-0.5	-5.5	0.1	-0.7	0.6
WWD-30	BG549421AA	A	0.9	1.8	-0.1	-4.2	0.4	-0.3	0.8
WWD-45	BG485361BA	A	0.3	0.5	-0.4	-5.3	0.2	-0.6	0.2
DEP-15	YV399518AA	B	0.2	0.6	-1.5	-6.3	-0.7	-1.7	0.1
DEP-16A	XV997655BA	B	-1000	-1000	-0.9	-5.7	-0.1	-1.1	-1000
DEP-17	YV578833AA	B	0.4	1.0	-1.3	-6.0	-0.5	-1.5	0.3
DEP-9	YV182483AA	B	0.3	1.2	-2.3	-6.2	-1.0	-2.5	0.1
MAF-S1(001/015)	ZV193035AA	B	-1000	-1000	-0.9	-5.7	-1000	-1.0	-1000
WWD-13	YB406953BA	B	0.3	0.5	-0.1	-6.2	0.3	-0.2	0.1
WWD-17	YA389228BA	B	0.0	0.0	0.0	-5.8	0.6	-0.2	-0.1
WWD-19	YA859494AA	B	1.0	2.1	-0.1	-6.4	0.6	-0.3	0.9
WWD-5	XA694716BA	B	-256	-512	0.0	-6.1	0.4	-0.2	-256
WWD-9	XA612881BA	B	0.5	1.6	-1.5	-5.4	-0.6	-1.7	0.3
001/014	ZV193035BA	C	0.2	0.7	-1.3	-5.6	0.2	-1.4	0.1
001/290	AF829201AA	C	0.1	0.4	-1.2	-5.8	0.4	-1.3	0.0
Bashn-1	CF035107AA	C	0.8	1.6	-1.3	-5.7	-0.4	-1.5	0.6
Bin Kh	BF080077AA	C	0.5	1.2	-1.2	-6.1	0.3	-1.4	0.3
DEP-14	XV876910AA	C	0.7	2.0	-1.8	-6.1	-1.2	-2.0	0.6
DEP-16	XV997655AA	C	0.5	1.7	-1.6	-6.2	-0.3	-1.8	0.3
DEP-18	BF223760AA	C	0.4	1.3	-1.6	-6.1	-0.6	-1.8	0.3
DEP-19	BF792149AA	C	0.5	1.4	-1.6	-5.2	0.1	-1.8	0.4
DEP-2	YV955966AA	C	0.5	1.6	-1.5	-5.3	0.2	-1.7	0.4
DEP-9A	YV182483BA	C	0.6	1.8	-1.4	-6.1	0.0	-1.6	0.4
Goshaml	CF179989AA	C	0.7	1.8	-1.2	-5.1	-0.4	-1.4	0.5
M.Sp	YV439388AC	C	0.7	1.3	-1.2	-5.7	-0.5	-1.4	0.5
Qitbit	BG317999AA	C	0.1	0.4	-0.8	-5.5	0.6	-1.0	0.0
Ranada-1	BF840101AA	C	0.4	1.2	-2.0	-6.0	-0.2	-2.1	0.3
RBK-C	BE050838AA	C	0.5	1.4	-2.2	-5.4	-0.3	-2.4	0.4
S.TMMI	YV347775AA	C	0.3	0.8	-1.1	-5.8	0.0	-1.3	0.2
UBAR Fm	YA819821AA	C	-0.1	0.2	-1.5	-6.2	0.0	-1.7	-0.2
W.Bharn1	BF040020AA	C	0.5	1.6	-1.7	-5.7	-0.1	-1.9	0.4
WWD-11	YA051882AA	C	1.0	2.3	-0.9	-6.2	0.2	-1.1	0.8
WWD-12	YB406944AA	C	0.5	1.3	-0.6	-6.1	0.3	-0.8	0.4
WWD-16	YA389227AA	C	0.5	1.2	-0.6	-6.1	0.5	-0.7	0.4
WWD-2	XA557476BA	C	1.1	2.3	-1.1	-6.3	0.0	-1.3	1.0
WWD-21	YA858545AA	C	0.7	1.7	-1.1	-6.1	0.3	-1.3	0.5
WWD-22	BG200046AA	C	0.5	1.3	-0.8	-6.0	0.4	-1.0	0.4
WWD-25	BG000002AA	C	0.5	1.4	-0.9	-6.0	0.3	-1.1	0.4
WWD-27	BG110099AA	C	0.1	0.6	-1.0	-6.1	0.4	-1.2	0.0
WWD-32	CG034063BA	C	0.4	1.1	-1.2	-4.6	0.2	-1.4	0.2

Table 4.6 Continued

Local Name	Site ID	Aquifer	Calcite	Dolomite	Gypsum	Halite	Fluorite	Anhydrite	Aragonite
WWD-34	AG856280BA	C	1.0	2.1	-0.5	-5.5	0.6	-0.7	0.8
WWD-35	YB809472AA	C	0.7	1.7	-0.7	-6.2	0.3	-0.8	0.6
WWD-36	CG085491AA	C	0.7	1.9	-0.9	-4.2	0.4	-1.1	0.6
WWD-39	BG367633AA	C	0.7	1.6	-0.7	-4.9	0.5	-0.8	0.5
WWD-7	XA694716DA	C	0.6	1.5	-0.9	-6.0	0.2	-1.1	0.4
WWD-8	XA612881AA	C	0.5	0.7	-1.2	-5.3	-0.8	-1.4	0.4
332/014	AE989051AA	D	0.1	0.5	-1.4	-5.7	0.2	-1.5	-0.1
AQSR	BE202783AA	D	0.6	1.3	-1.0	-5.3	-0.1	-1.2	0.4
DEP-10	YV322265AA	D	0.1	0.4	-1.2	-6.1	0.0	-1.4	-0.1
DEP-11A	YV356616BA	D	0.7	2.1	-1.8	-5.9	-0.4	-1.9	0.5
DEP-14A	XV876910BA	D	0.6	2.0	-1.6	-5.9	-0.4	-1.8	0.5
DEP-3	BE162450AA	D	0.3	1.2	-3.0	-5.7	-0.1	-3.2	0.1
DEP-4	YV937394AA	D	-1000	-1000	-1.2	-5.5	-0.8	-1.4	-1000
DEP-5	BE149620AA	D	0.2	1.1	-2.5	-5.9	-0.4	-2.7	0.1
DEP-6	YV123115AA	D	0.0	0.2	-1.3	-5.5	0.0	-1.5	-0.1
DEP-7	BE127955AA	D	1.6	3.4	-1.3	-5.5	0.2	-1.5	1.5
DEP-8	XV935678AA	D	0.4	1.2	-1.7	-6.2	-0.5	-1.8	0.2
DWS-15	YU181909AA	D	0.0	-0.1	-1.2	-6.7	-0.7	-1.4	-0.2
H.R.C(103/395)	AF828170BA	D	0.2	0.8	-2.0	-5.8	-0.3	-2.1	0.0
HAD-49	ZV084571AA	D	0.3	1.2	-2.5	-6.2	-0.1	-2.7	0.1
LobFr	AE818982AA	D	0.4	1.0	-1.4	-5.9	-0.6	-1.6	0.3
Mathira 2	YV826752AA	D	0.8	2.0	-1.4	-6.1	0.2	-1.6	0.7
MOD-15	AE853383AA	D	-1000	-1000	-1.2	-5.6	0.2	-1.3	-1000
QISB	AE915009AA	D	0.3	0.5	-1.6	-6.5	-1.1	-1.8	0.2
RBK-D	BE094486AA	D	0.4	1.4	-2.9	-5.6	-0.3	-3.0	0.3
TOSNAT	XV849043AA	D	0.3	0.9	-1.1	-6.3	0.0	-1.3	0.2
WSW-3	BE991437AA	D	0.2	0.6	-1.5	-6.3	-0.4	-1.7	0.1
WWD-14	YB406954CA	D	0.3	0.9	-0.9	-5.1	0.6	-1.0	0.2
WWD-37	CG085490BA	D	0.5	1.4	-1.0	-3.5	1.2	-1.2	0.4
WWD-6	XA694716CA	D	0.8	1.9	-1.0	-5.9	0.4	-1.1	0.6

Note: Bold numbers are excluded from these calculations

4.4.5 Lithology of aquifer matrixes

The aquifer matrix analysis is used in the study as a parameter in order to find out if water-rock interaction influences the groundwater hydrochemistry. It furthermore helps for evaluation of groundwater ages by the ^{14}C method in limestone aquifers. The lithological samples covered 9 boreholes from aquifers A to D (A=2, B=1, C=3, D=3) (Table 4.7 a+b). The analysis shows that the elements Ca, Mg, Al, Si, S, Sr, Na, K and Fe occupy the majority in the aquifer matrix of each well. Consequently, it was suggested to ignore other elements or oxides.

Data reveals that Ca is the most dominant element in all boreholes with percentages of total elements ranging from 21.37% to 34.99% (Table 4.7b). Sulphur is the second

dominant in WWD-20 (aquifers A) (14.78%), WWD-13 (aquifer B) (13.13%) and WWD-25 (aquifer C) (9.44%); however it is less than 1% in the remaining samples. In addition Mg is the third dominant element in some boreholes located in aquifers A, B and C; with a percentage of 3.34% (WWD-20), 3.49% (WWD-13) and 5.23% (WWD-25) respectively. Whereas Mg occupied the second rank in several boreholes of aquifer D with values range between 0.9% and 2% (Table 4.7b).

Table 4.7 (a-b) Lithological results for 9 boreholes in Najd analyzed by using XRF

a) Related to oxides for light elements (according to the XRF analysis procedure)

Aquifer	Well Name	CaO %	MgO %	Al ₂ O ₃ %	SiO ₂ %	S %	Na ₂ O %	K ₂ O %	Fe ₂ O ₃ %	Sr %	Total Comp	Ignition Loss%	Total %
A	WWD-20	29.97	5.57	0.13	1.44	13.13	0.03	0.04	0.09	1.25	51.65	29.5	81.2
A	WWD-24	47.61	0.88	0.75	5.24	0.55	0.03	0.13	0.49	0.06	55.74	42.2	97.9
B	WWD-13	33.03	5.82	0.10	1.33	14.78	0.06	0.05	0.06	0.14	55.36	21.7	77.0
C	WWD-12	49.60	1.77	0.06	0.64	0.11	0.05	0.02	0.13	0.15	52.52	45.9	98.4
C	WWD-25	29.91	8.72	1.26	7.24	9.44	0.05	0.17	0.86	0.29	57.92	29.0	86.9
C	WWD-36	48.99	1.61	0.04	0.95	0.21	0.11	0.01	0.64	0.55	53.11	44.5	97.6
D	DEP-6	47.87	3.13	0.19	1.05	0.11	0.03	0.04	0.14	0.18	52.75	44.8	97.5
D	WWD-14	47.64	3.38	0.06	0.90	0.16	0.04	0.01	0.21	0.38	52.78	45.3	98.1
D	WWD-37	48.92	1.58	0.19	1.37	0.13	0.10	0.03	0.70	0.32	53.33	44.4	97.7

b) Related to element concentrations (calculated from the oxides)

Aquifer	Well Name	Ca %	Mg %	Al %	Si %	S %	Na %	K %	Fe %	Sr %	Total Elem%
A	WWD-20	21.41	3.34	0.07	0.67	13.13	0.02	0.03	0.06	1.25	39.99
A	WWD-24	34.01	0.53	0.40	2.44	0.55	0.02	0.11	0.35	0.06	38.46
B	WWD-13	23.59	3.49	0.05	0.62	14.78	0.04	0.04	0.04	0.14	42.80
C	WWD-12	35.43	1.06	0.03	0.30	0.11	0.03	0.02	0.09	0.15	37.22
C	WWD-25	21.37	5.23	0.66	3.38	9.44	0.03	0.14	0.60	0.29	41.14
C	WWD-36	34.99	0.97	0.02	0.44	0.21	0.08	0.01	0.45	0.55	37.72
D	DEP-6	34.20	1.88	0.10	0.49	0.11	0.02	0.03	0.10	0.18	37.11
D	WWD-14	34.03	2.03	0.03	0.42	0.16	0.03	0.01	0.15	0.38	37.23
D	WWD-37	34.94	0.95	0.10	0.64	0.13	0.07	0.02	0.49	0.32	37.67

On the other hand four boreholes were selected on the bases of one borehole from each aquifer to discuss the aquifer matrix. These boreholes are WWD-24, WWD-13, WWD-25 and WWD-14 for aquifers from A to D respectively. Despite the boreholes having being scattered in the Study Area, they reflect the matrix composition at selected locations and an overall idea about different aquifers. Therefore the plot of these elements for the previous boreholes (Figure 4.16) using Table 4.7b data shows the dominance of Ca in all aquifers with the highest percentage in aquifer D followed by sulphur rises in aquifers B and C.

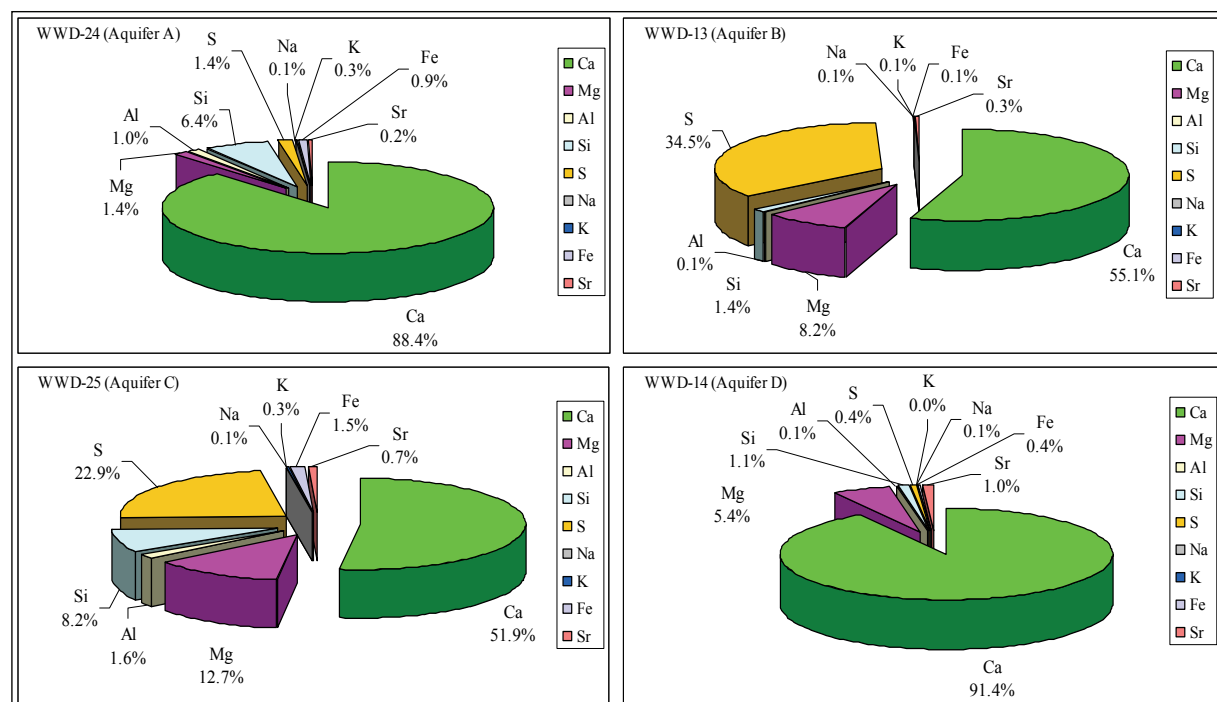


Figure 4.16 Aquifer matrix compositions in different aquifers

The Study Area lithological matrix consists of marine carbonate. The matrix composition varies sometimes depending on the inter-bedded layer which exists in different formations. As a result, it was observed that thin layers of marl were present in Dammam, gypsum in Rus and biomicrite and shale in UER formations. These layers form the aquifer matrix in combination with the limestone dissolved and produced different elements or compounds mainly found in the lithological analyses. This type of carbonate rocks is an important source for Ca, Mg, Sr as well with gypsum and especially for Ca and S. However, layers like shale and clay materials mainly govern the Al and Si form as aluminosilicates. Other elements are of minor relevance for the matrix formation.

Therefore, from the lithological analysis we can calculate the matrix composition based on the chemical composition by the XRF analysis. These were performed by using atomic or mole weight and elements percentage in each sample. For example, borehole WWD-25 in aquifer C (Table 4.8):

Calcium occurs in two dominant compounds: CaCO_3 and CaSO_4 . This has been taken into account when calculating the mineral composition. Gypsum contributions can be calculated depending on S concentration because S is forming sulphate.

Table 4.8 Elements obtained from borehole WWD-25 by using (XRF) analysis

Oxid g/100	Element	Atom g	Element 100g/57.7	mol 100g	Element % /41g	Minerals as	Mineral mol/100g	Minerals as	Mineral mol/100g	Minerals %
29.914	Ca	40	21.37	0.53	51.93	CaCO ₃ +CaSO ₄	0.53	CaCO ₃	0.24	26.40
8.72	Mg	24	5.23	0.22	12.71	MgCO ₃	0.22	MgCO ₃	0.22	24.49
1.26	2Al	54	0.67	0.01	1.62	Al ₂ O ₃ *SiO ₂	0.13	Al ₂ O ₃ *SiO ₂	0.13	14.94
7.241	Si	28	3.38	0.12	8.21	Al ₂ O ₃ *SiO ₂				
0.86	2Fe	111	0.60	0.01	1.46	Fe ₂ O ₃	0.01	Fe ₂ O ₃	0.01	0.61
9.44	S	32	9.44	0.30	22.94	CaSO ₄	0.30	CaSO ₄	0.30	33.15
0.29	Sr	87.6	0.29	0.00	0.70	SrCO ₃	0.00	SrCO ₃	0.00	0.37
57.73			40.98		99.58				0.89	99.97

Assuming for sample WWD-25 the following processes based on 100g of mineral samples and expressed in %:

- All Mg occurs as MgCO₃ giving then MgCO₃ ≈24.5%
- All S dominantly occurs as sulphate giving then CaSO₄ ≈33%
- All Ca occurs as CaCO₃ and CaSO₄ giving then CaCO₃ reduced by part of CaSO₄ ≈ 26%
- All Si + Al₂O₃ occur as aluminum silicates in a form of SiO₂+ Al₂O₃.SiO₄ giving then ≈14.9%

Based on the above calculations the main components are following the order CaSO₄ > CaCO₃ > MgCO₃ > (SiO₂+Al₂O₃.SiO₄) and all together consisting of 98%. The remaining elements Sr, Na, Fe, P, K, Ti, V, Cr, and Mn are all together constitute ≈1%.

The result of WWD-25 shows a high percentage of CaSO₄ over all the other components. This indicates that the source of sulphate at WWD-25 is related to an aquifer matrix such as gypsum (CaSO₄.2H₂O) or anhydrite (CaSO₄) rather than pyrite (FeS₂) where Fe was found in the X-RF in this sample, contributing as a minor component. Additionally, other S-containing organic matter should be of minor importance (Hem, 1989), besides CaSO₄ has a reversible relationship with CaCO₃. Although FeS₂ is found as a common minor component in black shale which originated from marine deposits or brackish water (Konrad B, et al, 1995), and does not have the potential to produce that amount of sulphur as indicated in the X-RF.

The X-Y plot of sulphate (XRF) versus sulphate (groundwater) shows an excess of sulphate in groundwater over the XRF sulphate percentage in most of the sampled boreholes regardless different scales. Only three boreholes in aquifers A (WWD-20),

B (WWD-13) and C (WWD-25) divert from that trend (Figure 4.17). The highest and lowest sulphate values in groundwater were recorded in aquifer D, however the highest XRF sulphate percentage values were found in aquifer B (WWD-13) located in the north portion of the Study Area. The high sulphate in groundwater may result from gypsum layers dissolution and organic matter especially near WWD-14. On the other hand boreholes such as WWD-13, WWD-20 and WWD-25 were associated with high sulphate percentages in the aquifer matrix representing an enrichment with sulphate and dissolution processes could be reduced. This rise of sulphate in the aquifer matrix is probably related to evaporites such as gypsum, and pyrite deposits occurring in the aquifers.

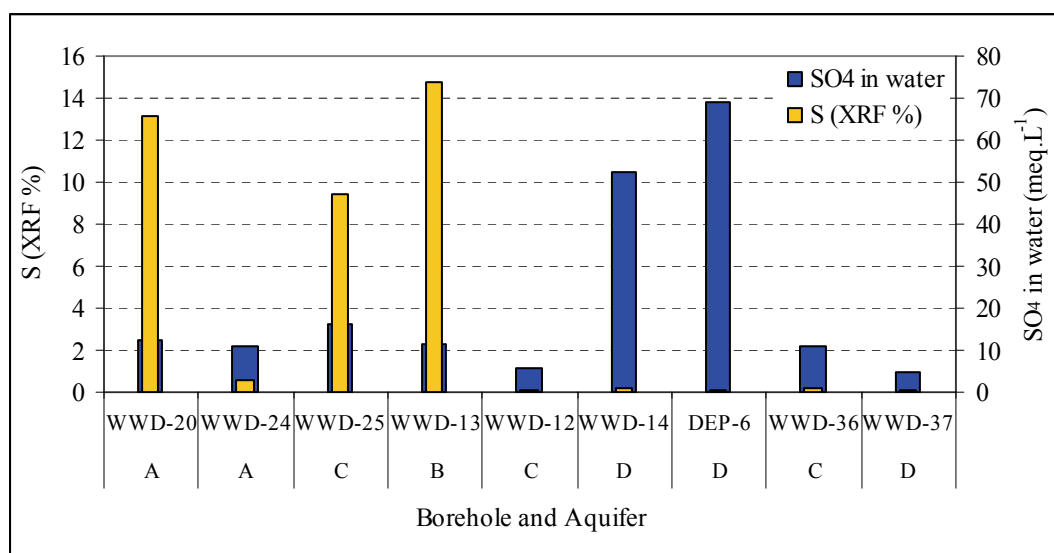


Figure 4.17 Sulphur in aquifer matrix and sulphate in groundwater in different aquifers

In Figure 4.18 the plot of elements Ca versus Mg shows a general dominance of Ca in almost all selected boreholes regardless of the scale. It has an excess of 2 to 4 times in comparison with Mg. This high value of Ca might be related to limestone and specifically gypsum layers existing in the Rus formation and U.UER which are restricted with aquifer A and B. On other hand L.UER consists of limestone, and is repeatedly inter-bedded with pyritic mudstones and shale. As a result, additions of Ca over Mg could be related to aquifer limestone and ion exchange especially in the replacement of Na by Mg on clay minerals. In addition, the solubility and alteration of elements like Mg, Ca, Na, and K with clay minerals can form different types of clay

minerals such as kaolinite and Ca-montmorillonite and increase the Ca value. Concurrently, possibilities of dolomitisation could occur in the mineral matrix of the boreholes WWD-13, WWD-20 and may be WWD-25.

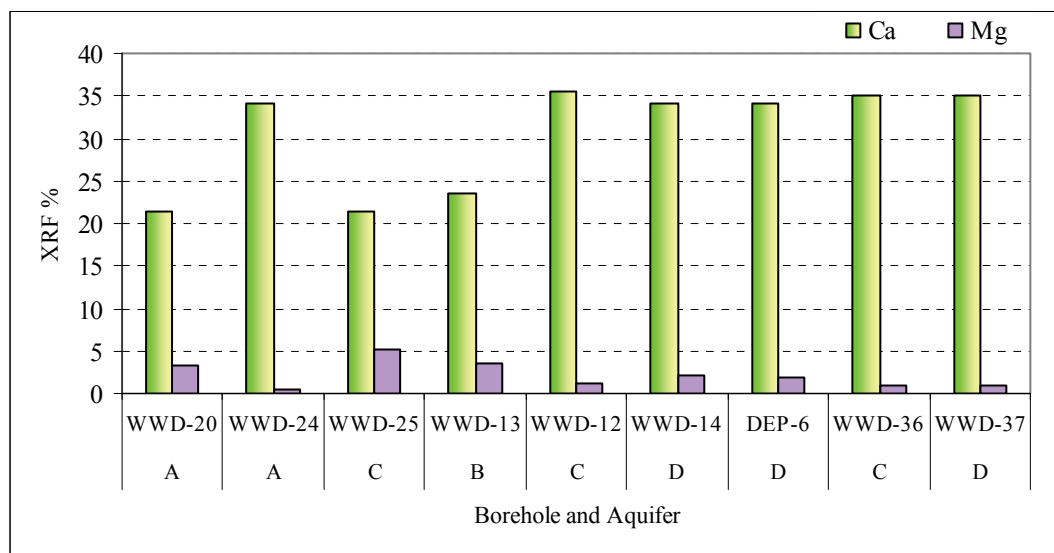


Figure 4.18 Calcium and magnesium in aquifer matrix of Najd aquifers based on XRF analyses

Overall, all minor elements reveal (Figure 4.19) close concentration in most of the core samples with some exceptions. Simultaneously, boreholes from different aquifers located close to each other seem to be semi-homogenous in components such as Si, Al, Sr, Fe, Na and K. The borehole WWD-20 (aquifer A) was recorded with the highest percentage in Sr. However boreholes WWD-24 (aquifer A) and WWD-25 (aquifer C) which are located within a distance of less than 50m were found with highest percentage of Si.

The strontium (Sr) which is excised overall at WWD-20 (aquifer A) may relate to ion exchange and replacement of aragonite instead of calcite. The Fe of marine origin appears first as iron sulphide of FeS type and changes later onto pyrite (FeS₂) (Konrad B, et al, 1995). In fact, the excess of Fe appears in one of the highest mineralization sites in the Study Area. Consequently, the rise of iron could be related to these marine deposits abundant in sulphate and organic matter. Si and Al elements are usually associated with clay minerals. Therefore, their rises in some different boreholes may be related to clay minerals reaction like ion exchange (equation below) and formation of kaolinite.

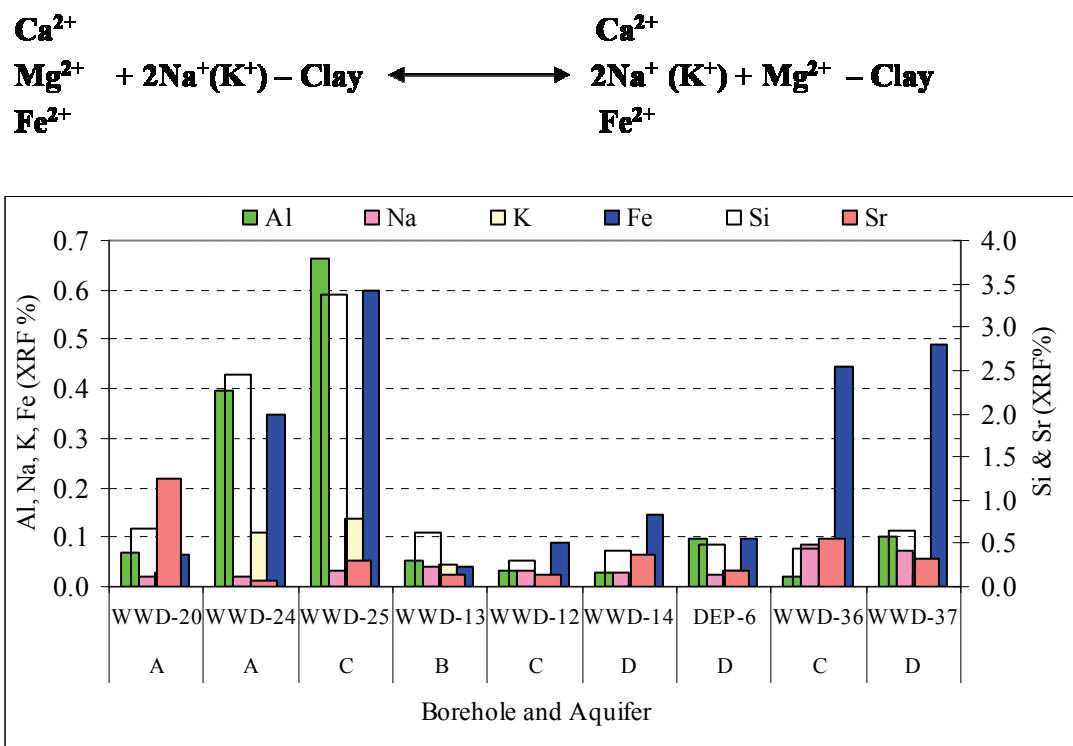


Figure 4.19 Comparison of trace element in the matrix of different aquifers

X-RF analysis shows dominance of Ca over all the selected wells with a percentage range from 21% to 35%. S – appearing as sulphate – is recorded the second highest ratio of 14.78% (Table 4.7ab) in borehole WWD-13 located in aquifer B.

On other hand, from aquifer matrix analyses, the dominance of elements following the order: Ca > S > Mg > Si > Sr > Fe.

4.5. Environmental Isotopes in Groundwater of the Najd Aquifers

4.5.1 Stable isotopes of water and tritium

Water isotopic signatures and stable isotopes of dissolved compounds were taken during this survey to evaluate recharge sources, and elucidate the relationship between the different aquifers and groundwater flow direction. 76 wells and 3 springs, in addition to rain water, were analyzed for hydrogen and oxygen stable isotopes.

Comparable to the hydrochemistry of the groundwater, the variation of $\delta^2\text{H}$ and $\delta^{18}\text{O}$ reflects a grouping with a tendency to decrease with depth from A to C; however, the

H and O isotope values in the D aquifer shows a higher variation and the highest enrichment in heavier isotopes ^2H and ^{18}O . Remarkably, groundwater from both aquifers A ($\pm 15.0\%$ and $\pm 2.1\%$ for $\delta^2\text{H}$ and $\delta^{18}\text{O}$, respectively), and D ($\pm 12.55\%$ and $\pm 1.54\%$ for $\delta^2\text{H}$ and $\delta^{18}\text{O}$, respectively), were highly variable with respect to changes in their isotope signature (Table 4.9).

Table 4.9 Minimum and maximum concentration of isotopes in each aquifer

Aquifer	Range	$\delta^{18}\text{O}[\text{‰}]$	$\delta^2\text{H}[\text{‰}]$	$\delta^{34}\text{S}_{\text{sulphate}}[\text{‰}]$	$\delta^{18}\text{O}_{\text{sulphate}}[\text{‰}]$	$\delta^{13}\text{C}_{\text{DIC}}[\text{‰}]$	$^3\text{H}[\text{TU}]$	Count
A	Min	-6.54	-43.78	13.10	7.30	-11.10	0.25	12
	Max	0.38	6.40	31.90	15.50	-6.30	1.2	
B	Min	-5.72	-39.56	9.50	12.00	-10.30	0.25	10
	Max	-3.71	-24.52	25.50	14.90	-4.50	1.2	
C	Min	-6.52	-47.57	12.70	10.50	-13.10	0.25	33
	Max	-3.71	-22.15	55.70	17.30	-2.50	0.25	
D	Min	-6.11	-47.14	4.00	8.70	-10.90	0.25	24
	Max	-0.06	5.09	101.10	16.00	-1.63	1.3	

Tritium was measured at groundwater level from 48 wells and springs distributed along the aquifers (Annex A-3). The data ranges between 0.25 TU which refers to the detection limit, and up to 1.2 TU in DWS-15 (aquifer D). Only five out of 39 samples have ^3H values greater than 0.25 TU belonging to DWS-15 (aquifer D), DEP-9 (B), M.Masin, Mathira1 and spring SHTH (all in A).

The $\delta^{13}\text{C}_{\text{DIC}}$ measured in 79 wells and springs (Table 4.10) show slight enrichment from aquifer A to D and a higher variability in C and D.

$\delta^{34}\text{S}_{\text{Sulphate}}$ and $\delta^{18}\text{O}_{\text{Sulphate}}$ are generally enriched with depth from A to D with exception of $\delta^{34}\text{S}_{\text{sulphate}}$ in aquifer B; this part will be discussed later on.

Values of stable water isotopes from the groundwater and spring water samples were shifted from the GMWL and indicate that the groundwater within the Najd formation differs from the GMWL by slightly lower amounts of $\delta^2\text{H}$ and $\delta^{18}\text{O}$. The relationship, depicted by the Najd Groundwater Line (NGL) in Figure 4.20, between hydrogen and oxygen isotopes in these aquifers can be described by the equation $\delta^2\text{H} = 7.79 \delta^{18}\text{O} + 5.54$. Also depicted on the graph are the Southern Oman meteoric water line (SOMWL, $\delta^2\text{H} = 7.2 \delta^{18}\text{O} - 1.1$) and the Northern Oman meteoric water line (NOMWL, $\delta^2\text{H} = 5.1 \delta^{18}\text{O} + 8.0$) (Macumber et al., 1997).

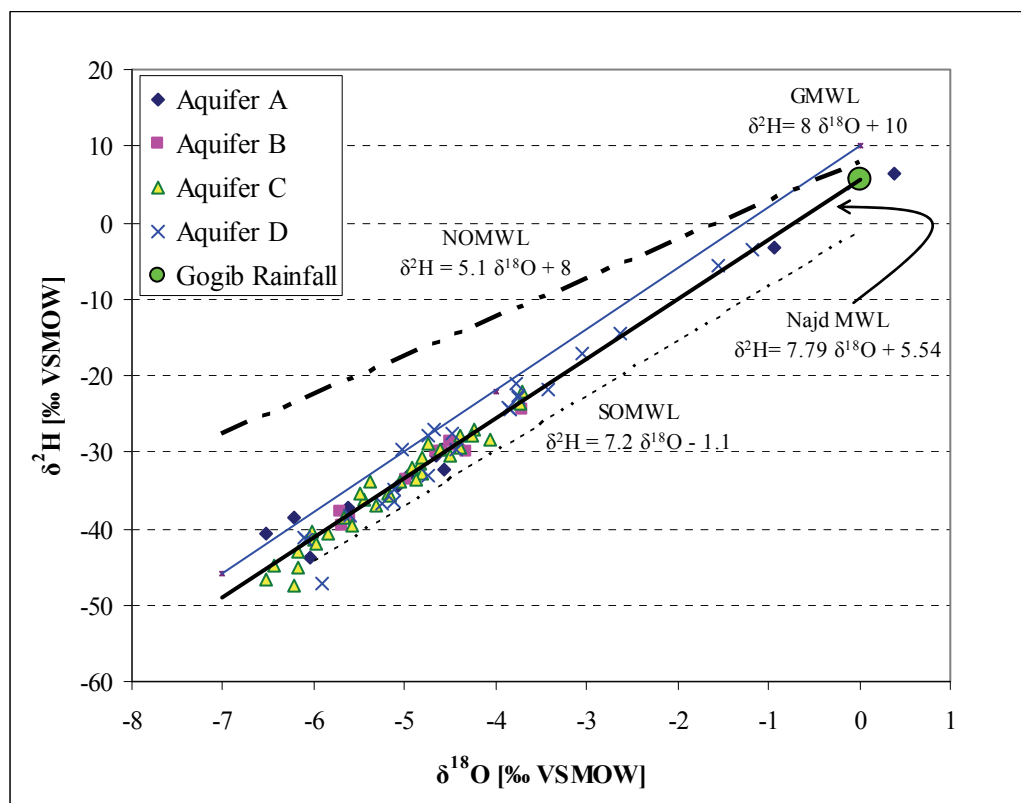


Figure 4.20 $\delta^2\text{H}$ - $\delta^{18}\text{O}$ diagram of groundwater, spring water, and precipitation from the Dhofar region and the different Najd aquifers (Najd Groundwater Line [NGL]: black line bold); further: Northern Oman Meteoric Water Line (NOMWL: dotted), Southern Meteoric Water Line (SOMWL: dashed-dotted), Global Meteoric Water Line (GMWL) are depicted for reference

The NOMWL represents a reference value for water that is influenced by precipitation from the Northwesterlies (Macumber et al., 1997), whereas tropical cycles from the south have the strongest influence on the SOMWL (Macumber et al., 1995). Similarities between the hydrogen and oxygen isotope relationships in the Najd aquifer and the SOMWL reveal that southern precipitation and rainfall in the Jabal chain have contributed significantly to the water constituting from aquifers A through D. Three samples collected during this survey show an enrichment of ^{18}O and ^2H , one spring (SHTH, +0.38‰ in $\delta^{18}\text{O}$, +6.4‰ in $\delta^2\text{H}$) from aquifer A, one well (QISB, -0.06‰, +5.1‰) from aquifer D, and the rainfall sample Gobib (+0.01‰, +5.5‰). All of these sites are located in the monsoon recharge area. The majority of samples from the groundwater including the Mudy-Spring (M.sp) in aquifer C are grouped in a range of less than -3.7‰ for $\delta^{18}\text{O}$ and -20.8‰ for $\delta^2\text{H}$ which indicates a decrease of

monsoon recharge by infiltration processes. Waters heavily enriched in ^{18}O and less in ^2H in comparison to the GMWL indicates that complex water-rock exchange processes influence the groundwater signature known as sedimentary rocks, including brines and solutions in contact with clay layers (IAEA, 1981). However, there are no indications of sedimentary rock interactions from any of the samples collected during this survey.

The isotopic enriched spring (SHTH) and well (QISB) affected by monsoon rainfall along the southern edge of the Study Area indicates that infiltration processes are occurring through fractures or dissolution channels of the limestone matrix located in the groundwater recharge area. Previous studies have suggested this process as a common phenomenon in geological formations from this region (Tetra Tech, 1978). The groundwater from aquifers B, C, and most of D have $\delta^2\text{H}$ values below -20‰ and $\delta^{18}\text{O}$ values of -3.7‰. The similar slope in $\delta^2\text{H}$ and $\delta^{18}\text{O}$ compared to GMWL indicates that the water here was not affected by evaporation during infiltration. Moreover, the $^2\text{H}/^{18}\text{O}$ relationship of groundwater from this formation suggests that atmospheric circulation systems from the Indian Ocean would be a likely source of precipitation during recharge (Macumber et al., 1995). They reported a variation in $\delta^2\text{H}$ range from (-51.6) to (+25.1) and $\delta^{18}\text{O}$ values between (-7.04) to (+7.35).

The depletion of ^2H and ^{18}O in the groundwater pool also suggest that colder and wetter climate conditions were present during the initial infiltration of groundwater into this area. These environmental changes may have led to higher recharge and infiltration process rates. Clark *et al.* (1987, 1997) supports this hypothesis and they concluded that the water in the UER formation was mostly comprised of paleo-groundwater in an area close to the recharge basin. However, mixing processes in the recharge area close to the Jabal chain and further into the northern interior of Najd can be suggested from data collected herein.

Tritium (^3H , half-life time 12.43 years) is widely used as a radioisotope tracer to identify the modern recharge. The tritium input function is coupled to the H-bomb peak of the 1960s, groundwater with high tritium concentrations >30 TU indicates a recharge during and after the 1960s. Recent precipitation and recharged groundwater

in the northern hemisphere has tritium concentrations up to 9 TU (IAEA GNIP). Groundwater containing ^3H values <1 TU is often classified as submodern. Groundwater with ^3H values originates as a mixture of submodern and shallow modern groundwater discharging as springs or wells (Clark, et al., 1997).

The tritium analyses from groundwater samples of boreholes from all aquifers show that most of this groundwater has no significant indication of any modern recharge since the early 1960's, the H-bomb tritium input. However, a mixture of submodern and fossil water could also mask input of modern recharge. Concerning the tritium values, only few groundwater samples with >0.5 TU point to mixing of modern recharge with the submodern groundwater.

Overall, at this time, it is difficult to identify individual recharge sources for each aquifer in this area based only on ^3H measurements. Moreover, from the isotopic studies it has been determined that groundwater behaviors in all aquifers were generally close to each other except in the recharge area which was restricted to the Jabal chain in the south. In this area or nearby, two boreholes (MOD-15, 332/014) belong to aquifer D and are located in the interior of Najd; ^2H becomes enriched which reflects recharge signature. Two hypotheses could be proposed from the water isotopic signatures: (i) groundwater within the aquifers is being mixed with modern water particularly in aquifers A and D, (ii) the water initially infiltrated the aquifers under more humid conditions and is affected by hydraulic processes. The first assumption could be responsible for most of the recharge to Najd aquifers, however the second assumption is probably considered for part of it as well. ^2H and ^{18}O depletion signatures within all four aquifers would better support the second hypothesis. Only two springs (SHTH, NKR) from the A aquifer and five wells (QISB, DEP-6, LobFr, MOD-15, 332/014) from the D aquifer support the first assumption that these aquifers were filled via a paleo-recharge process and mixed with modern water.

Table 4.10 Results of isotope analyses of water, sulphate, DIC and tritium from water, in addition to ¹³C of lithology

All [‰] are related to VSMOW [H₂O], CDT [S] and VPDB [C].

Local Name	Site ID	Aquifer	Sampling Date	δ ¹⁸ O [‰]	δ ² H [‰]	δ ³⁴ S _{sulphate} [‰]	δ ¹⁸ O _{sulphate} [‰]	³ H [TU]	± 2σ [TU]	δ ¹³ C _{DIC} [‰]	δ ¹³ C _{Lithology} [‰]
KhT-A	BG117784AA	A	3/5/09	-4.42	-29.2	31.9	15.5	0.3	0.25	-6.3	
M.Masin	YA729072AA	A	29/4/08	-4.97	-33.1	14.0	12.2	0.6	0.20	-8.5	
Mathira 1	YV826752BA	A	26/5/09	-6.22	-38.7	13.1	12.8	0.8	0.25	-11.1	
NKR Sp	BE105632AC	A	24/5/08	-0.94	-3.3	14.9	7.3			-10.2	
O.R	ZV191273AA	A	5/4/09	-5.08	-34.3	15.5	11.0	0.3	0.25	-8.4	
SHTH Sp	AE803515AC	A	24/5/08	0.38	6.4	16.7	8.5	1.2	0.30	-8.6	
TWIRISH	AF123492AA	A	29/4/08	-4.60	-29.7	15.1	12.3	0.3	0.25	-8.5	
WWD-20	YA859494BA	A	6/5/09	-6.54	-40.7	18.7	13.8	0.3	0.25	-7.7	-3.4
WWD-24	BG200046CA	A	21/4/08	-4.65	-30.5	30.3	14.2	0.3	0.25	-9.8	-7.1
WWD-26	BG409917AA	A	3/5/09	-5.63	-37.4	25.1	13.7	0.3	0.25	-7.1	
WWD-30	BG549421AA	A	3/5/09	-6.04	-43.8	20.9	13.1	0.3	0.25	-7.4	
WWD-45	BG485361BA	A	21/4/09	-4.58	-32.3	20.7	13.9	0.3	0.25	-8.0	
DEP-15	YV399518AA	B	21/5/08	-4.51	-28.6	9.5	12.5			-9.1	
DEP-16A	XV997655BA	B	4/5/08	-3.71	-24.5	12.8	14.3			-6.7	
DEP-17	YV578833AA	B	11/4/09	-4.59	-30.1	10.8	12.5	0.3	0.25	-8.5	
DEP-9	YV182483AA	B	3/5/08	-4.41	-29.1	11.0	12.5	1.2	0.30	-10.3	
MAF-S1(001/015)	ZV193035AA	B	18/11/09	-4.65	-30.0	22.2	15.4	0.3	0.25	-9.7	
WWD-13	YB406953BA	B	31/3/09	-5.69	-39.6	21.2	13.4	0.3	0.25	-4.5	-3.0
WWD-17	YA389228BA	B	31/3/09	-5.72	-37.8	18.8	12.0			-5.6	
WWD-19	YA859494AA	B	3/5/09	-5.61	-38.8	18.5	13.7	0.3	0.25	-7.1	
WWD-5	XA694716BA	B	13/4/08	-4.98	-33.5	19.4	14.0	0.3	0.25	-8.3	
WWD-9	XA612881BA	B	4/5/08	-4.31	-29.9	25.5	14.9			-6.6	
001/014	ZV193035BA	C	28/4/08	-4.62	-29.7	22.0	12.1			-4.3	
001/290	AF829201AA	C	29/4/08	-4.83	-31.6	22.3	12.7			-3.2	
Bashn-1	CF035107AA	C	21/4/08	-5.59	-39.7	32.0	15.0			-6.8	
Bin Kh	BF080077AA	C	16/4/08	-5.67	-38.4	23.0	13.6			-3.2	
DEP-14	XV876910AA	C	4/5/08	-4.50	-30.4	21.2	13.4			-7.6	
DEP-16	XV997655AA	C	4/5/08	-3.71	-22.1	15.5	13.1			-2.5	
DEP-18	BF223760AA	C	17/5/08	-4.74	-28.8	16.4	12.8			-5.5	
DEP-19	BF792149AA	C	3/5/09	-5.84	-40.8	43.6	13.5			-4.8	
DEP-2	YV955966AA	C	8/4/09	-4.23	-27.2	27.5	15.0			-4.9	
DEP-9A	YV182483BA	C	3/5/08	-3.73	-23.7	13.5	14.3			-2.8	
Gosham1	CF179989AA	C	5/5/09	-5.45	-36.2	36.6	15.5			-3.0	
M.Sp	YV439388AC	C	6/5/08	-5.38	-33.9	15.8	10.5			-10.3	
Qitbit	BG317999AA	C	3/5/09	-6.45	-44.8	22.8	11.6			-7.1	
Ranada-1	BF840101AA	C	5/5/09	-5.49	-35.4	55.7	17.3			-7.9	
RBK - C	BE050838AA	C	19/8/09	-4.92	-32.0	44.1	9.6	0.3	0.25	-13.1	
S.TMMI	YV347775AA	C	11/4/09	-4.39	-29.3	12.7	12.9			-5.3	
Ubar Fm	YA819821AA	C	29/4/08	-4.81	-30.7	14.8	13.2			-3.2	
W Bharna1	BF040020AA	C	2/5/09	-4.26	-27.9	47.6	16.5			-8.7	
WWD-11	YA051882AA	C	14/4/08	-4.82	-32.9	15.1	13.7			-5.0	
WWD-12	YB406944AA	C	31/3/09	-5.31	-36.9	20.9	14.0	0.3	0.25	-5.6	3.5
WWD-16	YA389227AA	C	31/3/09	-4.87	-33.7	19.6	14.8			-3.0	
WWD-2	XA557476BA	C	13/4/08	-4.40	-28.0	13.9	13.4			-4.4	
WWD-21	YA858545AA	C	6/5/09	-5.17	-35.5	19.3	13.9			-3.7	
WWD-22	BG200046AA	C	17/4/08	-6.02	-40.5	22.1	12.9	0.3	0.25	-5.6	
WWD-25	BG000002AA	C	16/4/08	-5.99	-41.5	21.0	13.6			-5.6	-5.5

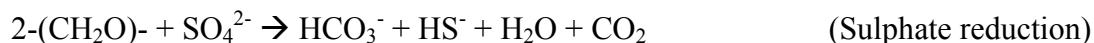
Table 4.10 Continued

Local Name	Site ID	Aquifer	Sampling date	$\delta^{18}\text{O}$ [‰]	$\delta^2\text{H}$ [‰]	$\delta^{34}\text{S}_{\text{sulphate}}$ [‰]	$\delta^{18}\text{O}_{\text{sulphate}}$ [‰]	^3H [TU]	$\pm 2\sigma$ [TU]	$\delta^{13}\text{C}_{\text{DIC}}$ [‰]	$\delta^{13}\text{C}_{\text{Lithology}}$ [‰]
WWD-27	BG110099AA	C	3/5/09	-6.17	-43.1	21.2	13.8	0.3	0.25	-2.7	
WWD-32	CG034063BA	C	5/5/09	-6.52	-46.7	41.0	14.2	0.3	0.25	-5.5	
WWD-34	AG856280BA	C	17/4/08	-5.98	-42.0	22.3	14.6			-4.3	
WWD-35	YB809472AA	C	17/4/08	-5.16	-35.7	19.7	13.3			-5.6	
WWD-36	CG085491AA	C	5/5/09	-6.21	-47.6	27.2	13.5	0.3	0.25	-5.0	2.1
WWD-39	BG367633AA	C	21/4/09	-6.18	-45.1	23.4	13.8	0.3	0.25	-4.9	
WWD-7	XA694716DA	C	1/4/09	-5.04	-33.9	17.8	13.6			-5.5	
WWD-8	XA612881AA	C	4/5/08	-4.07	-28.4	15.6	13.7			-7.3	
332/014	AE989051AA	D	28/4/08	-2.62	-14.6	27.5	11.6			-3.3	
AQSR	BE202783AA	D	10/5/08	-3.86	-24.2	4.0	13.6			-4.2	
DEP-10	YV322265AA	D	13/5/08	-5.25	-36.6	11.2	12.2			-4.9	
DEP-11A	YV356616BA	D	3/5/08	-3.83	-24.5	9.6	13.8			-5.8	
DEP-14A	XV876910BA	D	4/5/08	-4.75	-33.2	19.6	13.6			-3.7	
DEP-3	BE162450AA	D	25/5/09	-3.77	-21.1	101.1	15.8	0.3	0.25	-4.3	
DEP-4	YV937394AA	D	26/5/09	-4.43	-29.7	17.4	15.1	0.3	0.25	-10.9	
DEP-5	BE149620AA	D	2/5/09	-5.04	-29.7	47.8	15.2	0.3	0.25	-1.8	
DEP-6	YV123115AA	D	3/6/09	-1.55	-5.5	15.2	12.6	0.3	0.25	-1.6	2.7
DEP-7	BE127955AA	D	25/5/09	-4.75	-27.9	78.7	15.6	0.3	0.25	-4.7	
DEP-8	XV935678AA	D	13/5/08	-3.76	-22.9	25.0	13.2			-7.6	
DWS-15	YU181909AA	D	24/4/08	-4.49	-27.7	14.8	12.5	1.3	0.30	-7.9	
H.R.C(103/395)	AF828170BA	D	29/4/08	-5.60	-38.2	39.3	9.8			-5.7	
HAD-49	ZV084571AA	D	6/4/09	-6.08	-41.4	60.0	15.9	0.3	0.25	-8.3	
LobFr	AE818982AA	D	3/6/09	-1.19	-3.5	13.5	8.8	0.3	0.25	-3.7	
Mathira 2	YV826752AA	D	26/5/09	-4.68	-27.0	16.3	8.9	0.3	0.25	-4.1	
MOD-15	AE853383AA	D	29/1/10	-3.05	-17.2	16.6	13.0			-3.4	
QISB	AE915009AA	D	11/5/08	-0.06	5.1	15.3	8.7			-5.1	
RBK-D	BE094486AA	D	2/5/09	-3.41	-21.9	78.3	13.8	0.3	0.25	-4.8	
TOSNAT	XV849043AA	D	14/5/08	-3.75	-22.6	11.0	13.4			-3.2	
WSW-3	BE991437AA	D	5/5/09	-6.11	-41.2	11.7	9.0	0.3	0.25	-5.7	
WWD-14	YB406954CA	D	31/3/09	-5.13	-36.5	21.2	13.6	0.3	0.25	-7.3	2.9
WWD-37	CG085490BA	D	5/5/09	-5.91	-47.1	37.1	16.0	0.3	0.25	-4.7	2.1
WWD-6	XA694716CA	D	13/4/08	-5.13	-35.0	14.8	13.4	0.3	0.25	-2.6	
Gogib Rainfall	AE902477AF	Rainfall	July-Aug08	0.01	5.5			0.3	0.3	-15.5	

4.5.2 Sulphate and oxygen isotopes of sulphate

In the subsurface, the major forms of sulphur compounds are sulphate and sulphide which occur in minerals or dissolved as sulphate: (SO_4^{2-}), sulphide (HS^-), and hydrogen sulphide (H_2S). Their oxidation and recycling in soils produce terrestrial sulphates which is common in semi-arid regions. The main source of sulphate is sedimentary evaporites, like gypsum ($\text{CaSO}_4 \cdot 2\text{H}_2\text{O}$) or anhydrite (CaSO_4). These two components form evaporate rocks or layers in formations such as Rus and UER, as it is also known in other arid rock formations (Khayat et al., 2006). The other earth

alkaline sulphates such as strontium and barium sulphates are relatively rare, and less soluble in comparison with calcium sulphate (Hem, 1989). The dissolution of gypsum often results in a re-crystallization of limestone when CO₂ or bicarbonate occurs induced by mineralization of organic matter:



These processes are responsible for variation of S and C isotopes in sulphate, carbonate, DIC and CO₂. That means S and O isotopes become enriched with the sulphate reduction: during oxidation of organic carbon (CH₂O) the C isotopic composition of DIC and CO₂ is influenced by depleted carbon from organic material whereas S and O isotopes are enriched in the residual sulphate phase and depleted in the reaction product sulphide,

Data variation obtained from groundwater of the Najd aquifers shows that groundwater in aquifer D has the highest value of $\delta^{34}\text{S}_{\text{sulphate}}$ while the isotope enrichment follows the trend from aquifer B to aquifer D (Table 4.10). The enrichment with $\delta^{34}\text{S}_{\text{sulphate}}$ in aquifer D may be related to gypsum dissolution or ion exchange in this deep aquifer. Similar dissolution processes are also discussed in groundwater of the Lissan formation in Pleistocene aquifers of the Jordan Valley (Khayat et al., 2006). The $\delta^{18}\text{O}_{\text{sulphate}}$ slightly increases in groundwater from aquifer A downward to the aquifers which lie beneath.

Source of sulphate

In general, the aquifer matrix which mainly consists of limestone embedded with fossiliferous limestone, micritic limestone, shale and minor layers of pyrite mudstone, gypsum and marl may be important for the increase of sulphate concentration. The $\delta^{34}\text{S}_{\text{sulphate}}$ enrichment, however, is related to hydrochemical processes in the aquifer. These types of sediments are common sources for sulphur production (Repcok, et al, 2000). In addition, secondary processes with organic matters, such as fossiliferous and micritic limestone during sulphate reduction, probably contribute in this field and

influence the increase of $^{34}\text{S}_{\text{sulphate}}$. On the other hand, X-RF analysis conducted for 9 samples collected from the saturation zone shows an excess of sulfur over the groundwater sulphate. This enrichment was observed in several boreholes from different aquifers where DEP-6 and WWD-14 (aquifer D) represent the highest values, and WWD-37 and WWD-13 record the lowest. The comparison between WWD-13, WWD-12 and WWD-14 (Figure 4.17) located nearby within a diameter of less than 100m and belong to aquifers B, C and D, respectively, shows variable concentrations of the lithological sulphate ($D > B > C$). However, the comparison of the same boreholes lithological sulphate with groundwater sulphate reveals the highest concentration of water sulphate in aquifer B which may be related to gypsum dissolution. Also, solubility of gypsum may help to accelerate this process in aquifer B more than other aquifers such as C and D.

The $\delta^{34}\text{S}_{\text{sulphate}}$ values increases from the central Najd towards the northeast in all aquifers. Ten out of 79 samples collected from all the Najd aquifers have values above 40‰ for $\delta^{34}\text{S}_{\text{sulphate}}$. Whereas, 5 samples have values $\geq 30 < 40$, in addition, 23 samples are in the range $\geq 20 < 30$, however 38 samples show values $\geq 10 < 20$ and rest of 3 samples are recorded with values < 10 . The highest δ -values in each aquifer were found +31.9‰ (KhT-A), +25.5‰ (WWD-9), +55.7‰ (Ranada1) and +101.1‰ (DEP-3) in aquifers from A to D, respectively. However, deeper aquifers (C&D) were recorded by the highest ten values. Boreholes with these high concentrations were concentrated in central to east of the Study Area. The sulphate of aquifers A and B are less enriched into ^{34}S between +9.5 and +31.5‰ (Table 4.10).

The plot of $\delta^{34}\text{S}_{\text{sulphate}}$ versus $\delta^{18}\text{O}_{\text{sulphate}}$ (Figure 4.21) shows characteristic variations of the sulphate isotopic composition of the stratified aquifers. Three processes (I), (II) and (III) may be identified from the clustering of S- and O-isotopes. Firstly (I) impact of source and variation with different mobile and biological activities in or close to recharge area ($\delta^{34}\text{S}_{\text{sulphate}} < 20\text{‰}$) and increase of $\delta^{18}\text{O}_{\text{SO}_4}$ due to enrichment of O isotopes in the soil and atmospheric oxygen. This is represented by springs and borehole data located in the area affected by monsoon rainfall or flood events.

The second process (II) reflects dissolution of sulphate (inside the circle) and the possibility of a mix between different water types especially in a closed system. The

evidence suggests either one or both reduction and oxidation processes occur at this stage. Presently, most of the data from all aquifers were accompanied; therefore, to the identification of interactions between aquifer matrix and dissolved sulphate is challenging. The third (III) processes ($\delta^{34}\text{S}_{\text{sulphate}} > 20\text{‰}$ and relative constance $\delta^{18}\text{O}_{\text{SO}_4}$) were represented by almost all groundwater from boreholes located in aquifer D and unexplainably from aquifer C. The ^{34}S enrichment in the direction from the circle towards (III) following the arrow direction may be related to bacterial sulphate reduction (BSR). At the same time data reveals consistency of $^{18}\text{O}_{\text{sulphate}}$ in this direction. This could be due to the aquifer being considered as a closed system. This idea agrees with the experiment result carried out by Turchyn et al (2010) using a simplified biochemical model called dissimilatory sulphate reduction (DSR). The experiment shows enrichment of $\delta^{34}\text{S}_{\text{sulphate}}$ in all strains and no (or minimal) change in $\delta^{18}\text{O}_{\text{SO}_4}$ over the growth of bacteria.

The ^{18}O in sulphate shows the highest variations in aquifer A and C ranging from 7.3‰ (Mathira1) in aquifer A, to 17.3‰ (Ranada1) in aquifer C.

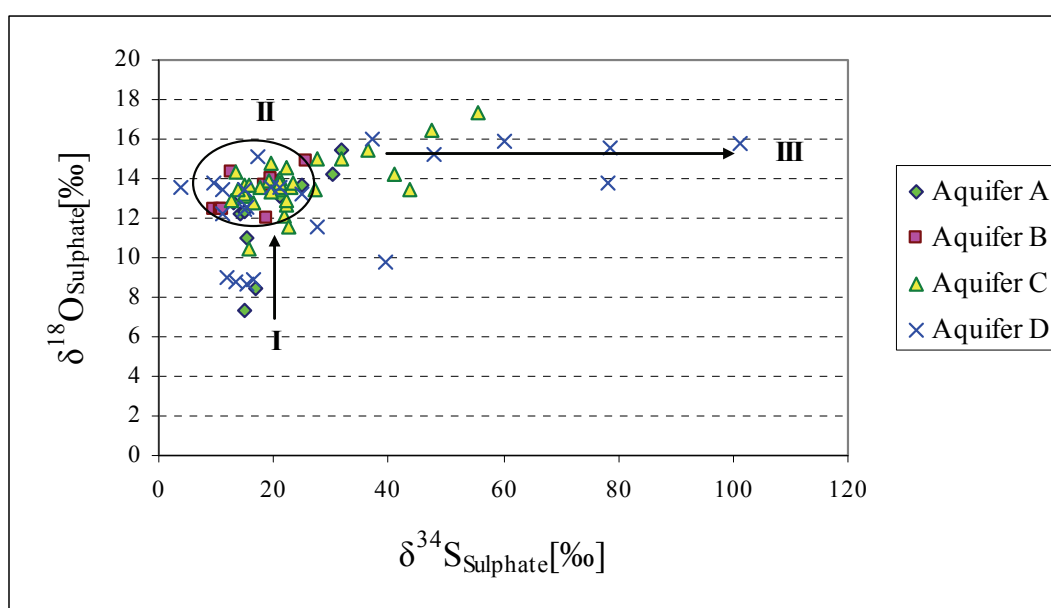
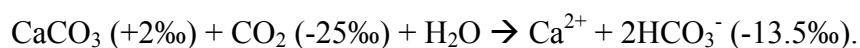


Figure 4.21 Relation of S and O isotopes in groundwater sulphate from the different aquifers

The sulphate reduction can contribute to DIC isotope composition in addition with other sources such as degradation of organic carbon, dissolution of atmospheric and

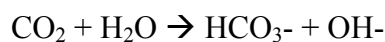
limestone CO₂. To make these reactions more simplify, it seems to be necessary to explain the carbon formation in groundwater.

The carbon source in groundwater in Najd aquifers system is mainly characterized by the limestone matrix and dissolution reactions. However, other carbon sources should be taken into account when the isotopic composition of DIC has to be assessed. The sources are CO₂ from the atmospheric input via recharge with $\delta^{13}\text{C} \sim -7\text{‰}$, organic carbon entered into the groundwater by sulphate reduction with $\delta^{13}\text{C} \sim -25\text{‰}$ for CO₂. All these carbon components dissolve to HCO₃⁻ and are summarized to DIC yielding an isotope mixture of all the constituents. In the case of sulphate reduction the isotopic composition of DIC should basically give a $\delta^{13}\text{C}_{\text{DIC}}$ as a mixture of the source values (δ -values in brackets):



Other reactions which contribute to the isotopic composition of DIC are:

(i) Dissolution of atmospheric CO₂:



(ii) Dissolution of limestone by atmospheric CO₂:



Taking all these reactions into account, an isotope mixture of DIC mixture is expected. However, a mean value cannot be calculated because of the different reactions being involved.

On account of the dominant limestone faces with characteristically enriches ¹³C the degraded by sulphate reduction organic carbon source can only marginally affect the ¹³C_{DIC} in the groundwater as observed by $\delta^{13}\text{C}$ values slightly $< -10\text{‰}$

This is observed from X-Y plot of ³⁴S_{Sulphate} versus ¹³C_{DIC} (Figure 4.22). The correlation shows that most of the water in all aquifers shifted towards an enrichment in ¹³C_{DIC} rather than figuring a sulphate reduction by both increasing of ³⁴S_{Sulphate} and ¹³C_{DIC} depletion. Evidently, the sulphate reduction in Najd aquifers probably depends on the processing inside the system of limestone matrix rather than on the organic carbon source which is used as a reduction mean. This assumption seems to be true because of the case of organic carbon influence the data should be in the shaded area (¹³C_{DIC} $< -10\text{‰}$ and ³⁴S_{Sulphate} $> +18\text{‰}$) (Figure 4.24). Based on this, the data filled with the shadow area is represented depletion of ¹³C_{DIC} and enrichment of ³⁴S_{Sulphate}

which means degradation of organic carbon (CH_2O). Only one sample from aquifer C (RBK-C) was restricted within that range which probably reflected influence of organic carbon.

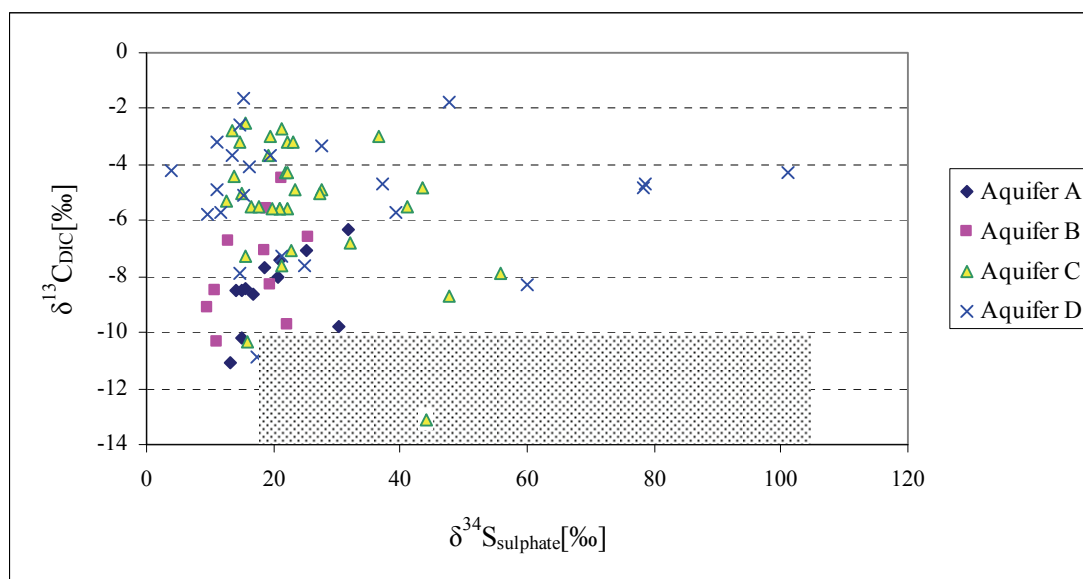


Figure 4.22 $\delta^{34}\text{S}_{\text{sulphate}}$ vs $\delta^{13}\text{C}_{\text{DIC}}$ in groundwater of Najd aquifers

The plot of $\delta^{34}\text{S}_{\text{sulphate}}$ versus sulphate concentration on a logarithmic scale reflects again the different behavior of groundwater in the aquifers. Groundwater from selected wells of aquifer C and D show a reverse linear relationship. This relationship can be interpreted as sulphate reduction (Figure 4.23).

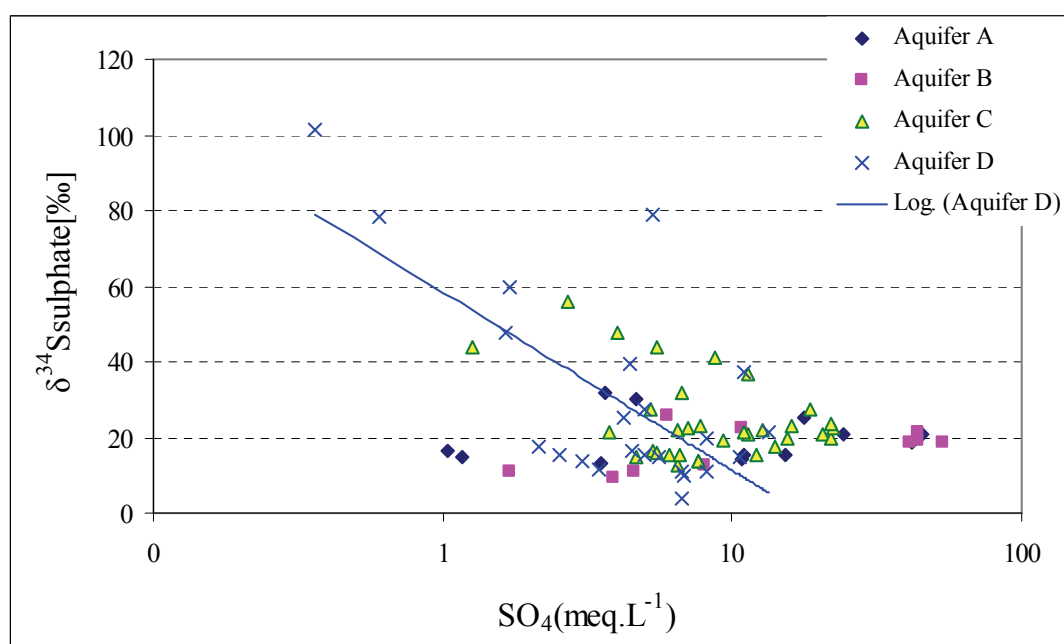


Figure 4.23 $\delta^{34}\text{S}_{\text{sulphate}}$ vs sulphate concentration in groundwater from all aquifers

In opposition, the groundwater from aquifer A and B does not follow the general sulphate reduction signature based on the Rayleigh relation; however it fits for some selected boreholes (see Table 4.11). The large isotopic variations in S and O points to redox reactions in these aquifers connected with isotopic fractionation and probably a mixing of other sulphate from dissolution processes.

This fractionation of the sulphate reduction the process with the highest isotope fractionation – can be derived from the modified Rayleigh equation expressed as $\delta^{34}\text{S} = \delta^{34}\text{S}_0 + \epsilon \ln f$ with f ($C_{\text{start(sulphate)}}/C_{\text{end}}$) as the ratio of initial sulphate concentration to the remaining sulphate, and ϵ as enrichment factor of the sulphate reduction.

Based on the above equation the enrichment factor (ϵ) for the sulphate reduction was calculated for some reasonable examples in each aquifer (Table 4.11). Two boreholes were selected for each aquifer following the flow pathway. As a result, the enrichment factor (ϵ) was found in aquifers from A to D between the ranges of -8.3‰ to -67.7‰. These values support the idea that from all aquifers A to D, the sulphate reduction is based on the Rayleigh relation.

Table 4.11 Enrichment factor for sulphate reduction (ϵ) along selected directions

Aquifer	Sample Source	Mixing line	SO ₄ [meq L ⁻¹]	$\delta^{34}\text{S}_{\text{sulphate}}$ [‰]	f	lnf	ϵ [‰]
A	KhT-A	$^{34}\text{S}_{\text{end}}$	3.6	31.9	0.8	-0.2	-67.7
	WWD-24	$^{34}\text{S}_0$	4.7	15.0			
B	WWD-13	$^{34}\text{S}_{\text{end}}$	44.1	21.2	0.8	-0.2	-12.8
	WWD-17	$^{34}\text{S}_0$	53.2	18.8			
C	WWD-36	$^{34}\text{S}_{\text{end}}$	18.5	27.2	0.8	-0.2	-22.9
	WWD-39	$^{34}\text{S}_0$	21.8	23.4			
D	DEP-3	$^{34}\text{S}_{\text{end}}$	0.4	101.1	0.1	-2.7	-8.3
	DEP-7	$^{34}\text{S}_0$	5.4	78.7			

In 2007, Mangalo et al, discussed stable isotope fractionation during bacterial sulphate reduction and its control by reoxidation to intermediates. The study was concluded that a non-linear relationship between the increase of $\delta^{34}\text{S}_{\text{sulphate}}$ and $\delta^{18}\text{O}_{\text{SO}_4}$ during sulphate reduction exists. Non-linear relationship between $^{34}\text{S}_{\text{sulphate}}$ and $^{18}\text{O}_{\text{sulphate}}$ was reported by Fritz et al (1989). Böttcher et al. (2001) and discussed

the possibility of decrease of $^{18}\text{O}_{\text{sulphate}}$ with an increase of $^{34}\text{S}_{\text{sulphate}}$ in deep groundwater systems in a marine environment. The sulfur enrichment factor was suggested to be controlled by the sulphate reduction. The sulphate reduction depends on the availability of sulphate (no limitation) and the type of sulphate reduction bacteria (Mangalo et al. (2007).

The comparison between sulphate (SO_4) in meq.L^{-1} and $\delta^{34}\text{S}_{\text{sulphate}}$ for all aquifers shows a general reversible relationship especially in aquifers C and D. This reveals initial bacterial reactions followed by reduction processes using the isotopically light sulphate as $^{32}\text{S}_{\text{sulphate}}$ more than $^{34}\text{S}_{\text{sulphate}}$. Consequently $^{34}\text{S}_{\text{sulphate}}$ concentration becomes enriched (Mangalo et al, 2007). At the same time sulphate in water is decreased. This relationship could be reacting in a reverse order as well depending on the aquifer conditions. This idea is probably supported by sulphate and $\delta^{34}\text{S}_{\text{sulphate}}$ results collected from boreholes WWD-17 and DEP-3. Both boreholes are located in aquifers B and D and recorded nonlinear relationship between sulphate and $\delta^{34}\text{S}_{\text{sulphate}}$. The wells show sulphate concentrations of 53.15 meq.L^{-1} and 0.36 meq.L^{-1} whereas $\delta^{34}\text{S}_{\text{sulphate}}$ values were $+18.8\%$ and $+101.1\%$ respectively (Figure 4.21). In addition WWD-17 was recorded with highest value of sulphate; however, DEP-3 occupied the lowest concentration of sulphate and the highest value of $\delta^{34}\text{S}_{\text{sulphate}}$.

The comparison between $\delta^{34}\text{S}$ in aquifers C and D shows a general enrichment of ^{34}S in aquifer D. The most enriched dominant range of $\delta^{34}\text{S}$ was between $+30$ to $+40\%$ in aquifer D, and between $+22$ to $+32\%$ in aquifer C (Table 4.10). Also, all values of $\delta^{34}\text{S}$ in aquifer C were less than $+60\%$ (Figure 4.24a). However, rising points in $\delta^{34}\text{S}$ ($>+60\%$) were observed in aquifer D following the flow direction passing through boreholes DEP-7, DEP-5, DEP-3 and RBK-D in addition with HAD-49 (Figure 4.24b). These increases could be related to spots with strong sulphate reduction resulting in the dominance of ^{34}S concentration.

Furthermore, two possibilities may occur in aquifer D and affect the high spots on the above aquifers. Due to the high altitude and the hydraulic conditions, sulphate is imported through fissures, fractures or faults to the upper aquifers. The second option can be said to relate to groundwater injected from aquifer D to upper aquifers,

however later on each aquifer developed by itself among bacterial reduction and oxidization. Taking the longer residence time into account ^{34}S appears with high concentrations as is observed in boreholes Ranada1, WWD-32, W.Bharna1 and DEP-19 in aquifer C as well as at WWD-24 and KhT-A in aquifer A.

As a result, the $\delta^{34}\text{S}_{\text{sulphate}}$ values are become enriched in central Najd and eastward more than in the west in aquifer C and D. However, $\delta^{34}\text{S}$ distribution and ^{34}S concentrations were recorded by higher rate in aquifer D more than in aquifer C due to the reduction process (BSR).

The enrichment in $\delta^{34}\text{S}_{\text{sulphate}}$ in these samples seems to be due to BSR in the stagnant groundwater. This is confirmed by the observation of a H_2S smell (IAEA, 1995) in most groundwater samples from aquifers B, C and D. Recent data obtained from drilling in the Najd points to H_2S smell being observed in groundwater samples of aquifer C and D to the north of UTM (1966814 N) with exceptions for some specific locations such at DEP-9A and DEP-16 east of Al Mazyunah. In aquifer B, H_2S a smell is found in groundwater located north of UTM (1996523 N). However this gas smell was not detected any where in aquifer A.

The presence of H_2S is detected in all Najd aquifers except A. Several scenarios have been discussed to find a reasonable link for this difference between aquifers, even though it was difficult to find a direct relation variation. However, aquifer matrix compositions seem to be the unique parameter which can answer this phenomenon. By referring to aquifers lithological description, aquifer A is mainly restricted with Rus formation which consists of Breccia, chalky dolomite, marl and gypsum limestone. On other hand, the rest of aquifers B to D contain either biomicritic and fossiliferous limestone or both. In addition, aquifers common with H_2S were altogether located in the UER formation. In this case, the formation may help to provide thin layers consisting of biomicritic or fossiliferous limestone inter-bedded with aquifer lithology and acting as a source for sulphate reduction developments. As a result, H_2S seems to be developed in these aquifers during microbial processes.

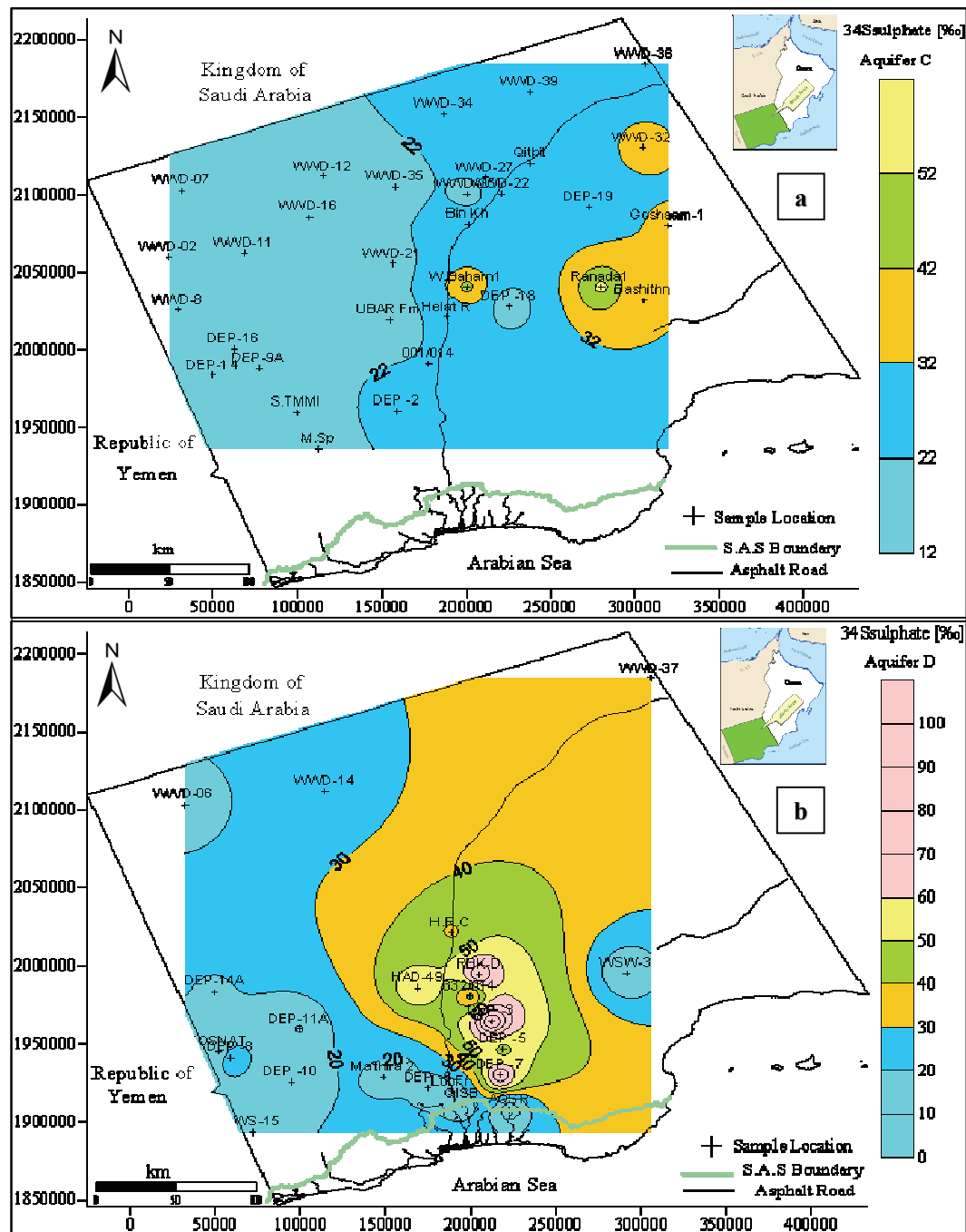


Figure 4.24 Distribution of $\delta^{34}\text{S}_{\text{sulphate}}$ in groundwater of aquifer C and D

4.6 Multiple Influences on Groundwater Recharge Processes

4.6.1 Groundwater flow dynamic in the upper aquifer A

After the study, the general consensus of aquifer A being representative of water from the entire Najd region can only be held for very limited areas within the aquifer

(GRC, 2008). Considering isotopic signatures of water, $\delta^2\text{H}$, $\delta^{18}\text{O}$, and ^3H , from this aquifer (Table 4.10), it is not likely to have raised from modern recharge sources alone. Consequently, the recharge of aquifer A cannot be completed by monsoon and direct rainfall events. It is further concluded that still uncharacterized recharge sources from below the formation of aquifer A, i.e., Dammam and Rus, contribute to the water pool in this aquifer. The soil coverage is very shallow in the Najd regions, often less than 4 m, underlain by hard limestone of the Dammam and Rus formation and the permeability of this base layer is low. Subsequently, aquifer A seems to be confined to most of the Study Area even though some reports say it is a semi-confined to confined aquifer (*i.e.*, PAWR, 1986).

Two observations emphasize the different hydraulic behavior of aquifer A, and its recharge sources are taken into account for future considerations. First, the spring SHTH close to aquifer A is located in the recharge area and contains water with an isotopic signature in $^2\text{H}/^{18}\text{O}$ and elevated tritium of modern precipitation. Additionally, water from borehole M.MASIN located in the centre of the desert (Shsir Village, aquifer A) has an isotopic signature in $^2\text{H}/^{18}\text{O}$ with less elevated tritium similarly to water from the Ubar Fm (aquifer C) well nearby.

As a result of that recharge to aquifer A - when it occurs in some specific places like Shsir and Helat Ar Rakah - probably does not infiltrate directly from the rainfall, however, it conducts through some faults in reaction with flood events. This may explain the difference in water levels between boreholes located within circle diameter less than 2-4 km.

4.6.2 Faults influences in the groundwater flow and behaviour

It was previously mentioned that two major and several minor fault lines for a Graben structure that runs through the center of the Najd region (Watson Hawksley, 1983; MPM, 1990; MMI, 1991). However, the recent seismic surveys conducted by oil companies in this area disagree with those hypotheses. The data shows that several faults exist in Hanfeet and Helat Ar Rakah and take the direction of southwest to northeast with some of them passing through the Hanfeet wellfield supporting drilling results at that field. The similarity was found to the east side close to DEP-3 and

DEP-5 one major and some minor faults were observed (more details in chapter 2). These faults have a strong influence on the groundwater flow dynamics in this formation. Chemical shifts were observed in aquifers B, C, and D along the areas close to the fault lines. Despite the uncertainty of the fault occurrence and direction in some places within the Najd region, however the hydrochemical and isotope data presented here can be used to assess the behavior and interaction of groundwater in the different aquifers.

4.6.3 Hydrochemistry and isotopes evidences

The heterogeneity between aquifers and in specific aquifers themselves was complicated to assess and trace the flowpath. This is due to the scattering of boreholes in different aquifers and the geological structures influences. Even though the study attempts to find relationships between boreholes in each aquifer which may help to understand the groundwater behavior and flow characteristic. These relationships - if they exist – can give further evidence about the groundwater movement and the effect of faults. Therefore, eight groundwater profiles were presented from aquifers A, B, C, and D. Each of the profiles formed at least three wells being consistent in both hydrochemistry H/O isotopes in any direction (see Figure 4.25, Figure 4.26 a-p).

Profile A ran from south to north starting at the STHH spring and passes along borehole M.Masin continuing northward to borehole WWD-20 (Figure 4.25 & 4.26 a-b). In this line, with the exception of HCO_3 all ions increase from south to north, however ^2H and ^{18}O depleted with the same direction following the groundwater flow direction in that area.

Profile B was chosen along a south to north transect through aquifer B (Figure 4.25 & 4.26 c-d) using boreholes DEP-16A, WWD-17, and WWD-13 located within the sand dunes. The groundwater mineralization along this transect is associated with very high concentrations of sulphate and calcium, and low concentrations of sodium and chloride. The increased sulphate and calcium ions could have originated from the dissolution of the gypsum layer present in the upper UER. Low concentrations of chloride, sulphate, and bicarbonate as marked in DEP-16A are usually indicative of surface water (rivers, wadi downflow) (Hem, 1989) by vertical recharge. However,

the tritium content of DEP-16A is too low. Also, groundwater from borehole WWD-13 along the profile B is tritium free. South of the profile B, a higher tritium content of 1.2 TU was analyzed in borehole DEP-9 located 50 km east of Al Mazyunah in the Wadi Aydim. Groundwater from aquifer B in this region - assumed from the profile - does not indicate recent vertical recharge northward and seems to have little contact with brine waters or halite layers which are abundant more in the north-east direction. In the south the watershed of Wadi Aydim could influence the groundwater due to recharge by flood events. This can also be verified by the well DWS-15 – built in aquifer D and located upstream DEP-9 (aquifer B) - with a tritium content of 1.3 TU. Flood and rainfall events along wadis seem to directly influence the recharge into aquifer systems independently of their position (Matter et al., 2005; Odeh et al. 2009).

The C1 and D1 profiles (see Figure 4.25) run parallel to the Saudi Arabian border, passing through wells WWD-7, WWD-12 and WWD-36 for aquifer C (Figure 4.26 e-f), and WWD-6, WWD-14, and WWD-37 for the D aquifer (Figure 4.26 m-n). In both profiles, sodium and chloride increases along the direction of groundwater flow and may indicate mixing of sodium-chloride bearing brines into the groundwater along the north-east direction, because limestone is the most dominant rock-type in this part of the aquifer and halite formations are extremely low here. The mixing hypothesis is supported by the existence of sabkhas in the Rub al Khali in the northeast edge of the Najd ranging to further NE direction. Brines from these geomorphic features in the Rub al Khali are highly concentrated in Na^+ , Mg^{2+} , Ca^{2+} , Cl^- , SO_4^{2-} (Alsaaran, 2008). The sabkhas are considered as result of uprising paleo-groundwater for wetter periods older than 6000 years BP and precipitation (Clark et al., 1987, Wood et al., 2002). The presence of marine fossils and brines justify the mixing hypothesis along the flow path.

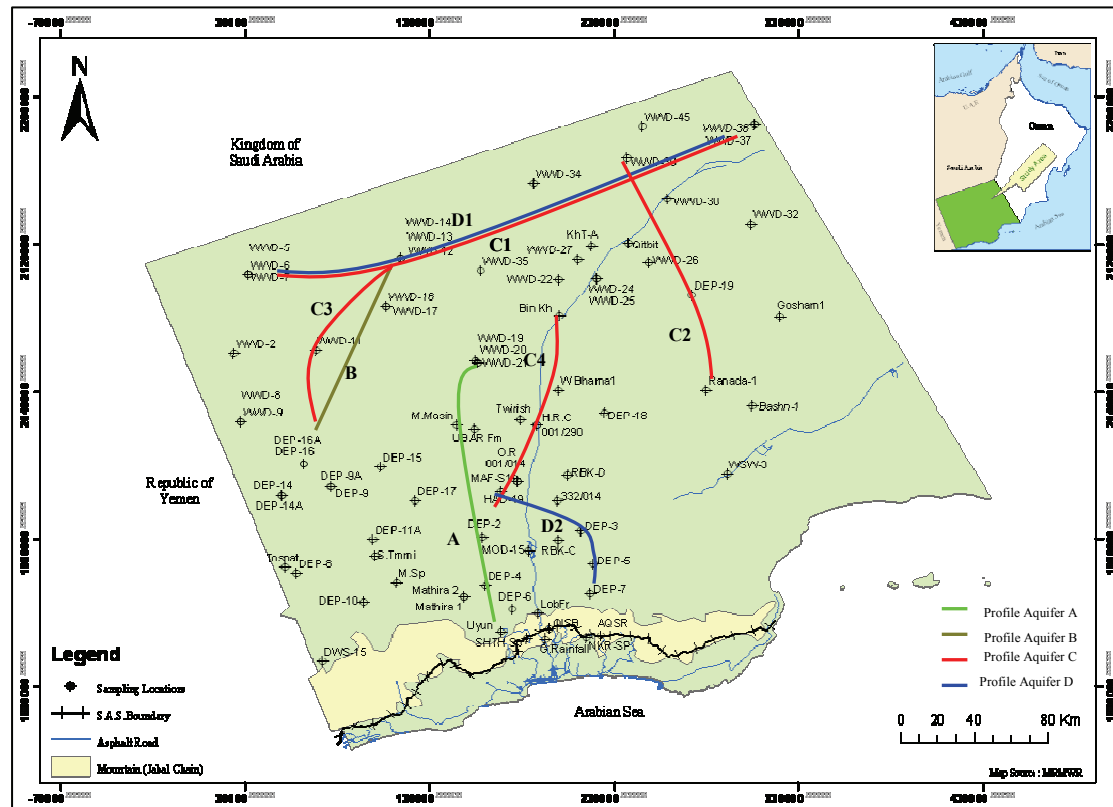


Figure 4.25 Profiles constructed in different aquifers based on the consistent relationship between hydrochemistry and isotope data, for an example from each aquifer (see Figure 4.26)

The "tritium free" groundwater has a value of the detection limit of 0.25 TU analyses in WWD-7 and WWD-12 and confirms the exclusion of any recent water compartments along the north-east flow direction.

Further profiling was done along the Study Area structure to further characterize the C aquifer using wells Ranada1, DEP-19 and WWD-39 in the east (profile C2, Figure 4.25 and 4.26, g-h), wells DEP-16, WWD-11 and WWD-16 in the west (profile C3, Figure 4.25 and 4.26, i-j) and wells DEP-2, 001/014, 001/290, Bin Kh (BF080077AA) and WWD-25 (profile C4, Figure 4.25 and 4.26, k-l). The hydrochemistry influences by the brine character observed in profiles C1 and D1. Following aquifer C from the recharge area north towards WWD-39, ^2H and ^{18}O steadily decreases from the well (001/290) at Helat Ar Rakah. Considering all C

profiles as a whole, we conclude that groundwater is particularly impacted by the fault structure as well as the fossil groundwater located along the northeast edge of the Study Area.

Overall, groundwater in middle Najd around (332/014) at east Hanfeet area is associated with low mineralized and remarkably enriched in ^2H and ^{18}O as it detected from profile D2 (Figure 4.25 and 4.26, o-p). From this observation, it can be concluded that groundwater recharge in the Jabal chain in/or the nearby north side in the southern part of aquifer D occurs by mixing recent precipitation from monsoon and cyclonic events (Macumber, 1995) with older groundwater from beneath the formation. Water from the west of this area at west Hanfeet is significantly depleted in ^2H and ^{18}O , particularly indicated around well HAD-49, and recharge from another area or at another time period must be assumed as well as structurally influenced flow system.

In addition to isotopes, it is also clear from the major ion concentrations in water the located within the area are highlighted with faults (see structure map in chapter 2), that the faults play an important role in determining groundwater chemistry. For example, ions such as Na^+ , Cl^- , SO_4^{2-} , Ca^{2+} and Mg^{2+} generally increase northwards in all profiles, where ^2H and ^{18}O are also depleted along the groundwater flow direction. The behaviors of these ions in aquifer C (C1) matches the profile of aquifer D (D1), and water taken from wells WWD-36 (aquifer C) and WWD-37 (aquifer D) (Figure 4.25 and 4.26, e-f, m-n) clearly have similar chemistry and isotopic signature. In addition to the chemistry, groundwater mixing is assumed between aquifer B and C.

From these profiles, it is suggested that another fault is expected to exist north of Dawkah. This fault probably takes a southwest to northeast direction and lies close to borehole Bin Kh (BF080077AA) at UTM WGS84 2080773N. Two reason can support this hypotheses (i) hydrochemistry data behavior among profile C4 did not follow the same trend when profile C4 extended to borehole WWD-25 (Figure 4.25 and 4.26, k) (ii) the hydrogeological cross section (A-A, see chapter 3) was detected possibility of fault between boreholes Bin Kh (BF080077AA) and WWD-25.

The major ion concentrations were observed to increase along the groundwater flow direction. Specifically with depth, sodium and chloride increase and sulphate and calcium decrease (aquifer A to D). These observations, taken together, suggest that ion exchange or sulphate-reducing processes occurs in the deepest parts of the formation. The A and B aquifers seems to be an outlier as far as ion concentrations are concerned, and hydrochemistry suggests that the formations matrix here probably consists of limestone, gypsum, and mixed layers of them, as well as sodium chloride. Considering the $\text{Ca}^{2+}/\text{Mg}^{2+}$ ratios, the majority of water samples in aquifers C and D (ranging from the Jabal foothills toward the Najd) tend to have a meq-ratio less than one which indicates that dolomitic dissolution and calcite precipitation occurs here. The ratios support the assumption of a groundwater flow towards north-east, and that groundwater of the deeper aquifers C and D interact with the aquifer matrix. Overall, groundwater in aquifers A, B and those samples from aquifer D located in or close to the recharge area (Jabal chain) is influenced by gypsum dissolution processes in these aquifers.

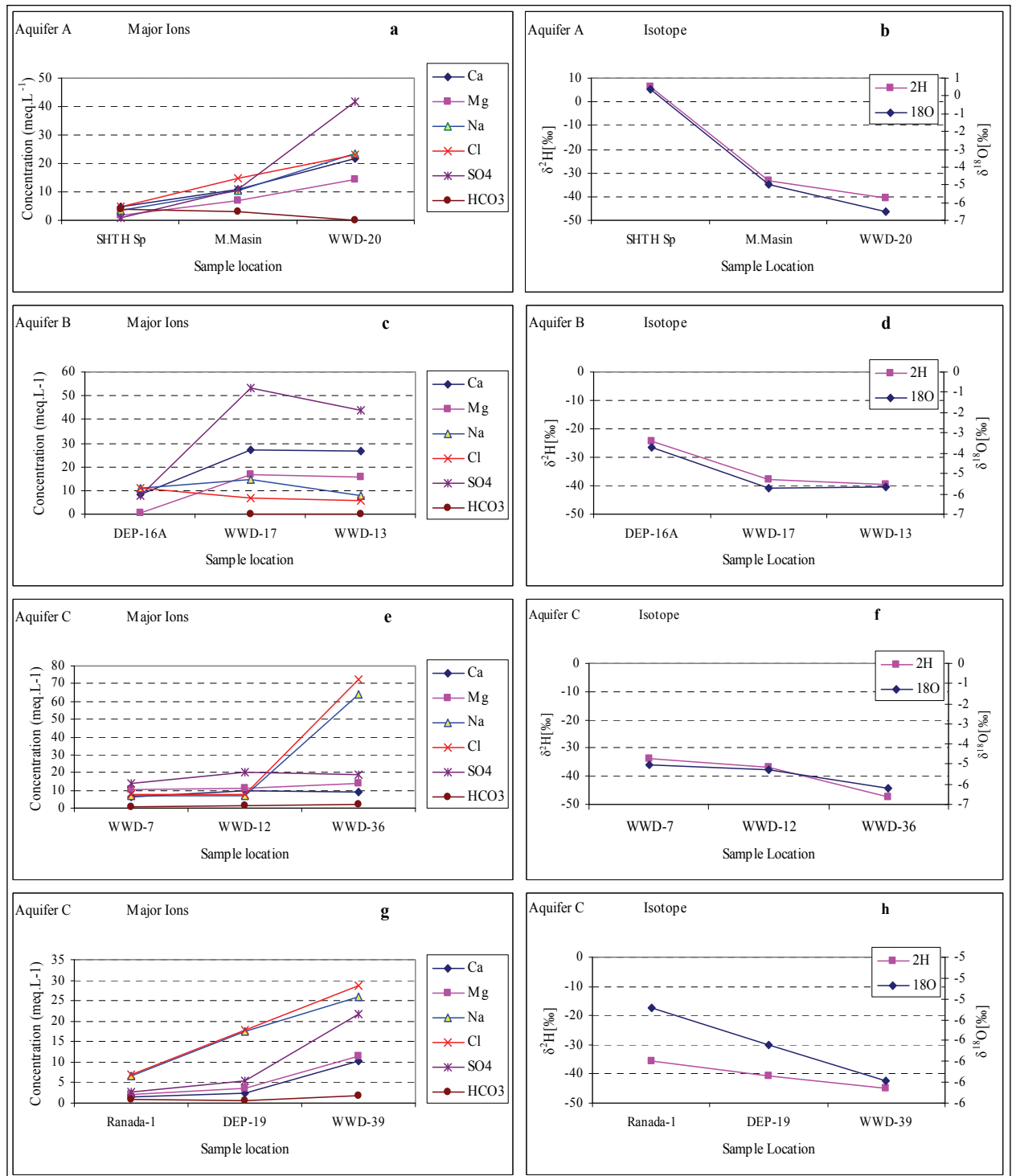
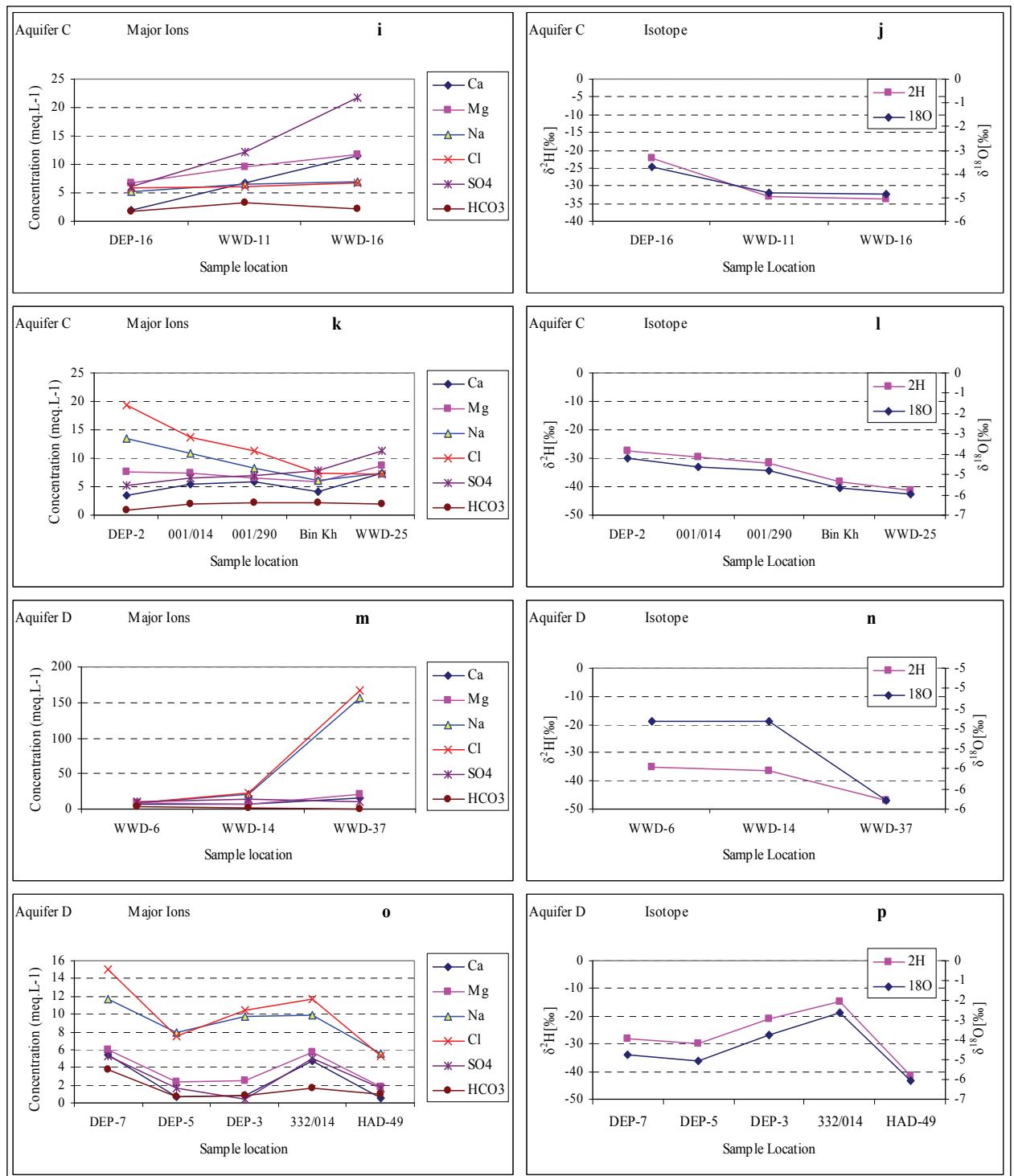


Figure 4.26 (a-p) Characteristic profiles reporting the hydrochemical and isotope development of the groundwater in aquifers A to D. The profiles follow the main directions of the groundwater flow: in aquifer A (a, b = A) and aquifer B (c, d = B) south to north, in aquifer C (e, h = C1, C2)



4.6.4 Recharge direction

According to the contour maps constructed in aquifer D for ^2H (Figure 4.27), the data reveals a possible connection between the groundwater in the recharge area in south and central Najd. This direction is distinguished through boreholes (LobFr) in the south, Thumrait (MOD-15) and east Hanfeet at the poultry farm (332/014), and probably continues northeastward to wadi Bin Khawtar near WWD-24. The similarity was observed in Figure 4.28 and shows the distribution of chloride in aquifer D. The chloride concentration increases with groundwater flow direction. This direction agrees with mineralization rises direction. This direction can be distinguished from $\delta^2\text{H}$ in aquifer D as well from Cl through the green colour in both figures. As a result, this direction is probably an important line in terms of groundwater recharges. Moreover, the water level contour maps for aquifer C and D (chapter 3) confirm the same flow direction.

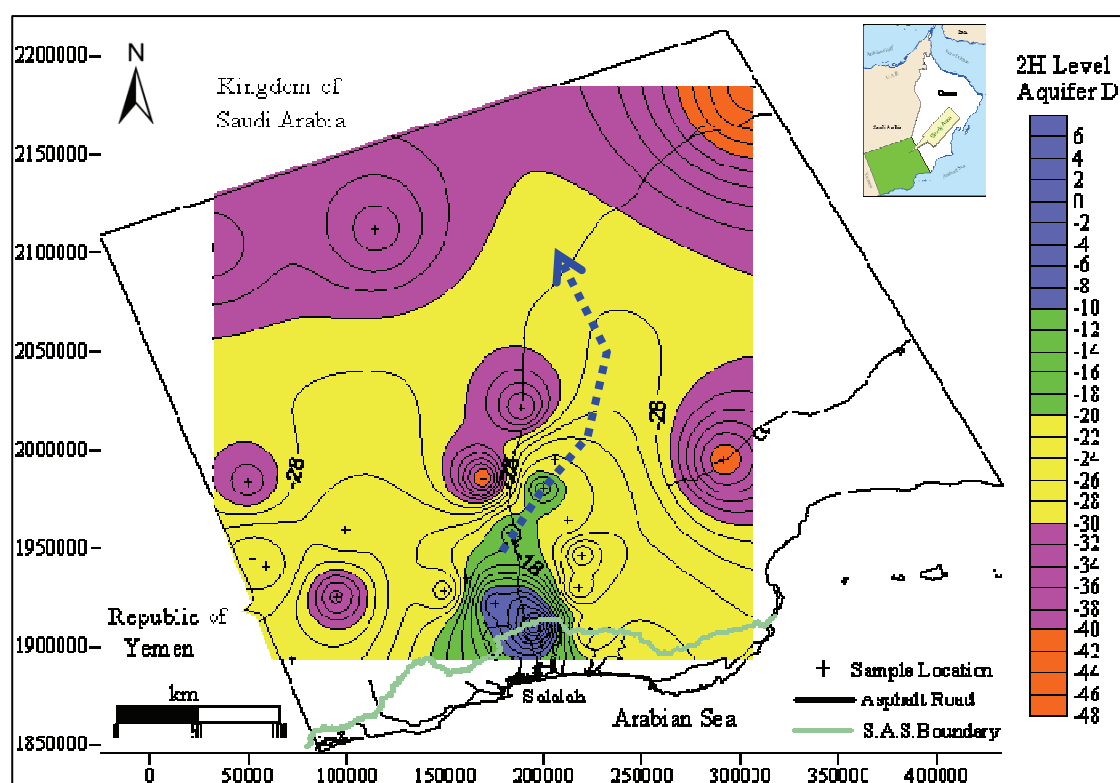


Figure 4.27 $\delta^2\text{H}$ distribution in aquifer D and direction of the recharge in dot line shows decrease of monsoon influence along the flow line; high depletion of ^2H could also point to strong pumping activities because of fossils water with depleted ^2H

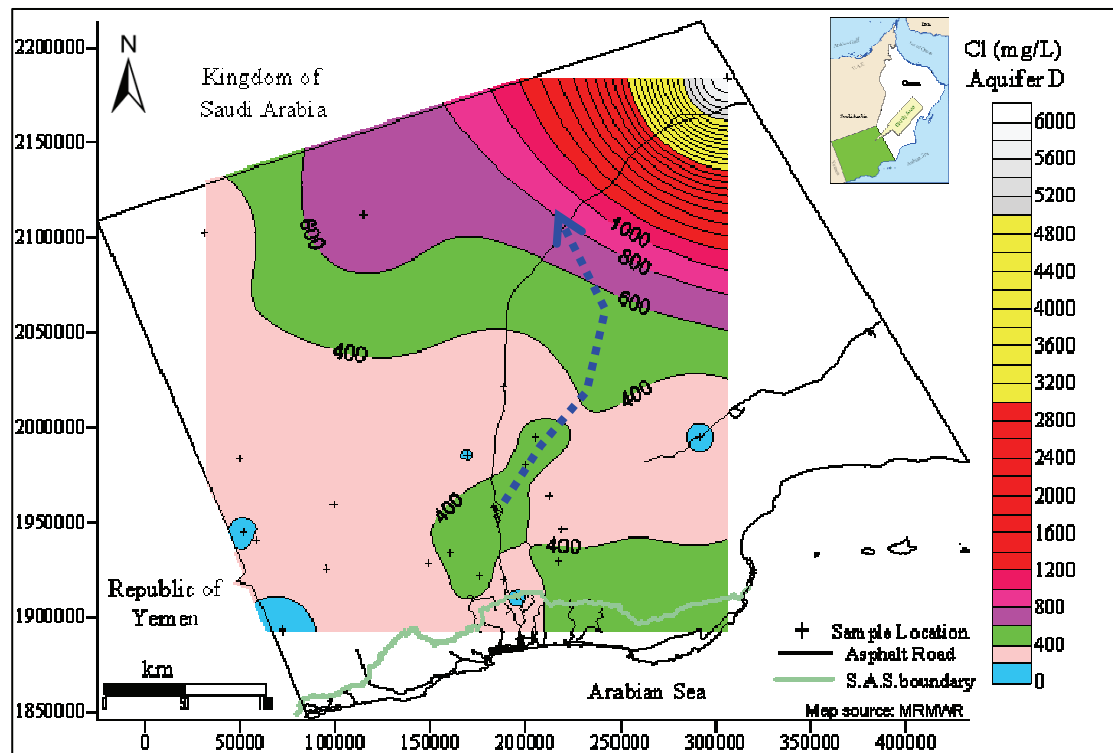


Figure 4.28 Cl ($\text{mg}\cdot\text{L}^{-1}$) distribution in aquifer D and proposed recharge direction in dot line

4.7 Water Quality

Aquifer A has the potential to produce a good amount of water for agriculture purposes in the previous highlighted areas (see chapter 3). The increasing discharge in this aquifer towards the north may be due to leakage from the lower aquifers. The quality of water decreases with the flow direction as well as with the other aquifers. Several studies conducted in the Najd region by MacDonald (1991, 1994b) and the Ministry of Water Resources (MWR 2000a) before 2005 have suggested that aquifer B could provide a significant portion of the water demands for the entire area. However the latest project carried out by the MRMWR (GRC, 2008) has confirmed that the B aquifer could provide significant amounts of water for western and central Najd only. This aquifer which occupies the Upper UER formation spreads north from DEP-17 (UTM WGS84 coordinate 1978362 N), with the western edge near WWD-9 and the international border of Yemen, and the eastern edge beyond Helat Ar Rakah close to DEP-18. Thicknesses in aquifer B are nonetheless largely diminished

northeast of Al Mazyunah in the middle and western regions of this area where thicknesses are less than one metre and were observed in boreholes for wells DEP-14, DEP-18, WWD-5, WWD-13, WWD-17, and WWD-19.

Since the primary investigations of groundwater in this region during the 1980s, it was assumed that aquifer C was the most important water resource. However, further characterization in 2004 revealed that the distribution of this aquifer was located more north than initially believed and is located north of UTM WGS84 coordinate (1959600N). South of this coordinate, near the Jabal, aquifer C is largely dry and its distribution along the southern edge of the Najd is currently unknown (GRC, 2005a).

Compared with all aquifers, the D aquifer is the most widely distributed as it starts on the northern side of the Jabal chain and covers the entire region. It is also suggested that this portion of the formation possesses the highest alluvial thickness, but lower transmissivity (see Table 3.1) than aquifer A, B, or C. Aquifer D also produces a lower discharge rate than aquifer C (MWR, 2000a). After the exclusion of three boreholes (WWD-30, WWD-36 and WWD-37) located in the north east part of the Najd was due to high salinity. Therefore, the study concludes from hydrochemical knowledge and a survey of the current information for this region that groundwater suitability for use as agricultural irrigation must be evaluated in a sequence as $D > C > A > B$.

4.7.1 Potable water

The groundwater in the Study Area consists partly of paleo-groundwater except in the recharge area (Jabal chain). The water quality varies between aquifers as well with different parts of the Najd area. Thus it is possible to find some of the groundwater elements' concentration fall within Omani Standard (almost same as WHO standard). However it is unusual to find all elements concentrations to agree with the maximum permissible limits of potable water. Also it was observed in several locations that almost all elements were fitting with the Omani Standard, however either or both F and SO_4 often pass the maximum permissible limit. In previous years most people in the desert drank natural groundwater precisely due to the shortage of potable water.

This type of water often has high concentrations of fluoride. Consequently, their affect is easily detected from the people's brown-tinted tooth colour. However, later the government constructed desalination plants in all cities or villages to provide potable water for citizens. The F is a common ion in Najd groundwater with high concentrations exceeding human drinking water permissibility. Therefore, the study suggests highlighting this ion particularly on its source and distribution.

4.7.1.1 Fluoride source and distribution

The F⁻ at low concentrations of drinking water has been considered beneficial in candy bar consuming countries (Appolo & Postma, 2005). Regularly, F is added to the water supply when it is absent or in very low concentration. The F can create some health problems when exceeding 3 mg.L⁻¹ and causing dental problems like tooth discolouration. Moreover, F is found in high concentrations and can cause bone deformation and joint pain for the elderly (Appolo & Postma, 2005). The effect of F in drinking water on animals is similar to the effects on humans. Water with small concentrations of 1 mg.L⁻¹ F is beneficial, but at concentrations which reach 30 mg.L⁻¹ of F in water is toxic to most livestock. Effects on livestock and people are basically the same and occur at about the same F levels (GRC, 2008).

Despite few references being discussed in detail, there is a source of fluoride in groundwater. However, the source of fluoride were mentioned by Hem (1989) to be found in the Fluorite (CaF₂) mineral which possibly to exists in both igneous and sedimentary rocks due to its low solubility. Also fluoride can be found in Apatite, Ca₅(Cl,F,OH) and (PO₄)₃. High fluoride concentrations are found more in water with low calcium concentration (Hem, 1989). Other authors related fluoride occurrences to different sources such as leaching from formations lithology without any specification (Handa, 1975; Jacks et al., 1993; Saxena and Ahmed, 2003).

Zack (1980) related the source of fluoride to dissolution of fossil shark teeth, containing fluoroapatite in the sedimentary rocks. Fluoride usually increases in groundwater by residence time and slow groundwater movement in deep aquifers systems. Under such conditions, the solubility of fluorite increases with increasing

temperatures and fluoride may be added by dissolution of HF gas (Frencken et al, 1992 and Brunt, et al, 2004). Battaleb-Looie and Moore, (2009) conducted studies to determine fluoride source in groundwater in Dashtestan area, south of Iran by using Petrographic analyses. The study indicates that mica minerals were the most probable source of fluoride content.

Coetsiers, et al. (2008) carried out hydrogeochemistry studies in the Nairobi area (Kenya) using the PHREEQC model to determine the influential source of fluoride ascents in groundwater. The study related fluoride increase were due to weathering of sodium-rich alkaline igneous rocks resulted in a pH increase followed by an increase in HCO_3^- and CO_3^{2-} by dissolution of CO_2 . As well, when groundwater becomes oversaturated with respect to calcite, Ca^{2+} will decrease while calcite precipitation occurs. At the same time this process causes a sub-saturation with respect to fluorite and dissolution of fluorite increases the F^- concentration.

In total 74 out of 79 of the collected samples were recorded as containing fluoride concentration exceeding the Omani standard for potable water. The fluoride concentrations were recorded the lowest value of 0.61 mg.L^{-1} in spring (SHTH) in aquifer A and the highest value 15.0 mg.L^{-1} in borehole (WWD-37) located in aquifer D with average of 0.75 mg.L^{-1} . These concentrations were found in the range ($0.61\text{-}8.7 \text{ mg.L}^{-1}$), ($1.9\text{-}5.4 \text{ mg.L}^{-1}$), ($1.5\text{-}7.4 \text{ mg.L}^{-1}$) and ($0.8\text{-}15 \text{ mg.L}^{-1}$) in aquifers A to D respectively. The X-Y plot of F with several elements such as Ca, SO_4 , Sr, Temp and EC were found with a maximum relationship (R^2) less than 0.4. These relations also varied between aquifers and increase northward with the flow direction.

Despite this, several calculations have been conducted in all aquifers in order to find out any direct relationship between F and other elements. However the scattered plots of F versus Sr shows a slightly stronger relationship ($R^2 = 0.5$) in aquifer A rather than what was found with the other elements (Figure 4.29). This linear relation is probably related to a source of Strontium and fluoride from SrF_2 or the combination from different components such as aragonite for Sr and CaF_2 for fluoride. Moreover due to its ion charge and radius, which is slightly similar to hydroxide ions, fluoride can replace each other in mineral structures like Cl or OH (Hem, 1989). On the other hand, the groundwater in Najd was described as paleo-groundwater (Clark, 1997).

Therefore temperature and residence time in addition with ions exchange are parameters which probably play a role in the elements behavior, as well with fluoride. Increasing concentrations of fluoride and strontium ions were also observed from the aquifer's A to D. These ions were recorded at the highest concentrations in aquifer C and the lowest concentration in aquifer A. Fossilized remains occur more frequently in the aquifer matrix of C than in other aquifers. The elevated content of limestone present here could also explain the higher strontium ion concentrations in this location (Hem, 1989). In particular, aragonite could be another source of strontium when altered to calcite (Sunagawa et al., 2007). The increased fluoride ion concentrations in the C and D aquifer may be due to weathering of the aquifer matrix, ion exchange capacity, or the presence of fossilized remains within the formation. Potassium concentrations generally increased with aquifer depth, but the highest concentrations were observed in the aquifer B and C reservoir.

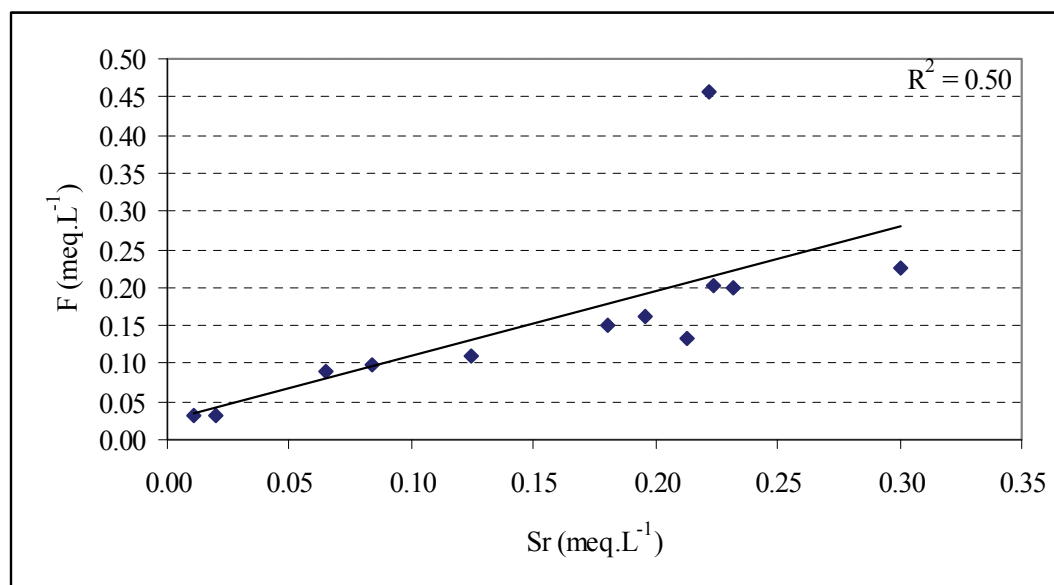


Figure 4.29 Sr versus F in aquifer A

The distribution of fluoride in aquifers C and D can be illustrated from Figures 4.30. The maps reveal that the majority of Najd groundwater was restricted within the fluoride values and range from 4.5 to 6 (mg.L⁻¹) in both aquifers C and D. The fluoride concentrations in both aquifers increase with the groundwater flow direction south or southwest to north or northeast with exceptional points. Regarding aquifers A

and B, due to their horizontal boundary limitation they ignored from this type of plot in bases of fluoride distribution.

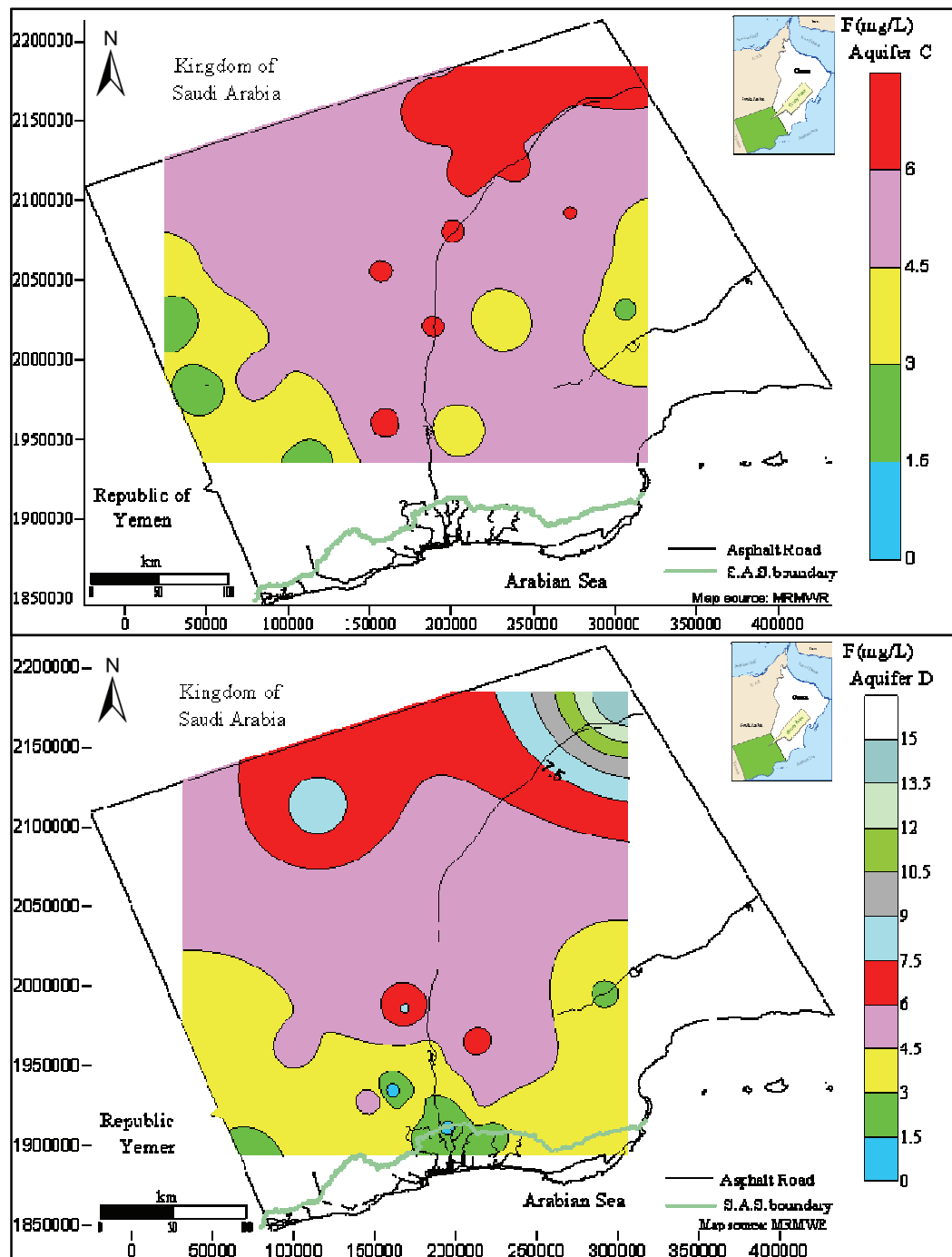


Figure 4.30 Distribution of fluoride in aquifers C and D

Fluoride occurs in aquifers A to D with concentrations exceeding the Omani standard for potable water and covered whole of the Study Area, except springs or wells located in the Jabal and DEP-14 (aquifer C) east of Mazyunah.

The linear plot of TDS versus Fluorite (SI) shows that around 50% of the samples were located either in oversaturated or under-saturated ranges with respect to fluoride. At the same time groundwater from all aquifers are likely to be in a mixing process between aquifers which is not easy to distinguish in the aquifers. The fluoride SI had slightly increased in all aquifers with the low mineralization range up to approximately TDS value reach 4000 mg.L⁻¹ (Figure 4.31).

The fluoride SI under-saturated indicates fluoride dissolution and may release fluoride in the matrix which is involved in other processes such as ion exchange. As a result, fluoride concentrations are relatively small in groundwater under-saturation with respect to fluoride. In parallel the aquifer system with oversaturated fluoride seems to precipitate fluoride and no more dissolution of fluoride. Therefore any addition of fluoride will release fluoride ion (F⁻) concentration as well with fluoride precipitation in the aquifer.

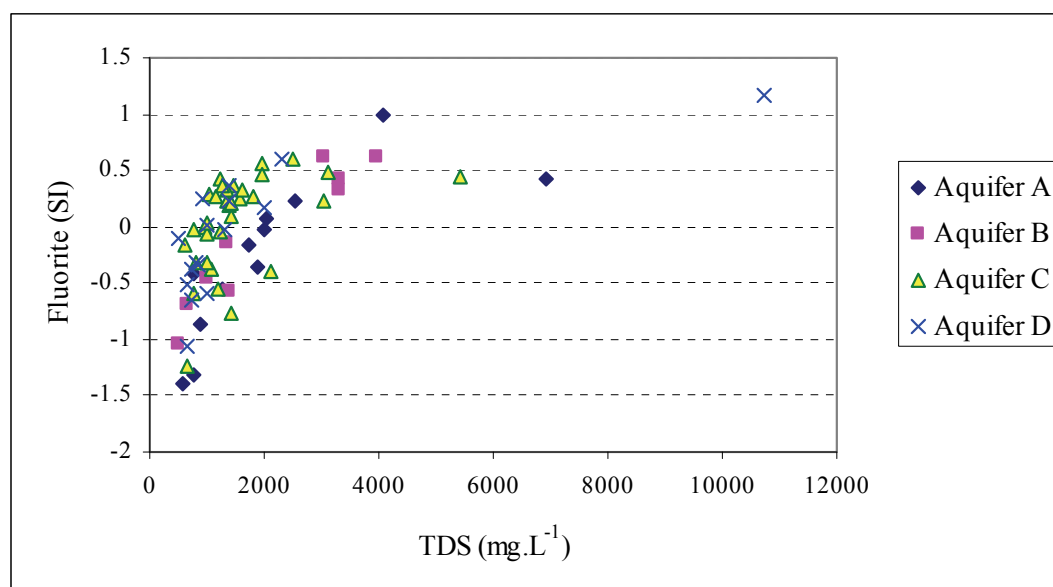


Figure 4.31 Total dissolved solids (TDS) versus Fluorite (SI)

In fact, all aquifers were oversaturated in respect to calcite, dolomite and aragonite which means the possibility of precipitate carbonate such as calcium. In comparison with SI, in respect to calcite and fluorite the precipitation of calcium with respect to calcite could be associated with fluorite process and increase of fluoride

concentration. This idea may agree with Coetsiers, et al. (2008) idea that related increases of F^- to dissolution of fluorite.

On other hand, the strontium is the main source is aragonite. Based on the linear relationship between fluoride and strontium the possibility of sharing the same source may be expected.

4.7.1.2 Nitrate

Fifteen samples out of 79 were recorded nitrate with values in the rang between 0.89 $mg.L^{-1}$ at Mather2 in aquifer D to 31 $mg.L^{-1}$ at O.R in aquifer A with exception of NKR spring which occupied the highest value of 81 $mg.L^{-1}$. These boreholes were distributed between three aquifers A, C and D only, however 7 out of 15 belong to aquifer A. Whereas NO_3 was not detected with considering levels except 0.22 which may related to measuring mistakes and ignored were in this counting. By referring to the Omani standard No.8 (2006) for potable water the maximum permissible limit of nitrate was 50 $mg.L^{-1}$, therefore groundwater from all locations are still within the range of potable water except NKR spring.

4.7.1.3. Total Hardness

The classification of groundwater based on total hardness shows varied values ranging between 123 to 2400 $mg.L^{-1}$ for all aquifers. In total, 31 out of 79 samples fitted below the maximum permissible limit for potable water, even though not one fits within the soft water range ($<75 mg.L^{-1}$). At the same time 3 boreholes from aquifer D located at Hanfeet (HAD-49, RBK-D) and Helat Ar Rakah (H.R.C) were recorded as moderately high water (75-150 $mg.L^{-1}$). Only 13 samples can be classified as hard (150-300 $mg.L^{-1}$) water according to Sawyer and McMearty's (1967) classification which was mentioned by Bahar and Reza (2010). However, the rest of the wells were defined as very hard water ($>300 mg.L^{-1}$). In addition, the total hardness increases in all aquifers A to D with the groundwater flow direction to the north and northeast ward.

4.7.2 Irrigation water for agriculture purposes

4.7.2.1 Salinity

The hydrochemical evaluation of the water quality of the four aquifers is highly relevant for the sustainable use of the water resources of the Najd region. Aquifer A is an important local source of water in central and northern Najd. This aquifer is the main reservoir for many local farms in the Helat Ar Rakah, Hanfeet and Bin Khawtar areas. The shallow depth of aquifer A and acceptable mineralization values for agriculture encouraged many local farmers to establish small farms which depend on aquifer A for a main water resource. Despite the highest rates of discharge in aquifer A found during drilling of well WWD-36, located in the northern corner of the Study Area. However, this area is also known to contain highly mineralized water (EC at $15,000 \mu\text{S.cm}^{-1}$). Additionally, high mineralization was also discovered along the western edge of the region, approximately 120 km parallel to the border with Saudi Arabia. Values here exceeded $9,000 \mu\text{S.cm}^{-1}$. As is consistent with mineralization values in this range, these two areas of the aquifer A do not represent potable sources.

Even though these high concentrations of EC in all Najd aquifers especially in the northeast portion, however this water can be categorised based on the type of use. In general Najd groundwater could be used for animal drinking. For animal drinking purposes, the FAO (1986) classified water based on mineralization (TDS) concentrations to several levels (Table 4.12). Base on this information, all groundwater from different aquifers seems to be fitting with FAO classification range for at least one type of animal.

Table 4.12 The FAO standards for the safe upper limits of total salts in water for stock in arid countries

Species	Data Source	TDS[mg.L^{-1}]	Approximately EC [$\mu\text{S.cm}^{-1}$]
Poultry	FAO	2800	4024
Horses	FAO	6400	9095
Cattle (Dairy)	FAO	7100	10081
Cattle (Beef)	FAO	10000	14165
Adult Dry Sheep	FAO	12800	18109
Donkeys	ILCA	10000	14165
Camels	MRMWR	10000	14165

The convert from TDS to EC was used the following equation ($\text{TDS} = 0.71 \text{ EC} - 57.38$)

The EC ($\mu\text{S}\cdot\text{cm}^{-1}$) values were used to create contour maps for each aquifer separately (Figure 4.32). In these maps the interval 2500 $\mu\text{S}\cdot\text{cm}^{-1}$ between contours was fixed for all aquifers. The purpose of the previous interval value was to determine the distribution of groundwater with semi equivalent EC to that of maximum limit for potable water (TDS=1500 $\text{mg}\cdot\text{L}^{-1}$) uses.

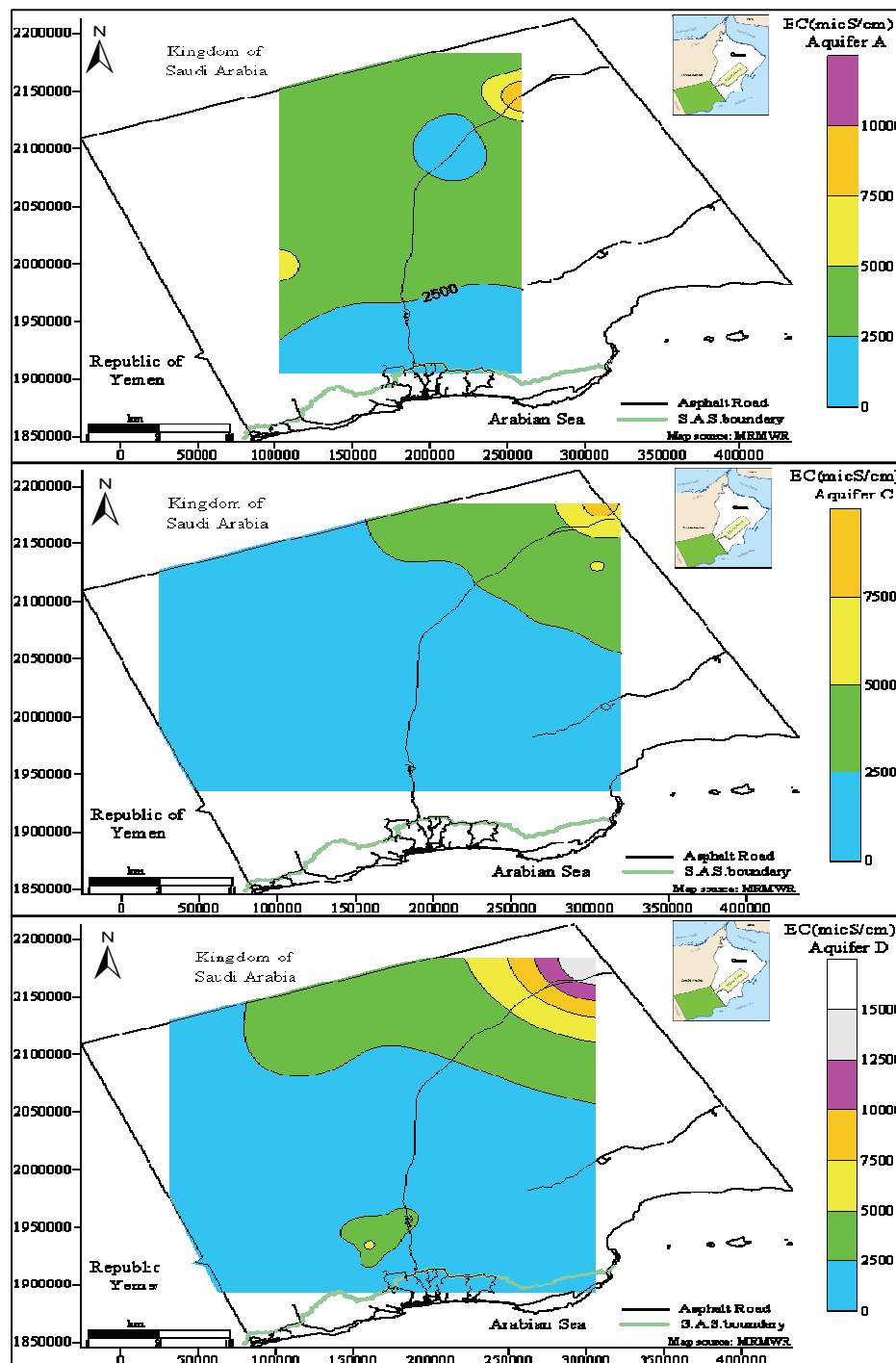


Figure 4.32 Electrical conductivity ($\mu\text{S}\cdot\text{cm}^{-1}$) distributions in aquifers A, C and D

The plots show a general dominant range for the first interval $<2500 \mu\text{S}\cdot\text{cm}^{-1}$ except in aquifer A which is slightly higher. The EC in all aquifers from A to D tends to increase with the groundwater flow direction.

4.7.2.2 Cl/Br ratio

This ratio was used to distinguish the origin of Cl and the possibility of saline water intrusion with fresh groundwater. The detected ratio of Cl/Br is about 300 when both elements are measured in $(\text{mg}\cdot\text{L}^{-1})$. The values close to this ratio were indicated by sea water intrusion or brine water intrusion, with fresh water in the aquifer system (Eriksson, 1981). When Cl and Br composition in sea water was at the value of 19000 $(\text{mg}\cdot\text{L}^{-1})$ for Cl and 67 $(\text{mg}\cdot\text{L}^{-1})$ for Br; this ratio will be at 284. In the Study Area Br was not analyzed for all samples due to some technical problems in the laboratory in Oman at that time. Therefore most of the data available was from aquifer C. The Cl/Br ratio for aquifer C was restricted between 20 in borehole WWD-11 and 794 at well 001/014 in Hanfeet, with average of 255.

Six out of 19 boreholes in aquifer C shows Cl/Br ratios within the range from 270 to 794. These boreholes are WWD-7(270), DEP-19(392), 001/290(588), WWD-12(640), DEP-2(725) and 001/014(794). Based on this, the high ratio in these wells may indicate brine water intrusion mixed with aquifer groundwater.

Cl versus Br scatter plot (Figure 4.33) for the available 35 samples collected from all aquifers during 2008 and 2009 shows that the majority of data falls below and close to sea water dilution line. Also almost all of the data was in the range of 20 $\text{meq}\cdot\text{L}^{-1}$ of Cl and 0.1 $\text{meq}\cdot\text{L}^{-1}$ of Br. Data with concentrations above the sea water dilution line from different aquifers belong to boreholes located in the north position of the Study Area. However, most of these boreholes are from aquifer C and D and some from aquifer B. These aquifers which were previously formed in marine deposits may contain brine groundwater. Therefore the data suggested general groundwater mixing with brines in the flow direction towards the northern east near WWD-37.

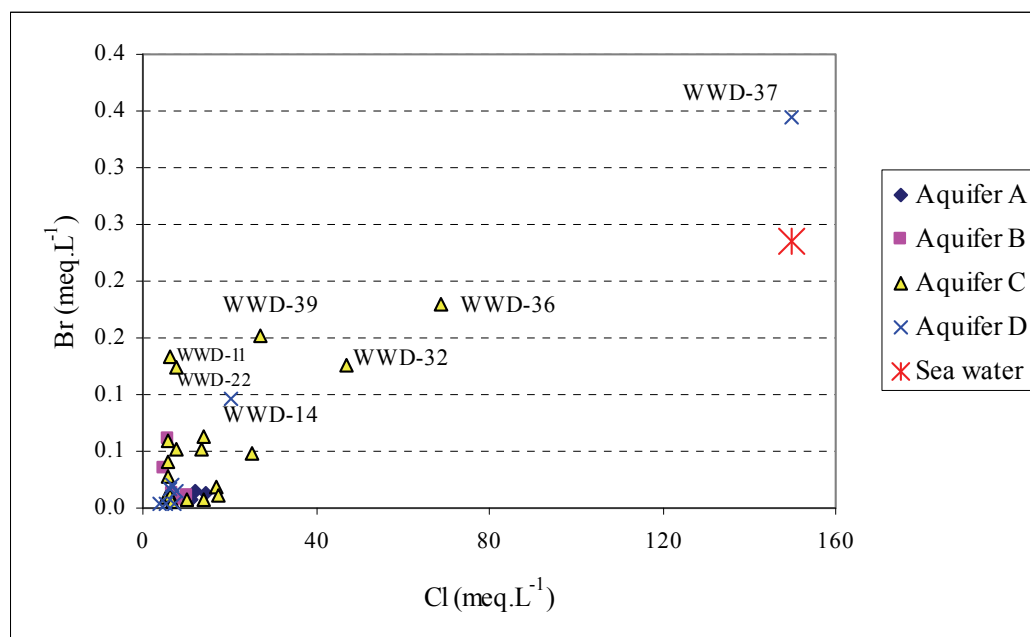


Figure 4.33 Cl versus Br compared with sea water

4.7.2.3 Sodium Adsorption Ratio (SAR)

Several studies have been conducted in the SAR in relation to EC (FAO, 1986; Driscoll, 1986); Glover (1996) classifications considered quality problems in terms of salinity. This classification is based on the presence or the absence of specific salts in irrigation water can lead to a reduction in soil permeability and hence infiltration rate, causing a drop in crop yield.

Very low salinity groundwater ($<200 \mu\text{S}\cdot\text{cm}^{-1}$) is corrosive and tends to leach calcium which reduces its strong stabilizing influence on soil and structure. Without salts and calcium, the soil disperses, sealing the surface and severely reducing the rate at which water infiltrates the soil surface. Where there are excessive levels of sodium in the groundwater ($\text{SAR} > 6$) ion exchange between sodium in the groundwater and calcium in the soil can occur, which may cause soil dispersion and plugging. A diagram showing the suitability of irrigation waters based on relationships between EC and SAR was developed by the U.S. Salinity Laboratory Glover (1996). The diagram divides groundwater quality into 16 areas which are used to indicate the degree in which particular water may cause salinity problems in plants and

undesirable ion exchange effects in soils. The interpretation of quality-class ratings of water for irrigation purposes are as follows (Driscoll, 1986):

- Low-salinity water (C1). This can be used for most crops and soils with little likelihood that soil salinity will develop. Some leaching is required, but this occurs under normal irrigation on all but the tightest of soils.
- Medium-salinity water (C2). This can be used where a moderate amount of leaching occurs. Plants with moderate salt tolerance can be grown in most cases without special practices for salinity control.
- High-salinity water (C3). This cannot be used on soils that have restricted drainage. With adequate drainage, special management for salinity control may be required and plants with good salt tolerance should be selected.
- Very-high salinity water (C4). This is not suitable for irrigation under ordinary conditions. If used, the soils must be permeable, drainage must be adequate, considerable excess irrigation water must be applied, and very salt tolerant crops should be selected.
- Low sodium water (S1). This can be used with little danger on nearly all soils. Sodium-sensitive crops such as stone fruit trees and avocados may accumulate injurious concentrations of sodium.
- Medium-sodium waters (S2). This is hazardous for use on fine-textured soils that have high cation-exchange capacity. This water may be used on coarse-textured or organic soils with good permeability.
- High-sodium water (S3). This may be harmful to most soils and thus requires special soil management such as good drainage, high leaching, and addition of organic matter. Chemical amendments may be necessary except for gypsiferous soils.
- Very-high-sodium water (S4). This is generally unsatisfactory for irrigation purposes, except at low salinity and where calcium from the soil or use of gypsum or other mineral additions may make these waters usable.

Sodium Adsorption Ratio (SAR) data was used in conjunction with EC for irrigation water assessment purposes and if it causes infiltration problems or not. This ratio was obtained from the following equation.

$$SAR = \frac{Na}{\sqrt{(Ca+Mg)^2}} \quad \text{Where ion concentration measured in (meq.L}^{-1}\text{)}$$

The data plot was performed by using Aquachem program. Later, the diagram was modified by some explanations (Figure 4.34). The assessment of SAR on the basis of salinity hazard was divided to four zones as follow (GRC, 2008):

- <2500 $\mu\text{S.cm}^{-1}$ potentially suitable for potable use.
- 2500 to 4000 $\mu\text{S.cm}^{-1}$ Suitable for most agriculture and livestock purposes.
- 4000 to 6000 $\mu\text{S.cm}^{-1}$ Suitable for selected crops, livestock and oilfield use.
- 6000 to 10000 $\mu\text{S.cm}^{-1}$ Suitable for more resistant crops, certain livestock and industrial use.
- >10000 $\mu\text{S.cm}^{-1}$ Suitable for industrial purposes only (e.g. oilfield).

Camels can drink water with an EC of more than 15000 $\mu\text{S.cm}^{-1}$. This is based on the evidence from local people who were camping behind the borehole WWD-36 in 2004 who were using a dug well in aquifer A and who saw camels drinking regularly. The measurements were taken by MRMWR staff during the drilling period of WWD-36 and found with EC exceeds 15000 $\mu\text{S.cm}^{-1}$.

The SAR data shows a varied distribution range from 1 to 36 and an average of 5. The lowest value was found in aquifer B in borehole WWD-19 whereas the highest value was detected in aquifer D at borehole WWD-37. SAR ratio recorded the second, third and fourth highest values in aquifer C at boreholes WWD-36, WWD-32 and WWD-8; and they were as following: 18, 12.5 and 10 respectively.

The sodium hazard versus salinity hazard diagram reveals that the majority of groundwater from all aquifers is located within the range of high salinity with a low to medium sodium hazard (S1, S2). This range is classified as suitable water for

agricultural purposes. Whereas the rest of groundwater data fall in the doubtful and unsuitable ranges.

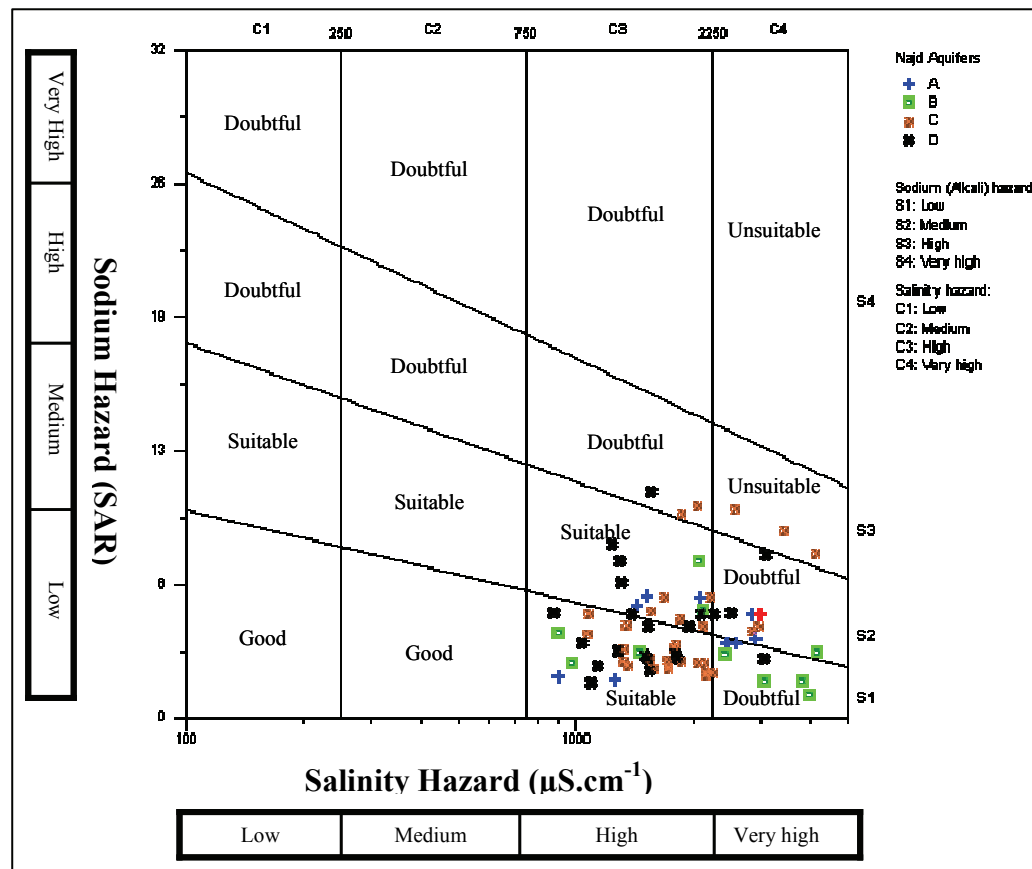


Figure 4.34 Sodium Adsorption Ratio (SAR) from the different aquifers

Overall, the recent EC and SAR data in this study shows that aquifer D seems to be the best for agricultural or irrigation purposes. Therefore the sequences of these aquifers in the case of irrigation suitability will follow the order $D > C > A > B$. This classification was excluded three boreholes (WWD-30, WWD-36, WWD-37) which belong to aquifers A, C and D due to their high salinity variation with other wells.

4.8 Conclusion

In general aquifers are heterogeneous with themselves and between each other with the exception of some particular places due to geological structure influences. The hydrochemistry and isotopes behavior are mainly controlled by these geological

structures such as faults, fissures, fractures, quantity and quality of recharge; and aquifer characteristics.

Mineralization increases in all aquifers from south and southwest to north and northeast following the groundwater flow direction. Four types of water Na-Ca-Cl-SO₄, Ca-Mg-Na-SO₄-Cl, Na-Mg-Cl-SO₄ and Na-Ca-Mg-Cl-SO₄ were found in aquifers A to D and overall the Najd groundwater type was Na-Ca-Mg-Cl-SO₄. With the exception of boreholes or springs located in the recharge area (Jabal), groundwater in Najd from all aquifers does not fit with the Omani standard for human drinking water. However majority of aquifers groundwater is suitable for agricultural irrigation purposes and generally ranked as follow: D>C>A>B.

The evidence of the recharge occurrence was detected along three directions, the first in two directions by the presence of ³H in aquifers A (SHTH, M.Masin) and B (DEP-9). However the third direction was in aquifer D and was detected from contour maps created for ²H and Cl. This direction located on the way from the recharge area (LobFr) passing through east of Thumrait (MOD-15) and east Hanfeet (332/014) towards wadi Bin Khawtar (WWD-24) in the northeast.

The constant presence of ¹⁸O_{SO4} and increasing levels of ³⁴S_{SO4} is likely to appear for the first time in the field and are probably due to bacterial sulphate reduction (BSR). The H₂S gas was detected in UER formation aquifers only due to its development in the formation during the reduction of microbial processes.

The interpretation of hydrochemical data variation (profile C4 Figure 4.25 & Figure 4.26, k) and hydrogeological cross section (A-A), all together suggest one additional fault in existence north of Dawkah and close to borehole Bin Kh (BF080077AA).

EVALUATION OF GROUNDWATER AGE IN ALL AQUIFERS WITH REGARDS TO PALEO-ENVIRONMENTAL DEVELOPMENT

This chapter emphasises the process of dating groundwater and the influences of paleo-climate in Najd aquifers, based on environmental isotopes and noble gases data. Two models with different factors were applied for groundwater dating calculations in order to compare the most reliable one to choose. The selected model results were used with different plots to detect recharge processes among groundwater young age. At the sometime the data was compared with noble gases data and especially noble gases temperature (NGT) to evaluate the paleo-climate conditions from the time the initial recharge occurrence.

5.1 Dating of Groundwater Using ^{14}C

5.1.1 Radiocarbon in groundwater and the problems of age dating

Radiocarbon or ^{14}C is used by hydrogeologists for the dating of groundwater. The radioactive nuclide ^{14}C has a half-life of 5730 years which is relevant to old groundwater systems. The ^{14}C activities are referenced to the international standard called modern Carbon (mC), which is observed to have 95% of its contents in surface seawater (Clark, 1997). Thus ^{14}C measurement is expressed as a percentage of modern carbon (pmC) which is being used nowadays. The concentration of ^{14}C in the atmosphere, ocean and biosphere is relatively constant and is set to ≈ 100 pmC (Clark, 1997). The common sources which can contribute DIC to groundwater are the carbonate dissolution initiated by atmosphere and soil CO_2 ; however the first processes are more applicable for arid regions. The atmosphere contains around $\sim 99\%$ of CO_2 as $^{12}\text{C}-\text{CO}_2$. The remaining 1% of carbon isotopes is found as ^{13}C and ^{14}C (Office of Health and Environmental Research U.S. Department of Energy, 1996).

Munich (1957) was proposed ^{14}C uses for groundwater dating (Gonfiantini and Zuppi, 2003). Subsequently, radiocarbon (^{14}C) was developed as a tool for archeological dating by Willard Frank Libby in 1960 (Clark, 1997) and then further applied in hydrogeology for groundwater dating. Groundwater dating is affected by dissolution and precipitation of carbonate as CaCO_3 . The process of isotopic exchange occurs

between DIC and the carbonate aquifer matrix with time and produces enriched ^{13}C and depleted ^{14}C , suggesting karsts groundwater (Pearson, 1965; Pearson and Hanshaw, 1970; Geyh, 1970; Wigley, 1976; Wigley et al., 1978; Evans et al., 1984; Gonfiantini and Zuppi 2003).

Two main sources control the carbon concentration. These sources are both organic and inorganic carbon. The first commonly contributes carbon to the groundwater system through the production of CO_2 from organic matter degradation with a mean of $\delta^{13}\text{C}$ values between -30‰ to -24‰. The second source is generated from marine carbonate dissolution at around 0‰ of $\delta^{13}\text{C}$ (Clark, 1997). In the carbonate system, like in the Najd area, sulphate reduction can be an additional source of dead carbon. This aims to measure the infiltration date of the groundwater entering the aquifer. The direct and absolute method is not available at the present time. Therefore several methods applied for these circumstances. In these measurements dissolved inorganic and organic carbon (DIC and DOC) will be taken into account because both enter the groundwater from the atmosphere among the soil as $^{14}\text{CO}_2$.

Scientists then introduced the groundwater age correction in the limestone system which was developed by Fontes and Garnier (1979; 1981). Subsequently, Maloszewski and Zuber, (1991); Clark, (1997); Gonfiantini and Zuppi, (2003); Carreira et al. (2010) were contributors to these methods.

The study carried out by Gonfiantini & Zuppi (2003) concluded that exchange rates of stable isotopes are 3 times less than the radioactive decay rate of ^{14}C between limestone groundwater and rock.

The high ^{14}C values in pmC reflect recharge to groundwater, these raw data do not indicate the real age of water which is more useful, unless they calibrated. Therefore several other indirect measurements were performed in order to apply in ^{14}C dating calculation processes. Based on that, ^{13}C from groundwater, soil and lithology were measured for calibration purposes.

The groundwater aquifers in the Study Area occur in Cenozoic (Paleocene to Eocene) and mainly consist of limestone. In comparison with the study carried out by

Gonfiantini and Zuppi (2003), northern Libya shows that groundwater occurs in Eocene to Oligocene limestone and the age of groundwater ranges from 5-23 ka BP. Even though there is difference in some periods of the geological scale and the lithology. However, this groundwater period is not far from (4,000 to 30,000 yr) that was given by (Clark, 1997) to Najd groundwater. In 2005, a study conducted at the University of Neuchâtel in Switzerland carried out chemical and isotope analyses of two natural springs and ten boreholes from aquifer C (GRC, 2008). These analyses were performed by GRC and concluded that the groundwater in the C aquifer was more than 3000 years old.

5.1.2. ^{14}C in groundwater of the Najd region – data and corrections

In total 38 samples were collected from the Study Area for ^{14}C . These samples are distributed between aquifers A to D (Table 5.1) as follow: A (n=7), B(n=7), C (n=10) and D(n=14). However 27 of the samples were analysed by AMS method due to low concentrations of bicarbonate, which makes collection of data by precipitation difficult. The ^{14}C results accounted for a percentage of modern Carbon (pmC) can not be used for interpretation of the water age, unless they are calibrated with other parameters such as ^{13}C of water, lithology and soil CO_2 . Therefore, all samples measured for DIC of ^{13}C in addition to four locations were measured for $^{13}\text{C}_{\text{soil}}$. The $\delta^{13}\text{C}$ results of the selected sites are in ‰ from M.Masin (-20.1‰), 001/290 (-16.5‰), M.sp (-14‰) and in the recharge area Tawi Atair (-19.7‰). In addition, all locations were already included in our sampling campaign except Tawi Atair. Moreover, ^{13}C for lithology (carbonate) were obtained by the analyses of 9 boreholes drilling cutting.

The ^{14}C values obtained in the groundwater of Najd ranged between 1.6 at borehole DEP-16 to 97 pmC at spring SHTH located in the recharge area (Table 5.1). Parameters such as $^{13}\text{C}_{\text{DIC}}$, $^{13}\text{C}_{\text{soil}}$ and the enrichment factor (ϵ) were included in the correction calculation of ^{14}C . The vegetation area is enriched with organic matters, consequently it produces CO_2 , which then degrades with a mean of $\delta^{13}\text{C}$ values ranging between -30‰ to -24‰ (Clark, 1997). The ^{13}C of limestone of the aquifer matrix was measured in several boreholes lithology by using XRF and was found in the δ -range between -7.1‰ and +3.5‰. However, negative values indicate dolomite

dissolution processes and are excluded from this specific correction calculation, for carbon 14. Other positive values greater than +2‰ may indicate marine limestone rather than limestone influences by other sources of carbon like CO₂. Thus +2‰ was selected to apply for $\delta^{13}\text{C}_{\text{carb}}$ in this type of correction.

By referring to the field data for $^{13}\text{C}_{\text{soil}}$, there are values ranging between -14‰ to -20.1‰. Also, the aquifers systems in the interior of Najd are usually confined or semi-confined and soil contribution to groundwater may be very low or non-relevant. This gives an impression that the possible recharge processes at present occur through the Jabal chain area in the south, which was furthermore found with a $\delta^{13}\text{C}_{\text{soil}}$ value of -19.7‰. Respectively, the value -19.7‰ seems to be a suitable representative more so than others, and was therefore fixed for all corrections as $^{13}\text{C}_{\text{soil}}$.

Due to fractionation of ^{14}C during organic and inorganic reactions, calibration with other isotopes such as $\delta^{13}\text{C}$ should be used. Therefore, in the open system condition $\delta^{13}\text{C}$ will be controlled by soil CO₂ because of the exchange of CO₂ between DIC and soil CO₂ in unsaturated zone of the groundwater. On the other hand, in the case of closed system conditions where there is no contact with CO₂ the groundwater in the aquifers will be diluted by DIC only, thus $\delta^{13}\text{C} = \approx 0\text{‰}$. In the case of the mix of $\delta^{13}\text{C}$ it can be used for correction purposes of ^{14}C activities by calculating the value of the **q-factor** using a carbon isotope mass balance formula (Clark, 1997).

CHAPTER 5

Table 5.1 ¹⁴C data and age calculations by different models

Local Name	Site ID	Aquifer	$\delta^{13}\text{C}_{\text{DIC}}$ [‰]	$\delta^{13}\text{C}_{\text{DIC}}$ [‰]	$\delta^{13}\text{C}_{\text{soil}}$ [‰]	$a_t^{14}\text{C}$ [pmC]	$^{13}\text{C}_{\text{Litho}}$ [‰]	ϵ [‰]	M1 q	M2 q	M1 q	M2 q	$a_0^{14}\text{C}$	1/ λ	M1 ¹⁴ C [yr]	M2 ¹⁴ C [yr]	* M1 ¹⁴ C [yr]	M2 ¹⁴ C [yr]
M-Masin	YA729072AA	A	-8.5	-8.5	-19.7	31.9	2	-7	0.48	0.67	0.48	0.67	100	-8267	3439	6121	3439	6121
O.R	ZV191273AA	A	-8.4	-8.4	-19.7	28.1	2	-7	0.48	0.66	0.48	0.66	100	-8267	4402	7065	4402	7065
SHTH Sp	AE803515AC	A	-8.6	-8.6	-19.7	97.0	2	-7	0.49	0.68	0.49	0.68	100	-8267			modern	
TWIRISH	AF123492AA	A	-8.5	-8.5	-19.7	45.6	2	-7	0.48	0.67	0.48	0.67	100	-8267	487	3169	487	3169
WWD-20	YA859494BA	A	-7.7	-7.7	-19.7		2	-7	0.45	0.61	0.09	0.00	100	-8267			n.c	
WWD-24	BG200046CA	A	-9.8	-7.0	-19.7	15.8	2	-7	0.54	0.77	0.42	0.55	100	-8267	10213	13107	7979	10332
WWD-26	BG409917AA	A	-7.1	-9.2	-19.7	30.3	2	-7	0.42	0.56	0.52	0.72	100	-8267	2685	5062	4402	7204
WWD-45	BG485361BA	A	-8.0	-7.8	-19.7	9.9	2	-7	0.46	0.63	0.45	0.62	100	-8267	12755	15339	12625	15177
MAF-S1(001/015)	ZV193035AA	B	-9.7	-1.3	-19.7	3.1	2	-7	0.54	0.76	0.15	0.10	100	-8267	23558	26437	13094	9822
DEP-16A	XV997655BA	B	-6.7	-8.9	-19.7	3.4	2	-7	0.40	0.53	0.50	0.70	100	-8267	20466	22735	22316	25066
DEP-17	YV578833AA	B	-8.5	-8.5	-19.7	17.1	2	-7	0.48	0.67	0.48	0.67	100	-8267	8599	11281	8599	11281
DEP-9	YV182483AA	B	-10.3	1.4	-19.7	93.3	2	-7	0.57	0.81	0.03	-0.11	100	-8267			modern	
WWD-13	YB406953BA	B	-4.5	-16.1	-19.7	70.3	2	-7	0.30	0.35	0.83	1.26	100	-8267			1394	4853
WWD-17	YA389228BA	B	-5.6	-13.2	-19.7	77.1	2	-7	0.35	0.44	0.70	1.04	100	-8267			modern	2484
WWD-19	YA859494AA	B	-7.1	-3.9	-19.7	79.7	2	-7	0.42	0.56	0.27	0.31	100	-8267			modern	
001/014	ZV193035BA	C	-4.3	-6.0	-19.7	7.7	2	-7	0.29	0.34	0.37	0.47	100	-8267	10936	12207	12911	14961
001/290	AF829201AA	C	-3.2	-3.2	-19.7	5.2	2	-7	0.24	0.25	0.24	0.25	100	-8267	12711	13126	12711	13126
DEP-16	XV997655AA	C	-2.5	-1.6	-19.7	1.6	2	-7	0.21	0.20	0.16	0.12	100	-8267	21175	20744	19261	16898
DEP-19	BF792149AA	C	-4.8	-18.0	-19.7	77.2	2	-7	0.31	0.38	0.92	1.42	100	-8267			1474	5032
DEP-9A	YV182483BA	C	-2.8	1.2	-19.7	1.7	2	-7	0.22	0.22	0.04	-0.09	100	-8267	21259	21232	6570	
S.TMMI	YV347775AA	C	-5.3	-5.3	-19.7	3.9	2	-7	0.34	0.42	0.34	0.42	100	-8267	17877	19659	17877	19659
WWD-12	YB406944AA	C	-5.6	-3.9	-19.7	19.4	2	-7	0.35	0.44	0.27	0.31	100	-8267	4886	6791	2793	3800
WWD-16	YA389227AA	C	-3.0	-3.5	-19.7	9.0	2	-7	0.23	0.24	0.25	0.28	100	-8267	7787	7993	8575	9267
WWD-27	BG110099AA	C	-2.7	2.3	-19.7	10.4	2	-7	0.22	0.21	-0.01	-0.18	100	-8267	6086	5932	n.c	
WWD-36	CG085491AA	C	-5.0	-0.4	-19.7	5.4	2	-7	0.32	0.39	0.11	0.03	100	-8267	14776	16423	5826	

Note: The bold digits are referring to ¹⁴C and ¹³C data analyzed by AMS,

* M1= The selected model

n.c: no calculation

Table 5.1 Continued

Local Name	Site ID	Aquifer	$\delta^{13}\text{C}_{\text{DIC}}$ [‰]	$\delta^{13}\text{C}_{\text{DIC}}$ [‰]	$\delta^{13}\text{C}_{\text{DIC}}$ [‰]	$\delta^{13}\text{C}_{\text{soil}}$ [‰]	$a_t^{14}\text{C}$ [pmC]	$^{13}\text{C}_{\text{Litho}}$ [‰]	ε [‰]	M1 q	M2 q	M1 q	M2 q	$a_0^{14}\text{C}$	1/- λ	M1 ^{14}C [yr]	M2 ^{14}C [yr]	* M1 ^{14}C [yr]	M2 ^{14}C [yr]
332/014	AE989051AA	D	-3.3	-3.3	-19.7	5.7	2	-7	0.24	0.26	0.24	0.26	0.26	100	-8267	12102	12614	12102	12614
DEP-14A	XV876910BA	D	-3.7	-7.4	-19.7	12.6	2	-7	0.26	0.29	0.43	0.58	0.58	100	-8267	6069	6925	10207	12659
DEP-3	BE162450AA	D	-4.3	-10.8	-19.7	35.8	2	-7	0.29	0.34	0.59	0.85	0.85	100	-8267	13803	11613	4141	7168
DEP-6	YV123115AA	D	-1.6	-1.6	-19.7	3.2	2	-7	0.17	0.13	0.17	0.13	0.13	100	-8267	13803	11613	13803	11613
DEP-7	BE127955AA	D	-4.7	-6.8	-19.7	51.4	2	-7	0.31	0.37	0.41	0.54	100	-8267	2297	4860	modern	modern	380
DWS-15	YU181909AA	D	-7.9	-10.2	-19.7	34.6	2	-7	0.46	0.62	0.56	0.81	100	-8267	421	3045	4042	6994	6994
H.R.C(103/395).	AF828170BA	D	-8.2	-8.2	-19.7	44.7	2	-7	0.47	0.65	0.47	0.65	100	-8267	9848	12492	10640	13464	3045
HAD-49	ZV084571AA	D	-8.3	-9.3	-19.7	14.4	2	-7	0.47	0.65	0.52	0.74	100	-8267	3120	3977	775	18	18
LobFr	AE818982AA	D	-3.7	-2.3	-19.7	18.0	2	-7	0.26	0.29	0.20	0.18	100	-8267	2975	4669	2975	4669	4669
QISB	AE915009AA	D	-5.1	-5.1	-19.7	22.8	2	-7	0.33	0.40	0.33	0.40	100	-8267	1926	modern	modern	modern	modern
RBK-D	BE094486AA	D	-4.8	-6.4	-19.7	52.8	2	-7	0.31	0.38	0.39	0.51	100	-8267	17683	20110	6699	modern	modern
WSW-3	BE991437AA	D	-5.7	-1.2	-19.7	35.6	2	-7	0.35	0.45	0.15	0.09	100	-8267	15041	16539	n.c	n.c	n.c
WWD-14	YB406954CA	D	-7.3	-0.5	-19.7	5.0	2	-7	0.43	0.57	0.11	0.04	100	-8267	15041	16539	n.c	n.c	n.c
WWD-37	CG085490BA	D	-4.7	3.2	-19.7	5.0	2	-7	0.31	0.37	-0.06	-0.25	100	-8267	15041	16539	n.c	n.c	n.c

Note: The bold digits refer to ^{14}C and ^{13}C data analyzed by AMS,

* M1= The selected model

n.c: no calculation

The measurement of groundwater dating by using ^{14}C is a difficult task due to the Study Area distribution being over approximately 88000 km² dealing with four heterogeneous aquifers at the same time. Moreover, the effect of the geological structure seems to dominate most of the groundwater flow directions. The Netpath model was applied for ^{14}C dating, however it doesn't accommodate the research which is probably due to heterogeneity of the aquifers and the flow path. Therefore the study suggested introducing extra parameters such as stable isotopes and hydrochemistry data for the calibration of age measurements. Yet, based on the complicated method and shortage of time, it is impossible to include in this thesis. As a result, two models (Model-1 & Model-2) were used depending on Eq.3. Model-1 assumes an open system, because the expected recharge had occurred on or close to the Jabal chain in the south. This model was calculated based on (Eq.1), using the real data obtained from lithology with a fixed value of +2‰. However, Model-2 was used for the closed system and calculations were based on (Eq.2), using carbon isotope fractionation between CO₂ and DIC assumed ($\varepsilon = -7$ ‰).

Both models were applied twice using different $^{13}\text{C}_{\text{DIC}}$ data calculated by precipitation (UFZ) and AMS (Heidelberg University). After the comparison between four different model results, Model-1 was selected. This model was advantageous and used $^{13}\text{C}_{\text{DIC}}$ data which was measured by the AMS method in addition to the real data of ^{13}C from soil and lithology. Moreover, the Model-1 results seem to be more reasonable to the Study Area conditions than the other models. All data and calculation results included in these models are summarized in Table 5.1.

In model-1 the correction factor was calculated based on the following equation:

$$q = \frac{\delta^{13}\text{C}_{\text{DIC}} - \delta^{13}\text{C}_{\text{Carb}}}{\delta^{13}\text{C}_{\text{Soil}} - \delta^{13}\text{C}_{\text{Carb}}} \quad \text{Eq.(1)}$$

Where: $\delta^{13}\text{C}_{\text{DIC}}$ = measured ^{13}C in groundwater (measured value)

$\delta^{13}\text{C}_{\text{soil}}$ = $\delta^{13}\text{C}$ of the soil CO₂ (-19.7 ‰; own field measurement)

$\delta^{13}\text{C}_{\text{carb}}$ = $\delta^{13}\text{C}_{\text{lithology}}$ by using XRF analysis (+2‰; measured value)

In model-2 carbon correction factor (q) was calculated by using equation **Eq.(2)**.

$$q = \frac{\delta^{13}C_{DIC} - \delta^{13}C_{MarinCarbon}}{\delta^{13}C_{Soil} - \varepsilon} \quad \mathbf{Eq.(2)}$$

Where: $\delta^{13}C_{DIC}$ = measured ^{13}C in groundwater (measured value)

$\delta^{13}C_{soil}$ = $\delta^{13}C$ of the soil CO_2 (-19.7 ‰; own field measurement)

$\delta^{13}C_{Marin Carbon}$ = Assumed to be 0 ‰

ε = carbon isotope fractionation between CO_2 and DIC assumed (-7‰)

The groundwater age in Najd aquifers was obtained by the substitution of q values from both models calculations in **Eq.(3)**.

$$^{14}C(age) = -8267 * LN\left(\frac{^{14}Ca_t}{(q * ^{14}Ca_o)}\right) \quad \mathbf{Eq.(3)}$$

Where: $a_t^{14}C$ = calculated from the Lab (pmC),

$a_o^{14}C$ = initial carbon (100),

q = correction factor for carbon activities.

-8267 = constant value of $(1/-\lambda)$,

The data analyses show a variation of age values between aquifers. At the sametime several locations have higher ^{14}C concentrations, however when applying the model, the reading become in negative values. These negative values depend on the rise of ^{14}C in the groundwater and ^{13}C concentrations in different sources like water, soil and lithology. Consequently, these values were classified within the range of "modern groundwater" and even they were excluded from all plots except (Figure 5.2).

The minimum model age (Figure 5.1) was 421 years (yr) at borehole H.R.C (103/395) in aquifer D and the maximum was found in borehole DEP-16A (22316 yr) in aquifer B located northeast of Al Mazyunah. However, the groundwater age generally seems to be older in aquifers B and C than A and D. Despite that, some boreholes were found with young water in all aquifers. Boreholes Twirish, WWD-13, DEP-19 and

H.R.C (103/395) in aquifers from A to D were recorded with the youngest age in each aquifer. The presence of young groundwater in particular areas in the Najd aquifers could be related to fault influences. Because aquifers from A to D are often found under confined conditions in interior of Najd, with exception of aquifer A in specific places like Helat Ar Rakah.

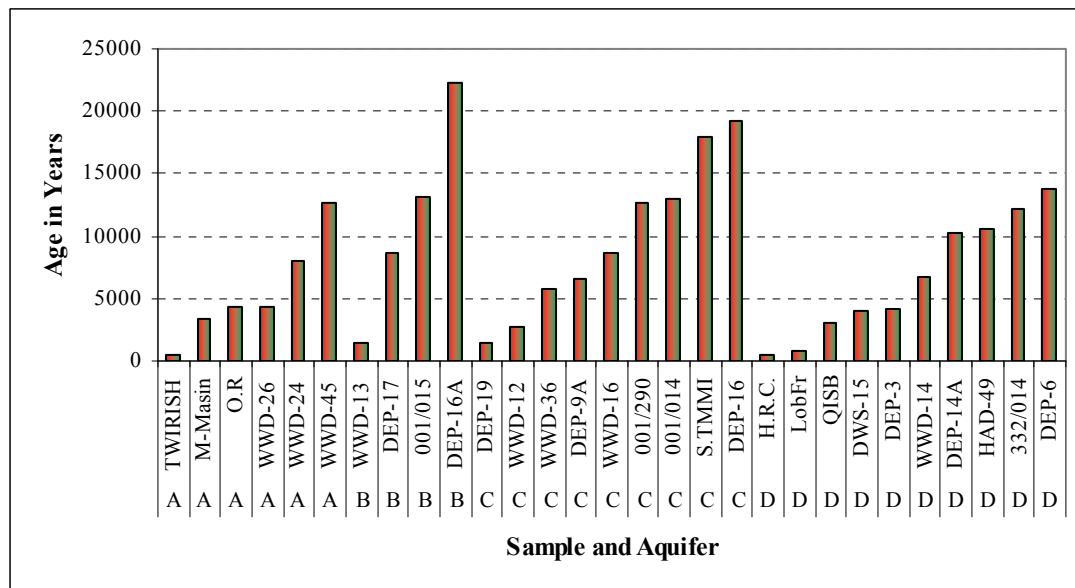


Figure 5.1 Groundwater age in different aquifers

5.1.3. Interpretation of ^{14}C data in relation to the carbon sources and the water origin

In aquifer A the borehole Twirish contains the second youngest water in Najd after H.R.C (103/395). At the same time a borehole located behind the fault which passes south of the Helat Ar Rakah MRMWR office may be responsible for the influence of recharge via the fault to groundwater occurrence in that area.

At aquifer B the borehole WWD-13 located in the north, within the sand dunes area, was appointed as young groundwater (1394 yr). In fact the borehole is faraway from any source of recharge; however the comparison of this borehole with others (WWD-17 & DEP-9) located in the same flow direction makes the signature of recharge probably reasonable. The distance from DEP-9 to WWD-17 is 98 km and from WWD-17 to WWD-13 is 26 km following the flow direction from south to north.

These boreholes recorded ^{14}C values of 93.3 pmC; 77.1 pmC and 70.3 pmC respectively. By making simple comparisons between the sites based on depleted ^{14}C and divided by the distance, it shows that ^{14}C depletes at the rate of 0,17 pmC per km from DEP-9 to WWD-17, whereas 0,26 pmC per km from WWD-17 to WWD-13 which seems to be acceptable. In so far as the source of recharge comes from the south and depletes northward. This consistency of recharge in aquifer B could be related to homogeneity developed in the aquifer.

The recharge signature was observed at DEP-19 (aquifer C) located 50 km south of Qitbit. The borehole was drilled in 2004 within the wadi's main channel and was found with a relatively young age of 1474 years. This age is young in comparison with other boreholes in the surrounding area. The aquifer is confined at that area and therefore regional fault influences could be expected for this recharge.

In aquifer D the borehole H.R.C (421 yr) is located at the MRMWR office in Helat Ar Rakah and not far away from the borehole Twirish. Despite both boreholes have a low groundwater age and are occurred nearby fault. However, the young water at H.R.C (103/395) could be related to dewatering processes acceleration from aquifer D to C due to high abstraction in C. Consequently, more modern water replaces the lack of groundwater, and mixing of modern water with older ones occurs in aquifer D.

This young water in different aquifers when it occurs probably indicates recharge sources, eventhough this recharge could result from mixing between two types of water at the location. This may be due to developed canals along some faults or due to intensive abstraction which allows young water from nearby to be mixed together.

The groundwater ages for all aquifers obtained from Model-1 (including ^{13}C measured by AMS) and those with negative values were used to create contour maps in the Study Area (Figure 5.2). The negative values were considered as modern recharge. Therefore the negative values were replaced by the range of "0 to 2000" to represent the boreholes locations purposes. The figure reveals that the majority of the groundwater age is in the range between 2000 yr's to 10000 yr's old. The oldest groundwater occurs in the west of Najd around borehole WWD-16A (aquifer B) as well in the northeastern corner close to borehole WWD-45 (aquifer A).

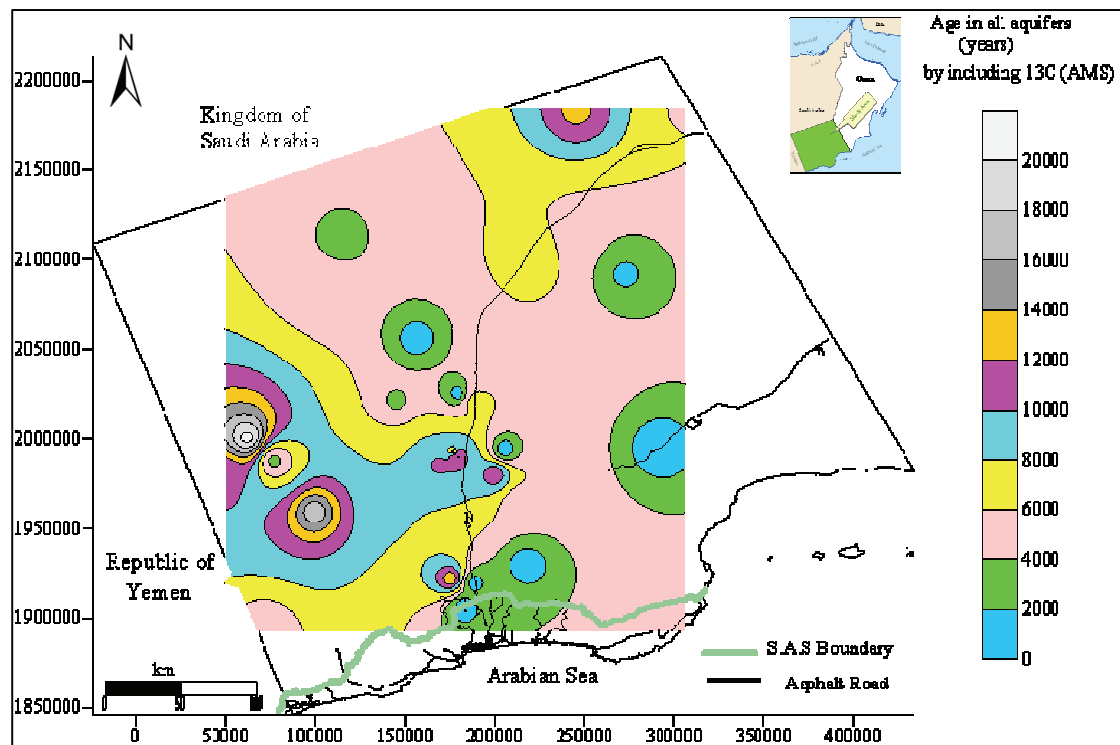


Figure 5.2 Groundwater age in years BP from all aquifers using Mod-1 with ^{13}C (AMS)

In addition, the positive values of age obtained from ^{14}C calculation in model-1 (see, M-1, AMS, ^{13}C) with and other models (Table 5.1) were plotted against ^{14}C concentrations in pmC for all aquifers (Figure 5.3). The data shows a nonlinear relationship for aquifers A to D. The variation between model-1 depends on ^{13}C analyses methods either by precipitation or by AMS and the similarity with Model-2. The figure reflects close relationship between aquifers. Even though, the majority of variations in groundwater age were restricted with an age of less than 5000 yr. However, minimal variations were observed above the age 10000 yr. In addition most of the groundwater in all aquifers fits with the Holocene period (0-10,000 yrs).

The data plot for ^{13}C versus ^{14}C (Figure 5.4) is mainly categorized into three groups. The first group on the left consists of samples which are enriched in ^{14}C pmC and depleted in ^{13}C . The $\delta^{13}\text{C}$ of DIC with depleted values around -15‰ to -20‰ usually occurs during the dissolution of soil CO_2 indicating influence of soil organic carbon (Gonfiantini and Zuppi, 2003). The $\delta^{13}\text{C}$ of soil containing CO_2 collected from the

Study Area agrees with this range and was found with a valued range between -14‰ to -20‰. At the same time, boreholes located within this range in the first group belong to aquifer B and C. Too were they highlighted with high ^{14}C pmC values which reflected influences of cyclone events. The second group in the middle consists of boreholes belonging to aquifers A, B and D. All these boreholes are expected to be influenced by the mixing of recent recharge due to their locations close to the recharge area (SHTH-spring) or as a effect of faults and fissures. These boreholes are associated with both moderate and high ^{14}C >30 pmC values and $\delta^{13}\text{C}$ values close to that of the atmosphere (-7 to -8‰), which may reflect rapid infiltration during the recharge process. The third group consists of ^{14}C values <20 pmC and of an enrichment of ^{13}C . The $\delta^{13}\text{C}$ was found with values around 0‰ to +2‰ in the limestone (Gonfiantini and Zuppi, 2003). The lithological samples collected from several boreholes in Najd aquifers show $\delta^{13}\text{C}_{\text{Carbon}}$ values ranging from -7.1‰ to +3.5‰. This range reflects the carbonate influences in a closed system more than in other sources. With the exception of DEP-19, all boreholes from aquifer C fall within this group.

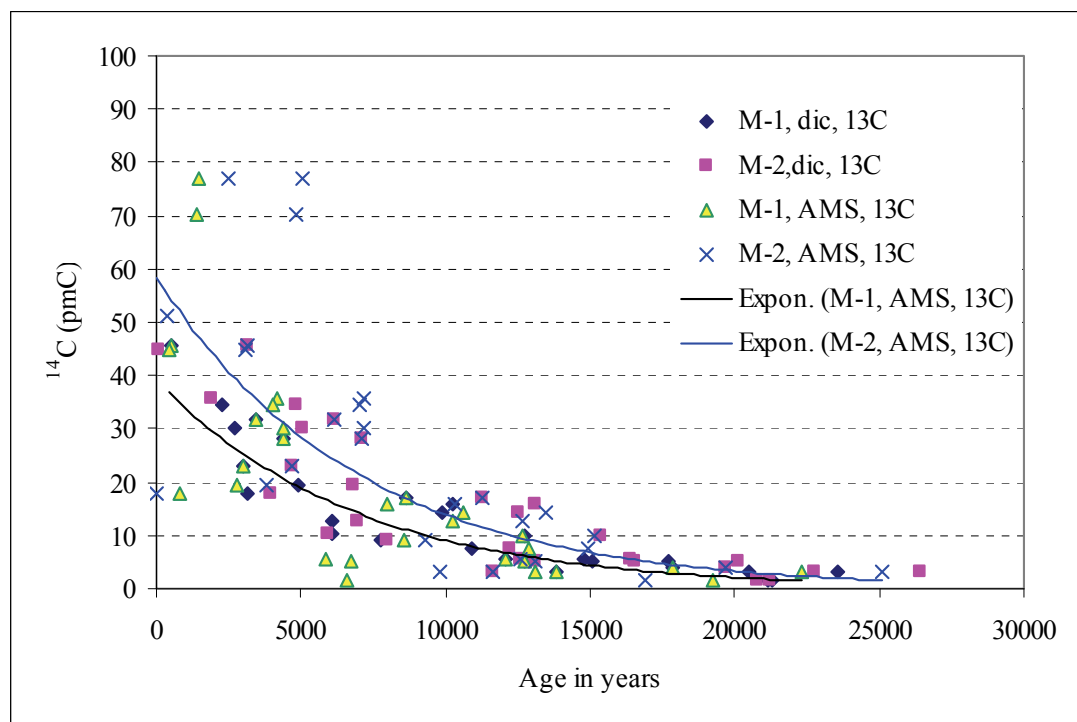


Figure 5.3 Groundwater age versus ^{14}C concentration

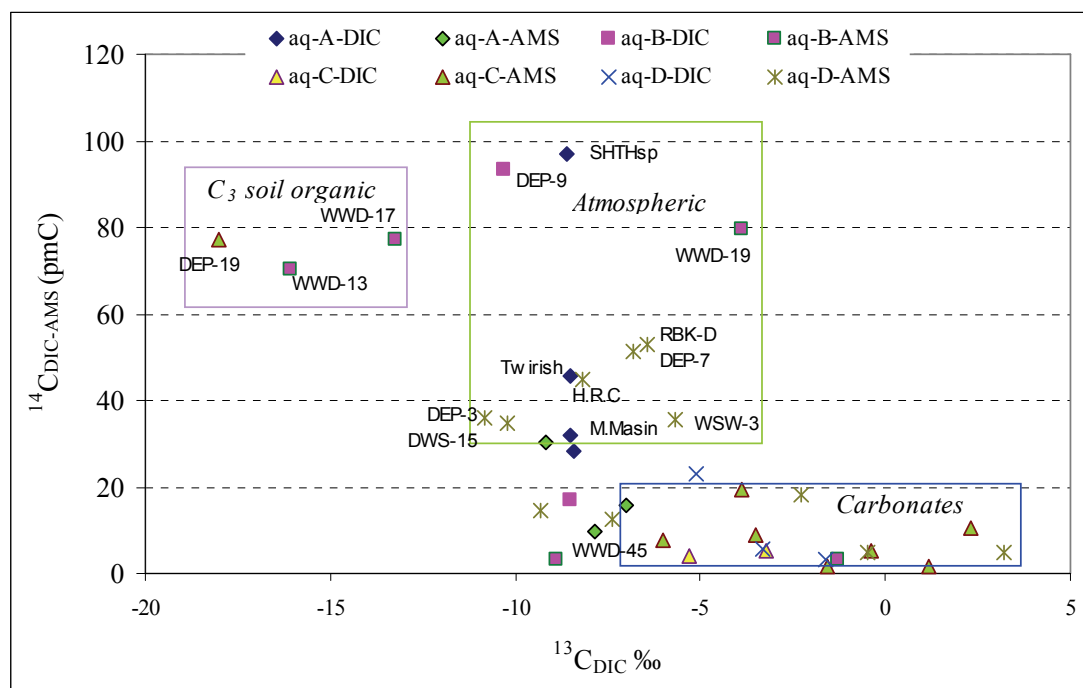


Figure 5.4 Comparisons between ^{13}C and ^{14}C showing three types of influences, (^{14}C values were plot in DIC and AMS for each aquifer)

The plot of $\delta^{18}\text{O}$ versus ^{14}C (Figure 5.5) shows that all boreholes are grouped together (figure 5.4) and are either effected by soil, organic or atmospheric carbon, which indicates cyclonic influences. Also, two boreholes and one spring located in/or close to the recharge area show enrichments in ^{18}O which relate to a monsoon source. The third part containing percentages of ^{18}O between -6‰ to -4‰ in Figure 5.5, has a majority of boreholes belonging to aquifer C and sparsely from other aquifers. These boreholes are associated with depleted ^{18}O and low ^{14}C pmC values seem to be fossil water. Despite these classifications, mixing processes are assumed between the groups. This idea could be supported by the plot of $\delta^{18}\text{O}$ versus $\delta^{13}\text{C}$ (Figure 5.6) which reveals the possibility of groundwater mixing processes between the recharge area and aquifers further northward, with fossils water in the direction from QSIB to 332/014 in aquifer D.

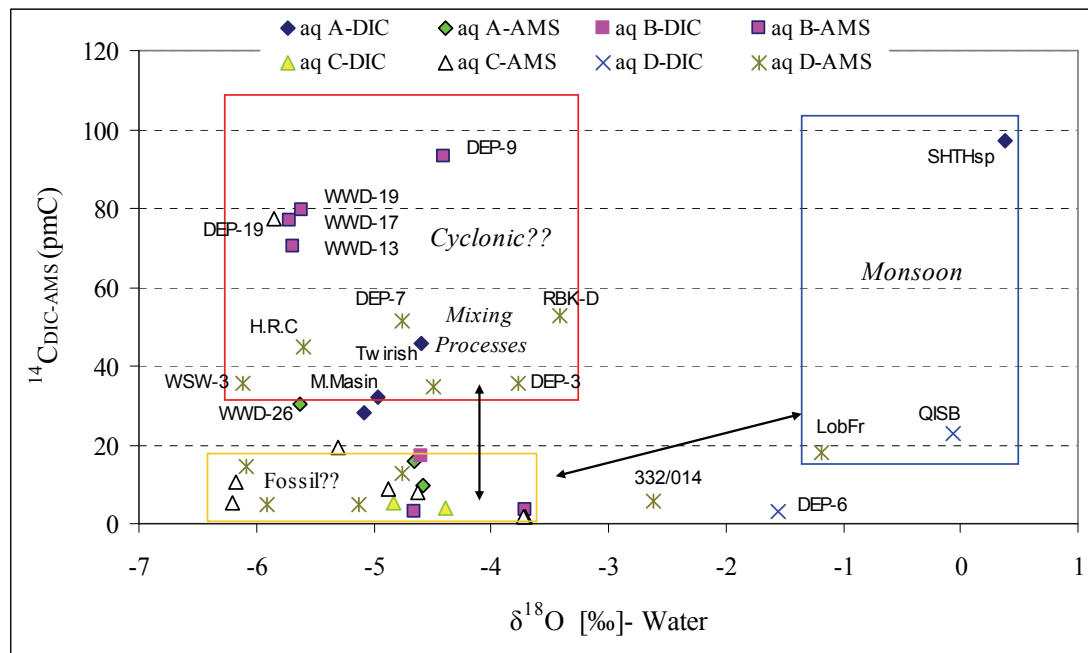


Figure 5.5 ^{18}O of water versus ^{14}C classified the source of groundwater in Najd to three groups, (^{14}C values were plot in DIC and AMS for each aquifer)

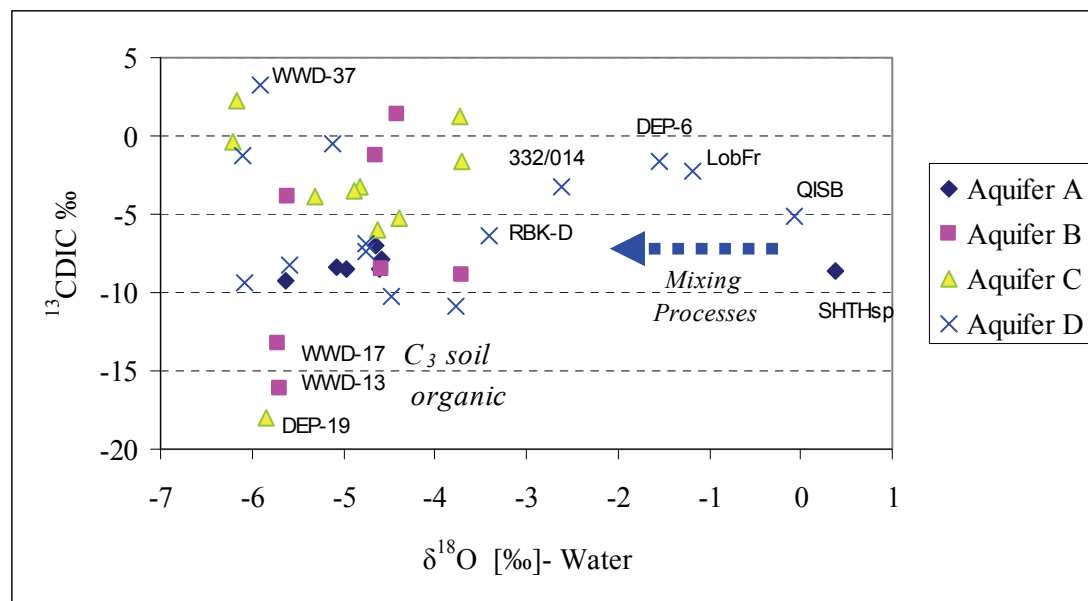


Figure 5.6 ^{18}O versus $^{13}\text{C}_{\text{DIC}}$ for different aquifers in Najd, reflecting soil organic matter and mixing processes

These correlations clearly confirm hypothesis one and two which discussed the source and mechanism of recharge. This can be observed from several groundwater (Figure 5.4) indicating soil, organic and atmospheric influences. The data leads our attention

to cyclonic events which could be the main source of the recharge to Najd aquifers. In figure 5.5 the mixing processes may occur between monsoon and cyclone water with fossils groundwater, evidentially in aquifer D (Figure 5.6) which is the dominant aquifer in/around the recharge area in the Jabal chain south of the Study Area. In addition, the data reveals that aquifer C probably recharged during the Holocene via aquifer D. Later, when huge amount of water accumulated in between confining layers of aquifer C, recent recharge from aquifer D can not enter and due to the pressure, faults and fissures, above aquifers B and A are dewatered. This hypothesis likes to be true by the focus on the ^{13}C , ^{14}C and ^{18}O results in (Figures 5.4, 5.5).

5.1.4. Comparison of ^{14}C data with data from other sources

In 1985, the groundwater sampled by Clark for ^{14}C shows a variation of age between 9000-30000 yr's old. However boreholes with ^{14}C values of more than 32 pmC were classified as modern age. These boreholes were distributed between the recharge area and the interior of Najd. For example the borehole RBK-D (BE894486AA) is located in aquifer D east of Hanfeet. The groundwater of this borehole was found in November 1985 with ^{14}C value of 2.7 pmC; the same borehole ^{14}C in November 2009 had the value 52.8 pmC. This high value may relate to the recover of aquifer D with modern water, due to influences of dewatering between aquifer D and C because the borehole locates close to one of the intensive abstraction area at Helat Ar Rakah.

In another case, borehole YV187500AA located about 6 km east of borehole DEP-9 shows a ^{14}C value of 32.44 pmC (1985), whereas in a recent sample (2009) DEP-9 was 93.3 pmC. This difference in ^{14}C values may be due to the location of DEP-9, the mean wadi channel or holding the possibility of recent recharge occurring during the last 24 years in both locations.

The "corrected age" was calculated by several models (Clark, 1997) for RBK-D and was found in the range 17000-31000 yr. However the borehole YV187500AA was classified as modern age. Based on the recent data calculation (Model-1) in this study, both boreholes (DEP-9 and RBK-D) give negative values as a result of the classification within the modern groundwater age. Moreover, PDO (1994) stated the age of the groundwater in Marmul (WSW-3) in aquifer D is around 7000 yr⁻¹.

GRC in 2008 calculated the groundwater age for 10 samples collected from aquifer C by a Swiss group in 2005. The age ranged from 3000 yr in the recharge area to 21000 yr in central Najd at Helat Ar Rakah (001/290) and >48 yr at WWD-34. The groundwater age calculated by Model-1 for borehole 001/290 gave a value of 12711 yr which was less than that calculated by GRC (21000 yr). However, the GRC calculation seems not to calibrate, and therefore these values may be over the reasonable age.

5.2 Estimation of Paleo-Recharge Temperatures by Noble Gas Thermometry

5.2.1 Noble gases importance and types of applications

The noble gases are naturally concentrated in the atmosphere. When these gases dissolve in groundwater their concentrations increase and exceed the equilibrium solubility of groundwater. Due to the composition of noble gases which has a similarity to that of air, it was used as indicators for recharge temperatures (Bradley, 2008). Up to now noble gases are considered as one of the best parameters which can detect the paleo-groundwater conditions in the geological periods. The groundwater in Najd was described as paleo-groundwater (Clark, 1997), keeping in mind that none of the previous studies carried out the noble gases analysis. For more understanding about this area of vital paleo-environmental conditions, it is suggested to collect noble gases samples.

In total 27 groundwater samples were collected from the study during November 2009. The samples represent groundwater from the all aquifers A to D and distributed between them in the following order, 5, 6, 8 and 8 respectively. The results of these analyses were completed in January 2011.

Based on the analysis of noble gases consisting of an estimation of Helium (He) isotopes, Neon (Ne) and Argon (Ar), Krypton (Kr) and Xenon (Xe) a kind of thermometer is used to calculate noble gases temperature (NGT) (Annex A-5). The NGT and helium isotopes are considered as important parameters for the paleo-climate conditions interpretation of the Study Area.

The NGT can indicate climate conditions from thousands of years ago. In addition NGT is recognized as a significant parameter in terms of groundwater infiltration to the aquifer. The evidence of this data is important in characterizing the aquifers relationship with each other and also for groundwater dating. The paleo-water temperatures can be calculated by using noble gas thermometer tools. This calculation uses a simple physical principle which is a temperature dependency of the solubility of noble gases in water (W. Aeschbach, et al, 2002). Therefore, NGT can be distinguished between two types of groundwater occurred in different periods; old (>10,000 yr) and young like the Holocene (<10,000 yr). In this case the Holocene period will be associated with a higher than 4-7 k temperature range than in the old period (Porcelli et al. 2002).

Helium with its stable isotopes ^3He and ^4He is good indicator for determining groundwater residence time and to reflect the geological structures, such as faults. This noble gas is mainly generated in the Earth mantle and the Earth crust. The gas occurrence in groundwater is evidence for the presence of faults as a source of connection between groundwater aquifers and deeper parts of the lithosphere. The groundwater residence time tends to increase He concentration due to accumulation of radiogenic He as ^4He generated by α -decay of Uranium (U) and Thorium (Th) in crustal minerals (W. Aeschbach-Hertig et al, 2002). Noble gases are often generated from the atmosphere. Even though some noble gas isotopes originate from others such as an ^4He source in the Earth's crust (Ozima and Podosek, 1983). The main source of ^3He in the upper Mantle is commonly characterized by a high ratio of $^3\text{He}/^4\text{He}$. Additionally, ^3He is produced by the tritium decay (W. Aeschbach-Hertig et al, 1999).

The presence of ^4He is generated from the crust in young groundwater, which is evidence of mixing with He traveling along the thrust fault below the aquifers (Phillips, 1994, Clark, 1997). Other studies suggest that the ^4He concentration in groundwater is related to diffusion of adjacent confining layers (Andrews and Lee. 1979 and Tolstikhin et al. 1996). As a result of its abundance in the crustal rocks and existence in groundwater, ^4He concentrations increase with the traveling time of groundwater (Andrews and Lee. 1979 and Porcelli et al. 2002).

5.2.2 Noble gases interpretations and evidence of recharge

In the Study Area, the linear relationship obtained from the X-Y plot (Figure 5.7) for Ne/He versus $^3\text{He}/^4\text{He}$ reveals a mixing area between a pure radiogenic He isotope ratio of about (2.10^{-8}) and an atmospheric end-member (1.36×10^{-6}). On this mixing line it was observed that boreholes belonging to aquifers A, B and D were more influenced by He with atmospheric source and shifting towards atmospheric endmember than those from aquifer C. However almost all boreholes from aquifer C and others from aquifers B and D which are located further north, especially within the sand dunes portion were shifted to He with radiogenic endmember.

Based on this evidence, it seems that aquifer C is mainly constituted by fossil water and has less of a chance of coming into direct contact with cyclonic recharge, whereas other aquifers probably do. Moreover, this could be explained in two ways: (i) that aquifer C recharged in the Holocene and due to its characteristics can not capture more recharge in regional scale, or (ii) the three aquifers A, B and C are basically feeding from aquifer D. Saying this, the aquifers A and B are mixing with some recent recharge though some faults, fissures and fractures. Even though, this idea is likely to be a first impression with a limited number of samples available at hand at the moment. Data involved in these calculations are summarized in Table 5.2.

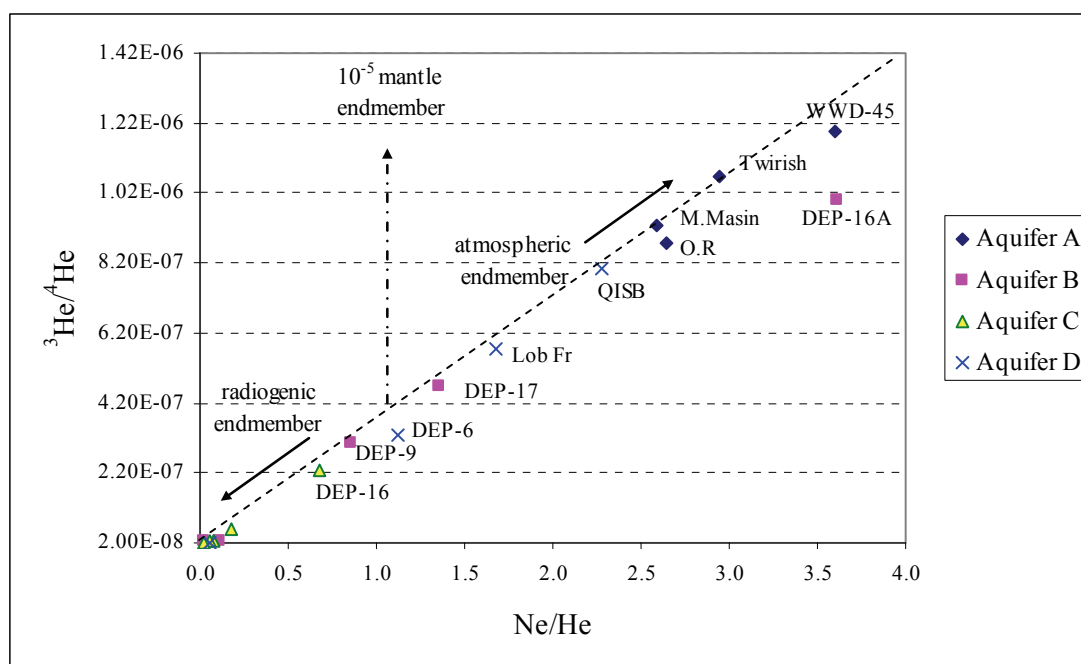
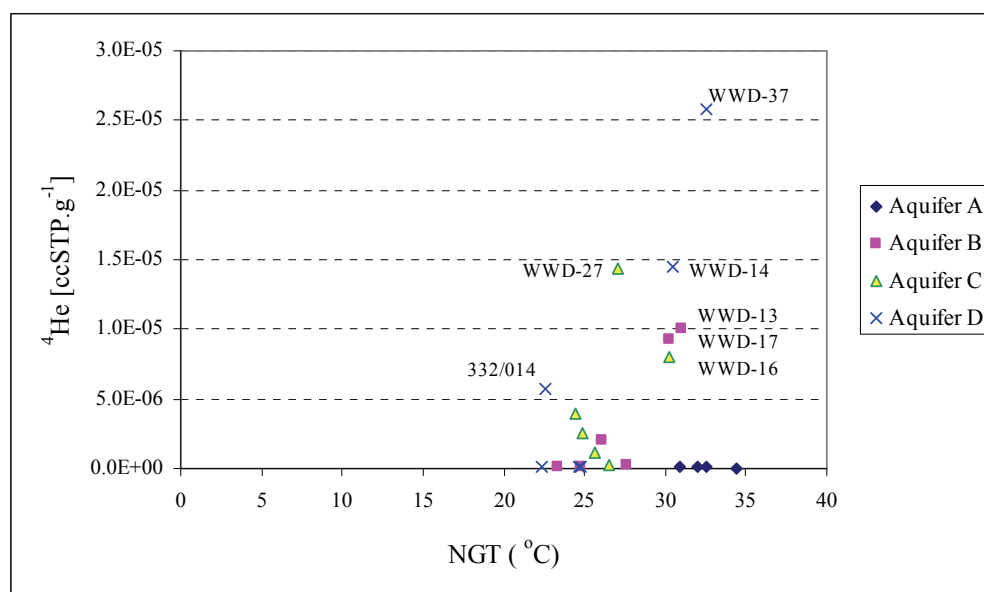


Figure 5.7 Ne/He versus $^3\text{He}/^4\text{He}$ ratio in aquifers A to D as evidently for influence of different inputs: atmospheric and radiogenic

Table 5.2 Comparison between NGT, helium isotopes and groundwater age

Well name	Aquifer	Ne/He	$^3\text{He}/^4\text{He}$	$^4\text{He}[\text{ccSTP.g}^{-1}]$	NGT[°C]	Age [yr]
M-Masin	A	2.641	8.74E-07	6.6E-08	30.9	3439
O.R	A	2.592	9.28E-07	7.6E-08	32.5	4402
TWIRISH	A	2.946	1.06E-06	6.4E-08	32.0	487
WWD-45	A	3.601	1.20E-06	5.0E-08	34.5	12625
MAF-S1(001/015)	B	0.106	2.68E-08	2.0E-06	26.1	13094
DEP-16A	B	3.615	9.99E-07	7.0E-08	23.4	22316
DEP-17	B	1.351	4.66E-07	1.6E-07	24.7	8599
DEP-9	B	0.851	3.05E-07	2.4E-07	27.6	
WWD-13	B	0.022	1.25E-08	1.0E-05	31.0	1394
WWD-17	B	0.025	2.56E-08	9.3E-06	30.3	
001/014	C	0.082	2.66E-08	2.6E-06	24.9	12911
001/290	C	0.060	2.50E-08	4.0E-06	24.4	12711
DEP-16	C	0.681	2.26E-07	3.0E-07	26.6	19261
DEP-9A	C	0.182	6.09E-08	1.1E-06	25.6	6570
WWD-16	C	0.026	1.95E-08	7.9E-06	30.2	8575
WWD-27	C	0.017	1.41E-08	1.4E-05	27.1	
332/014	D	0.052	1.77E-08	5.7E-06	22.6	12102
DEP-6	D	1.125	3.26E-07	1.8E-07	22.3	13803
LobFr	D	1.681	5.76E-07	1.3E-07	24.6	775
QISB	D	2.273	8.03E-07	1.2E-07	24.7	2975
WWD-14	D	0.015	1.54E-08	1.5E-05	30.5	6699
WWD-37	D	0.007	1.26E-08	2.6E-05	32.6	

The scatter plot of NGT versus ^4He (Figure 5.8) reflects a slightly linear relationship. The figure shows a mixing between aquifers B to D a central and west of central Najd together with the recharge area close to the Jabal chain. With the exception of aquifer A, ^4He concentration increases towards the north in all aquifers B to D. This decreases in parallel, with an increase of NGT following the groundwater flow direction.

Figure 5.8 NGT versus ^4He in aquifers A to D

In general, the NGT in groundwater increased towards the north. This is detected from boreholes, WWD-45, WWD-16 and WWD-14 (Figure 5.9) located in the north portion of the Study Area. Although these boreholes were represented the highest groundwater temperatures in aquifers A (34.5 °C), C (30.2 °C) and D (30.5 °C), which are relatively high. However, assuming that most of the cyclones occurred in summer-time as is the case now, these temperatures are still low in comparison with the recent groundwater temperatures which sometimes exceed 40 °C in the summer. The lowest groundwater temperature occurred in aquifer D at boreholes DEP-6 near the Jabal chain and 332/014 located east of Hanfeet (poultry farm). In particular, the low temperatures in aquifer D were reflected close to the recharge area and the flow path, probably in the direction along well 332/014. This direction agreed with chemical and stable isotopes discussed in previous chapters. NGT of groundwater in aquifer A seems to occur in warmer weather conditions than in the other aquifers B to D. However groundwater temperatures in aquifers B and C which are close to each other, indicate a medium temperature between aquifer A and D. Furthermore, the boreholes DEP-16A (aquifer B) and DEP-16 (aquifer C) are indicated as slightly higher temperatures in both aquifers. Remembering that, they located in the same site within a distance of less than 50 m between each other. A similarity was observed between DEP-9 and DEP-9A; and WWD-16 and WWD-17 located together in one site. Consequently the variations at the same location in groundwater temperatures reflected different climate conditions where the recharge occurred in these aquifers.

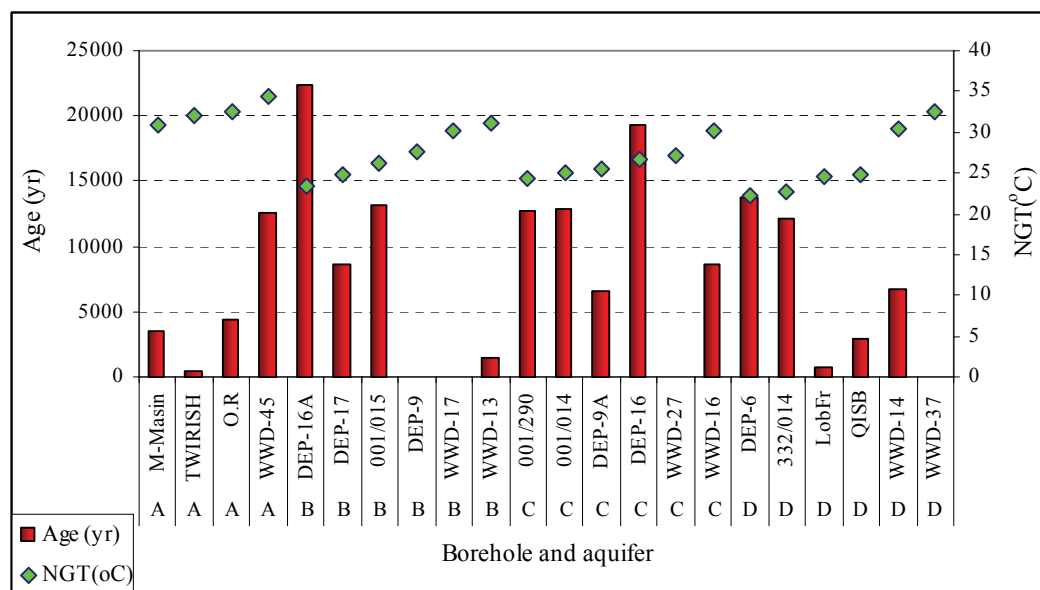


Figure 5.9 Groundwater age in comparison with NGT for different aquifers

The linear plot of the water age versus NGT (Figure 5.10) shows a general decline of NGT with the groundwater age. The boreholes from all aquifers located within the sand dunes in the north portion were recorded as having a NGT greater than 30 °C. This probably reflects the climate influence from previously within the Najd area and seems to increase towards the north and northeast direction.

Based on that, this high temperature may indicate that climate conditions are warmer than expected. The NGT in all aquifers seems to increase with the groundwater flow direction. If that is true, contribution from flood events rather than direct rainfall may be taken into account.

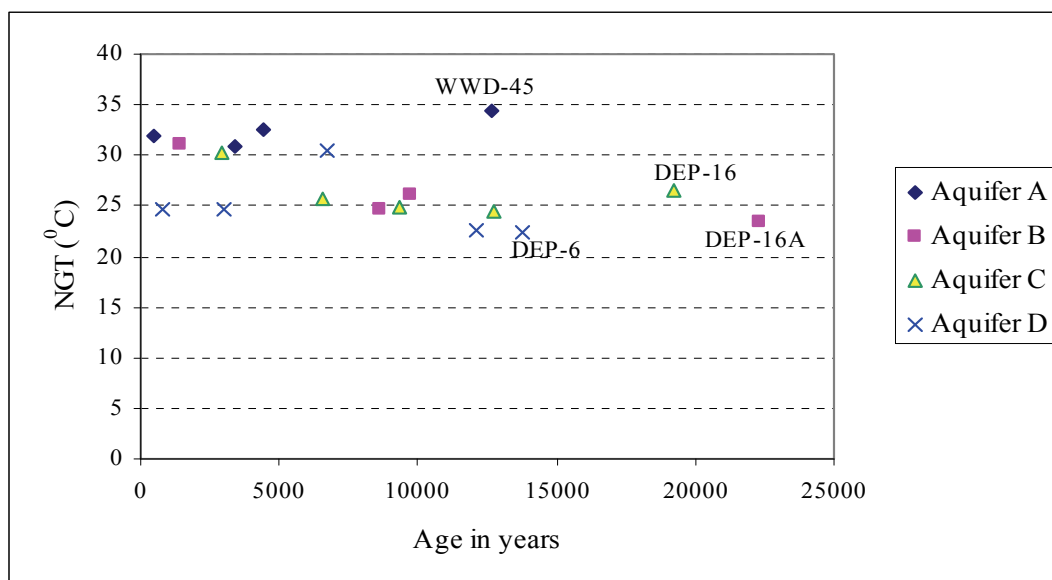


Figure 5.10 Groundwater age versus NGT in different aquifers

The paleo-climatic conditions in the Study Area were affected by the environmental issues of the Intertropical Convergence Zone (ITCZ) during the Holocene. The migration of ITCZ from the south to the north in the early period (9.5-10.5 ka BP) was associated with high humidity and rainfall changes in the Study Area. However, from 7.8 ka BP to the present the ITCZ migrated southward (Fleitmann, et al, 2007). As a result, weather conditions moved to aridity which influenced the recharge processes in the Najd area. Despite this, the recharge conditions were probably different in the past and far better than in recent times.

5.3 Conclusion

The groundwater age in Najd is in the range between (Modern to 22300 yr), however it varies between aquifers. With the exception of the recharge area (Jabal chain), several locations were reflected as being modern recharge and possibly based on their young groundwater in different aquifers. These locations are Helat Ar Rakah (Twirish) in aquifer A, east of Al Mazyunah and northward to the sand dunes (DEP-9, WWD-17, WWD-13, WWD-19) in aquifer B, south of Qitbit (DEP-19) in aquifer C and in Hanfeet and Helat Ar Rakah (RBK-D, H.R.C) in aquifer D.

The cyclonic contribution to groundwater recharge was observed from ^{14}C , ^{13}C and ^{18}O data analyses, which show three sources of groundwater origin; monsoon waters are collected at aquifer D; mainly cyclone recharge in aquifers (A, B, D) and fossil water concentrated in aquifer C; in addition to mixing processes between these types. Evidentially, the recharge processes started by dewatering of aquifer C from aquifer D in the previous (say early Holocene), and due to the steady state condition of aquifer C and the water pressure, the recent water is allowed to pass to aquifers B and A via faults, fissures and fractures.

The groundwater NGTs increases from south to north and northeast in all aquifers which indicates a similarity with the present temperature increase direction. However, the climate conditions are much warmer at present than in the past. The recharge to Najd aquifers occurred in the past within climate conditions much colder than now, and the Jabal chains in the south still play the role of this recharge generation.

The presence of recharge in aquifers A to D at different locations probably reflects the influences of some faults allowing an amount of recent water to be mixed with old groundwater. Even though, the young groundwater could explain the high abstraction which accelerates the mixing between old and recent groundwater.

NAJD GROUNDWATER SITUATION AND FUTURE MANAGAMENT

Groundwater in the Study Area can be explained in lay-man terms, as having four layers above each other called aquifers. The deepest one, called aquifer D is distributed over all Najd. However the other three are restricted in some places even though the aquifer C (the second from the bottom) becomes the second in the distribution bases. The remaining two layers, aquifer B and A occupy limited areas. Aquifer B is located east of Mazyunah to Hanfeet and extends northward to North Shsir and Dawkah, whereas aquifer A is distributed between Shsir, Hanfeet, Helat Ar Rakah and Bin Khawtar; however its quality becomes worse in the area north to northeast of Bin Khawtar. Nevertheless, in the importance of all aquifers, aquifer C should be prioritised in the case of a significant classification. This aquifer's characteristics, such as transmissivity and storage coefficient enables it to produce and recover faster than the other aquifers. As a result, three pilot government agricultural projects are establishing themselves at Hanfeet, Dawkah and Bin Khawtar, and depend on aquifer C as main water source. From the other three aquifers only aquifer A is used at present and mainly for agriculture by local farms concentrated in Shsir, Helat Ar Rakah, Hanfeet and some scattered farms at Bin Khawtar. The other aquifers, such as aquifer D, are used for water supply, whereas B is used in a very limit scale.

On other hand, the future abstraction from the three proposed pilot wellfields was limited to $30 \text{ Mm}^3.\text{yr}^{-1}$ from Hanfeet and $25 \text{ Mm}^3.\text{yr}^{-1}$ from both Dawkah and Bin Khawtar. In opposition, the estimated total inflow to Najd aquifers was at $15 \text{ Mm}^3.\text{yr}^{-1}$ (GRC, 2008) which means a deficit of about $65 \text{ Mm}^3.\text{yr}^{-1}$ plus the local farms consumption. The flood data analyses during the period 1985 to 2008 from four main wadis in Najd shows an approximate average flow of $10 \text{ Mm}^3.\text{yr}^{-1}$. However, many of the wadis were not measured with gauges which may contribute to such amount of recharge and without taking it into account. In addition, the flood measurements in these wadi gauges take place at 30 to 50 km away from the surface watershed division; this is often associated with maximum rainfall occurrences. Therefore, such an amount of recharge is expected and occurs before these gauges. Assuming this, if all the flood volumes are penetrated as recharge, this amount is still one third less than

the estimated recharge in the previous studies ($15 \text{ Mm}^3 \cdot \text{yr}^{-1}$). Therefore, the recharge amount is probably more or less than what was expected. By taking into account the contribution from ungauged wadis, this amount may approximate around $10 \text{ Mm}^3 \cdot \text{yr}^{-1}$, thus three detailed dimension models with extra wadi gauges are required in that area to determine the reasonable recharge going to Najd. A type of this modeling is recently being run by the Helmholtz Centre for Environmental Research UFZ (T. Müller, PhD Thesis, in progress).

The cyclonic events are the main source for groundwater recharge in Najd area. This idea is supported by evidence collected from water level monitoring wells, compared with flood event periods, was found to respond in all aquifers; varying on time, depending on distance from the recharge source occurred and the aquifer's characteristics. This recharge process usually occurs in the south in/or close to the Jabal chain among aquifer D, then further north, and the above aquifers feeds due to elevation differences through faults, fissures and fractures with the exception of some limited areas being influenced by local faults such as in Helat Ar Rakah. The accumulation of ^{13}C , ^{14}C and ^{18}O data reveals that groundwater is mainly related to an atmospheric source in an area not influenced by monsoons. This indicates recharge due to cyclone events. Too, monsoon and fossil water sources which are mixed between these groups are expected. Moreover, by using hydrochemical parameters (Cl) and stable isotopes (^2H), the data suggests the direction for recharge conducted modern groundwater through aquifer D from the recharge area northward. This flow path canal may pass through Thumrait (MOD-15) to the poultry farm (332/014) and continue in a northeastward direction. In addition the ^3H data collected from 50 locations shows a possibility of recent recharge in the recharge area (Jabal) wells and springs, and only in two other locations, one in aquifer A (M.Masin) in Shsir and the other one in aquifer B (DEP-9) east of Mazyunah.

^{14}C dating and noble gas analysis were conducted in all aquifers from A to D. The groundwater age is found in the range from modern to 22000 yr old groundwater. The youngest groundwater in addition to the recharge area was detected at several locations in different aquifers such as Helat Ar Rakah at boreholes Twirish and H.R.C (aquifer A, D), east and northeast of Mazyunah at DEP-9, WWD-17 and WWD-13

(aquifer B), south of Qitbit near DEP-19 (aquifer C) and RBK-D in Hanfeet (aquifer D), however the oldest groundwater was found in aquifer B at borehole DEP-16A at Qobat al Nsir northeast of Mazyunah. In fact heterogeneity of the aquifers themselves and between each other makes age calculations more difficult, even though all the important parameters were provided for, such as a real data measured in the field in order to avoid assumptions.

The noble gases analyses were carried out for all aquifers in order to understand the paleo-climate and the influences of geological structure. Noble gases are one of the best indicators still used worldwide to measure the groundwater temperature at the time of infiltration occurring thousands of years ago. Due to the climatical conditions of the Study Area the noble gas temperature (NGT) and Helium isotopes (^3He , ^4He) were used. The NGT reveals that groundwater temperatures increased in all aquifers from the south to north or northeast following the groundwater flow direction. However, they were colder in the past, more so than at the infiltration time at present. On the other hand, the relationship between Ne/He versus $^3\text{He}/^4\text{He}$ reflects a general influence of atmospheric helium in boreholes located in/or close to the Jabal chain in the south (recharge area) and generally in all aquifers further north except aquifer C. As a result, it seems that the contribution of recharge to Najd aquifers is less in aquifer C than the other aquifers A, B and D. This confirms fossils' water existence especially in aquifer C, probably recharged during the paleo-climate (Holocene period).

Despite the uses of different chemical and environmentally stable and radioactive isotopes analyses, it was difficult to separate between aquifers in the regional scale. It seems however, to be rather possible with limited areas. Therefore mixing processes occurred between aquifers depending on special development among and between the layers structure. This mixing may be more restricted within the area of Helat Ar Rakah due to intensive drilling activities rather than in the north. In addition, non-natural leakages between aquifers also exist due to unmaintained boreholes and non-cased wells from the Petroleum Development Oman (PDO).

The water level data collected from all aquifers shows a general decrease, even though it can vary specifically between them. Therefore, a maximum drawdown with an accuracy of 1cm recorded in all aquifers from A to D during the period (1989-1993) and up to Feb2010 was; 6.27m (HRB-19), 2.23m (001/018), 34.79m (JICA-6) and 8.9m (RBK-D) respectively (details see chapter 3). However the maximum drawdown was observed in aquifer C at Helat Ar Rakah (JICA-6) and 13m out of the total drawdown (34.79m) had occurred within the last 4 years after 2006 and associated with the expansion of the Zinat al Sahra farm. In addition, aquifers such as B and D also decrease even though they are not involved in any intensive abstraction. This is except for water supply using aquifer D in limited areas such as the poultry farm at eastern Hanfeet. This decrease indicates a mix or leakage between aquifers (GRC, 2008). The water level decline for aquifers was calculated by using the maximum drawdown values and divided by the monitoring period. As a result, the annual decreasing rate for aquifers A to D is 0.33m, 0.12m, 2.05m and 0.42m respectively. However the boreholes from aquifer A and C involved in this calculation were located in Helat Ar Rakah, whereas the others in aquifer B and D were from the Hanfeet area at around 30 km south of Helat Ar Rakah.

The groundwater quality in all aquifers exceeds the maximum permissible limit which means it does not fit with the Omani standard (8/2006) for human drinking water. However, boreholes or springs located within the recharge area (Jabal) often fall within the permissible human drinking water range. Common ions/variables such as SO_4 , F, and TDS often found with high concentrations exceed the Omani standard. On the other hand based on SAR comparison with EC, the majority of groundwater from all aquifers in Najd is suitable for agricultural irrigation purposes. The existing aquifers around Shsir, Hanfeet, Helat Ar Rakah, Dawkah and Bin Khawtar are the best locations for any agricultural development. The quantities and quality of water and the advantage of some locations which is close to the main cities like Thumrait and Salalah also not far away from the main road. Further north (sand dunes) and northeast towards Maqshin and Ramlat Maqshin (close to WWD-37) the quality becomes worse eventhough the quantity is abundant. Overall, the irrigation water quality decreases towards the north and northeast in all available aquifers. Based on this, groundwater suitability for agricultural irrigation should be ranked in the

following order: D>C>A>B with exceptions of three boreholes close to the northeast corner belonging to different aquifers. However, on the bases of quantity and economy these aquifers ranking order could be change to C>D>B>A.

In general, the groundwater pressure increases northward and water levels start to flow artesian north of Dawkah and before borehole Bin Kh (BF080077AA). In the area between this well and the Hanfeet well, water levels, particularly in aquifers C and D could rise from the water strike at 200-300m below ground level up to less than 30 meters below the ground surface, which means a sub-artesian condition. In the meanwhile, local people have drilled, at random, more than 1200 boreholes in aquifer A. These boreholes were not cased at all and were left as open holes. If farmers dip those boreholes to beneath artesian and sub-artesian aquifers C and D, an enormous leakage will occur among these wells to the upper layers and the situation would spin out of control. At the sametime, the groundwater abstraction should not concentrate in a specific aquifer and in the same area. However, the distribution of agricultural well fields is recommended. Therefore the drilling or rehabilitation in Najd should be performed with special borehole construction design and under MRMWR engineering supervision regardless of the privatization of the property. As well as without good understanding of the artesian aquifers condition the future development in the area may be threatened. Consequently, the expected running period for the agriculture development will be dramatically shorter.

On the other hand, Management in Najd is different from the typical agriculture systems in other regions. It is therefore difficult to compare this area with other locations such as Salalah or the Batinah coastal plains. This because the climate conditions normally affect most of the principal operations such as irrigational systems. Consequently, the investment in Najd requires more focus in many aspects; however, the water quality and quantity should be a priority. Therefore a prudent dealing with aquifers is important in order to achieve long term goals even though it adds a heavy extra cost.

This requires several technical parameters to be taken into account as following:

- installing data loggers around the well fields to monitor the actual water level fluctuation,

- continuing monitoring hydrochemistry such as EC, pH, temperature and major ions analyses,
- installing discharge meters in all discharging wells to determine the total abstraction, educating the farmers through different campaigns about how to economize water, and at the very least choosing the best time for irrigation.

Despite the weather in Najd, the area has the capability to lose a big amount of water during the irrigation period as evaporation happens due to high temperatures. Importantly, to imply instructions which control water management and conservation based on Najd circumstances. Finally, water level monitoring networks should be expanded to include recent boreholes.

REFERENCES

- Aeschbach-Hertig, W., Peeters, F., Beyerle, U., Kipfer, R. (1999): Interpretation of dissolved atmospheric noble gases in natural waters. *Water Resources Research*, 35, 2779-2792
- Aeschbach-Hertig, W., Peeters, F., Beyerle, U., Kipfer, R. (2000): Palaeotemperature reconstruction from noble gases in ground water taking into account equilibration with entrapped air. *Letters to Nature* 405, 1040-1044
- Aeschbach-Hertig, W., Stute, M., Clark, J.F., Reuter, R.F., Schlosser, P. (2002): A paleotemperature record derived from dissolved noble gases in groundwater of the Aquia Aquifer (Maryland, USA). *Ceochimica et Cosmochimica Acta* 66, 797-817
- Alsaaran, N.A. (2008): Origin and geochemical reaction paths of Sabkha brines: Sabkha Jayb Uwayyid, eastern Saudi Arabia. *Arab. J. Geosci.* 1, 63-74
- Andrews, J.N. (1985): The isotopic composition of radiogenic helium and its use to study groundwater movement in confined aquifers. *Chem. Geol.* 49, 339-351
- Andrews, J.N., Lee, D.J. (1979): Inert gases in groundwater from the Bunter Sandstone of England as indicators of age and palaeoclimatic trends. *J. Hydrol* 41, 233-252
- Appelo, C. A. J., Postma, D., (2005): *Geochemistry, Groundwater and Pollution*. 2nd edition, Balkema, Publishers, Leiden, The Netherlands, 404p
- Bahar, M., Reza, S. (2010): Hydrochemical characteristics and quality assessment of shallow groundwater in a coastal area of southwest Bangladesh, *Environ Earth Science Journal* 61, 1065-1073
- Battaleb-Looie, S., Moore, F. (2009): Determination of fluoride source in ground water using petrographic studies in Dashtestan area, south of Iran. Department of Earth Sciences, Faculty of Sciences, Shiraz University, Shiraz, Iran
- Birkle, P., García, B.M., Milland Padrón., C.M., Eglinton, B.M. (2009): Origin and evolution of formation water at the Jujo-Tecominoacan oil reservoir, Gulf of Mexico. Part 2: Isotopic and field-production evidence for fluid connectivity, *Applied Geochemistry* 24, 543-554
- Böttcher, M., Thamdrup, B., Vennemann, T.W. (2001): Oxygen and sulphur isotope fractionation during anaerobic bacterial disproportionation of sulphur. *Geochim, Cosmochim. Acta* 60, 1601-1609
- Bradley, D., Cey, G., Hudson, B., Moran, J.E., Scanlon, B.R. (2008): Impact of Artificial Recharge on Dissolved Noble Gases in Groundwater in California. *Environ. Sci. Technol.* 42, 1017-1023
- Brunt, R., Vasak, L., Griffioen, J. (2004): Fluoride in groundwater: probability of occurrence of excessive concentration on global scale. International groundwater resources assessment centre, Report nr. SP 2004-2, Utrecht, UNESCO.
- Carreira, P.M., Marques, J.M., Pina, A., Gomes, A.M., Galego Fernandes, P.A., Santos, F.M. (2010): Groundwater Assessment at Santiago Island (Cabo Verde): A Multidisciplinary Approach to a Recurring Source of Water Supply. *Water Resour Management* 24, 1139-1159
- CCEWR (1986b): Regional Hydrogeological Evaluation of Najd. R-48-86
- CCEWR (Council for the Conservation of Environment and Water Resources) (1986a): The Najd Exploratory Drilling Investigation, 1985-1986. OFR-40-86
- Clark, I., Fritz, P. (1997): *Environmental Isotopes in Hydrogeology*. Lewis Publishers, New York

REFERENCES

- Clark, I.D., Fritz, P., Quinn, O.P., Rippon, P.W., Nash, H., Al-Said, S.B. (1987) Modern and fossil groundwater in an arid environment: a look at the hydrogeology of southern Oman. Proceed. Use of stable isotopes in water resources development, IAEA-SM-299, pp 167-187, Vienna, Austria
- Coetsiers, M., Kilonzo, F., Walrevens, K. (2008): Hydrochemistry and source of high fluoride in groundwater of the Nairobi area. *Hydrological Sciences Journal*, 2150-3435, 53, 6, 1230 – 1240
- Cresswell, R.G., Herczeg, A.L. (2004): Groundwater recharge, mixing and salinity across the Angas-Bremer Plains, South Australia: Geochemical and Isotopic contents. CSIRO Land and Water Technical Report No.29/04, Australia
- Datta, D.K., Subramanian, V. (1997): Nature of solute loads in the rivers of Bengal drainage basin, Bangladesh. *J. Hydrol* 198, 196-208
- Dewandel, B., Lachassagne, P., Boudier, F., Al-Hattali, S., Ladouche, B., Pinault, J.L., Al-Suleimani, Z. (2005): A conceptual hydrogeological model of ophiolite hard-rock aquifers in Oman based on a multiscale and a multidisciplinary approach. *Hydrogeological Journal* 13, 708-726
- Doerr, H., Mueanich, O. (1980): Carbon-14 and carbon-13 in soil CO₂. *Radiocarbon* 22, 909-918
- Driscoll, F.G. (1986): *Groundwater and Wells*. Johnson Filtration Systems, Inc., St. Paul, Minnesota
- ESI Ltd., Century Architects, Andam International LLC. (2007): *Groundwater Modeling of the Nejd Aquifers*.
- Evans, G.V., Otlet, R.L., Wassell, L.L., Bath, A.H. (1984): Verification of the presence of carbon-14 in secondary carbonates within a sandstone aquifer and its hydrological implications. *Isotope Hydrology*, IAEA, Vienna, 1983, 577-590
- FAO (Food and Agriculture Organisation of the United Nations) (1986): *Water for Animals*, Document No. AGL/MISC/4/85.
- Fleitmann, D., Burns, S.J., Manfini, A., Mudelsee, M., Kramers, J., Villa, I., Neff, U., Al-Subbary, A.A., Buettner, A., Hippler, D., Matter, A. (2007): Holocene ITCZ and Indian monsoon dynamics recorded in stalagmites from Oman and Yemen (Socotra). *Quaternary Science Reviews*, 26: 170-188
- Fleitmann, D., Burns, S.J., Mudelsee, M., Neff, U., Kramers, J., Manfini, A., Matter, A. (2003): Holocene Forcing of the Indian Monsoon Recorded in a Stalagmite from Southern Oman, Report, Science VOL 300.
- Frencken, J.E., König, K.G., Mulder, J., Truin, G.J. (1992): Exposure to Low Levels of Fluoride and Dental Caries in Deciduous Molars of Tanzanian Children. *Caries Research*, 26, 379-383
- Fritz, P., Basharmal, G. M., Drimmie, R. J., Ibsen, J., Qureshi, R. M. (1989): Oxygen isotope exchange between sulphate and water during bacterial reduction of sulphate. *Chem. Geol.* 79: 99-105
- Gehre, M., Strauch, G. (2003): High-temperature elemental analysis and pyrolysis techniques for stable isotope analysis. *Rapid Commun Mass Spectrum* 17, 1497-1503
- Geyh, M.A. (1970): Carbon-14 concentration of lime in soil and aspects of the carbon-14 dating of groundwater. *Isotope Hydrology*, IAEA, Vienna, pp. 215-223
- Glover, C.R. (1996): *Irrigation Water Classification systems*, Guide A-116, New Mexico University (NMSU), U.S. Department of Agriculture
- Gonfiantini, R., Zuppi, G.M. (2003): Carbon isotope exchange rate of DIC in karst groundwater. *Chemical Geology* 197, 319-336

REFERENCES

- GRC (Geo-Resources Consultants) (2007): Drilling and Aquifer Testing Programme in the Dhofar Governorate. Inception Report, Sultanate of Oman
- GRC (2008): Drilling & Aquifer Testing in the Dhofar Governorate, MRMWR, Sultanate of Oman.
- GRC (2005a): Drilling and Aquifer Testing Project in the Western Al Wusta (Najd) Desert, Oman. Final Report, unpublished, Ministry of Regional Municipality and Water Resources (MRMWR), Sultanate of Oman
- GRC., Aquaterra. (2005b): Detailed Water Resources Management and Planning Study for the Salalah Region: Part A - Review; Part B - Modelling; Part C - Planning; and Part D – Monitoring. MRMWR
- GTZ & DCo (Deutsche Gesellschaft für Technische Zusammenarbeit in association with Dornier Consulting) (2009): Groundwater Quality-Hydrochemistry, 11, Ministry of Electricity and Water, Kingdom of Saudi Arabia
- Hahm, D., Kim, K.R. (2001): An estimation of the new production in the southern East Sea using helium isotopes. *J Korean Soc Oceanogr* 36, 19-26
- Hahm, D., Postlethwaite, C.F., Tamaki, K., Kim, K.R. (2004): Mechanisms controlling the distribution of helium and neon in the Arctic seas: the case of the Knipovich Ridge. *Earth Planet Sci Lett* 229, 125-139.
- Handa, B. K. (1975): Geochemistry and genesis of fluoride-containing ground waters in India. *Groundwater* 13, 275–281
- Hem, J.D. (1989): Study and Interpretation of the Chemical Characteristics of Natural Water. 3rd Edition, Geological Survey, Water-Supply Paper 2254, Library of Congress, Washington, USA
- Herb, Christian. (~2011) Paleoclimate study based on noble gases and other environmental tracers in groundwater in Dhofar (Southern Oman), Diploma Thesis, University of Heidelberg
- Hesse, K-H., Hissene, A., Kheir, O., Schnacker, E., Schneider, M., Thorweihe, U. (1987): Hydrogeological Investigations in the Nubian Aquifer System, Eastern Sahara. *Berlin geowiss. Abh A75.2*, 397-464
- Hörling, B. (1992): Hydrogeologie, Kapitel 4.2.2.10, Ferdinand Enke Verlag, Stuttgart, p 207
- Hydrotechnica (1985) Thumrait Military Camp, Reappraisal of Groundwater Supply - Report Nr. 6.324/R1, Sultanate of Oman
- IAEA (1981): Stable Isotope Hydrology, ¹⁸O and ²H in the Water Cycle, Technical Reports Series No. 210, IAEA, Vienna
- IAEA (1995): Isotopes in Water Resources Management. In: Proceedings of a Symposium, Reports No. 20-24. Volume 2, IAEA, Vienna
- IPCC (Intergovernmental Panel on Climate Change) (2008): Fourth assessment Report: climate change in the Middle East and North Africa," The World Bank
- Jacks, G., Rajagopalan, K., Alveteg, T. and Jönsson, M.(1993) Genesis of high-F groundwaters, Southern India. *Appl. Geochem. (Suppl.)*, 2, 241–244
- Jagannathan, N. V., Shawky, A., Kremer, A. (2009): Water in the Arab World: management perspectives and innovations, Middle East and North Africa region. The World Bank
- Janza, M. (2010): Hydrological modelling in the karst area, Rižana spring catchment, Slovenia. *Environmental Earth Science Journal* 61, 909-920

REFERENCES

- JICA (Japanese International Corporation Agency) (1988, 1989): The Study on the Agricultural Development Project in the Najd Region, Ministry of Agriculture and Fisheries, Sultanate of Oman
- Kebede, S., Travi, Y., Stadler, S. (2010): Groundwaters of the Central Ethiopian Rift: diagnostic trends in trace elements, $\delta^{18}\text{O}$ and major elements. *Environ Earth Sci*, 61, 1641-1655
- Khayat, S., Hötzl, H., Geyer, S., Ali, W., Knöller, K., Strauch, G. (2006): Sulphur and Oxygen Isotopic Characters of Dissolved Sulphate in Groundwater from the Pleistocene Aquifer in the Southern Jordan Valley (Jericho Area, Palestine). *Isotopes Environm Health Stud* 42, 289-302
- Kipfer, R. (1991): Primordiale Edelgase als Tracer für Fluide aus dem Erdmantel, ETH Zürich. Diss. 9463
- Kipfer, R., Aeschbach-Hertig, W., Peeters, F., Stute, M. (2002): Noble gases in lake and ground waters, Vol. 47, Geochemical Society, Mineralogical Society of America
- Koepfen, W.S., (1923): Die Klimate der Erde. Walter der Grayter Verlag, Berlin
- Krauskopf, K.B., Bird, D.K. (1995): Introduction to Geochemistry, Third Edition, McGraw-Hill International, Library of Congress, USA
- Land, L., Huff, G.F. (2010): Multi-tracer investigation of groundwater residence time in a karstic aquifer: Bitter Lakes National Wildlife Refuge, New Mexico, USA. *Hydrogeology Journal* 18, 455-472
- Lee, J., Jung, B., Kim, J.M., Ko, K.S., Chang, H.W. (2010): Determination of groundwater flow regimes in underground storage caverns using tritium and helium isotopes, *Environ Earth Sci*, DOI 10.1007/s12665-010-0747-4
- Macumber, P.G., Barghash, S.G., Kew, G.A., Tennakoon, T.V. (1995): Hydrogeologic implications of a cyclonic rainfall event in central Oman. In: Nash H, McCall GJH (eds), *Groundwater Quality*. Chapman and Hall, London, pp 87-97
- Macumber, P.G., Niwas, J.M., Al Abadi, A., Seneviratne, R. (1997): A new isotopic water line for northern Oman. paper presented at the third gulf water conference, ministry of water resources, sultanate of Oman
- Mangalo, M., Meckenstock, R.U., Stichler, W., Einsiedl, F. (2007): Stable isotope fractionation during bacterial sulfate reduction is controlled by reoxidation of intermediates. *Geochimica et Cosmochimica Acta* 71, 4161-4171
- Matter, J.M., Waber, H.N., Loew, S., Matter, A. (2005): Recharge areas and geochemical evolution of groundwater in an alluvial aquifer system in the Sultanate of Oman. *Hydrogeol Journal* 14, 203-224
- Ministry of National Economy, census administration (2003), Sultanate of Oman
- MMI -Mott MacDonald International- (1991): Detailed Investigations for Development of up to 1000ha of Irrigated Land: Nejd Region. *Hydrogeology Interim Report (Final)*, Ministry of Water Resources, Sultanate of Oman
- MMI -Mott MacDonald International (1994b): Detailed Investigations for Development of up to 1000ha of irrigated Land: Negd Region. *Final Mathematical Modelling Report (Draft)*, Ministry of Water Resources, Sultanate of Oman
- Moncaster, S.J., Bottrell, S.H., Tellam, J.H., Lloyd, J.W., Konhauser, K.O. (2000): Migration and attenuation of agrochemical pollutants: insights from isotopic analysis of groundwater sulphate. *Journal of Contaminant Hydrology* 43, 147-163

REFERENCES

- Morikawa, N. (2004): Dissolved helium distribution in deep groundwaters from the Tono area, central Japan: a tool for tracing groundwater flow in fractured granite. *The Japanese Society of Limnology* 5, 61-69
- Morrow, D.W., Mayers, I.R. (1978): Simulation of limestone diagenesis-a model based on strontium depletion. *Can. J. Earth Sci.* 15, 3, 376-396
- MPM (Ministry of Petroleum and Minerals) (1992b): Geological Map of Hawf, Sheet NE39-16 (scale 1:250,000), Oman. Directorate General of Minerals and Geological Survey of Japan, Ministry of Petroleum and Minerals, Sultanate of Oman
- MPM (1992a): Geological Map of Marmul, Sheet NE40-05 (scale 1:250,000), Oman. Directorate General of Minerals and Geological Survey of Japan, Ministry of Petroleum and Minerals, Sultanate of Oman
- Münnich, K.O. (1957): Messungen des ^{14}C -Gehaltes von hartem Grundwasser. *Naturwissenschaften* 44, 32-33
- MWR (Ministry of Water Resources) (1993): Report on the pumping test analysis and hydrochemistry at the MAF proposed pilot farm, Sultanate of Oman
- MWR (1994c): Najd Regional Assessment. Test Pumping Analyses and Hydrochemistry at West Hanfeet, Dhofar, Sultanate of Oman
- MWR (1994d): Najd Regional Assessment. Test Pumping Analyses and Hydrochemistry at JICA Farm, Dhofar. The purpose of the work was also to obtain detailed C aquifer characteristics at Helat Ar Rakah. Sultanate of Oman
- MWR (1995a): Najd Regional Assessment report. Helat Ar Rakah Pumping Test Program, Sultanate of Oman
- MWR (2000a): Water Resources Assessment Report for Najd Water Assessment Area, Sultanate of Oman
- Odeh, T., Salameh, E., Schirmer, M., Strauch, G. (2009): Structural control of groundwater flow regimes and groundwater chemistry along the lower reaches of the Zerka River, West Jordan, using remote sensing, GIS, and field methods. *Environm Geol.* DOI 10.1007/s00254-008-1678-1
- Office of Health and Environmental Research U.S. Department of Energy, 1996
- Ozima, M., Podosek, F.A. (1983): Noble gas geochemistry. Cambridge Univ. Press, Cambridge, London, New York
- Parkhurst, D.L. (1995): User's guide to PHREEQC-a computer program for speciation, reaction-path, advective-transport, and inverse geochemical calculations. U.S. Geological Survey Water-Resources Investigations Report 95-4227, 143 p
- PAWR (Public Authority for Water Resources) (1986): Regional Hydrogeological Evaluation of the Najd, Sultanate of Oman. pp 48-86
- PAWR (1986d): Programme for Further Exploration Wells and Discussion of Limited Pilot Development in the Najd region, Sultanate of Oman. PAWR 86-I-13
- PAWR (1986a): Report on Microfossil Content Najd Exploratory Boreholes. PAWR 86-2
- PDO (Petroleum Development Oman) (1994): The Desert Agricultural Project. A Report on Project Development to December 1993
- Pearson, Jr., F.J. (1965): Use of $\text{C}^{13}/\text{C}^{12}$ ratios to correct radiocarbon ages of materials initially diluted by limestone. *Proc. Int. Conf. on Radiocarbon and Tritium Dating, Pullman, USA*, 357-366

REFERENCES

- Pearson, Jr., F.J., Hanshaw, B.B. (1970): Source of dissolved carbonate species in groundwater and their effects on carbon-14 dating. *Isotope Hydrology*, IAEA, Vienna, pp. 271-286
- Peh, Z., Miko, S., Hasan, O. (2010): geochemical background in soils: a linear process domain? An example from Istria (Croatia). *Environ Earth Sci* 59, 1367-1383
- Pilla, G., Sacchi, E., Zuppi, G., Braga, G., Ciancetti, G. (2006): Hydrochemistry and isotope geochemistry as tools for groundwater hydrodynamic investigation in multilayer aquifers: a case study from Lomellina, Po plain, South-Western Lombardym Italy. *Hydrogeology Journal*, 14, 795-808
- Porcelli, D., Ballentine, C.J., Wieler, R. (2002): An Overview of Noble Gas Geochemistry and Cosmochemistry, *Mineralogical Society of America*, V. 47; p 1-19
- Powers, R.W., Ramirez, L.F., Redmond, C.D., Elberg, E.L (1966): *Geology of the Arabian Peninsula, Sedimentary Geology of Saudi Arabia*: U.S. Geological Survey, Professional Paper 560D, p147
- Rajmohan, N., Al-Futaisi, A., Al-Touqi, S. (2009): Geochemical process regulating groundwater quality in a coastal region with complex contamination sources: Barka, Sultanate of Oman. *Environmental Earth Science*, DOI 10.1007/s12665-009-0037-1
- Rashidi, M., Seilsepour, M. (2008): Sodium Adsorption Ratio Pedotransfer Function for Calcareous Soils of Varamin Region. *International Journal of Agriculture and Biology* 10, 6, 715-8
- Repčok, I., Mišík, M., Eliáš, K., Ferencikova, E., Harcova, E., Jablonsky, J., Rucka, I., (2000): Extremely isotopically heavy sulphur in barite concretions from Slovakia. *Geologica Carpathica*, 51, 301-308
- Roger, J., Platel, J.P., Bourdillon-de-Crissac, C., Cavelier, C. (1992): *Geological of Dhofar (geology and geodynamic evolution during the Mesozoic and Cenozoic)*. Ministry of Petroleum and Minerals, Sultanate of Oman
- Sawyer, G.N., McMartyly, D.L. (1967): *Chemistry of sanitary engineers*. 2nd ed. McGraw Hill, New York, p518
- Saxena, V. K., Ahmed, S. (2003) Inferring the chemical parameters for the dissolution of fluoride in groundwater. *Environ. Geol.* 43, 731–736
- Schlosser, P., Winckler, G. (2002): Noble Gases in Ocean Waters and Sediments, noble gases in geochemistry and cosmochemistry 47, *Geochemical Society, Mineralogical Society of America*.
- Sharaf, M.A.M. (2001): Review of the hydrogeological and hydrochemical aspects of groundwater in the Umm-Er-Radhuma aquifer system, Arabian Peninsula. *Journal of African Earth Sciences* 33, 349-362
- Singh, A.K., Hasnain, S.I. (1998): Major ion chemistry and weathering control in a high altitude basin: Alaknanda River, Garhwal Himalaya, India. *Hydrol. Sci. J.* 43, 825-843
- Stuiver, M., Polach, H. (1977): Reporting of ¹⁴C data. *Radiocarbon* 19, 355-363
- Sunagawa, I., Takahashi, Y., Imai, H. (2007): Strontium and aragonite-calcite precipitation. *J. Mineralogical and Petrological Sciences*, 102, 174-181
- Tetra Tech International, Inc (1978): *Groundwater System of Jabal Al Qara and its Relation to the Occurrence and Quality of Groundwater in Adjacent Salalah Coastal Plain and Najd*, PAWR, Sultanate of Oman
- The Omani Standard (8/2006): Directorate General for Specifications and Measurements, Ministry of Commerce and Industry, Sultanate of Oman.

REFERENCES

- Tolstikhin, I., Lehmann, B.E., Loosli, H.H., Gautschi, A. (1996): Helium and argon isotopes in rocks, minerals, and related groundwaters: A case study in northern Switzerland. *Geochim Cosmochim Acta* 60, 1497-1514
- Turchyn, A.V., Bruchert, V., Lyons, T.W., Engel, G. S., Balci, N., Schrag, D. P., Brunner, B. (2010): Kinetic oxygen isotope effects during dissimilatory sulfate reduction: A combined theoretical and experimental approach. *Geochimica et Cosmochimica Acta* 74, 2011-2024
- UN.(United Nation) (2010): World Water Day (22 March). UN-Water official site
- Wang, G.W., Guanlin, G., Shi, Y.B., Wu, S. L., Wu, J. Q. (2010): Large differential land subsidence and earth fissures in Jiangyin, China. *Environmental Earth Science*, 61, 1085-1093
- Watson Hawksley (1983): Thumrait Water Resources and Treatment Study, Oman, 1981-1983
- WBCSD (world business council for sustainable development) (2005): The role business can play as an active stakeholder in collaborative processes for water management, discussion paper prepared by the WBCSD program on water and sustainable development
- Weyhenmeyer, C.E., Burns, S.J., Waber, H.N., Macumber, P.G. (2002): Isotope study of moisture sources, recharge area, and groundwater flow path within the eastern Batinah coastal plain, Sultanate of Oman. *Water Res. Res.* 38, 10, 2-1-2-22
- Wigley, T.M.L. (1976): Effect of mineral precipitation on isotopic composition and ^{14}C dating of groundwater. *Nature* 263: 219-221
- Wigley, T.M.L., Plummer, L.N., Pearson, Jr., F.J (1978): Mass transfer and carbon isotope evolution in natural water systems. *Geochim, Cosmochim. Acta* 42, 1117-1139
- Wood, W.W., Sanford, W.E., Al Habshi, A.R.S. (2002): The source of solutes to the coastal-sabkha aquifer of Abu Dhabi. *Geol. Soc. Amer. Bull.* 114, 259–268
- Xiangquan Li., Li Zhang., Xinwei Hou. (2008): Use of hydrogeochemistry and environmental isotopes for evaluation of groundwater in Qingshuihe Basin, north-western China. *Hydrogeology Journal* 16, 335-348
- Xubo Gao, Yanxin Wang, Penglin Wu, Qinghai Guo (2010): Trace elements and environmental isotopes as tracers of surface water-groundwater interaction: a case study at Xin'an Karst water system, Shanxi Province, Northern China, *Environ Earth Sci* 59, 1223-1234
- Zack, A.L. (1980): Geochemistry of fluoride in the Black Creek aquifer system of Horry and Georgetown Countier, South Carolina- and its physiological implications. US Geological Survey Water-Supply Paper 2067, 40

In order to evaluate the amount of recharge to Najd aquifers, three dimension modeling in the south part of the Study Area is recently being run by the Helmholtz Centre for Environmental Research UFZ (T. Müller, PhD Thesis, in progress)..

ANNEX

A-1 Results of chemical data and precipitation collected in 2008 and 2009 (mg.L⁻¹)

Local Name	Site ID	Aquifer	Sample Date	Temp °C	pH	EC µS.cm ⁻¹	Ca ²⁺ mg.L ⁻¹	Mg ²⁺ mg.L ⁻¹	Na ⁺ mg.L ⁻¹	K ⁺ mg.L ⁻¹	Sr ²⁺ mg.L ⁻¹	HCO ₃ ⁻ mg.L ⁻¹	Cl ⁻ mg.L ⁻¹	SO ₄ ⁻² mg.L ⁻¹	NO ₃ ⁻ mg.L ⁻¹	F ⁻ mg.L ⁻¹	Br ⁻ mg.L ⁻¹	Si mg.L ⁻¹	SiO ₂ mg.L ⁻¹	SAR	TDS mg.L ⁻¹	T.Hardness mg.L ⁻¹
KhT-A	BG117784AA	A	3/5/09	31.3	8.4	2095	127.5	31.9	278.6	16.4	2.9	24.2	607.0	175.2	0.0	1.7	0.6	1.2	5.7	1252	452	
M.Masin	YA729072AA	A	20/4/09	32.6	7.2	2460	217.3	82.1	241.9	4.1	9.3	174.8	528.4	520.5	19.9	2.5	3.6	13.9	29.2	3.5	1739	886
M.Masin	YA729072AA	A	29/4/08	32.6	7.6	2003	202.5	69.0	233.5	15.4	9.9	151.4	343.2	422.4	12.4	1.8	0.0	15.2	31.9	3.6	1415	794
Mathira I	YV826752BA	A	26/5/09	32.8	8.0	1449	32.7	34.1	183.8	8.7	10.2	56.5	323.0	170.2	0.0	3.8	0.3	0.7	5.3	785	224	
NKR sp	BE105632AC	A	24/5/08	26.4	7.4	1275	125.3	24.8	85.9	10.1	0.9	293.7	221.1	56.3	81.2	0.6	0.0	8.2	17.1	1.8	771	417
O.R	ZV191273AA	A	5/4/09	32.8	7.4	2864	202.7	71.7	323.0	6.5	5.5	142.9	607.0	524.0	31.0	2.1	0.0	12.0	25.2	5.0	1870	806
SHTH sp	AE803515AC	A	7/6/09	28.7	7.8	941	91.9	24.1	92.2	0.2	0.5	196.4	58.7	12.8	0.7			18.4			605	330
SHTH sp	AE803515AC	A	24/5/08	26.0	7.9	909	95.1	19.9	80.0	1.5	0.5	234.1	167.5	49.8	20.8	0.6		11.5	24.1	1.9	580	321
TWIRISH	AF123492AA	A	5/4/09	33.2	7.1	2590	249.6	80.6	253.3	4.5	7.9	176.1	513.6	735.4	21.7	2.9	1.6	15.2	31.9	3.6	1988	960
TWIRISH	AF123492AA	A	29/4/08	32.0	7.6	2089	235.0	70.0	212.0	15.9	9.1	153.6	339.5	535.0	11.3	2.1	0.0	17.3	36.5	3.1	1542	879
WWD-20	YA859494BA	A	6/5/09	30.1	8.1	5400	435.7	172.8	536.9	47.0	9.7	5.9	809.3	2009.0	0.0	8.7	9.7	20.4	5.5	4088	1809	
WWD-20	YA859494BA	A	11/5/08	32.7	8.7	5750	605.0	251.2	809.4	85.2	15.2	32.9	977.6	3324.8	12.2	5.1	11.3	23.9	7.0	6116	2559	
WWD-24	BG200046CA	A	3/5/09	29.0	8.8	1537	44.7	32.5	209.6	10.0	3.7	34.9	343.3	224.9	0.0	1.9	0.4	1.0	5.8	885	247	
WWD-24	BG200046CA	A	21/4/08	31.1	8.2	1603	77.0	46.5	208.0	12.2	4.1	24.0	324.2	281.5	0.2	1.2	0.3	0.7	4.6	964	386	
WWD-26	BG409917AA	A	3/5/09	33.7	8.6	2902	269.7	71.0	267.1	11.0	8.6	33.3	553.0	857.0	0.0	3.1	0.5	1.0	3.7	2049	970	
WWD-26	BG409917AA	A	21/4/08	32.0	6.9	2971	349.1	78.2	292.1	11.6	8.6	15.3	509.4	1067.7	0.2	3.3	0.3	0.6	3.7	2320	1198	
WWD-30	BG549421AA	A	3/5/09	32.9	8.6	9880	627.0	199.9	1373.3	46.6	13.2	35.8	2486.0	2175.0	0.0	4.3	0.7	1.5	12.2	6932	2400	
WWD-45	BG485361BA	A	21/4/09	32.3	8.2	2982	288.3	88.1	371.4	15.5	9.8	28.7	592.1	1162.2	0.0	3.8	2.1	0.5	1.1	4.9	2537	1088
MAF-S1(001/015)	ZV193035AA	B	18/11/09	35.0	7.0	2420	176.8	103.4	206.3	18.1			405.9	520.4	0.1		0.1					
DEP-17	YV578833AA	B	21/5/08	32.0	7.8	1310	67.2	48.0	159.6	10.5	17.1	180.3	254.8	203.7	0.2	4.5	0.0	11.1	23.4	3.6	866	368
DEP-15	YV399518AA	B	21/5/08	32.3	8.1	981	63.4	36.9	106.7	7.4	3.2	102.0	178.6	185.4	0.2	1.9	0.0	2.2	4.7	2.6	638	317
DEP-16A	XV997653BA	B	12/4/09	29.9	11.1	2126	169.0	5.6	250.2	55.2	17.0	-134.8	381.0	385.5	0.0	2.4	1.6	2.3	4.7	5.2	1339	446
DEP-16A	XV997653BA	B	4/5/08	30.4	11.3	2062	114.0	3.0	269.0	85.7	20.6	166.7	344.0	386.0	0.2	2.3	3.0	6.3	6.8	1303	298	
DEP-17	YV578833AA	B	11/4/09	35.9	7.5	1467	107.6	61.4	162.0	2.5	16.5	224.1	294.4	218.7	0.0	2.3	0.0	18.6	39.2	3.1	1008	525
DEP-9	YV182483AA	B	12/4/09	32.1	8.9	904	18.5	30.1	121.8	5.6	4.8	40.6	206.0	82.0	0.0	2.2	1.0	0.2	0.4	4.0	506	172
DEP-9	YV182483AA	B	3/5/08	33.5	7.7	1412	75.1	51.3	162.6	8.7	9.4	140.7	258.5	233.6	0.2	2.2	3.1	6.4	3.5	869	401	
WWD-13	YB406953BA	B	31/3/09	33.2	9.2	3840	532.9	192.9	179.9	42.4	13.5	7.9	200.8	2116.0	0.0	3.8	8.3	0.7	1.5	1.7	3306	2136
WWD-13	YB406953BA	B	13/4/08	32.4	9.8	4340	658.0	194.0	229.0	45.8	12.8	33.2	170.0	2510.0	9.2	2.1	0.0	0.3	0.6	2.0	3859	2453
WWD-17	YA389228BA	B	31/3/09	31.6	8.6	4170	539.7	199.8	334.2	51.5	14.4	5.7	240.0	2553.0	0.0	5.3	14.6	2.8	5.8	3.1	3962	2182
WWD-17	YA389228BA	B	13/4/08	29.9	9.7	4120	461.1	135.9	195.0	34.4	10.2	29.7	173.0	1986.0	0.0	5.4	3.5	0.4	0.8	2.0	3055	1719
WWD-19	YA859494AA	B	6/5/09	31.5	8.5	3990	471.9	201.0	106.9	32.0	10.8	58.3	172.0	1986.0	0.0	5.4	10.3	21.6	1.0	3031	2017	
WWD-19	YA859494AA	B	11/5/08	33.7	7.8	3880	660.6	288.1	176.9	60.9	17.1	32.9	222.4	3055.0	0.2	3.7	12.7	26.7	1.4	4517	2852	
WWD-5	XA694716BA	B	1/4/09	27.0	8.8	3479	501.4	197.7	198.7	27.3	15.4	-3.2	241.9	2263.0	0.0	4.0	2.0	1.6	3.3	1.9	3455	2077
WWD-5	XA694716BA	B	13/4/08	31.5	8.6	3820	532.0	191.0	183.0	32.2	16.9	13.1	239.0	2123.8	0.0	4.1	0.0	0.4	0.7	1.7	3314	2126
WWD-9	XA612881BA	B	4/5/08	31.7	8.7	2067	58.5	95.8	398.2	17.9	9.4	38.2	499.0	288.9	0.2	2.8	0.8	1.6	7.4	1386	545	

ANNEX

A-1. Continued

Local Name	Site ID	Aquifer	Sample Date	Temp °C	pH	EC $\mu\text{S cm}^{-1}$	Ca ²⁺ mg.L ⁻¹	Mg ²⁺ mg.L ⁻¹	Na ⁺ mg.L ⁻¹	K ⁺ mg.L ⁻¹	Si ²⁺ mg.L ⁻¹	HCO ₃ ⁻ mg.L ⁻¹	Cl ⁻ mg.L ⁻¹	SO ₄ ²⁻ mg.L ⁻¹	NO ₃ ⁻ mg.L ⁻¹	F ⁻ mg.L ⁻¹	Br ⁻ mg.L ⁻¹	Si mg.L ⁻¹	SiO ₂ mg.L ⁻¹	SAR	TDS mg.L ⁻¹	T.Hardness mg.L ⁻¹
001/014	ZV193035BA	C	5/4/09	36.2	7.5	2240	123.8	98.5	260.7	11.6	24.6	146.5	561.3	367.7	0.0	6.5	1.9	9.7	20.4	4.2	1528	720
001/014	ZV193035BA	C	28/4/08	36.2	7.6	2132	108.5	88.5	251.0	27.9	57.4	119.0	488.4	310.8	0.2	5.3	0.0	10.9	23.0	4.3	1368	640
001/290	AF829201AA	C	29/4/08	32.6	7.6	1696	105.0	73.0	166.0	23.0	50.0	134.7	351.9	282.7	0.2	5.1	0.0	7.2	15.2	3.0	1092	567
001/290	AF829201AA	C	6/4/09	35.5	7.4	1795	117.8	78.2	190.5	10.6	23.8	138.8	402.4	338.9	0.0	6.3	1.8	9.6	20.3	3.3	1238	620
Bashn-1	CF035107AA	C	5/5/09	32.4	9.3	1691	78.2	34.0	241.6	16.0	9.6	28.6	372.8	324.1	0.0	2.7		0.1	0.2	5.7	1084	337
Bashn-1	CF035107AA	C	21/4/08	27.2	7.8	1603	76.5	29.0	264.5	36.4	13.0	13.7	344.9	289.1	0.2	2.1	0.0	0.2	0.4	6.5	1050	312
Bin Kh	BF080077AA	C	3/5/09	34.1	7.9	1717	83.0	71.0	141.0	17.2	6.4	133.8	264.0	372.0	0.0	6.2		9.5	19.9	2.7	1045	503
Bin Kh	BF080077AA	C	16/4/08	35.1	7.8	1592	96.0	77.0	145.0	30.6	45.4	119.4	285.3	248.1	0.2	5.5		9.7	20.3	2.7	972	561
DEP-14	XV876910AA	C	4/5/08	32.3	8.3	1071	32.6	44.3	149.7	12.4	0.7	63.0	205.0	181.8	0.2	1.5		0.6	1.4	4.0	661	266
DEP-16	XV997655AA	C	12/4/09	29.0	8.5	1372	39.0	83.0	119.0	3.8	28.0	107.6	209.0	293.0	0.0	4.1	9.4	1.4	2.9	2.5	824	443
DEP-16	XV997655AA	C	4/5/08	29.7	8.1	1491	69.5	52.8	151.2	9.3	21.2	198.7	208.8	355.2	0.2	3.7		3.2	6.6	3.3	957	394
DEP-18	BF223760AA	C	2/5/09	32.0	8.6	1349	34.4	35.3	153.7	26.7	7.6	71.5	217.0	255.0	0.0	3.0		1.3	2.7	4.4	764	233
DEP-18	BF223760AA	C	17/5/08	31.1	7.4	1456	66.4	45.2	196.9	9.0	11.5	78.3	359.0	215.0	0.2	3.3		0.7	1.4	4.6	935	354
DEP-19	BF792149AA	C	3/5/09	32.5	9.0	2575	50.1	43.8	400.1	27.1	17.3	34.8	632.0	263.0	0.0	6.1		0.3	0.5	9.9	1440	308
DEP-19	BF792149AA	C	21/4/08	32.1	8.8	2844	104.0	81.0	442.0	31.9	23.2	22.9	592.9	559.8	0.2	5.4	3.0	0.3	0.6	7.9	1835	598
DEP-2	YV955966AA	C	8/4/09	31.1	8.6	2229	69.0	93.4	309.4	12.8	23.6	54.5	682.4	251.3	0.0	6.5	1.7	2.9	6.0	5.7	1573	562
DEP-2	YV955966AA	C	16/5/08	31.7	7.8	2068	81.0	74.1	270.4	22.5	28.0	56.5	549.4	257.1	0.2	4.9	0.0	1.5	3.2	5.2	1291	511
DEP-4	YV937394AA	C	16/5/08	30.9	12.6	5180	462.0	0.2	349.0	50.4	12.4	170.0	847.0	175.0	0.2	1.7	0.0	3.6	7.6	4.5	2439	1156
DEP-9A	YV182483BA	C	12/4/09	32.9	8.5	1329	53.1	93.1	138.9	3.8	27.1	83.6	230.1	369.4	0.0	5.5	1.4	0.6	1.2	2.7	954	521
DEP-9A	YV182483BA	C	3/5/08	31.3	8.0	1419	64.2	64.2	143.4	10.4	21.8	143.1	179.5	318.2	0.2	4.4		0.7	1.5	3.0	857	428
Gosharnl	CF179989AA	C	5/5/09	32.6	8.5	3441	81.1	98.6	507.8	22.5	6.9	79.8	814.0	544.0	0.0	3.2	3.9	0.4	0.8	9.8	2111	614
Gosharnl	CF179989AA	C	21/4/08	29.4	8.6	3411	147.4	114.4	640.8	26.4	9.1	55.6	960.9	704.8	0.2	3.7	3.9	0.7	1.5	9.6	2632	845
M.sp	YV439388AC	C	6/5/08	29.8	7.8	1859	126.0	48.0	247.0	10.7	3.2	169.3	380.6	264.7	14.1	1.8		10.1	21.3	4.7	1203	515
Qitbit	BG317999AA	C	3/5/09	7.7	29.62	148.3	128.0	330.3	30.0	20.7	112.0	491.0	775.0	0.0	6.1		10.3	21.6	4.3	1961	904	
Qitbit	BG317999AA	C	21/4/08	37.8	8.4	2851	182.0	132.0	333.0	36.6	25.2	98.7	483.9	733.2	0.2	6.6	4.1	10.8	22.7	4.6	1988	1005
Ranada-1	BF840101AA	C	5/5/09	31.8	8.8	1088	28.3	26.0	151.1	10.5	14.8	49.4	250.0	130.1	0.0	5.1		0.3	0.7	4.9	626	179
Ranada-1	BF840101AA	C	20/4/08	30.8	7.7	1065	29.7	24.9	160.5	11.4	15.6	29.9	247.5	140.6	0.2	4.6	0.0	0.3	0.6	5.2	635	178
RBK-C	BE050838AA	C	18/8/09	32.6	9.3	1879	36.7	28.2	322.3	14.8	9.6	27.3	537.7	61.0	0.2	4.0		0.0	0.1	9.7	1018	209
S.TMMI	YV347775AA	C	11/4/09	33.0	7.4	1814	132.3	73.9	202.2	0.8	17.0	226.1	353.9	310.4	0.0	3.4	0.0	10.7	22.4	3.5	1216	639
S.TMMI	YV347775AA	C	3/5/08	33.9	7.7	5190	259.7	175.7	1074.0	32.5	34.5	167.3	1494.6	755.1	0.2	7.5		19.9	41.8	12.6	3934	1382
UBAR Fm	YA819821AA	C	29/4/08	36.3	7.9	1332	54.0	47.0	136.0	13.4	30.3	160.7	199.1	222.8	0.2	5.1	0.0	9.8	20.5	3.3	782	331
W Bhaml	BF040000AA	C	17/5/08	31.2	7.1	1445	39.7	43.8	211.2	16.9	17.2	25.3	399.6	188.5	0.2	4.2	0.0	0.2	0.4	5.5	917	282
W Bhaml	BF040020AA	C	2/5/09	31.5	8.9	1576	42.3	62.6	222.8	14.5	18.9	42.1	429.2	194.2	0.0	5.3		0.3	0.7	5.1	992	366
WWD-11	YA051882AA	C	13/4/08	36.7	7.8	1733	136.0	116.0	151.0	17.8	24.9	195.9	216.0	584.3	0.0	5.3	10.6	11.7	24.7	2.3	1354	823
WWD-12	YB406944AA	C	31/3/09	37.4	8.0	2277	197.6	134.3	154.2	25.0	18.3	75.9	260.7	978.7	0.0	5.1	0.8	12.0	25.2	2.1	1824	1054
WWD-12	YB406944AA	C	13/4/08	34.2	8.0	1952	143.0	97.0	117.0	33.7	21.3	98.0	225.5	597.6	0.0	3.7	0.0	12.8	27.0	1.8	1299	762
WWD-2	XA557476BA	C	13/4/08	36.6	7.6	1564	104.0	48.0	137.0	9.4	27.7	221.6	174.0	367.0	0.0	4.2	0.0	12.1	25.4	2.8	984	460

ANNEX

A-1. Continued

Local Name	Site ID	Aquifer	Sample Date	Temp °C	pH	EC $\mu\text{S}\cdot\text{cm}^{-1}$	Ca ²⁺ mg.L ⁻¹	Mg ²⁺ mg.L ⁻¹	Na ⁺ mg.L ⁻¹	K ⁺ mg.L ⁻¹	Sr ²⁺ mg.L ⁻¹	HCO ₃ ⁻ mg.L ⁻¹	Cl ⁻ mg.L ⁻¹	SO ₄ ²⁻ mg.L ⁻¹	NO ₃ ⁻ mg.L ⁻¹	F ⁻ mg.L ⁻¹	Br ⁻ mg.L ⁻¹	Si mg.L ⁻¹	SiO ₂ mg.L ⁻¹	SAR	TDS mg.L ⁻¹	T.Hardness mg.L ⁻¹	
WWD-16	YA389227AA	C	31/3/09	38.6	7.6	2163	231.6	142.0	158.5	23.7	20.1	135.1	236.5	1046.7	0.0	6.0	7.9	14.2	29.9	2.0	1949	1170	
WWD-16	YA389227AA	C	13/4/08	37.5	8.0	1973	178.0	143.0	144.0	31.9	21.3	136.5	206.3	717.0	0.0	4.9	1.8	13.8	29.0	1.9	1528	1041	
WWD-21	YA858545AA	C	6/5/09	36.5	8.0	1585	92.4	82.7	126.6	16.0	26.4	168.6	256.8	450.9	0.0	6.2		11.8	24.8	2.3	1145	575	
WWD-21	YA858545AA	C	11/5/08	39.2	7.5	1560	149.9	106.2	184.4	31.3	38.5	116.4	220.7	417.4	0.2	5.7		11.7	24.6	2.8	1219	817	
WWD-22	BG200046AA	C	17/4/08	36.6	7.7	2050	173.0	114.0	182.0	30.8	26.3	108.7	275.9	614.6	0.2	5.5	9.9	10.1	21.2	2.6	1476	908	
WWD-25	BG00002AA	C	16/4/08	37.6	7.8	1875	146.4	106.5	172.2	26.9	24.0	124.2	252.7	544.6	0.2	5.7	0.0	8.9	18.6	2.6	1339	809	
WWD-27	BG110099AA	C	3/5/09	38.3	7.5	2159	106.0	97.0	154.0	24.7	21.5	117.2	264.0	527.0	0.0	6.8		10.5	22.0	2.6	1265	669	
WWD-27	BG110099AA	C	17/4/08	37.1	7.7	2101	164.0	108.1	205.3	30.0	22.8	116.9	293.4	601.5	0.2	5.5	8.4	9.3	19.6	3.0	1490	860	
WWD-32	CG034063BA	C	5/5/09	31.4	9.0	5100	127.0	102.0	785.0	34.1	19.1	16.8	1537.0	421.0	0.0	5.4		0.3	0.6	12.5	3048	743	
WWD-32	CG034063BA	C	21/4/08	31.0	9.8	5040	156.8	122.9	985.2	44.3	24.9	16.6	1790.9	644.1	0.2	7.5	10.0	0.2	0.5	14.2	3785	904	
WWD-34	AGR56280BA	C	17/4/08	35.3	8.6	2855	275.7	154.0	343.2	42.3	19.9	87.4	505.7	1077.0	11.0	6.4	5.0	11.6	24.3	4.1	2495	1331	
WWD-35	YB809472AA	C	17/4/08	38.5	8.2	2169	228.5	129.6	157.2	37.7	21.3	104.3	214.3	744.7	4.6	4.9	2.2	12.2	25.7	2.1	1605	1111	
WWD-36	CG085491AA	C	5/5/09	35.0	8.2	8460	181.3	170.3	1466.7	54.7	28.3	121.5	2555.9	886.6	0.0	7.4		10.7	22.5	18.7	5411	1163	
WWD-36	CG085491AA	C	21/4/08	34.1	8.6	8230	247.3	198.0	909.6	63.4	34.1	103.3	2545.3	783.1	9.0	6.0	17.6	11.0	23.2	21.9	5850	1443	
WWD-39	BG367633AA	C	21/4/09	36.6	8.0	4150	204.3	138.5	593.8	38.9	22.1	112.7	1013.0	1047.0	0.0	6.8	19.1	11.7	24.6	7.8	3128	1088	
WWD-39	BG367633AA	C	17/4/08	36.6	8.9	4070	218.3	142.2	629.8	43.0	21.6	83.0	922.4	912.8	9.2	5.4	5.0	10.5	22.1	8.1	2968	1138	
WWD-7	XA694716DA	C	1/4/09	30.7	8.5	1742	122.0	126.0	159.0	14.6	24.0	48.9	269.7	669.8	0.0	5.0	1.7	5.5	11.5	2.4	1415	830	
WWD-7	XA694716DA	C	13/4/08	32.1	8.6	1530	63.0	51.0	156.0	16.7	18.6	33.2	181.0	392.0	0.0	3.8	0.0	2.3	4.9	3.5	889	370	
WWD-8	XA612881AA	C	4/5/08	32.4	8.6	2049	94.8	19.1	410.9	62.7	12.8	14.8	513.9	318.2	0.2	1.6		0.3	0.6	10.0	1431	317	
332/014	AE989051AA	D	15/6/09	36.7	7.8	1987	99.4	81.7	232.4	23.6	8.7		518.0	305.0	0.0	7.1			25.4		1362	589	
332/014	AE989051AA	D	28/4/08	38.6	7.5	1885	95.5	69.5	228.0	41.1	55.6	102.1	415.0	239.6	0.2	5.5	0.0	14.3	30.0	4.3	1182	528	
AQSR	BE202783AA	D	10/5/08	30.8	7.9	2522	238.3	131.3	389.5	11.6	21.8	319.4	558.7	323.6	11.2	2.6		9.2	19.4	5.0	1848	1143	
DEP-10	YV322265AA	D	26/5/09	32.7	8.9	1453	14.0	38.7	193.8	6.5	4.4	97.0	318.0	42.0	0.0	4.1		0.2	0.4	6.0	676	491	
DEP-10	YV322265AA	D	13/5/08	33.8	7.7	1515	97.0	59.8	151.8	7.8	12.4	218.9	240.0	321.5	0.2	4.0	0.0	10.6	22.2	3.0	1017	491	
DEP-11A	YV356616BA	D	11/4/09	31.1	9.2	1395	25.1	60.4	201.3	65.1	6.8	63.9	239.5	325.6	0.0	4.9	1.3	0.4	0.9	4.9	981	314	
DEP-11A	YV356616BA	D	3/5/08	32.7	9.0	1384	17.4	38.4	197.4	65.0	6.3	61.5	206.2	302.7	0.2	4.0		0.3	0.5	6.0	871	203	
DEP-14A	XV876910BA	D	12/4/09	31.7	8.8	1540	35.0	81.9	204.9	16.0	12.2	89.8	251.3	394.7	0.0	4.3	1.6	0.5	1.1	4.3	1048	429	
DEP-14A	XV876910BA	D	4/5/08	32.7	8.6	1543	28.9	62.8	211.3	19.6	12.2	89.8	227.8	381.7	0.2	3.9		0.4	0.9	5.0	986	334	
DEP-3	BE162450AA	D	25/5/09	32.6	8.8	1299	17.9	30.8	225.2	16.1	4.1	51.4	368.4	17.5	0.0	7.0		0.3	0.5	7.4	739	173	
DEP-3	BE162450AA	D	15/5/08	30.6	8.2	1213	19.8	30.9	201.4	15.1	6.3	70.0	366.8	26.8	0.2	6.1	0.0	0.2	0.4	6.6	702	178	
DEP-4	YV937394AA	D	26/5/09	32.2	11.7	5610	443.0	4.3	310.0	22.1	11.9	-1179.0	530.4	102.6	0.0	0.8		2.4	5.0	4.0	1999	1125	
DEP-5	BE149620AA	D	25/5/09	30.8	9.0	1320	13.6	28.5	181.8	23.7	4.4	41.0	264.0	79.0	0.0	5.4		0.3	0.7	6.4	642	152	
DEP-5	BE149620AA	D	15/5/08	30.8	8.3	1270	24.0	47.1	183.5	16.4	7.2	74.9	321.3	128.9	0.2	4.6	0.0	0.5	1.1	5.0	768	256	
DEP-6	YV123115AA	D	3/6/09	33.3	7.4																		
DEP-6	YV123115AA	D	28/4/08	32.7	7.7	2101	119.0	63.0	269.0	11.4	31.8	195.6	479.3	240.0	0.2	3.5		10.2	21.4	4.9	1308	560	
DEP-8	XV935678AA	D	13/5/08	32.3	8.4	1042	41.0	42.6	134.8	8.4	9.5	33.8	202.5	203.7	0.2	3.0	0.0	0.3	0.6	3.5	655	280	

ANNEX

A-1. Continued

Local Name	Site ID	Aquifer	Sample Date	Temp °C	pH	EC $\mu\text{S.cm}^{-1}$	Ca ²⁺ mg.L ⁻¹	Mg ²⁺ mg.L ⁻¹	Na ⁺ mg.L ⁻¹	K ⁺ mg.L ⁻¹	Si ²⁺ mg.L ⁻¹	HCO ₃ ⁻ mg.L ⁻¹	Cl ⁻ mg.L ⁻¹	SO ₄ ²⁻ mg.L ⁻¹	NO ₃ ⁻ mg.L ⁻¹	F ⁻ mg.L ⁻¹	Br ⁻ mg.L ⁻¹	Si mg.L ⁻¹	SiO ₂ mg.L ⁻¹	SAR	TDS mg.L ⁻¹	T.Hardness mg.L ⁻¹
DEP-7	BE127955AA	D	25/5/09	28.0	9.0	2273	109.5	72.0	269.1	6.0	21.9	229.6	533.0	257.0	0.0	4.9	0.0	9.1	19.2	4.9	1388	574
DEP-7	BE127955AA	D	15/5/08	28.9	7.7	2101	126.5	67.5	293.0	11.4	31.8	195.6	479.3	240.0	0.2	3.5	0.0	10.2	21.4	5.2	1344	598
DWS-15	YU181909AA	D	23/4/09	28.1	9.2	656	22.0	24.0	82.0	4.5	2.0	55.3	152.6	99.9	0.0	1.3	0.5	0.3	0.6	2.9	414	155
DWS-15	YU181909AA	D	24/4/08	31.2	7.7	1098	105.3	45.4	82.4	4.7	5.8	189.6	107.9	268.0	4.4	1.6	0.0	8.7	18.3	1.7	736	452
HR-C(103/395)	AF828170BA	D	6/4/09	33.0	9.5	1243	19.0	23.0	226.0	20.8	3.5	18.4	279.0	211.6	0.0	5.4	0.7	0.3	0.7	8.2	819	143
HR-C(103/395)	AF828170BA	D	29/4/08	30.3	8.8	1399	29.5	37.6	234.1	19.0	19.8	65.5	284.5	233.5	0.2	6.0	0.0	3.9	8.1	6.7	894	230
HAD-49	ZV084571AA	D	6/4/09	30.5	9.0	878	12.5	22.0	127.4	19.1	5.3	55.9	186.0	81.4	0.0	7.7	0.8	0.3	0.6	5.0	500	123
HAD-49	ZV084571AA	D	21/4/08	31.5	8.4	871	19.7	25.7	126.9	20.9	8.2	70.0	193.6	104.1	0.2	6.6	0.0	0.4	0.8	4.4	535	156
LobFr	AE818982AA	D	3/6/09	31.6	7.5	1807	120.1	57.5	162.4	3.4	4.4	245.2	362.0	145.2	18.6	1.7	0.0	6.8	14.4	3.0	1009	540
Mathira 2	YV826752AA	D	26/5/09	33.0	8.1	1541	83.7	65.0	141.6	5.1	7.0	215.7	261.0	216.0	0.9	5.6	0.0	13.2	27.8	2.8	920	480
MOD-15	AE853383AA	D	15/3/10	35.2	7.7	3070	195.0	131.0	206.0	4.1			580.0	240.0	11.0	4.0					1996	1028
QISB	AE915009AA	D	2/6/09	30.0	7.4	1140	79.8	27.3	99.5	4.3	2.0	303.4	132.0	121.0	10.6	1.1	0.0	8.6	18.2	2.4	647	313
QISB	AE915009AA	D	11/5/08	29.5	7.9	1597	181.1	64.8	257.5	6.0	6.5	243.0	343.6	146.8	7.5	1.5	0.0	10.6	22.2	4.2	1156	723
RBK-D	BE094486AA	D	2/5/09	32.5	9.0	1567	15.5	20.2	274.9	18.0	3.5	64.4	421.0	29.2	0.0	5.6	0.0	0.4	0.8	10.8	838	123
Tosnat	XV849043AA	D	14/5/08	33.6	7.7	1480	95.0	65.4	114.6	15.5	15.5	230.6	183.0	389.0	0.2	4.2	0.0	8.4	17.6	2.2	1002	510
WSW-3	BE991437AA	D	5/5/09	35.0	7.5	1287	67.3	33.1	127.8	5.2	7.8	226.1	178.0	165.0	4.0	2.8	0.0	9.0	19.0	3.2	718	306
WSW-3	BE991437AA	D	20/4/08	35.9	7.7	1240	78.4	34.3	142.1	5.6	9.9	168.7	200.5	185.3	3.1	2.6	0.0	7.8	16.5	3.4	755	339
WWD-14	YB406954CA	D	31/3/09	39.5	7.5	3101	155.7	93.1	497.4	24.9	29.3	143.0	793.9	644.7	0.0	8.2	15.2	14.3	30.1	7.8	2326	777
WWD-14	YB406954CA	D	13/4/08	39.7	7.5	2854	126.0	76.0	466.0	33.0	29.6	135.4	695.0	524.0	0.0	7.2	5.5	13.9	29.3	8.1	2030	632
WWD-37	CG085490BA	D	5/5/09	31.5	9.0	15140	197.1	199.7	2219.2	54.4	35.8	-22.0	4297.0	599.0	0.0	9.3		3.4	7.1	26.5	7616	1325
WWD-37	CG085490BA	D	21/4/08	32.0	9.3	14910	323.5	254.9	3591.1	74.6	58.0	22.0	5921.1	530.8	0.2	15.0	32.7	0.5	1.1	36.1	10747	1871
WWD-6	XA694716CA	D	1/4/09	34.0	7.9	1837	141.0	111.2	183.0	6.8	29.0	216.3	300.5	510.8	0.0	5.8	2.4	9.8	20.7	2.8	1391	816
WWD-6	XA694716CA	D	13/4/08	30.9	8.0	1640	115.6	92.8	171.0	9.9	21.4	191.4	260.1	430.4	0.0	4.6	0.0	6.6	13.9	2.9	1196	675
Gogib Raunfall	AE902477AF	Rainfall	Jul-Aug2008	229	0.1	0.6	0.1	0.6	0.1	3.1	0.2	108.8	20.7	11.6	0.2	0.1	0.4	0.9	0.9	0.0	91	3

ANNEX

A-2 Results of chemical analyses and precipitation collected in 2008 and 2009 (meq.L⁻¹)

Local Name	Site ID	Aquifer	Sample Date	Temp °C	pH	EC µS cm ⁻¹	Ca ²⁺ meq.L ⁻¹	Mg ²⁺ meq.L ⁻¹	Na ⁺ meq.L ⁻¹	K ⁺ meq.L ⁻¹	Sr ²⁺ meq.L ⁻¹	HCO ₃ ⁻ meq.L ⁻¹	Cl ⁻ meq.L ⁻¹	SO ₄ ²⁻ meq.L ⁻¹	NO ₃ ⁻ meq.L ⁻¹	F ⁻ meq.L ⁻¹	Br ⁻ meq.L ⁻¹	SAR	TDS mg.L ⁻¹	T.Hardness mg.L ⁻¹
KHT-A	BG117784AA	A	3/5/09	31.3	8.44	2095	6.4	2.6	12.1	0.4	0.1	0.4	17.1	3.6	0.0	0.1	0.0	5.7	1252	452
M.Masin	YA729072AA	A	20/4/09	32.6	7.18	2460	10.8	6.8	10.5	0.1	0.2	2.9	14.9	10.8	0.3	0.1	0.0	3.5	1739	886
M.Masin	YA729072AA	A	29/4/08	32.6	7.6	2003	10.1	5.7	10.2	0.4	0.2	2.5	9.7	8.8	0.2	0.1	0.0	3.6	1415	794
Marhira I	YV826752BA	A	26/5/09	32.8	7.95	1449	1.6	2.8	8.0	0.2	0.2	0.9	9.1	3.5	0.0	0.2	0.0	5.3	785	224
NKR sp	BE105632AC	A	24/5/08	26.4	7.44	1275	6.3	2.0	3.7	0.3	0.0	4.8	6.2	1.2	1.3	0.0	0.0	1.8	771	417
O.R	ZV191273AA	A	5/4/09	32.8	7.44	2864	10.1	5.9	14.1	0.2	0.1	2.3	17.1	10.9	0.5	0.1	0.0	5.0	1870	806
SHTH sp	AE803515AC	A	7/6/09	28.7	7.8	941	4.6	2.0	4.0	0.0	0.0	0.0	5.5	1.2	0.2	0.0	0.0	605	330	330
SHTH sp	AE803515AC	A	24/5/08	26	7.92	909	4.7	1.6	3.5	0.0	0.0	3.8	4.7	1.0	0.3	0.0	0.0	1.9	580	321
TWIRISH	AF123492AA	A	5/4/09	33.2	7.06	2590	12.5	6.6	11.0	0.1	0.2	2.9	14.5	15.3	0.4	0.2	0.0	3.6	1988	960
TWIRISH	AF123492AA	A	29/4/08	32	7.58	2089	11.7	5.8	9.2	0.4	0.2	2.5	9.6	11.1	0.2	0.1	0.0	3.1	1542	879
WWD-20	YA859494BA	A	6/5/09	30.1	8.1	5400	21.7	14.2	23.4	1.2	0.2	0.1	22.8	41.8	0.0	0.5	0.0	5.5	4088	1809
WWD-20	YA859494BA	A	11/5/08	32.7	8.66	5750	30.2	20.7	35.2	2.2	0.3	0.5	27.6	69.2	0.2	0.3	0.0	7.0	6116	2559
WWD-24	BG200046CA	A	3/5/09	29	8.83	1537	2.2	2.7	9.1	0.3	0.1	0.6	9.7	4.7	0.0	0.1	0.0	5.8	885	247
WWD-24	BG200046CA	A	21/4/08	31.1	8.16	1603	3.8	3.8	9.0	0.3	0.1	0.4	9.1	5.9	0.0	0.1	0.0	4.6	964	386
WWD-26	BG409917AA	A	3/5/09	33.7	8.6	2902	13.5	5.8	11.6	0.3	0.2	0.5	15.6	17.8	0.0	0.2	0.0	3.7	2049	970
WWD-26	BG409917AA	A	21/4/08	32	6.92	2971	17.4	6.4	12.7	0.3	0.2	0.2	14.4	22.2	0.0	0.2	0.0	3.7	2320	1198
WWD-30	BG549421AA	A	3/5/09	32.9	8.62	9880	31.3	16.5	59.7	1.2	0.3	0.6	70.1	45.3	0.0	0.2	0.0	12.2	6932	2400
WWD-45	BG485361BA	A	21/4/09	32.3	8.15	2982	14.4	7.2	16.2	0.4	0.2	0.5	16.7	24.2	0.0	0.2	0.0	4.9	2537	1088
MAF-S1(001/015)	ZV193035AA	B	18/11/09	35	7.01	2420	8.8	8.5	9.0	0.5	0.0	0.0	11.5	10.8	0.0	0.0	0.0	0.0	638	317
DEP-15	YV399518AA	B	21/5/08	32.3	8.12	981	3.2	3.0	4.6	0.2	0.1	1.7	5.0	3.9	0.0	0.1	0.0	2.6	638	317
DEP-16A	XV997655BA	B	12/4/09	29.9	11.1	2126	8.4	0.5	10.9	1.4	0.4	-2.2	10.7	8.0	0.0	0.1	0.0	5.2	1339	446
DEP-16A	XV997655BA	B	4/5/08	30.4	11.3	2062	5.7	0.2	11.7	2.2	0.5	2.7	9.7	8.0	0.0	0.1	0.0	6.8	1303	298
DEP-17	YV578833AA	B	11/4/09	35.9	7.52	1467	5.4	5.1	7.0	0.1	0.4	3.7	8.3	4.6	0.0	0.1	0.0	3.1	1008	525
DEP-17	YV578833AA	B	21/5/08	32	7.8	1310	3.4	3.9	6.9	0.3	0.4	3.0	7.2	4.2	0.0	0.2	0.0	3.6	866	368
DEP-9	YV182483AA	B	12/4/09	32.1	8.92	904	0.9	2.5	5.3	0.1	0.1	0.7	5.8	1.7	0.0	0.1	0.0	4.0	506	172
DEP-9	YV182483AA	B	3/5/08	33.5	7.71	1412	3.7	4.2	7.1	0.2	0.2	2.3	7.3	4.9	0.0	0.1	0.0	3.5	869	401
WWD-13	YB406953BA	B	31/3/09	33.2	9.2	3840	26.6	15.9	7.8	1.1	0.3	0.1	5.7	44.1	0.0	0.2	0.1	1.7	3306	2136
WWD-13	YB406953BA	B	13/4/08	32.4	9.81	4340	32.8	16.0	10.0	1.2	0.3	0.5	4.8	52.3	0.1	0.1	0.0	2.0	3859	2453
WWD-17	YA389228BA	B	31/3/09	31.6	8.63	4170	26.9	16.4	14.5	1.3	0.3	0.1	6.8	53.2	0.0	0.3	0.2	3.1	3962	2182
WWD-17	YA389228BA	B	13/4/08	29.9	9.65	4120	23.0	11.2	8.5	0.9	0.2	0.5	4.9	41.3	0.1	0.2	0.0	2.0	3055	1719
WWD-19	YA859494AA	B	6/5/09	31.5	8.5	3990	23.5	16.5	4.6	0.8	0.2	1.0	4.9	41.3	0.0	0.3	0.0	1.0	3031	2017
WWD-19	YA859494AA	B	11/5/08	33.7	7.75	3880	33.0	23.7	7.7	1.6	0.4	0.5	6.3	63.6	0.0	0.2	0.0	1.4	4517	2852
WWD-5	XA694716BA	B	1/4/09	27	8.83	3479	25.0	16.3	8.6	0.7	0.4	-0.1	6.8	47.1	0.0	0.2	0.0	1.9	3455	2077
WWD-5	XA694716BA	B	13/4/08	31.5	8.59	3820	26.5	15.7	8.0	0.8	0.4	0.2	6.7	44.2	0.0	0.2	0.0	1.7	3314	2126
WWD-9	XA612881BA	B	4/5/08	31.7	8.67	2067	2.9	7.9	17.3	0.5	0.2	0.6	14.1	6.0	0.0	0.1	0.0	7.4	1386	545

ANNEX

A-2. Continued

Local Name	Site ID	Aquifer	Sample Date	Temp °C	pH	EC $\mu\text{S cm}^{-1}$	Ca ²⁺ meq.L ⁻¹	Mg ²⁺ meq.L ⁻¹	Na ⁺ meq.L ⁻¹	K ⁺ meq.L ⁻¹	Si ²⁺ meq.L ⁻¹	HCO ₃ ⁻ meq.L ⁻¹	Cl ⁻ meq.L ⁻¹	SO ₄ ²⁻ meq.L ⁻¹	NO ₃ ⁻ meq.L ⁻¹	F ⁻ meq.L ⁻¹	Br ⁻ meq.L ⁻¹	SAR	TDS mg.L ⁻¹	T.Hardness mg.L ⁻¹
001/014	ZV193035BA	C	5/4/09	36.2	7.52	2240	6.2	8.1	11.3	0.3	0.6	2.4	15.8	7.7	0.0	0.3	0.0	4.2	1528	720
001/014	ZV193035BA	C	28/4/08	36.2	7.6	2132	5.4	7.3	10.9	0.7	1.3	1.9	13.8	6.5	0.0	0.3	0.0	4.3	1368	640
001/290	AF828201AA	C	29/4/08	32.6	7.58	1696	5.2	6.0	7.2	0.6	1.1	2.2	9.9	5.9	0.0	0.3	0.0	3.0	1092	567
001/290	AF829201AA	C	6/4/09	35.5	7.4	1795	5.9	6.4	8.3	0.3	0.5	2.3	11.4	7.1	0.0	0.3	0.0	3.3	1238	620
Bashn-1	CF035107AA	C	5/5/09	32.4	9.25	1691	3.9	2.8	10.5	0.4	0.2	0.5	10.5	6.7	0.0	0.1	0.0	5.7	1084	337
Bashn-1	CF035107AA	C	21/4/08	27.2	7.8	1603	3.8	2.4	11.5	0.9	0.3	0.2	9.7	6.0	0.0	0.1	0.0	6.5	1050	312
Bin Kh	BF080077AA	C	3/5/09	34.1	7.94	1717	4.1	5.8	6.1	0.4	0.1	2.2	7.4	7.7	0.0	0.3	0.0	2.7	1045	503
Bin Kh	BF080077AA	C	16/4/08	35.1	7.8	1592	4.8	6.3	6.3	0.8	1.0	2.0	8.0	5.2	0.0	0.3	0.0	2.7	972	561
DEP -18	BF223760AA	C	17/5/08	31.1	7.39	1456	3.3	3.7	8.6	0.2	0.3	1.3	10.1	4.5	0.0	0.2	0.0	4.6	935	354
DEP-14	XV876910AA	C	4/5/08	32.3	8.34	1071	1.6	3.6	6.5	0.3	0.0	1.0	5.8	3.8	0.0	0.1	0.0	4.0	661	266
DEP-16	XV997655AA	C	12/4/09	29	8.45	1372	1.9	6.8	5.2	0.1	0.6	1.8	5.9	6.1	0.0	0.2	0.1	2.5	824	443
DEP-16	XV997655AA	C	4/5/08	29.7	8.06	1491	3.5	4.3	6.6	0.2	0.5	3.3	5.9	7.4	0.0	0.2	0.0	3.3	957	394
DEP-18	BF223760AA	C	2/5/09	32	8.6	1349	1.7	2.9	6.7	0.7	0.2	1.2	6.1	5.3	0.0	0.2	0.0	4.4	764	233
DEP-19	BF792149AA	C	3/5/09	32.5	8.95	2575	2.5	3.6	17.4	0.7	0.4	0.6	17.8	5.5	0.0	0.3	0.0	9.9	1440	308
DEP-19	BF792149AA	C	21/4/08	32.1	8.83	2844	5.2	6.7	19.2	0.8	0.5	0.4	16.7	11.7	0.0	0.3	0.0	7.9	1835	598
DEP-2	YV955966AA	C	8/4/09	31.1	8.62	2229	3.4	7.7	13.5	0.3	0.5	0.9	19.3	5.2	0.0	0.3	0.0	5.7	1573	562
DEP-2	YV955966AA	C	16/5/08	31.7	7.84	2068	4.0	6.1	11.8	0.6	0.6	0.9	15.5	5.4	0.0	0.3	0.0	5.2	1291	511
DEP-4	YV937394AA	C	16/5/08	30.9	12.55	5180	23.1	0.0	15.2	1.3	0.3	2.8	23.9	3.6	0.0	0.1	0.0	4.5	2439	1156
DEP-9A	YV182483BA	C	12/4/09	32.9	8.53	1329	2.7	7.7	6.0	0.1	0.6	1.4	6.5	7.7	0.0	0.3	0.0	2.7	954	521
DEP-9A	YV182483BA	C	3/5/08	31.3	8	1419	3.2	5.3	6.2	0.3	0.5	2.3	5.1	6.6	0.0	0.2	0.0	3.0	857	428
Gosham I	CF179989AA	C	5/5/09	32.6	8.54	3441	4.0	8.1	22.1	0.6	0.2	1.3	23.0	11.3	0.0	0.2	0.0	9.8	2111	614
Gosham I	CF179989AA	C	21/4/08	29.4	8.58	3411	7.4	9.4	27.9	0.7	0.2	0.9	27.1	14.7	0.0	0.2	0.0	9.6	2632	845
M.sp	YV439388AC	C	6/5/08	29.8	7.78	1859	6.3	3.9	10.7	0.3	0.1	2.8	10.7	5.5	0.2	0.1	0.0	4.7	1203	515
Qitbit	BG317999AA	C	3/5/09		7.7	2962	7.4	10.5	13.1	0.8	0.5	1.8	13.9	16.1	0.0	0.3	0.0	4.3	1961	904
Qitbit	BG317999AA	C	21/4/08	37.8	8.44	2851	9.1	10.9	14.5	0.9	0.6	1.6	13.7	15.3	0.0	0.3	0.1	4.6	1988	1005
Ramada-1	BF840101AA	C	5/5/09	31.8	8.82	1088	1.4	2.1	6.6	0.3	0.3	0.8	7.1	2.7	0.0	0.3	0.0	4.9	626	179
Ramada-1	BF840101AA	C	20/4/08	30.8	7.69	1065	1.5	2.0	7.0	0.3	0.4	0.5	7.0	2.9	0.0	0.2	0.0	5.2	635	178
RBK-C	BE050838AA	C	18/8/09	32.6	9.26	1879	1.8	2.3	14.0	0.4	0.2	0.4	15.2	1.3	0.0	0.2	0.0	9.7	1018	209
S.TMMI	YV347775AA	C	11/4/09	33	7.38	1814	6.6	6.1	8.8	0.0	0.4	3.7	10.0	6.5	0.0	0.2	0.0	3.5	1216	639
S.TMMI	YV347775AA	C	3/5/08	33.9	7.69	5190	13.0	14.5	46.7	0.8	0.8	2.7	42.2	15.7	0.0	0.4	0.0	12.6	3934	1382
UBAR F'm	YA819821AA	C	29/4/08	36.3	7.9	1332	2.7	3.9	5.9	0.3	0.7	2.6	5.6	4.6	0.0	0.3	0.0	3.3	782	331
W Bham I	BF040000AA	C	17/5/08	31.2	7.06	1445	2.0	3.6	9.2	0.4	0.4	0.4	11.3	3.9	0.0	0.2	0.0	5.5	917	282
W Bham I	BF040020AA	C	2/5/09	31.5	8.88	1576	2.1	5.1	9.7	0.4	0.4	0.7	12.1	4.0	0.0	0.3	0.0	5.1	992	366
WWD-11	YA051882AA	C	13/4/08	36.7	7.83	1733	6.8	9.5	6.6	0.5	0.6	3.2	6.1	12.2	0.0	0.3	0.1	2.3	1354	823

ANNEX

A-2. Continued

Local Name	Site ID	Aquifer	Sample Date	Temp °C	pH	EC $\mu\text{S cm}^{-1}$	Ca ²⁺ meq.L ⁻¹	Mg ²⁺ meq.L ⁻¹	Na ⁺ meq.L ⁻¹	K ⁺ meq.L ⁻¹	Si ²⁺ meq.L ⁻¹	HCO ₃ ⁻ meq.L ⁻¹	Cl ⁻ meq.L ⁻¹	SO ₄ ²⁻ meq.L ⁻¹	NO ₃ ⁻ meq.L ⁻¹	F ⁻ meq.L ⁻¹	Br ⁻ meq.L ⁻¹	SAR	TDS mg.L ⁻¹	T.Hardness mg.L ⁻¹
WWD-12	YB406944AA	C	31/3/09	37.4	8	2277	9.9	11.1	6.7	0.6	0.4	1.2	7.4	20.4	0.0	0.3	0.0	2.1	1824	1054
WWD-12	YB406944AA	C	13/4/08	34.2	8.03	1952	7.1	8.0	5.1	0.9	0.5	1.6	6.4	12.4	0.0	0.2	0.0	1.8	1299	762
WWD-16	YA389227AA	C	31/3/09	38.6	7.61	2163	11.6	11.7	6.9	0.6	0.5	2.2	6.7	21.8	0.0	0.3	0.1	2.0	1949	1170
WWD-16	YA389227AA	C	13/4/08	37.5	8.03	1973	8.9	11.8	6.3	0.8	0.5	2.2	5.8	14.9	0.0	0.3	0.0	1.9	1528	1041
WWD-2	XA557476BA	C	13/4/08	36.6	7.61	1564	5.2	3.9	6.0	0.2	0.6	3.6	4.9	7.6	0.0	0.2	0.0	2.8	984	460
WWD-21	YA858545AA	C	6/5/09	36.5	8	1585	4.6	6.8	5.5	0.4	0.6	2.8	7.2	9.4	0.0	0.3	0.0	2.3	1145	575
WWD-21	YA858545AA	C	11/5/08	39.2	7.51	1560	7.5	8.7	8.0	0.8	0.9	1.9	6.2	8.7	0.0	0.3	0.0	2.8	1219	817
WWD-22	BG200046AA	C	17/4/08	36.6	7.71	2050	8.6	9.4	7.9	0.8	0.6	1.8	7.8	12.8	0.0	0.3	0.1	2.6	1476	908
WWD-25	BG000002AA	C	16/4/08	37.6	7.81	1875	7.3	8.8	7.5	0.7	0.5	2.0	7.1	11.3	0.0	0.3	0.0	2.6	1339	809
WWD-27	BG110099AA	C	3/5/09	38.3	7.51	2159	5.3	8.0	6.7	0.6	0.5	1.9	7.4	11.0	0.0	0.4	0.0	2.6	1265	669
WWD-27	BG110099AA	C	17/4/08	37.1	7.67	2101	8.2	8.9	8.9	0.8	0.5	1.9	8.3	12.5	0.0	0.3	0.1	3.0	1490	860
WWD-32	CG034063BA	C	5/5/09	31.4	8.95	5100	6.3	8.4	34.1	0.9	0.4	0.3	43.4	8.8	0.0	0.3	0.0	12.5	3048	743
WWD-32	CG034063BA	C	21/4/08	31	9.76	5040	7.8	10.1	42.9	1.1	0.6	0.3	50.5	13.4	0.0	0.4	0.1	14.2	3785	904
WWD-34	AG856280BA	C	17/4/08	35.3	8.57	2855	13.8	12.7	14.9	1.1	0.5	1.4	14.3	22.4	0.2	0.3	0.1	4.1	2495	1331
WWD-35	YB809472AA	C	17/4/08	38.5	8.2	2169	11.4	10.7	6.8	1.0	0.5	1.7	6.0	15.5	0.1	0.3	0.0	2.1	1605	1111
WWD-36	CG085491AA	C	5/5/09	35	8.16	8460	9.0	14.0	63.8	1.4	0.6	2.0	72.1	18.5	0.0	0.4	0.0	18.7	5411	1163
WWD-36	CG085491AA	C	21/4/08	34.1	8.59	8230	12.3	16.3	83.1	1.6	0.8	1.7	71.8	16.3	0.1	0.3	0.2	21.9	5850	1443
WWD-39	BG367633AA	C	21/4/09	36.6	8.02	4150	10.2	11.4	25.8	1.0	0.5	1.8	28.6	21.8	0.0	0.4	0.2	7.8	3128	1088
WWD-39	BG367633AA	C	17/4/08	36.6	8.85	4070	10.9	11.7	27.4	1.1	0.5	1.4	26.0	19.0	0.1	0.3	0.1	8.1	2968	1138
WWD-7	XA694716DA	C	1/4/09	30.7	8.5	1742	6.1	10.4	6.9	0.4	0.5	0.8	7.6	13.9	0.0	0.3	0.0	2.4	1415	830
WWD-7	XA694716DA	C	13/4/08	32.1	8.64	1530	3.1	4.2	6.8	0.4	0.4	0.5	5.1	8.2	0.0	0.2	0.0	3.5	889	370
WWD-8	XA612881AA	C	4/5/08	32.4	8.56	2049	4.7	1.6	17.9	1.6	0.3	0.2	14.5	6.6	0.0	0.1	0.0	10.0	1431	317
332/014	AE989051AA	D	15/6/09	36.7	7.75	1987	5.0	6.7	10.1	0.6	0.2	0.0	14.6	6.4	0.0	0.4	0.0		1362	589
332/014	AE989051AA	D	28/4/08	38.6	7.47	1885	4.8	5.7	9.9	1.1	1.3	1.7	11.7	5.0	0.0	0.3	0.0	4.3	1182	528
AQSR	BE202783AA	D	10/5/08	30.8	7.86	2522	11.9	10.8	16.9	0.3	0.5	5.2	15.8	6.7	0.2	0.1	0.0	5.0	1848	1143
DEP-6	YV123115AA	D	28/4/08	32.7	7.69	2101	5.9	5.2	11.7	0.3	0.7	3.2	13.5	5.0	0.0	0.2	0.0	4.9	1308	560
DEP-10	YV322265AA	D	26/5/09	32.7	8.91	1453	0.7	3.2	8.4	0.2	0.1	1.6	9.0	0.9	0.0	0.2	0.0	6.0	676	491
DEP-10	YV322265AA	D	13/5/08	33.8	7.73	1515	4.8	4.9	6.6	0.2	0.3	3.6	6.8	6.7	0.0	0.2	0.0	3.0	1017	491
DEP-11A	YV356616BA	D	11/4/09	31.1	9.2	1395	1.3	5.0	8.8	1.7	0.2	1.0	6.8	6.8	0.0	0.3	0.0	4.9	981	314
DEP-11A	YV356616BA	D	3/5/08	32.7	9	1384	0.9	3.2	8.6	1.7	0.1	1.0	5.8	6.3	0.0	0.2	0.0	6.0	871	203
DEP-14A	XV876910BA	D	12/4/09	31.7	8.8	1540	1.7	6.7	8.9	0.4	0.3	1.3	7.1	8.2	0.0	0.2	0.0	4.3	1048	429
DEP-14A	XV876910BA	D	4/5/08	32.7	8.6	1543	1.4	5.2	9.2	0.5	0.3	1.5	6.4	7.9	0.0	0.2	0.0	5.0	986	334
DEP-3	BE162450AA	D	25/5/09	32.6	8.82	1299	0.9	2.5	9.8	0.4	0.1	0.8	10.4	0.4	0.0	0.4	0.0	7.4	739	173
DEP-3	BE162450AA	D	15/5/08	30.6	8.24	1213	1.0	2.5	8.8	0.4	0.1	1.1	10.3	0.6	0.0	0.3	0.0	6.6	702	178

ANNEX

A-2. Continued

Local Name	Site ID	Aquifer	Sample Date	Temp °C	pH	EC $\mu\text{S cm}^{-1}$	Ca ²⁺ meq.L ⁻¹	Mg ²⁺ meq.L ⁻¹	Na ⁺ meq.L ⁻¹	K ⁺ meq.L ⁻¹	Si ²⁺ meq.L ⁻¹	HCO ₃ ⁻ meq.L ⁻¹	Cl ⁻ meq.L ⁻¹	SO ₄ ²⁻ meq.L ⁻¹	NO ₃ ⁻ meq.L ⁻¹	F ⁻ meq.L ⁻¹	Br ⁻ meq.L ⁻¹	SAR	TDS mg.L ⁻¹	T.Hardness mg.L ⁻¹
DEP-4	YV937394AA	D	26/5/09	32.2	11.7	5610	22.1	0.4	13.5	0.6	0.3	-19.3	15.0	2.1	0.0	0.0	0.0	4.0	1999	1125
DEP-5	BE149620AA	D	25/5/09	30.8	9.02	1320	0.7	2.3	7.9	0.6	0.1	0.7	7.4	1.6	0.0	0.3	0.0	6.4	642	152
DEP-5	BE149620AA	D	15/5/08	30.8	8.29	1270	1.2	3.9	8.0	0.4	0.2	1.2	9.1	2.7	0.0	0.2	0.0	5.0	768	256
DEP-6	YV123115AA	D	3/6/09	33.3	7.41		0.0	0.0	0.0	0.0	0.0	0.0	0.0	0.0	0.0	0.0	0.0			
DEP-7	BE127955AA	D	25/5/09	28	9	2273	5.5	5.9	11.7	0.2	0.5	3.8	15.0	5.4	0.0	0.3	0.0	4.9	1388	574
DEP-7	BE127955AA	D	15/5/08	28.9	7.69	2101	6.3	5.6	12.7	0.3	0.7	3.2	13.5	5.0	0.0	0.2	0.0	5.2	1344	598
DEP-8	XV935678AA	D	13/5/08	32.3	8.35	1042	2.0	3.5	5.9	0.2	0.2	0.6	5.7	4.2	0.0	0.2	0.0	3.5	655	280
DWS-15	YU181909AA	D	23/4/09	28.1	9.2	656	1.1	2.0	3.6	0.1	0.0	0.9	4.3	2.1	0.0	0.1	0.0	2.9	414	155
DWS-15	YU181909AA	D	24/4/08	31.2	7.65	1098	5.3	3.7	3.6	0.1	0.1	3.1	3.0	5.6	0.1	0.1	0.0	1.7	736	452
H.R.C(103/395)	AF828170BA	D	6/4/09	33	9.5	1243	0.9	1.9	9.8	0.5	0.1	0.3	7.9	4.4	0.0	0.3	0.0	8.2	819	143
H.R.C(103/395)	AF828170BA	D	29/4/08	30.3	8.83	1399	1.5	3.1	10.2	0.5	0.5	1.1	8.0	4.9	0.0	0.3	0.0	6.7	894	230
HAD-49	ZV084571AA	D	6/4/09	30.5	8.96	878	0.6	1.8	5.5	0.5	0.1	0.9	5.2	1.7	0.0	0.4	0.0	5.0	500	123
HAD-49	ZV084571AA	D	21/4/08	31.5	8.42	871	1.0	2.1	5.5	0.5	0.2	1.1	5.5	2.2	0.0	0.3	0.0	4.4	535	156
LobFr	AE818982AA	D	3/6/09	31.6	7.5	1807	6.0	4.7	7.1	0.1	0.1	4.0	10.2	3.0	0.3	0.1	0.0	3.0	1009	540
Mathira 2	YV826752AA	D	26/5/09	33	8.1	1541	4.2	5.3	6.2	0.1	0.2	3.5	7.4	4.5	0.0	0.3	0.0	2.8	920	480
MOD-15	AE853383AA	D	15/3/10	35.2	7.65	3070	9.7	10.8	9.0	0.1	0.0	0.0	16.4	5.0	0.2	0.2	0.0		1996	1028
QISB	AE915009AA	D	2/6/09	30	7.4	1140	4.0	2.2	4.3	0.1	0.0	5.0	3.7	2.5	0.2	0.1	0.0	2.4	647	313
QISB	AE915009AA	D	11/5/08	29.5	7.88	1597	9.0	5.3	11.2	0.2	0.1	4.0	9.7	3.1	0.1	0.1	0.0	4.2	1156	723
RBK-D	BE094486AA	D	2/5/09	32.5	8.98	1567	0.8	1.7	12.0	0.5	0.1	1.1	11.9	0.6	0.0	0.3	0.0	10.8	838	123
Tosnat	XV849043AA	D	14/5/08	33.6	7.71	1480	4.7	5.4	5.0	0.4	0.4	3.8	5.2	8.1	0.0	0.2	0.0	2.2	1002	510
WSW-3	BE991437AA	D	5/5/09	35	7.47	1287	3.4	2.7	5.6	0.1	0.2	3.7	5.0	3.4	0.1	0.1	0.0	3.2	718	306
WSW-3	BE991437AA	D	20/4/08	35.9	7.72	1240	3.9	2.8	6.2	0.1	0.2	2.8	5.7	3.9	0.1	0.1	0.0	3.4	755	339
WWD-14	YB406954CA	D	31/3/09	39.5	7.54	3101	7.8	7.7	21.6	0.6	0.7	2.3	22.4	13.4	0.0	0.4	0.2	7.8	2326	777
WWD-14	YB406954CA	D	13/4/08	39.7	7.53	2854	6.3	6.3	20.3	0.8	0.7	2.2	19.6	10.9	0.0	0.4	0.1	8.1	2030	632
WWD-37	CG085490BA	D	5/5/09	31.5	8.96	15140	9.8	16.4	96.5	1.4	0.8	-0.4	121.2	12.5	0.0	0.5	0.0	26.5	7616	1325
WWD-37	CG085490BA	D	21/4/08	32	9.3	14910	16.1	21.0	156.2	1.9	1.3	0.4	167.0	11.1	0.0	0.8	0.4	36.1	10747	1871
WWD-6	XA694716CA	D	1/4/09	34	7.88	1837	7.0	9.1	8.0	0.2	0.7	3.5	8.5	10.6	0.0	0.3	0.0	2.8	1391	816
WWD-6	XA694716CA	D	13/4/08	30.9	8.01	1640	5.8	7.6	7.4	0.3	0.5	3.1	7.3	9.0	0.0	0.2	0.0	2.9	1196	675
Gogtib Rainfall	AE902477AF	Rainfall	Jul-Aug2008			229	0.0	0.1	0.0	0.1	0.0	1.8	0.6	0.2	0.0	0.0	0.0	0.0	9.1	3

ANNEX

A-3 Stable isotopes and tritium for groundwater and precipitation analyses collected during 2008 and 2009

All [‰] are related to VSMOW [H₂O], CDT [S] and VPDB [C].

Sample Local Name	Aquifer	Sampling Date	$\delta^{18}\text{O}$ [‰]	$\delta^2\text{H}$ [‰]	$\delta^{34}\text{S}_{\text{sulphate}}$ [‰]	$\delta^{18}\text{O}_{\text{sulphate}}$ [‰]	^3H [TU]	$\pm 2\sigma$ [TU]	$\delta^{13}\text{C}_{\text{DIC}}$ [‰]	$\delta^{13}\text{C}_{\text{Lithology}}$ [‰]
KhT-A	A	3/5/09	-4.42	-29.2	31.9	15.5	0.3	0.3	-6.3	
M.Masin	A	29/4/08	-4.97	-33.1	14.0	12.2	0.6	0.2	-8.5	
M.Masin	A	20/4/09	-4.89	-32.6	13.1	13.5	0.3	0.3	-8.2	
M.Masin	A	18/11/09	-4.80	-32.8						
Mathira 1	A	26/5/09	-6.22	-38.7	13.1	12.8	0.8	0.5	-11.1	
NKR Sp	A	14/1/09			14.8	6.8			-10.9	
NKR Sp	A	24/5/08	-0.94	-3.3	14.9	7.3			-10.2	
NKR Sp	A	8/11/08	-0.73	-2.1						
O.R	A	16/11/09	-5.42	-35.4	15.9				-10.4	
O.R	A	5/4/09	-5.08	-34.3	15.5	11.0	0.3	0.3	-8.4	
SHTH Sp	A	14/1/09			16.6	1.4			-10.7	
SHTH Sp	A	24/5/08	0.38	6.4	16.7	8.5	1.2	0.3	-8.6	
SHTH Sp	A	7/6/09	0.76	8.6			0.6	0.5	-7.7	
TWIRISH	A	14/1/09			15.0	12.6			-9.9	
TWIRISH	A	29/4/08	-4.60	-29.7	15.1	12.3	0.3	0.3	-8.5	
TWIRISH	A	5/4/09	-4.52	-29.6			0.3	0.3	-7.3	
TWIRISH	A	13/11/09	-4.52	-30.7						
WWD-20	A	11/5/08	-6.27	-39.9	19.0	12.6			-8.3	
WWD-20	A	6/5/09	-6.54	-40.7	18.7	13.8	0.3	0.3	-7.7	-3.4
WWD-24	A	3/5/09	-4.60	-29.9	41.3	14.9	0.3	0.3	-9.9	
WWD-24	A	21/4/08	-4.65	-30.5	30.3	14.2	0.3	0.3	-9.8	
WWD-24	A	14/11/09	-4.69	-31.0	15.1				-9.4	-7.1
WWD-26	A	21/4/08	-5.53	-37.9	22.1	15.4			-18.4	
WWD-26	A	3/5/09	-5.63	-37.4	25.1	13.7	0.3	0.3	-7.1	
WWD-30	A	3/5/09	-6.04	-43.8	20.9	13.1	0.3	0.3	-7.4	
WWD-45	A	14/11/09	-4.98	-36.0	17.0				-9.8	
WWD-45	A	21/4/09	-4.58	-32.3	20.7	13.9	0.3	0.3	-8.0	
001/015 = MAF-S1	B	18/11/09	-4.65	-30.0	22.2				-9.7	
DEP-15	B	21/5/08	-4.51	-28.6	9.5	12.5			-9.1	
DEP-16A	B	12/4/09	-3.44	-22.4	13.7	14.7	0.3	0.3	-12.1	
DEP-16A	B	20/11/09	-3.66	-24.0	13.0				-9.9	
DEP-16A	B	4/5/08	-3.71	-24.5	12.8	14.3			-6.7	
DEP-17	B	11/4/09	-4.59	-30.1	10.8	12.5	0.3	0.3	-8.5	
DEP-17	B	21/5/08	-4.49	-28.8	14.9	13.1			-5.9	
DEP-17	B	21/11/09	-3.72	-24.3						
DEP-9	B	12/4/09	-4.54	-28.8	41.7	14.9	1.2	0.5	-10.4	
DEP-9	B	3/5/08	-4.41	-29.1	11.0	12.5	1.2	0.3	-10.3	
DEP-9	B	21/11/09	-4.14	-27.7	6.0				-3.4	
WWD-13	B	14/4/08	-5.70	-40.0	22.0	13.1	0.3	0.3	-6.3	
WWD-13	B	31/3/09	-5.69	-39.6	21.2	13.4	0.3	0.3	-4.5	
WWD-13	B	19/11/09	-5.64	-39.3						-3.0
WWD-17	B	14/4/08	-5.42	-36.6	23.1	12.5			-9.2	
WWD-17	B	31/3/09	-5.72	-37.8	18.8	12.0			-5.6	
WWD-17	B	19/11/09	-5.83	-38.5						
WWD-19	B	11/5/08	-5.65	-39.1	18.9	12.9			-10.7	
WWD-19	B	3/5/09	-5.61	-38.8	18.5	13.7	0.3	0.3	-7.1	
WWD-5	B	13/4/08	-4.98	-33.5	19.4	14.0	0.3	0.3	-8.3	
WWD-5	B	1/4/09	-4.97	-33.6	18.6	13.8			-6.6	
WWD-9	B	4/5/08	-4.31	-29.9	25.5	14.9			-6.6	
001/014	C	14/1/09			21.1	14.4			-5.8	
001/014	C	28/4/08	-4.62	-29.7	22.0	12.1			-4.3	
001/014	C	5/4/09	-4.64	-29.8			0.3	0.3		
001/014	C	17/11/09	-4.67	-30.0						
001/290	C	14/1/09			22.1	14.5			-6.9	
001/290	C	29/4/08	-4.83	-31.6	22.3	12.7			-3.2	
001/290	C	6/4/09	-4.91	-31.5			0.3	0.3	-1.4	
001/290	C	18/11/09	-4.89	-31.6						
Bashn-1	C	21/4/08	-5.59	-39.7	32.0	15.0			-6.8	
Bashn-1	C	14/1/09			33.0	13.4			-10.6 ± 1,8	

ANNEX

A-3 Continued

Sample Local Name	Aquifer	Sampling Date	$\delta^{18}\text{O}$ [‰]	$\delta^2\text{H}$ [‰]	$\delta^{34}\text{S}_{\text{sulphate}}$ [‰]	$\delta^{18}\text{O}_{\text{sulphate}}$ [‰]	^3H [TU]	$\pm 2\sigma$ [TU]	$\delta^{13}\text{C}_{\text{DIC}}$ [‰]	$\delta^{13}\text{C}_{\text{Lithology}}$ [‰]
Bashn-1	C	5/5/09	-5.70	-39.3						
Bin Kh	C	14/1/09			22.3	13.5			-6.4	
Bin Kh	C	16/4/08	-5.67	-38.4	23.0	13.6			-3.2	
Bin Kh	C	3/5/09	-5.65	-37.9						
DEP-14	C	4/5/08	-4.50	-30.4	21.2	13.4			-7.6	
DEP-16	C	20/11/09	-3.67	-22.0	14.8				-4.2	
DEP-16	C	12/4/09	-3.65	-22.3	19.5	15.0	0.3	0.3	-3.9	
DEP-16	C	4/5/08	-3.71	-22.1	15.5	13.1			-2.5	
DEP-18	C	2/5/09	-4.57	-28.0	25.6	15.7			-8.4	
DEP-18	C	17/5/08	-4.74	-28.8	16.4	12.8			-5.5	
DEP-19	C	21/4/08	-5.96	-41.2	27.6	13.7			-5.7	
DEP-19	C	3/5/09	-5.84	-40.8	43.6	13.5			-4.8	
DEP-19	C	15/11/09	-6.08	-41.2	42.2				no CO2	
DEP-2	C	16/5/08	-4.12	-26.4	30.0	16.0			-6.1	
DEP-2	C	8/4/09	-4.23	-27.2	27.5	15.0			-4.9	
DEP-9A	C	21/11/09	-4.03	-25.7	12.8				-10.2	
DEP-9A	C	12/4/09	-3.72	-23.2	18.5	15.8	0.3	0.3	-4.0	
DEP-9A	C	3/5/08	-3.73	-23.7	13.5	14.3			-2.8	
Gosham1	C	21/4/08	-5.47	-35.9	33.5	14.3			-7.9	
Gosham1	C	5/5/09	-5.45	-36.2	36.6	15.5			-3.0	
M.Sp	C	14/1/09			15.9	9.9			-11.4	
M.Sp	C	6/5/08	-5.38	-33.9	15.8	10.5			-10.3	
M.Sp	C	5/11/08	-5.34	-34.3						
Qitbit	C	3/5/09	-6.45	-44.8	22.8	11.6			-7.1	
Qitbit	C	21/4/08	-6.44	-45.0	23.0	12.4			-4.6	
Ranada-1	C	5/5/09	-5.49	-35.4	55.7	17.3			-7.9	
Ranada-1	C	20/4/08	-5.34	-34.7	53.6	15.4			-6.6	
RBK - C	C	19/8/09	-4.92	-32.0	44.1				-13.1	
S.TMMI	C	11/4/09	-4.39	-29.3	12.7	12.9			-5.3	
S.TMMI	C	3/5/08	-4.50	-29.2	13.1	12.2			-5.2	
Ubar Fm	C	29/4/08	-4.81	-30.7	14.8	13.2			-3.2	
W Bharna1	C	2/5/09	-4.26	-27.9	47.6	16.5			-8.7	
W Bharna1	C	17/5/08	-4.67	-29.1	44.2	14.1			-5.8	
WWD-11	C	14/4/08	-4.82	-32.9	15.1	13.7			-5.0	
WWD-12	C	31/3/09	-5.31	-36.9	20.9	14.0	0.3	0.3	-5.6	3.5
WWD-12	C	14/4/08	-5.27	-36.9	20.5	13.4	0.3	0.3	-5.2	
WWD-16	C	14/4/08	-4.87	-33.8	19.2	13.2			-6.3	
WWD-16	C	31/3/09	-4.87	-33.7	19.6	14.8			-3.0	
WWD-16	C	19/11/09	-4.86	-34.1						
WWD-2	C	13/4/08	-4.40	-28.0	13.9	13.4			-4.4	
WWD-21	C	6/5/09	-5.17	-35.5	19.3	13.9			-3.7	
WWD-21	C	11/5/08	-5.20	-34.8	19.1	12.8			-3.2	
WWD-22	C	17/4/08	-6.02	-40.5	22.1	12.9	0.3	0.3	-5.6	
WWD-25	C	16/4/08	-5.99	-41.5	21.0	13.6			-5.6	-5.5
WWD-27	C	17/4/08	-6.20	-42.9	22.2	12.9			-6.6	
WWD-27	C	3/5/09	-6.17	-43.1	21.2	13.8	0.3	0.3	-2.7	
WWD-27	C	14/11/09	-6.18	-42.8						
WWD-32	C	21/4/08	-5.70	-40.3	35.8	13.8			-6.2	
WWD-32	C	5/5/09	-6.52	-46.7	41.0	14.2	0.3	0.3	-5.5	
WWD-34	C	17/4/08	-5.98	-42.0	22.3	14.6			-4.3	
WWD-35	C	17/4/08	-5.16	-35.7	19.7	13.3			-5.6	
WWD-36	C	5/5/09	-6.21	-47.6	27.2	13.5	0.3	0.3	-5.0	2.1
WWD-36	C	21/4/08	-6.28	-47.3	27.2	14.2			-4.7	
WWD-36	C	15/11/09	-6.18	-46.6						
WWD-39	C	17/4/08	-6.32	-45.5	24.1	13.2			-6.2	
WWD-39	C	21/4/09	-6.18	-45.1	23.4	13.8	0.3	0.3	-4.9	
WWD-7	C	14/4/08	-5.02	-33.9	19.9	12.0			-7.8	
WWD-7	C	1/4/09	-5.04	-33.9	17.8	13.6			-5.5	
WWD-8	C	4/5/08	-4.07	-28.4	15.6	13.7			-7.3	

ANNEX

A-3 Continued

Sample Local Name	Aquifer	Sampling Date	$\delta^{18}\text{O}$ [‰]	$\delta^2\text{H}$ [‰]	$\delta^{34}\text{S}_{\text{sulphate}}$ [‰]	$\delta^{18}\text{O}_{\text{sulphate}}$ [‰]	^3H [TU]	$\pm 2\sigma$ [TU]	$\delta^{13}\text{C}_{\text{DIC}}$ [‰]	$\delta^{13}\text{C}_{\text{Lithology}}$ [‰]
332/014	D	14/1/09			26.8	16.2			-7.1	
332/014	D	28/4/08	-2.62	-14.6	27.5	11.6			-3.3	
332/014	D	15/6/09	-2.68	-14.4			0.3	0.3	-1.5	
332/014	D	16/11/09	-2.63	-14.5						
AQSR	D	10/5/08	-3.86	-24.2	4.0	13.6			-4.2	
DEP-10	D	26/5/09	-5.11	-35.9	11.2	15.0	0.3	0.3	-8.3	
DEP-10	D	13/5/08	-5.25	-36.6	11.2	12.2			-4.9	
DEP-11A	D	3/5/08	-3.83	-24.5	9.6	13.8			-5.8	
DEP-11A	D	11/4/09	-3.88	-24.4	14.2	14.4			-4.1	
DEP-14A	D	12/4/09	-4.67	-32.6	23.8	15.7	0.3	0.3	-4.7	
DEP-14A	D	4/5/08	-4.75	-33.2	19.6	13.6			-3.7	
DEP-3	D	15/5/08	-3.71	-20.8	86.1	15.3			-5.5	
DEP-3	D	25/5/09	-3.77	-21.1	101.1	15.8	0.3	0.3	-4.3	
DEP-4	D	16/5/08	-4.43	-29.1	17.4	15.0			-19.0	
DEP-4	D	26/5/09	-4.43	-29.7	17.4	15.1	0.3	0.3	-10.9	
DEP-5	D	15/5/08	-4.99	-29.8	36.6	15.5			-4.9	
DEP-5	D	2/5/09	-5.04	-29.7	47.8	15.2	0.3	0.3	-1.8	
DEP-6	D	28/4/08	-1.57	-6.3	14.7	13.2	0.3	0.3	-2.0	
DEP-6	D	3/6/09	-1.55	-5.5	15.2	12.6	0.3	0.3	-1.6	
DEP-6	D	17/11/09	-1.62	-5.9						2.7
DEP-7	D	25/5/09	-4.75	-27.9	78.7	15.6	0.3	0.3	-4.7	
DEP-7	D	15/5/08	-4.79	-28.1	43.7	15.5			-4.1	
DEP-8	D	13/5/08	-3.76	-22.9	25.0	13.2			-7.6	
DWS-15	D	23/4/09	-4.49	-28.0	51.6	15.1	1.2	0.5	-8.3	
DWS-15	D	24/4/08	-4.49	-27.7	14.8	12.5	1.3	0.3	-7.9	
H.R.C(103/395)	D	14/1/09			43.1	13.6			-8.6	
H.R.C(103/395)	D	13/11/09	-5.70	-38.6	52.2				-8.2	
H.R.C(103/395)	D	29/4/08	-5.60	-38.2	39.3	9.8			-5.7	
H.R.C(103/395)	D	6/4/09	-5.52	-37.5			0.3	0.3		
HAD-49	D	6/4/09	-6.08	-41.4	60.0	15.9	0.3	0.3	-8.3	
HAD-49	D	16/11/09	-6.17	-41.9	69.5				-5.6	
HAD-49	D	21/5/08	-6.13	-42.4	44.6	14.0			-4.3	
LobFr	D	3/6/09	-1.19	-3.5	13.5	8.8	0.3	0.3	-3.7	
LobFr	D	17/11/09	-1.28	-4.5						
Mathira 2	D	26/5/09	-4.68	-27.0	16.3	8.9	0.3	0.3	-4.1	
MOD-15	D	29/1/10	-3.05	-17.2	16.6	13.0			-3.4	
QISB	D	14/1/09			15.3	9.5			-7.5	
QISB	D	2/6/09	-0.08	4.4			0.3	0.3	-6.7	
QISB	D	11/5/08	-0.06	5.1	15.3	8.7			-5.1	
QISB	D	17/11/09	-0.10	3.4						
RBK-D	D	2/5/09	-3.41	-21.9	78.3	13.8	0.3	0.3	-4.8	
TOSNAT	D	14/1/09			9.5	13.2			-4.1	
TOSNAT	D	14/5/08	-3.75	-22.6	11.0	13.4			-3.2	
TOSNAT	D	6/11/08	-3.85	-23.3						
WSW-3	D	20/4/08	-6.15	-41.3	12.0	11.4			-5.9	
WSW-3	D	5/5/09	-6.11	-41.2	11.7	9.0	0.3	0.3	-5.7	
WSW-3	D	20/4/08					0.3	0.3		
WWD-14	D	31/3/09	-5.13	-36.5	21.2	13.6	0.3	0.3	-7.3	
WWD-14	D	14/4/08	-5.13	-36.9	21.0	14.3	0.3	0.3	-6.2	
WWD-14	D	19/11/09	-5.07	-36.4						2.9
WWD-37	D	21/4/08	-5.93	-47.0	39.0	14.2	0.3	0.3	-5.8	
WWD-37	D	5/5/09	-5.91	-47.1	37.1	16.0	0.3	0.3	-4.7	
WWD-37	D	15/11/09	-5.86	-46.5						2.1
WWD-6	D	1/4/09	-5.13	-34.9	15.8	14.3			-3.0	
WWD-6	D	13/4/08	-5.13	-35.0	14.8	13.4	0.3	0.3	-2.6	
Gogib Rainfall	Rainfall	July-Aug 2008	0.01	5.5					-15.5	

A-4 Results of trace elements and precipitation collected in 2008

Local Name	Site ID	Sample Date	Aquifer	Fe mg.L ⁻¹	As mg.L ⁻¹	B mg.L ⁻¹	Cu mg.L ⁻¹	Cr mg.L ⁻¹	Ni mg.L ⁻¹	Cd mg.L ⁻¹	Pb mg.L ⁻¹	Al mg.L ⁻¹	Mn mg.L ⁻¹	Zn mg.L ⁻¹	PO4 mg.L ⁻¹	P mg.L ⁻¹	V mg.L ⁻¹	Co mg.L ⁻¹	Mo mg.L ⁻¹
M-MASIN	YA729072AA	29/4/08	A	0.512	0.00168	0.2011	0.0193	0.00793	0.00722	<0.00005	<0.00001	0.4266	<0.02	<0.04	0.12	<0.1	23	<0.001	0.015
NKR-SP	BE105632AC	24/5/08	A	<0.03	<0.0003	0.1472	0.0187	0.00225	0.0049	<0.00005	0.00046	<0.03	<0.02	<0.04	<0.05	<0.1	6.11	<0.001	0.001
SHTH-SP	AE803515AC	24/5/08	A	0.1222	0.00182	0.2097	0.00553	0.00373	0.00196	0.00027	0.00444	<0.03	<0.02	0.1463	<0.05	<0.1	7.44	<0.001	<0.001
TWIRISH	AF123492AA	29/4/08	A	5.99	0.00213	12.89	0.00115	0.00508	0.0102	0.00018	<0.00001	0.1149	0.042	0.0503	<0.05	<0.1	25	0.002	0.016
WWD-20	YA859494BA	11/5/08	A	3.329	0.00831	0.0497	0.0157	0.00372	0.00649	0.00015	0.0101	<0.03	0.0631	<0.04	0.24	3.12	0.003	0.011	
WWD-24	BG200046CA	21/4/08	A	0.4518	0.00061	0.1058	0.0039	0.00211	0.00526	0.00021	0.00534	0.354	0.0859	<0.04	<0.05	2.64	0.002	0.02	
WWD-26	BG409917AA	21/4/08	A	0.0614	<0.0003	0.0915	0.00097	0.00123	0.00274	0.00007	<0.00001	<0.03	0.2661	<0.04	<0.05	1	<0.001	0.001	
DEP-15	YV399518AA	21/5/08	B	<0.03	<0.0003	0.1171	0.0017	0.00661	0.00259	0.00005	<0.00001	<0.03	0.0246	<0.04	<0.05	<0.1	2.71	0.001	0.005
DEP-17	YV578833AA	21/5/08	B	0.1217	<0.0003	0.0956	0.017	0.0109	0.0169	0.00006	0.0127	0.1173	<0.02	<0.04	0.38	<0.1	1.99	<0.001	0.007
DEP-16A	XV997655BA	4/5/08	B	0.997	<0.0003	0.1289	0.00353	0.00476	0.0124	0.0001	0.00445	0.0512	0.1691	<0.04	<0.05	<0.1	0.83	0.001	0.006
DEP-9	YV182483AA	3/5/08	B	1.82	0.00227	0.819	0.0131	0.00188	0.00568	0.0002	<0.00001	0.2093	0.0756	<0.04	<0.05	0.2746		0.003	0.003
WWD-05	XA694716BA	13/4/08	B	<0.03	<0.0003	2.552	0.0122	0.00065	0.00311	0.00025	0.0124	<0.03	0.0389	<0.04	<0.05	0.3459		0.003	0.003
WWD-13	YB406953BA	13/4/08	B	0.1904	<0.0003	8.83	0.00065	0.00066	0.00465	0.00021	0.00295	0.1786	0.0641	<0.04	<0.05	0.2038		0.004	0.004
WWD-17	YA389228BA	13/4/08	B	0.221	<0.0003	3.926	0.00234	0.00271	0.0113	<0.00005	0.00266	<0.03	0.1494	<0.04	<0.05	<0.1	1.26	0.002	0.004
WWD-19	YA859494AA	11/5/08	B	0.306	<0.0003	0.2126	0.0105	0.00152	0.00071	0.00017	0.00033	0.1665	0.0361	<0.04	<0.05	<0.1	10.89	0.002	0.049
WWD-9	XA612881BA	4/5/08	B	0.3519	<0.0003	0.2299	0.0124	0.00313	0.00852	<0.00005	0.00377	0.4161	<0.02	<0.04	<0.05	<0.1	9.5	0.002	0.003
001/014	ZV193035BA	28/4/08	C	0.552	0.00006	0.2603	0.0119	0.00139	0.00205	0.00007	0.00347	0.4405	<0.02	<0.04	<0.05	<0.1	1	0.002	0.01
001/290	AF829201AA	29/4/08	C	0.0363	<0.0003	0.1785	0.00418	0.00379	0.00199	0.00018	0.00436	<0.03	0.041	<0.04	<0.05	<0.1	3	0.001	0.011
Bashn-1	CF035107AA	21/4/08	C	0.905	<0.0003	0.4587	0.00412	0.00259	0.00604	<0.00005	0.00817	0.703	0.1051	<0.04	0.06	<0.1	1.6	0.002	0.002
Bin Kh	BF080077AA	16/4/08	C	0.6	<0.0003	0.1413	0.00419	0.00122	0.00324	0.00028	<0.00001	0.4334	0.0715	<0.04	0.11	<0.1	2.93	0.001	0.006
DEP-14	XV876910AA	4/5/08	C	0.1714	<0.0003	0.2086	0.0107	0.00899	0.0191	0.00021	<0.00001	0.0572	0.0888	<0.04	0.12	<0.1	0.73	0.003	0.002
DEP-16	XV997655AA	4/5/08	C	0.1235	0.00037	0.242	0.0124	0.00443	0.00182	0.00012	<0.00001	<0.03	0.0649	<0.04	<0.05	<0.1	1.53	0.001	0.008
DEP-18	BF223760AA	17/5/08	C	0.2944	0.00037	1.202	0.0105	0.00572	0.00947	<0.00005	0.00527	0.1942	0.1354	<0.04	<0.05	<0.1	1.48	0.001	0.004
DEP-19	BF792149AA	21/4/08	C	0.2372	<0.0003	0.185	0.0109	0.00017	0.00059	0.00011	0.00312	<0.03	0.0396	0.0401	<0.05	<0.1	1.35	0.001	0.002
DEP-2	YV955966AA	16/5/08	C	0.0952	<0.0003	0.4709	0.013	0.00772	0.0539	0.00009	0.00388	0.0718	0.1612	<0.04	<0.05	<0.1	1.37	0.002	0.003
DEP-9A	YV182483BA	3/5/08	C	0.0663	0.00091	1.038	0.00187	0.00191	0.00524	0.00028	0.00868	<0.03	0.0491	<0.04	<0.05	<0.1	4.93	0.001	0.033
Gosham1	YV439388AC	6/5/08	C	0.2916	0.00103	0.1477	0.00505	0.00926	0.00219	0.00014	0.00912	0.1334	0.0248	<0.04	<0.05	<0.1	2.74	0.001	0.007
M.sp	YV439388AC	6/5/08	C	0.699	<0.0003	1.359	0.00393	0.00452	0.0063	0.0001	0.00666	0.654	0.0317	<0.04	<0.05	<0.1	0.87	0.003	0.005
Qitbit	BG317999AA	21/4/08	C	0.1216	0.00194	0.1593	0.011	0.00149	0.00681	0.00023	0.00535	<0.03	0.0206	<0.04	<0.05	<0.1	3.2	0.002	0.01
Ranada1	BF840101AA	20/4/08	C	0.3135	<0.0003	0.3359	0.00521	0.00858	0.0152	<0.00005	0.011	0.3334	<0.02	0.0816	0.17	<0.1	2.38	0.002	0.008
S.TMMI	YV347775AA	3/5/08	C	0.458	0.00717	0.1344	0.0258	0.00303	0.00512	0.00021	<0.00001	0.0667	0.1208	<0.04	<0.05	0.1673	0.4	0.002	0.002
UBAR fm	YA819821AA	29/4/08	C	0.0378	0.00031	0.3194	0.000941	0.00263	0.00287	0.00053	0.00834	<0.03	<0.02	<0.04	<0.05	<0.1	3.42	0.001	0.003
W. Bhamra1	BF040000AA	17/5/08	C	0.1273	<0.0003	0.3162	0.00042	0.00063	0.00157	0.00012	0.00188	0.0334	0.0803	<0.04	<0.05	<0.1		0.002	0.002
WWD-11	YA051882AA	13/4/08	C	0.2562	<0.0003	0.586	0.014	0.00093	0.00307	0.00006	0.00299	<0.03	0.0838	<0.04	<0.05	<0.1		0.003	<0.001
WWD-12	YB406944AA	13/4/08	C	0.798	<0.0003	0.586	0.014	0.00053	0.0003	0.0011	0.00148	<0.03	1.507	<0.04	<0.05	<0.1		0.003	0.003
WWD-16	YA389227AA	13/4/08	C	0.3525	<0.0003	0.225	0.0118	0.00134	0.00013	0.00022	0.00553	0.4267	<0.02	<0.04	<0.05	<0.1		0.003	0.003
WWD-2	XA557476BA	13/4/08	C	0.718	<0.0003	0.3282	0.00483	0.00555	0.00349	0.00012	0.00505	0.4235	<0.02	<0.04	<0.05	<0.1	0.95	0.003	0.002
WWD-21	YA858545AA	11/5/08	C	0.561	<0.0003	0.76	0.00339	0.00139	0.00185	<0.00005	<0.00001	0.4897	0.0973	<0.04	<0.05	<0.1	2.78	0.002	0.003
WWD-22	BG200046AA	17/4/08	C																

ANNEX

A-4 Continued

Local Name	Site ID	Sample Date	Aquifer	Fe mg.L ⁻¹	As mg.L ⁻¹	B mg.L ⁻¹	Cu mg.L ⁻¹	Cr mg.L ⁻¹	Ni mg.L ⁻¹	Cd mg.L ⁻¹	Pb mg.L ⁻¹	Al mg.L ⁻¹	Mn mg.L ⁻¹	Zn mg.L ⁻¹	PO4 mg.L ⁻¹	P mg.L ⁻¹	V mg.L ⁻¹	Co mg.L ⁻¹	Mo mg.L ⁻¹
WWD-25	BG00002AA	16/4/08	C	0.16	<0.0003	0.74	0.00425	0.00061	0.0035	0.00009	0.00529	0.0786	0.0633	<0.04	<0.05	<0.1	2.62	0.002	0.003
WWD-27	BG110099AA	17/4/08	C	0.4778	0.00038	0.888	0.0197	0.00198	0.00656	0.00024	0.00646	0.3291	<0.02	<0.04	<0.05	<0.1	1.29	0.002	0.002
WWD-32	CG034063BA	21/4/08	C	0.1099	<0.0003	2.13	0.0174	0.00068	0.00444	<0.00005	0.00292	<0.03	0.0451	<0.04	<0.05	<0.1	1.16	0.001	0.001
WWD-34	AG856280BA	17/4/08	C	0.1419	<0.0003	1.222	0.0128	0.00104	0.00211	<0.00005	0.00446	0.1486	0.0568	<0.04	<0.05	<0.1	1.36	0.002	0.002
WWD-35	YB809472AA	17/4/08	C	0.308	<0.0003	0.815	0.0144	0.00167	0.00357	0.00024	0.00353	0.2311	0.0548	<0.04	<0.05	<0.1	<0.10	0.003	0.002
WWD-36	CG085491AA	21/4/08	C	0.2874	<0.0003	2.274	0.00207	0.00143	0.00504	<0.00005	<0.0001	0.1432	0.0603	<0.04	<0.05	<0.1	1.18	0.002	0.003
WWD-39	BG367633AA	17/4/08	C	0.655	<0.0003	1.831	0.00119	0.00356	0.00561	<0.00005	0.00267	0.3841	0.0534	<0.04	<0.05	<0.1	<0.10	0.001	0.002
WWD-7	XA694716DA	13/4/08	C	0.779	0.00045	0.389	0.0147	0.00588	0.00575	0.00029	0.00468	0.3303	0.2339	0.0424	<0.05	0.3014	<0.10	0.001	0.002
WWD-8	XA612881AA	4/5/08	C	0.1894	<0.0003	0.168	0.0136	0.0173	0.00811	<0.00005	0.00073	0.1764	<0.02	<0.04	<0.05	<0.1	3.65	0.002	0.019
H.R.C(103/395)	AF828170BA	29/4/08	D	0.513	<0.0003	0.865	0.00182	0.00208	0.0049	0.00036	0.00889	0.3608	0.0233	<0.04	<0.05	<0.1	2	0.003	0.006
332/014	AE989051AA	28/4/08	D	0.2163	0.00002	0.3738	0.0012	0.00235	0.00258	0.00021	0.00108	0.1819	<0.02	<0.04	<0.05	<0.1	1	0.003	0.004
AQSR	BE202783AA	10/5/08	D	0.0822	<0.0003	0.371	0.0178	0.00413	0.0763	0.00025	0.00343	<0.03	0.0376	<0.04	0.39	<0.1	32.39	0.002	0.033
DEP-10	YV322265AA	13/5/08	D	0.056	0.00032	0.1796	0.0167	0.00488	0.0107	0.00012	0.00257	<0.03	<0.02	0.0572	0.08	<0.1	1.99	0.001	0.003
DEP-11A	YV356616BA	3/5/08	D	6.11	0.00663	0.2439	0.0229	0.00556	0.00842	0.00017	0.0394	0.2683	<0.02	<0.04	0.05	0.652	2.78	0.002	0.03
DEP-14A	XV876910BA	4/5/08	D	0.56	0.00031	0.3824	0.00541	0.00236	0.00351	0.00026	0.00778	0.4063	0.0372	<0.04	0.06	<0.1	1.35	0.002	0.01
DEP-3	BE162450AA	15/5/08	D	0.0668	0.00045	0.1633	0.00114	0.00441	0.00219	0.00032	0.00818	<0.03	0.0301	<0.04	<0.05	<0.1	7.91	<0.001	0.048
DEP-4	YV937394AA	16/5/08	D	0.0523	<0.0003	0.0753	0.0006	0.206	0.00801	0.00013	0.016	0.0517	<0.02	<0.04	<0.05	<0.1	1.26	<0.001	<0.001
DEP-5	BE149620AA	15/5/08	D	0.0831	<0.0003	0.2253	0.00177	0.00527	0.00763	0.00015	0.0121	0.0428	0.0223	<0.04	<0.05	<0.1	1.56	<0.001	0.003
DEP-6	YV123115AA	28/4/08	D	0.4565	<0.0003	0.3055	0.018	0.00208	0.00284	0.00016	0.00397	<0.03	<0.02	<0.04	<0.05	<0.1	0.01	0.003	0.004
DEP-7	BE127955AA	15/5/08	D	0.0544	<0.0003	0.1584	0.0113	0.00451	0.0216	0.00009	0.0057	<0.03	<0.02	<0.04	<0.05	<0.1	0.3	<0.001	0.004
DEP-8	XV935678AA	13/5/08	D	0.891	<0.0003	0.0795	0.0139	0.00638	0.0485	0.0001	<0.0001	0.675	<0.02	<0.04	<0.05	<0.1	1.24	0.001	0.004
DWS-15	YU181909AA	24/4/08	D	0.693	0.00072	0.076	0.0165	0.00842	0.0141	<0.00005	0.00146	0.1596	<0.02	<0.04	<0.05	<0.1	5	0.001	0.01
HAD-49	ZV084571AA	21/4/08	D	0.0543	<0.0003	0.3357	0.00217	0.00197	0.0108	<0.00005	0.00274	<0.03	0.0405	<0.04	<0.05	<0.1	2.09	<0.001	0.009
QISB	AE915009AA	11/5/08	D	2.151	0.00093	0.1251	0.0185	0.00346	0.0131	<0.00005	0.00424	0.1222	<0.02	0.1038	<0.05	0.2242	7.9	0.002	0.009
TOSNAT	XV849043AA	14/5/08	D	0.979	<0.0003	0.1585	0.000996	0.00651	0.00696	<0.00005	0.00072	<0.03	0.0809	<0.04	0.12	<0.1	1.96	0.001	<0.001
WSW-3	BE991437AA	20/4/08	D	0.631	0.00095	0.1483	0.0127	0.00073	0.0092	0.00054	0.0184	0.4136	<0.02	<0.04	<0.05	<0.1	20.82	<0.001	0.013
WWD-14	YB406954CA	13/4/08	D	0.4267	0.00746	0.892	<0.0001	0.0011	0.00077	<0.00005	0.00498	0.3535	0.0366	<0.04	<0.05	<0.1	<0.10	0.001	0.001
WWD-37	CG085490BA	21/4/08	D	0.1015	<0.0003	2.789	0.00092	0.00277	0.00505	<0.00005	<0.0001	0.3176	0.2898	<0.04	<0.05	<0.1	1.89	0.002	0.002
WWD-6	XA694716CA	13/4/08	D	0.3364	<0.0003	0.3221	0.00463	0.00715	0.00453	0.00014	0.00278	0.0834	0.0846	<0.04	<0.05	<0.1	<0.10	0.002	0.002
Gogib Rainfall	AE902477AF	Jul-Aug 2008	Rainfall	0.018	0.000	0.000	0.000	0.000	0.000	0.000	0.000	0.000	0.014	0.000	0.000	0.000	0.000	0.000	0.000

ANNEX

A-5 Results of noble gases collected in 2009
 All units [ccSTP.g⁻¹] except NGT [°C] (see also, Herb, 2010)

Well name	Aquifer	He	err He	Ne	err Ne	Ar	err Ar	Kr	err Kr	Xe	err Xe	³ He	err ³ He	³ He/ ⁴ He	^{err} ³ He/ ⁴ He	NGT	err NGT
M-Masin	A	6.63E-08	6.63E-10	1.75E-07	8.76E-10	2.50E-04	2.00E-06	5.37E-08	1.14E-09	6.87E-09	1.11E-10	5.80E-14	2.82E-15	8.74E-07	4.27E-08	30.9	0.9
O.R	A	7.58E-08	7.58E-10	1.96E-07	9.82E-10	2.58E-04	2.06E-06	4.93E-08	9.56E-10	6.69E-09	7.62E-11	7.03E-14	2.58E-15	9.28E-07	3.44E-08	32.5	0.7
TWIRISH	A	6.31E-08	1.15E-09	1.86E-07	9.29E-10	2.63E-04	2.10E-06	5.44E-08	1.19E-09	6.83E-09	1.00E-10	6.81E-14	7.15E-16	1.06E-06	3.13E-08	32.0	1.4
WWD-45	A	5.04E-08	5.04E-10	1.81E-07	9.07E-10	2.52E-04	2.02E-06	5.35E-08	1.11E-09	6.46E-09	1.06E-10	6.02E-14	2.95E-15	1.20E-06	5.89E-08	34.5	1.6
MAF-SI (001/015)	B	2.04E-06	2.04E-08	2.15E-07	1.08E-09	3.01E-04	2.41E-06	6.42E-08	1.16E-09	8.01E-09	8.63E-11	5.45E-14	3.08E-15	2.68E-08	1.52E-09	26.1	0.7
DEP-16A	B	6.81E-08	6.81E-10	2.46E-07	1.23E-09	3.27E-04	2.61E-06	6.80E-08	1.16E-09	8.68E-09	1.01E-10	7.03E-14	3.51E-15	9.99E-07	5.01E-08	23.4	0.6
DEP-17	B	1.57E-07	1.57E-09	2.13E-07	1.06E-09	2.89E-04	2.31E-06	6.30E-08	1.24E-09	8.19E-09	1.25E-10	7.34E-14	3.55E-15	4.66E-07	2.26E-08	24.7	0.7
DEP-9	B	2.41E-07	2.41E-09	2.05E-07	1.02E-09	2.77E-04	2.22E-06	5.71E-08	1.25E-09	7.52E-09	1.18E-10	7.33E-14	3.74E-15	3.05E-07	1.56E-08	27.6	0.8
WWD-13	B	9.99E-06	9.99E-08	2.21E-07	1.10E-09	2.90E-04	2.32E-06	5.98E-08	1.01E-09	7.27E-09	7.56E-11	1.24E-13	9.87E-15	1.25E-08	9.90E-10	31.0	0.8
WWD-17	B	9.33E-06	9.33E-08	2.37E-07	1.18E-09	3.09E-04	2.47E-06	6.09E-08	1.15E-09	7.61E-09	8.45E-11	2.39E-13	1.38E-14	2.56E-08	1.48E-09	30.3	1.0
001/014	C	2.59E-06	2.59E-08	2.13E-07	1.06E-09	2.93E-04	2.34E-06	6.23E-08	1.51E-09	8.14E-09	1.33E-10	6.89E-14	4.10E-15	2.66E-08	1.59E-09	24.9	0.8
001/290	C	4.00E-06	4.00E-08	2.39E-07	1.20E-09	3.13E-04	2.51E-06	6.53E-08	1.43E-09	8.41E-09	1.25E-10	9.99E-14	5.99E-15	2.50E-08	1.50E-09	24.4	0.7
DEP-16	C	3.03E-07	3.03E-09	2.06E-07	1.03E-09	2.81E-04	2.25E-06	5.97E-08	1.03E-09	7.68E-09	7.68E-11	6.87E-14	2.63E-15	2.26E-07	8.74E-09	26.6	0.5
DEP-9A	C	1.12E-06	1.12E-08	2.04E-07	1.02E-09	2.86E-04	2.29E-06	6.08E-08	1.05E-09	7.88E-09	9.18E-11	6.83E-14	3.66E-15	6.09E-08	3.28E-09	25.6	0.6
WWD-16	C	7.95E-06	7.95E-08	2.08E-07	1.04E-09	2.76E-04	2.21E-06	5.60E-08	1.17E-09	7.19E-09	1.06E-10	1.55E-13	1.22E-14	1.95E-08	1.54E-09	30.2	0.8
WWD-27	C	1.41E-05	3.81E-07	2.46E-07	1.23E-09	3.14E-04	2.51E-06	6.43E-08	1.15E-09	8.06E-09	1.19E-10	2.02E-13	2.96E-14	1.41E-08	2.12E-09	27.1	0.8
332/014	D	5.66E-06	5.66E-08	2.93E-07	1.47E-09	3.53E-04	2.83E-06	7.20E-08	1.24E-09	9.09E-09	9.41E-11	1.00E-13	4.57E-15	1.77E-08	8.12E-10	22.6	0.6
DEP-6	D	1.79E-07	1.79E-09	2.01E-07	1.01E-09	2.89E-04	2.31E-06	6.13E-08	1.32E-09	8.61E-09	1.38E-10	5.84E-14	2.84E-15	3.26E-07	1.59E-08	22.3	0.7
LobFr	D	1.29E-07	1.29E-09	2.17E-07	1.08E-09	2.93E-04	2.35E-06	6.20E-08	1.39E-09	7.93E-09	1.23E-10	7.42E-14	3.63E-15	5.76E-07	2.83E-08	24.6	0.8
QISB	D	1.22E-07	1.22E-09	2.76E-07	1.38E-09	3.24E-04	2.59E-06	6.49E-08	1.36E-09	8.14E-09	1.26E-10	9.77E-14	4.87E-15	8.03E-07	4.02E-08	24.7	0.8
WWD-14	D	1.44E-05	1.44E-07	2.09E-07	1.05E-09	2.72E-04	2.17E-06	5.78E-08	1.31E-09	7.09E-09	1.11E-10	2.23E-13	1.76E-14	1.54E-08	1.21E-09	30.5	0.8
WWD-37	D	2.58E-05	2.58E-07	1.79E-07	8.96E-10	2.60E-04	2.08E-06	5.26E-08	1.04E-09	6.85E-09	6.85E-11	3.26E-13	1.45E-14	1.26E-08	5.67E-10	32.6	2.1

